Modulating the activity of NADPH oxidase by oxidative stress participants ; lipids and nanoparticles A cell-free system study

Rawand Masoud

NNT : 2016SACLS028

THESE DE DOCTORAT

DE

L'UNIVERSITE PARIS-SACLAY

PREPAREE A

L'UNIVERSITE PARIS-SUD

ÉCOLE DOCTORALE N°571

Sciences chimiques : molécules, matériaux, instrumentation et biosystèmes

Spécialité de doctorat : Chimie

Par

Mme Rawand Masoud

Modulating the activity of NADPH oxidase by oxidative stress participants; lipids and nanoparticles A cell-free system study.

Thèse présentée et soutenue à Orsay, le 16 février 2016 :

Composition du Jury :

Mme S. Lacombe	Professeure, Université Paris-Sud	Présidente du Jury
M. F. Fieschi	Professeur, Université Joseph Fourier	Rapporteur
Mme. P.M .Dang	Chargée de Recherche, CNRS	Rapporteur
M. M. Ostuni	Professeure, Université Paris Diderot	Examinateur
Mme. C. Houee-Levin	Professeur, Université Paris-Sud	Co-directeur de thèse
Mme. T. Bizouarn	Chargée de Recherche, CNRS	Co-directeur de thèse

université PARIS-SACLAY
ÉCOLE DOCTORALE
Sciences chimiques : molécules, matériaux, instrumentation et biosystèmes

Titre : Modulation de l'activité de la NADPH oxydase par des participants au stress oxidatif, les nanoparticules et le cholesterol

Mots clés : NADPH oxydase, stress oxydatif, cholestérol lipides nanoparticules

Résumé : La NADPH oxydase de phagocyte est un complexe enzymatique impliqué dans la défense immunitaire contre les pathogènes. Elle est constituée du flavocytochrome b_{558} membranaire (Cyt b_{558}), composé de deux sous-unités (gp91^{phox} et p22^{phox}) et de quatre sous-unités cytosoliques, p47^{phox}, p67^{phox}, p40^{phox}, et Rac. Sa fonction est de produire les anions superoxyde ($O_2^{\bullet-}$) qui sont transformés en d'autres espèces réactives de l'oxygène (ROS) qui vont détruire les agents pathogènes mais aussi dans certains situations pathologiques attaquer les lipides, les protéines et l'ADN environnants. Après activation du phagocyte, les sous-unités cytosoliques subissent des modifications post-traductionnelles et transloquent vers la membrane pour former avec le Cyt b_{558} le complexe NADPH oxydase activé. Le rôle délétère des ROS dans les maladies inflammatoires est connu depuis longtemps. Le but de ma thèse a été d'étudier l'influence de molécules exogènes qui induisent une augmentation du stress oxydatif, sur l'activité de la NADPH oxydase.

Dans ce travail, nous avons étudié le fonctionnement de la NADPH oxydase dans un système *in vitro* dans lequel l'enzyme était activée par la présence d'acide arachidonique (AA). J'ai étudié l'influence de deux types de molécules: une classe de lipides et des nanoparticules (NPs). Pour simplifier le système, nous avons remplacé l'ensemble des sous-unités cytosoliques par une protéine unique appelé trimère qui correspond à une fusion des trois protéines cytosoliques p47^{phox}, p67^{phox} et Rac. Nous avons montré que le trimère est fonctionnellement comparable aux sous-unités cytosoliques séparées. La vitesse de production de $O_2^{\bullet-}$, sa dépendances en fonction de la concentration en AA et et sa sensibilité aux radicaux libres sont comparables lorsque le trimère ou les sous-unités séparées sont utilisés.

J'ai étudié les conséquences de la présence du cholestérol et de ses formes oxydées sur la production de $O_2^{\bullet-}$ par la NADPH oxydase.

Nos résultats montrent clairement que le cholestérol et les oxystérols ne sont pas des activateurs efficaces de la NADPH oxydase. L'addition d'une quantité physiologique de cholestérol déclenche une faible production d'anions superoxyde. L'addition de cholestérol à des concentrations du même ordre de grandeur pendant le processus d'assemblage (en présence de AA), a un rôle inhibiteur sur la production d'$O_2^{\bullet-}$. Le cholestérol ajouté agit sur les composantes, cytosoliques et membranaires, conduisant à un assemblage imparfait. En conclusion, le cholestérol déjà présent dans la membrane des neutrophiles est optimal pour le fonctionnement de la NADPH oxydase.

Il était intéressant de vérifier l'influence des nanoparticules de dioxyde de titane (TiO_2) et de platine (Pt) sur le comportement de la NADPH oxydase sachant que l'internalisation cellulaire de ces NPs a pour effet d'activer les neutrophiles et les macrophages et contribue à une sur-production de ROS. En l'absence d'activateur mais en présence de NPs de TiO_2 ou Pt, aucune production de $O_2^{\bullet-}$ n'était détectée indiquant que les NPs de TiO_2 et Pt sont incapables d'activer le complexe par eux-mêmes aussi bien dans le système acellulaire que dans les neutrophiles. Cependant, une fois la NADPH oxydase activée (par AA), les NPs de TiO_2 entrainent une augmentation de la production des $O_2^{\bullet-}$ jusqu'à 40% en comparaison aux conditions où elles sont absentes. Cet effet est dépendent de leur concentration. Par contre, les NPs de Pt n'ont aucun effet sur l'activité de la NADPH oxydase aussi bien *in vitro* que dans les neutrophiles. En conclusion, l'hyperactivation de la NADPH oxydase et l'augmentation subséquente de la production des ROS induites par les NPs de TiO_2 pourraient participer au développement du stress oxydatif ce qui ne serait pas le cas de Pt NPs étant donnée leur absence d'effet.

université PARIS-SACLAY
ÉCOLE DOCTORALE
Sciences chimiques : molécules, matériaux, instrumentation et biosystèmes

Title : Modulating the activity of NADPH oxidase by oxidative stress participants, nanoparticles and cholesterol
Keywords : NADPH oxidase, lipids oxidative stress, cholesterol, nanoparticles

Abstract: NADPH oxidase from phagocytes is a multi-subunit enzyme complex involved in the innate defense of organisms against pathogens. It is composed of the membrane-bound flavocytochrome b_{558} (Cyt b_{558}), comprising two subunits (gp91^{phox}, and p22^{phox}) and four cytosolic components, p47^{phox}, p67^{phox}, p40^{phox}, and Rac. Its function is to produce superoxide anions that are transformed subsequently into other reactive oxygen species (ROS) and will destroy the pathogens but also can damage in certain pathological situations lipids, proteins and DNA. Upon phagocyte activation, the cytosolic subunits undergo posttranslational modifications and migrate to the membrane bound Cyt b_{558} to constitute the activated NADPH oxidase complex. The damaging role of oxidative stress induced by ROS in cardiovascular diseases has been known for some decades. The aim of my thesis was to study the influence on NADPH oxidase activity, of molecules coming from food and industrial products and known to be involved in increase of oxidative stress.

In this work, we studied the NADPH oxidase functioning in an in vitro system in which the components of the enzyme are mixed and activated by the introduction of an amphiphile the arachidonic acid (AA). During my PhD, I have studied the influence of two types of oxidative stress participants: lipids and nanoparticles (NPs). For simplicity, we have replaced the cytosolic subunits by a single protein called trimera, which is a fused construction of three cytosolic proteins p47^{phox}, p67^{phox} and Rac. We have shown that trimera is functionally comparable with the separated cytosolic subunits. The rates of production of $O_2^{\bullet-}$, the dependences of the activity in function of AA concentration and temperature, the presence of two states in the activation process and the sensitivity of NADPH oxidase to free radicals were comparable when either trimera or separated subunits were used.

I investigated the consequences of the addition of cholesterol on NADPH oxidase, on the production of ROS. Our results clearly show that cholesterol and oxysterols are not efficient activators of NADPH oxidase. Concentrations of cholesterol similar to what found in neutrophiles trigger a low superoxide production. Addition of cholesterol during the assembly process (in presence of AA) at similar or higher concentrations, has an inhibitory effect on the production of $O_2^{\bullet-}$. Added cholesterol acts on both cytosolic and membrane components, leading to imperfect assembly and decreasing the affinity of cytosolic subunits to the membrane ones. In conclusion, we showed that the cholesterol already present in the phagocyte membrane is optimal for the function NADPH oxidase.

It was of interest to check the influence of titanium dioxide (TiO_2) and platinum (Pt) NPs on NADPH oxidase especially that cellular internalization of NPs was shown to activate neutrophils and contribute to $O_2^{\bullet-}$ overproduction via NADPH oxidase. In the absence of activators and presence of TiO_2 or Pt NPs, no production of $O_2^{\bullet-}$ could be detected in in vitro system as well as in neutrophils indicating that TiO_2 and Pt NPs were unable to activate by themselves the complex. However once the NADPH oxidase was activated by AA, TiO_2 NPs increased the rate of $O_2^{\bullet-}$ production by up to 40%, this effect being dependent on their concentration. Differently, Pt NPs had no effect both on in vitro system as well as on neutrophils. In conclusion, the hyper-activation of NADPH oxidase and the subsequent increase in ROS production by TiO_2 NPs could participate to oxidative stress development while the absence of Pt NPs effect suggest that they do not induce inflammation status via this complex.

"As far as you dream goes, the earth will get bigger"

Mahmud Darwich

ACKNOWLEDGEMENTS

I would like to express my gratitude to many people who supported and helped me to bring this research project to fruition.

First and foremost I offer my sincerest gratitude to Pr. Mehran MOSTAFAVI and Pr. Philippe MAITRE for welcoming me in the laboratory and for their venerable suggestions.

A very special thanks goes out to Pr. Chantal HOUEE-LEVIN who gave me the opportunity to work on this subject. She is the one professor who truly made a difference in my life. It was under her tutelage that I developed myself. I am not sure that many students are given the opportunity to develop their own individuality and self-sufficiency by being allowed to work with such independence such as I had. She provided me with aspiring guidance, unlimited support and friendly advice. I doubt that I will ever be able to convey my appreciation fully, but I owe her my eternal gratitude.

I think that no word can express the gratitude I have to my supervisor Dr. Tania BIZOUARN, without her, I would not have been able to achieve my PhD. I am sincerely grateful for her understanding, patience and availability throughout these years. She supported me not only by providing a research assistantship, but also emotionally through the rough road to finish this thesis. I could not have imagined having a better supervisor and mentor for my PhD study.

I would like to express my deepest gratitude to Pr. Frank FIESCHI and Dr. My-chan DANG for accepting to be the rapporteurs of my thesis and for their careful reading and valuable comments on my work. I also thank Pr. Sandrine LACOMBE and

Dr. Mariano OSTUNI for having agreed to judge this work and to participate in the jury.

I would like to record my deep sense of gratitude to Dr. Laura BACIOU and Dr. Florence LEDERER for the help, encouragement and valuable scientific discussion. My sincere thanks go to Dr. Hynd REMITA for her continuous support and valuable advices throughout my PhD.

I gratefully thank Dr. Sergio MARCO for the work collaboration we had at Institut Curie which was very fruitful for shaping up my ideas and research. I also benefited by outstanding works from Dr. Sylvain TREPOUT's help with his particular skill in handling precisely the transmission electron microscope. My thanks to Dr. Frank WEIN and Dr. Matthieu REFREGIERS for their help in achieving CD experiments in Soleil synchrotron.

I must acknowledge Abdel Karim EL OMAR for his moral support, he was a true friend ever since. Karim is an amazing person in too many ways. I must also thank Daniela SALADO for the great cooperation and nice times we had together.

I also extend my thanks for all the members of the laboratory, the professors, the researchers and particularly: Marie ERARD, Delphine ONIDAS, Sophie BERNAD, Fabienne MEROLA, Cecile SICARD, Emilie BRUN, Filippo RUSCONI and Valerie DERRIEN for creating a pleasant working atmosphere. I wish also to record my thanks to Paul MACHILLOT who has been an inspiration on how to make experiments perfect and for sharing with me his remarkable knowledge. And I also thank Yasmina BOUSMAH who has been a source of love and energy ever since. Additionally, I express my warm thanks to all the administrative members

especially Marie-François LECANU and Severine BOURGUIGNON for their indispensable help dealing with travel funds, administration.

In my daily work I have been blessed with a friendly and cheerful group of friends with whom I have shared good times particularly Myriam MOUSSAOUI, Guilda KARIMI, Cornelia ZIEGLER, Xavier SERFATY.

Where would I be without my family? My parents and especially my mother deserve special thanks for their inseparable support, love and prayers. Even if they are far away, it was with their help and under their watchful eye that I gained so much drive and an ability to tackle challenges head on. Words fail me to express my appreciation to my husband Mohammed ABUOLBA whose unwavering love, quiet patience, encouragement and persistent confidence in me, has taken the load off my shoulder. He was always there cheering me up and stood by me through the good and bad times. This accomplishment would not have been possible without him.

I want to especially thank my sisters Dalia and Lina and my brother Mohammed who provided me with advice at times of critical need and consistently supported me despite the thousands of miles that separate us.

Finally, and most importantly, I must thank my daughter Louna who was born during my PhD, her smile was the biggest support during the hard times.

I would like to thank everybody who contributed to my success. Thank you all for supporting me during these years in both private life and in work.

SUMMARY

Introduction 18

I. NADPH oxidase history 19

II. NADPH oxidase family 21

1. Structure and Function 21

2. Tissue distribution and physiological roles 22

III. Reactive oxygen species production 23

IV. Phagocyte NADPH oxidase 26

1. Composition of the NADPH oxidase complex 28

2. Structure and functions of the membrane subunits 28

i. $gp91^{phox}$ 28

ii. $p22^{phox}$ protein 30

3. Structure and functions of cytosolic subunits 31

i. $p47^{phox}$ protein 31

ii. $p67^{phox}$ protein 33

iii. $p40^{phox}$ protein 34

iv. Rac 35

v. Trimera 37

V. Activation of NADPH oxidase complex 38

1. Physiological activation 38

2. Non physiological activation 40

VI. Diseases related to the malfunction of the NADPH oxidase 41

VII. Membrane lipids 42

1. Phospholipids 44

2. Glycolipids 44

3. Sphingolipids 45

4. Sterols 46

VIII. Lipid rafts 48

IX. NADPH oxidase and lipids 49

X. Nanoparticles 51

1. Generalities 51

2. Titanium dioxide nanoparticles 53

3. Platinum nanoparticles 54

***Objectives* 56**

***Materials & Methods* 58**

I. Preparation of proteins 59

1. Preparation of membrane fractions 59

2. Expression and purification of cytosolic proteins 60

***i.* Culture of bacteria expressing cytosolic proteins in *E.coli* 60**

ii. Extraction of proteins 61

iii. Purification of $p47^{phox}$ 62

iv. Purification of $p67^{phox}$ and Rac1Q61L 64

v. Purification of trimera 65

II. Proteins analysis 66

1. Determination of proteins concentration 66

2. Evaluation of protein purification by SDS-PAGE 67

III. Functional study of NADPH oxidase proteins 68

1. Measurement of superoxide anion production rate 68

2. Determination of enzymatic parameters 70

IV. Neutrophil cell activity measurement 70

V. Structural study of NADPH oxidase proteins 71

1. Intrinsic fluorescence Assays 71

2. Circular dichroism 71

VI. Cholesterol measurements 72

1. Quantification of intrinsic cholesterol in neutrophil membrane fractions 72

2. Depletion of cholesterol 75

VII. Quantification of H_2O_2 produced upon NADPH oxidase activation 75

VIII. Nanoparticles characterization 76

1. Dynamic light scattering measurement 76

2. Transmission electron microscopy 77

IX. Gamma irradiations 77

***Results & Discussion* 80**

CHAPTER 1: CHARACTERIZATION OF TRIMERA 81

I. Introduction 82

II. Characterization and assessing the validity of the trimera as a replacement of the cytosolic proteins 82

1. Purification of trimera 83

2. Optimization of AA activation with the trimera 84

3. Structural effects of AA 86

i. Effect of AA on soluble and membrane proteins 86

ii. Effect of AA on the secondary structure of the trimera 87

iii. Effect of AA on the tryptophan intrinsic fluorescence of the trimera 88

4. Kinetic parameters of superoxide anion production in the presence of trimera . 89

5. Assembly of NADPH oxidase in the presence of trimera 90

6. Quantification of H_2O_2 produced upon NADPH oxidase activation 91

7. Effect of H_2O_2 addition during the assembly phase 92

8. Sensitivity of cytosolic proteins to free radicals 93

9. Influence of temperature on the activity of NADPH oxidase 94

III. Discussion: trimera instead of separated proteins 97

1. On the role of AA with trimera 97

2. On the structural effect of AA on trimera 98

3. On the comparison between separated proteins and trimera 99

CHAPTER 2: EFFECT OF CHOLESTEROL ON NADPH OXIDASE 101

I. Introduction 102

II. Intrinsic cholesterol concentration and effect of cholesterol depletion by Methyl-β-cyclodextrin on superoxide production rate 102

III. Cholesterol as a Nox-activating molecule? 103

IV. Superoxide production in the presence of AA and added cholesterol 105

1. The addition of cholesterol inhibits NADPH oxidase activity 105

2. Effect of cholesterol on AA activation profile 109

3. Modification of kinetic parameters in the presence of added cholesterol 110

4. Effect of cholesterol addition during the assembly phase 112

V. Structural effects of added cholesterol 113

1. Effect of cholesterol on water-soluble and membrane proteins 113

2. Effect of cholesterol on the tryptophan intrinsic fluorescence of the trimera 115

3. Effect of cholesterol on the secondary structure of the trimera 116

VI. Discussion on the effect of lipids on NADPH oxidase 117

1. On the required cholesterol presence in neutrophils 118

2. On the target sites of cholesterol 119

3. On the conformation of the cytosolic partner 120

CHAPTER 3: EFFECT OF TITANUM DIOXIDE NANOPARTICLES ON NADPH OXIDASE 121

I. Introduction 122

II. TiO_2 NPs size characterization 123

III. Structural effects 125

1. Tryptophan fluorescence of the trimera in the presence of TiO_2 NPs 125

2. Effect of TiO_2 NPs on the secondary structure of the trimera 127

IV. Effects on the functionality 129

1. Effects of TiO_2 NPs on the NADPH oxidase activity 129

2. Effect of TiO_2 NPs addition at different sequences of cell free system assay 132

3. TiO_2 NPs effect on neutrophil cells 133

V. Discussion on the effect of TiO_2 NPs 134

CHAPTER 4: EFFECT OF PLATINUM NANOPARTICLES ON NADPH OXIDASE 137

I. Introduction 138

II. Synthesis and characterization of platinum nanoparticles 138

III. Interaction of Pt NPs with the trimera determined by fluorescence emission 140

IV. Effects on the functionality of NADPH oxidase 141

1. Pt PEG NPs as an activating molecule? 141

2. NADPH oxidase activation by AA in the presence of Pt-NPs 142

3. Effect of Pt PEG NPs on the AA-dependent activation profile 144

4. Pt PEG NPs effect on neutrophil cells 144

5. Influence of gamma irradiation on the functioning of the cell free system 145

V. Discussion on the effect of Pt NPs 147

Conclusions & Perspectives **149**

References **152**

List of publications **181**

Conferences **181**

LIST OF FIGURES

Figure 1: Scheme of NADPH oxidase family members present in human complexed with their regulatory proteins 21
Figure 2: Representative structure of the core region of NADPH oxidase enzymes 22
Figure 3: ROS production by a cascade of reactions initiated by NOX enzymes 25
Figure 4: The steps of phagocytosis and the action of NADPH oxidase 27
Figure 5: Electron transfer mechanism model catalyzed by flavocytochrome b_{558} 30
Figure 6: Scheme of cytochrome b_{558} 31
Figure 7: $p47^{phox}$ organization 32
Figure 8: Model of $p47^{phox}$ activation 33
Figure 9: $p67^{phox}$ organization 34
Figure 10: $p40^{phox}$ organization 35
Figure 11: Model of Rac activation 36
Figure 12: Trimera organization 37
Figure 13: Assembly of the phagocyte NADPH oxidase 40
Figure 14: Lipid bilayer with embedded lipid and protein molecules 43
Figure 15: Example of the structure of a phospholipid, the phosphatidylcholine 44
Figure 16: Structure of Glycolipid 45
Figure 17: Structure of sphingolipids 45
Figure 18: Structure of main sterols 46
Figure 19: Structures and sources of selected oxysterols 48
Figure 20: Scheme of lipid rafts 49
Figure 21: Absorption difference spectrum of Cyt b_{558}. 60
Figure 22: Separation of proteins of various charges by ion exchange chromatography 63
Figure 23: Principle of proteins separation by affinity chromatography 64
Figure 24: Separation of proteins of various sizes on a gel filtration column 66
Figure 25: Schematic representation of the migration of SDS PAGE 67
Figure 26: Example of kinetics of superoxide anion production 69
Figure 27: Michaelis–Menten curve for an enzyme reaction showing the relation between the protein concentration and reaction rate. 70

Figure 28: Schematic representation of Circular Dichroism spectrophotometer 72
Figure 29: Enzymatic Reaction for Cholesterol Quantitation. 73
Figure 30: Normalized absorption and fluorescence emission spectra of resorufin 73
Figure 31: Detection of cholesterol using the Amplex® Red reagent–based assay 74
Figure 32: Structural representations of α, β and γ cyclodextrin 75
Figure 33: Radioactive decay of cobalt-60 78
Figure 34: SDS–PAGE of trimera solutions after Ni column and gel filtration chromatography. 83
Figure 35: Superoxide anion production in function of AA concentrations for separate proteins 84
Figure 36: Arachidonic acid dependence of NADPH oxidase activity with the trimera. 85
Figure 37: Effect of AA activation of membrane fraction and trimera. 86
Figure 38: SR-CD spectra of trimera in the presence of increasing amounts of AA 87
Figure 39: Fluorescence of trimera treated with AA. 88
Figure 40: NADPH oxidase activity dependence on trimera concentration 89
Figure 41: Time course of the superoxide anion production catalyzed by the NADPH oxidase complex. 91
Figure 42: Effect of H_2O_2 on NADPH-oxidase activity. 93
Figure 43: Activity measurement in presence of irradiated $p47^{phox}$ or trimera 94
Figure 44: Dependence of NADPH oxidase activity as a function of temperature 95
Figure 45: Arrhenius plot of NADPH oxidase activity 96
Figure 46: Dependence of NADPH oxidase activity as a function of cholesterol concentration in the absence of arachidonic acid. 103
Figure 47: Dependence of NADPH oxidase activity as a function of oxysterols concentration in the absence of arachidonic acid. 104
Figure 48: NADPH-oxidase activity inhibition by cholesterol 106
Figure 49: NADPH-oxidase activity inhibition by cholesterol in the presence of separated cytosolic proteins. 107
Figure 50: NADPH-oxidase activity inhibition by cholesterol at 37 °C 108
Figure 51: NADPH-oxidase activity inhibition by addition of cholesterol to neutrophil membrane fractions from hypercholesteremic donor 109

Figure 52: Effect of cholesterol on the AA-dependent activation profile.....110
Figure 53: Effect of cholesterol on the trimera dependence NADPH oxidase activity 111
Figure 54: Effect of the addition time of cholesterol on NADPH-oxidase activity.....112
Figure 55: Effect of cholesterol on AA activation of membrane fraction and trimera. 114
Figure 56: Fluorescence of trimera treated with cholesterol or/and AA. 116
Figure 57: Effect of cholesterol on the SRCD spectra of trimera. 117
Figure 58: TEM images of TiO_2 NPs alone and with proteins.....124
Figure 59: Fluorescence spectrum of trimera in the presence and absence of TiO_2 NPs.....125
Figure 60: Enlargement of the fluorescence spectrum in the region 360-500 nm. 126
Figure 61: Variation of the emission fluorescence intensity of the trimera-TiO_2 NP suspensions.....126
Figure 62: Fluorescence spectrum of Trp in the presence and absence of TiO_2 NPs. 127
Figure 63: SRCD spectra of trimera alone and with either TiO_2 NPs or AA.....128
Figure 64: Kinetics of superoxide anion production in presence of TiO_2 129
Figure 65: Dependence of NOX activity as a function of TiO_2 NPs concentration.....130
Figure 66: Dependence of NADPH oxidase activity as a function of TiO_2 NPs concentrations in the absence of arachidonic acid. 131
Figure 67: Effect of TiO_2 NPs on the AA-dependent activation profile. 132
Figure 68: Effect of TiO_2 NPs as a function of its sequence of addition in the cell free system. 133
Figure 69: Characterization of platinum nanoparticles by transmission electron microscope 139
Figure 70: Size distribution histogram generated using TEM for (A) Pt PEG NPs, (B) naked Pt NPs. 140
Figure 71: Fluorescence emission spectra of the trimera-Pt PEG NPs solutions.....141
Figure 72: Dependence of NADPH oxidase activity as a function of Pt PEG NPs concentrations in the absence of arachidonic acid. 142
Figure 73: Dependence of Nox activity as a function of Pt NPs concentration 143
Figure 74: Effect of Pt PEG NPs on the AA-dependent activation profile 144
Figure 75: Influence of Gamma irradiation of Nox proteins and Pt PEG NPs on NADPH oxidase activity.....146

LIST OF TABLES

Table 1: Major reactions initiated by NOX enzymes.....25

Table 2: Plasma membrane lipid composition by weight percent of mammalian red blood cells.....43

Table 3: Kinetics parameters for cytosolic proteins using Michaelis-Menten equation in presence of AA.....90

Table 4: kinetic parameters of the fit by a two inhibitory sites equation. 106

Table 5: Values of the parameters of the fit by Michaelis-Menten equation are shown 111

Table 6: Analysis of the SRCD spectra of trimera alone, with AA and with TiO_2 NPs, using BestSel software.....128

Table 7: Rates of superoxide anion production in neutrophil cells 134

Table 8: Rates of superoxide anion production in neutrophil cells 145

LIST OF ABBREVIATIONS

AA: arachidonic acid

AIR: auto-inhibitory region

Amp: ampicillin

AuNPs: gold nanoparticles

BCA: bicinchoninic acid

BSA: bovine serum albumin

CD: circular dichroism

cDNA: complementary DNA

CGD: chronic granulomatous disease

Chl: chloramphenicol

C-ter: C-terminal

CDs: Cyclodextrins

Cyt b_{558}: cytochrome b_{558}

Cyt c: cytochrome *c*

DLS: Dynamic light scattering

DNase: deoxyribonuclease

DSB: double-strand breaks

DTT: dithiothreitol

DUOX: dual oxidase

E. coli*: Escherichia coli*

EDTA: ethylenediaminetetraacetic acid

FAD: flavin adenine dinucleotide

fMLP: formylmethionine leucyl-phenylalanine

GEF: GDP/GTP exchange factor

GDP: guanosine diphosphate

GTP: guanosine triphosphate

Gy: Gray

HDL: High-density lipoprotein

HEPS: 4-(2-hydroxyethyl)-1-piperazineethanesulfonic acid

IPTG: Isopropylthiogalatoside

IC50: half maximal inhibitory concentration

Kd: dissociation constant

K_M: Michaelis constant

kDa: Kilodalton

LB: Luria Bertoni

LDL: low-density lipoprotein

LiDS: lithium dodecyl sulfate

LR: lipid raft

MβCD: methyl-β-cyclodextrin

MPO: myeloperoxidase

MF: Membrane Fraction

NADP: nicotinamide adenine dinucleotide phosphate oxidized form

NADPH: nicotinamide adenine dinucleotide phosphate reduced form

NCF: neutrophil cytosolic factor

NOX: NADPH oxidase

NOS: NO synthase

NOXA1: Nox activator 1

NOXO1: Nox organisator1

NPs: nanoparticles

N-ter: N-terminal

$O_2^{\bullet-}$: superoxide anion

PA: phosphatidic acid

PAGE: polyacrylamide gel electrophoresis

PBS: Phosphate buffer saline

PB1: phox bem1 domain

phox: phagocyte oxidase

Pt: platinum

PI: Phosphoinositides

PI(3)P: phosphatidylinositol 3-phosphate

PI(3,4)P2: phosphatidylinositol 3,4-disphosphate

PIP: phosphatidylinositol

PMA: phorbol 12-myristate 13-acetate

PMN: polymorphonuclear neutrophils

PMSF: phenylmethylsulfonyl fluoride

PRR: proline rich region

PX: phagocyte oxidase domain

ROS: reactive oxygen species

RNOS: reactive nitrogen species

RhoGDI: GDP dissociation Inhibitor

rpm: rotation per minute

SEM: standard error of the mean

SH3: src homology 3 domain

SDS: sodium dodecyl sulfate

SDS-PAGE: sodium dodecyl sulfate polyacrylamide gel electrophoresis

SOD: superoxide dismutase

SP Sepharose: sulfopropyl sepharose

SRCD: synchrotron radiation circular dichroism

TB: terrific broth

TEM: transmission electron microscopy

TiO_2: Titanium dioxide

TPR: tetratricopeptide repeat

Tris: tris (hydroxymethyl) aminomethane

VLDL: very low-density lipoprotein

Introduction

"Research is creating new knowledge."

Neil Armstrong

I. NADPH oxidase history

The discovery of NADPH oxidase is strongly linked to that of the oxidative burst. In the early thirties, the correlation between phagocytosis, a process used by many organisms to destroy pathogens, and oxygen metabolism, was made by Baldrige and Gerard, who found that phagocytosis, was accompanied by a strong increase of the oxygen consumption [1]. It was found that functioning of phagocytes is accompanied by an important consumption of oxygen, called the respiratory burst, although the NADPH oxidase was not yet discovered.

The respiratory burst, i.e. this increase of oxygen consumption, was initially attributed to the mitochondrial respiration. In 1959, Sbarra and Karnovsky [2] described that the phagocyte respiratory burst was an energy requiring process that depended on glucose metabolism. Shortly after, in 1961, Iyer et al. [3] demonstrated that the phagocyte respiratory burst leads to the production of hydrogen peroxide. There was at that point a major controversy over whether the main substrate for the enzyme system was NADPH or NADH. In 1964, Rossi and Zatti [4] correctly suggested that an NADPH oxidase was responsible for the respiratory burst. Then, in 1965-78 NADPH oxidase was discovered in professional immune cells called phagocytes such as neutrophils, eosinophils, monocytes and macrophages [5-7]. In 1968, Fridovich and McCord discovered the enzymatic activity of copper, zinc superoxide dismutase (SOD) to protect organisms and made the hypothesis of the formation and the toxic effects of superoxide anion [8]. Later in 1973, Babior et al. [9] demonstrated that the initial product of the respiratory burst oxidase was superoxide anion and not hydrogen peroxide.

A second important topic of studies that resulted in the discovery of the phagocyte NADPH oxidase came from clinical research. In 1957, Berendes et al. [10] identified a new and relatively rare syndrome in young boys who suffered from recurrent pyogenic infections. Quie et al. [11] reported that phagocytes of chronic granulomatous disease (CGD) patients have diminished bactericidal capacity, although many phagocyte functions, such as chemotaxis, phagocytosis, and degranulation, were shown to be intact. In 1967, it was demonstrated that the respiratory burst was absent in the phagocytes of CGD patients [12, 13].

Finally, in 1975, further characterization of the reactive oxygen species (ROS) production by phagocytes showed that NADPH oxidase: 1) produced superoxide anions and its downstream

metabolite hydrogen peroxide, 2) was insensitive to cyanide, distinguishing it from mitochondria complexes and myeloperoxidase (MPO), 3) was present in phagocytes from MPO-deficient patients, but absent in those of CGD patients; and 4) was selective for NADPH over NADH by a factor of 100 [5].

The precise identification of the proteins responsible for ROS generation in phagocytes was the next challenge. A breakthrough happened in 1978, when Segal, Jones, and colleagues [7] characterized cytochrome b_{558} (Cyt b_{558}), which was absent in the leukocytes of many CGD patients. In the late 1980s, the gene coding for the catalytic subunit of the phagocyte NADPH oxidase, gp91^{phox} (also called NOX2), was cloned by Royer-Pokora et al. [14] and Teahan et al. [15].

However, it was rapidly revealed that NOX2 was not the only constituent of the phagocyte enzyme. In 1987, the protein p22^{phox} was discovered as the transmembrane subunit linked to NOX2 [16-18]. The development in 1984-85 of a cell-free system permitted the activation of the phagocyte NADPH oxidase using cytosol and membrane fractions [19, 20]. This system gave important tools to discover the cytosolic subunits p47^{phox} and p67^{phox} [21, 22] and to identify the roles of Rac1 and Rac2 [23, 24]. In 1993, Wientjes et al. [25] described a fourth cytosolic subunit, p40^{phox}.

In parallel with the progress toward understanding the phagocyte NADPH oxidase, during the 90s, the improvement in sensitivity of ROS detection methods allowed their identification in small amounts in different cell types and tissues other than phagocytic cells (epithelial, muscle, endothelial, neuronal ...) [26, 27]. In 1999, the first homolog of NOX2 was identified, NOX1 [28, 29].

Afterwards, six homologs of the phagocyte NADPH oxidase were identified in mammals based on sequence homology with gp91^{phox} (NOX2) [30-34]. They are listed in two subfamilies: NOX 1-5 (for NADPH oxidase) and DUOX 1-2 (for Dual Oxidase) (Figure 1) [35]. Together with the phagocyte NADPH oxidase, these homologs are now known as the NOX family [36]. In addition, new regulatory subunits called NOXO1 (NOX organizer 1) and NOXA1 (NOX activator 1) homologues of p47^{phox} and p67^{phox} were identified [37, 38].

II. NADPH oxidase family

1. Structure and Function

The NOX family is composed of proteins that share the capacity to transfer electrons across biological membranes from NADPH to dioxygen. The final product of the electron transfer reaction is either superoxide anion (NOX 1-2-3-5) or hydrogen peroxide (NOX4-DUOX1-2) [35, 39]. The biological function of NOX enzymes is therefore the generation of ROS [40] (Figure 1).

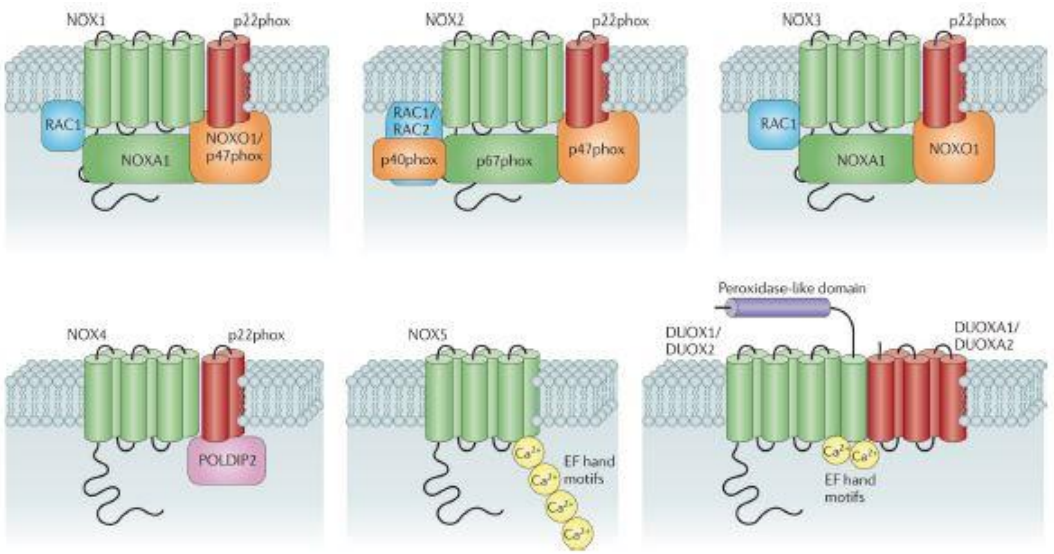

Figure 1: Scheme of NADPH oxidase family members present in human complexed with their regulatory proteins

(According to Drummond 2011) [41].

All Nox family members share a core structure consisting of: 1) six transmembrane helices, 2) NADPH and FAD binding sites at the C- terminus, and 3) four heme-binding histidines, two in the third and two in the fifth transmembrane helix (Figure 2) [42, 43]. Certain family members have additional structures. NOX5 has two polybasic domains with a domain rich in serines and a binding site for the calmodulin in the C terminal part and, in the N-terminal part, four EF-hand domains required for the protein activation by calcium [34, 44, 45]. DUOX1 and DUOX2 have two EF-hand domains followed by a seventh transmembrane helix and peroxidase homology

domain, which may allow the transformation of superoxide anion into hydrogen peroxide [33, 46].

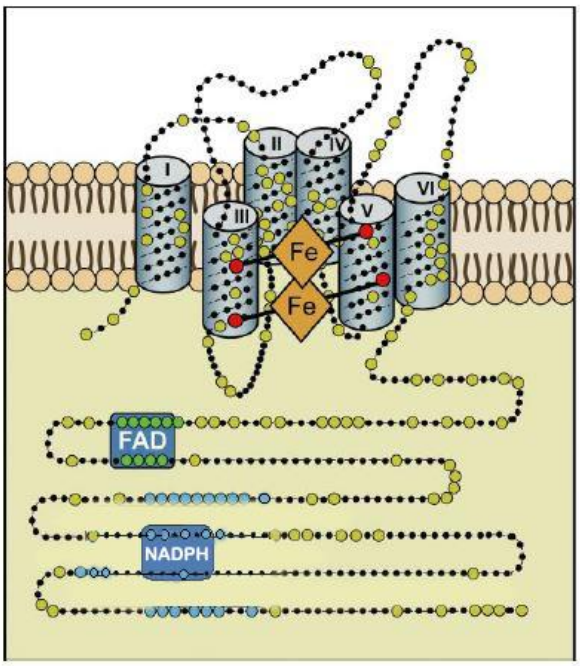

Figure 2: Representative structure of the core region of NADPH oxidase enzymes

All NOX family members contain six transmembrane domains with four histidine residues (red dots) involved in the coordination of two hemes (orange) in addition to FAD and NADPH binding domains at the C-terminus (Modified from Bedard and Krause 2007) [40].

2. Tissue distribution and physiological roles

NOX family members have been found nearly in all superior organisms such as fungi, plants and mammals [42]. In humans, many cell types express NOX family members [26]. NOX2, the phagocyte NADPH oxidase, is the most widely distributed among the NOX isoforms. It is present in a large number of tissues, such as small intestine, colon, spleen, pancreas, ovary, placenta, prostate, and testis [47]. It is expressed in non-phagocytic cells, including neurons, cardiomyocytes, skeletal muscle myocytes, hepatocytes, endothelial cells, and hematopoietic stem cells [40]. NOX2 is a clearly established host defense enzyme [48], but it is also involved in signaling functions [49]. NOX1 is most highly expressed in the colon; however, it is also expressed in other cell types, including vascular smooth muscle cells, endothelial cells, uterus, placenta, prostate and osteoclasts [40]. NOX1 was suggested to play a role in host defense and in

blood pressure regulation [26]. NOX3 is mainly expressed in the inner ear, where it is involved in otoconia morphogenesis. Low level of NOX3 can be detected in kidney, liver and fetal tissues [50, 51]. NOX4, is strongly expressed in kidney but it is also found in vascular cells, endothelial cells, smooth muscle cells, hematopoietic stem cell, fibroblasts, keratinocytes, melanoma cells, and neurons and osteoclasts [31, 39]. NOX4 is probably involved in the oxygen sensing in the kidney cortex. NOX5, a Ca^{2+} activated enzyme is predominantly expressed in lymphoid tissues and testis, where it might be involved in signaling processes [44, 45]. DUOX1 is expressed in the thyroid and in respiratory epithelia while DUOX2 is found basically in the thyroid and in gastrointestinal glandular epithelia [52]. DUOX2 is clearly involved in thyroid hormone synthesis, but possibly also in epithelial host defense [33, 48, 53, 54]. The role of DUOX1 remains unclear.

III. Reactive oxygen species production

ROS are derivatives of oxygen which are very unstable and react very easily with other molecules; they can free radicals or not free radicals. A free radical is any chemical species possessing one or more unpaired electrons. Free radicals of importance in living organisms include superoxide ($O_2^{\bullet -}$), hydroxyl ($OH^{\bullet}$), nitric oxide ($NO^{\bullet}$), peroxyl ($RO_2^{\bullet}$). Hypochlorous acid (HOCl), peroxynitrite ($ONOO^-$), hydrogen peroxide (H_2O_2), singlet oxygen ($^1O_2$) and ozone (O_3) are not free radicals but can easily lead to free radical reactions in living organism. [55]. ROS are produced *in vivo* from various endogenous sources such as the mitochondrial electron transport chain [56], xanthine oxidase, cytochrome P450, peroxisome, NOX and DUOX enzymes [57]. ROS are also produced by exogenous sources such as tobacco, smoke, pollutants, drugs and ionizing radiation [58].

NADPH oxidase is the major source of non-mitochondrial cellular ROS in many cells including renal cells, and vascular tissues**.** NOX-dependent ROS production can be depicted generally as coming from a cascade of reactions that starts with the production of superoxide anion [27] (Figure 3, table 1). NOX enzymes reduce dioxygen to form superoxide anion as their sole enzymatic function (equation 1) [59]. Although superoxide is the species produced by NOX enzymes, it seems doubtful that superoxide itself is directly implicated in microbial killing. $O_2^{\bullet -}$ is not highly reactive and since it is a charged molecule, it does not diffuse across the membrane. It has been known that superoxide is not reactive enough towards proteins, DNA or lipids, to be an

essential player on its own [60-62]. $O_2^{\bullet-}$ is the conjugate base of the perhydroxyl radical ($HO_2^{\bullet}$) with an acid dissociation constant (pKa) of 4.8, thus superoxide will be present in appreciable concentrations when the pH is above 4.8 [62]. Some reports have proposed that in nonpolar environment the reactivity of superoxide is boosted and at low pH, $HO_2^{\bullet}$, the more reactive protonated form of superoxide is abundant and could participate to the bactericidal destruction [63]. Therefore, under relevant physiological situations, such as the low pH in the phagosome and the nonpolar environment in the vicinity of cell membrane, superoxide itself could potentially be a direct player in microbial killing in addition to its role of being a substrate for the formation of secondarily derived ROS. $O_2^{\bullet-}$ rapidly dismutates to H_2O_2 either spontaneously, or catalyzed by superoxide dismutase (SOD) (equation 2) [3, 64]. H_2O_2 is relatively stable and has a bactericidal capacity. In fact, H_2O_2 is less reactive thus it can easily diffuse through the membrane and react in a different area from the area where it was produced. Other elements in the cascade of ROS generation include the iron-catalyzed Fenton reaction leading to the generation of the most powerful oxidizing agent ($OH^{\bullet}$) (equation 3) [65, 66], the myeloperoxidase (MPO) catalyze formation of potent oxidant (HOCl) from H_2O_2 and Cl^- (equation 4) [67], and the reaction of $O_2^{\bullet-}$ with $NO^{\bullet}$ to form $ONOO^-$ (equation 5) [68], a powerful oxidant capable of fragmenting the DNA and oxidizing lipids and proteins. In addition to the high level of ROS production by the phagocyte NADPH oxidase for the defense mechanisms against microbes [69], lower levels of ROS production have been found in non-phagocytic cells. The discovery of NOX family led to the concept that ROS are generated in these cells with distinctive cellular functions. It is now well-established that NADPH oxidases participate in important cellular processes including signal transduction, cell proliferation, differentiation and development [70, 71].

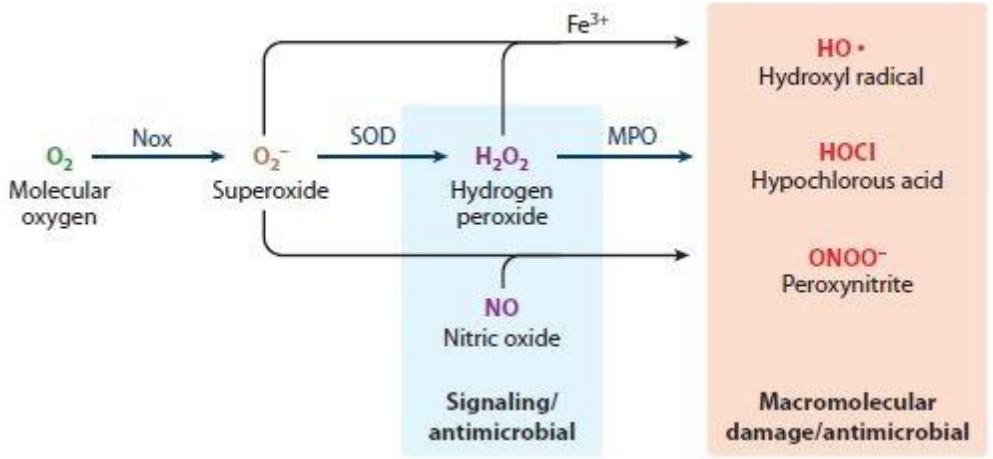

Figure 3: ROS production by a cascade of reactions initiated by NOX enzymes

(Modified from Lambeth 2014)

Table 1: Major reactions initiated by NOX enzymes

Reactions	Equations
$NADPH + 2O_2 \rightarrow NADP^+ + H^+ + 2\ O_2^{\bullet-}$	1
$O_2^{\bullet-} + HO_2^{\bullet} + H^+ \rightarrow O_2 + H_2O_2$	2
$Fe^{+2} + H_2O_2 \rightarrow Fe^{+3} + OH^{\bullet} + OH^-$	3
$H_2O_2 + Cl^- \rightarrow HOCl + OH^-$	4
$^{\bullet}NO + O_2^{\bullet-} \rightarrow ONOO^-$	5

Despite the important role of ROS in the immune defence, they can have harmful effects. ROS are considered as toxic molecules due to their high reactivity to many biological macromolecules which may lead to DNA damage, oxidations of polyunsaturated fatty acids and amino acids, and oxidative inactivation of specific enzymes which can contribute to the pathology of human diseases [71]. Thus, their production must be tightly controlled.

There are protection systems, enzymatic and non-enzymatic, that allow limitation of ROS concentration and their effects. The steady state of ROS is controlled by endogenous enzymatic regulatory systems. Intracellular levels of $O_2^{\bullet-}$ are controlled by different types of SOD: the

cytosolic CuSOD, ZnSOD and mitochondrial MnSOD. SOD accelerate the dismutation rate of $O_2^{\bullet -}$ to H_2O_2 by about four orders of magnitude [72] (equation 2). Catalase catalyzes the reduction of H_2O_2 to H_2O and O_2 and is located in the peroxisomes of most mammalian cells [73]. However, it is likely that the major H_2O_2 removing enzyme in mammalian cells are peroxidases, some of them possess a selenium active site [74]. There are also antioxidant molecules which protect the organisms by interacting with ROS. They can have anti-catalytic effect by interfering with the enzymes producing ROS or with the signalization cascade implicated in their production. Some of these molecules are produced by the body, it is the case of uric acid and Glutathione [75], Some of the antioxidants are taken from nutrients in food such as tocopherol (vitamin E), ascorbic acid (Vitamin C), β-Carotene and vitamin A. Those molecules act generally as scavengers but they are more and more studied for their anti-catalytic capacities. Oxidative stress is the term referring to imbalance between generation of ROS and the activity of the antioxidant defenses. Finally, the balance between ROS and antioxidants must be optimal as both extremes are damaging [76].

IV. Phagocyte NADPH oxidase

The human polymorphonuclear neutrophil (PMN) play an essential role in innate immunity intervening in the defense of the host against pathogens (bacteria, fungi, and virus) [77]. This cell will acquire during its maturation in the marrow, azurophilic granules (primary), specific granules (secondary), granules rich in gelatin (tertiary) and secretory vesicles that contain antimicrobial peptides and proteolytic enzymes. After maturation, the PMN remain 0-5 days in the marrow then pass into the bloodstream where its half-life is typically few hours. Under the influence of various stimuli, the PMN who are at rest in the circulating blood, will adhere to the vascular wall, slipping through endothelial cells then migrate through the tissues to the site of infection following a gradient of chemoattractant substances. At this level, adhesion to the target followed by its ingestion result in the formation of the phagosome and will engage the PN in bactericidal response (Figure 4). The PMN use in cooperative way two systems to destroy the infectious agent: the first system which is independent of the oxygen, involves the release, in the phagosome, anti-microbial peptides and lytic enzymes originally contained in the granules. The second system is dependent of oxygen and involves massive and rapid production of superoxide anions by NOX2 (Figure 4).

All the experiments present in my thesis have been performed with NOX2 from neutrophils. As said in paragraph I, NOX2 was first described in neutrophils and macrophages and is known as the "phagocyte NADPH oxidase". In these cells, NOX2 is localized in both intracellular and plasma membranes [78, 79]. In resting neutrophils, most of the NOX2 is localized in intracellular compartments, the granules (60-70% in secondary granules, 20-25% in tertiary granules, 5-20% in membrane) [80].

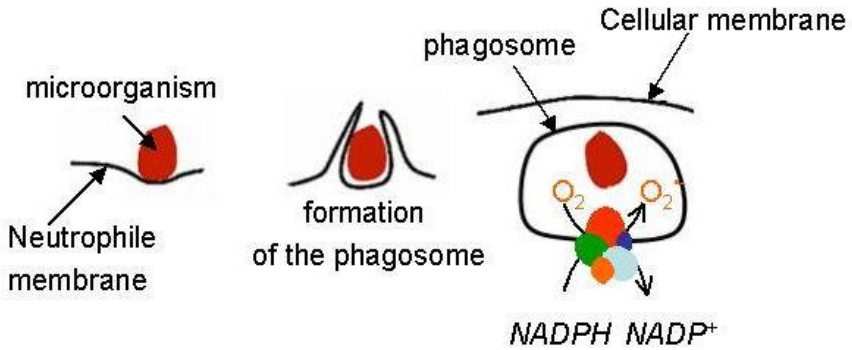

Figure 4: The steps of phagocytosis and the action of NADPH oxidase

During phagocytosis of invading microbes, the phagocyte NADPH oxidase becomes activated and generates superoxide anion, a precursor of microbicidal ROS.

Upon phagocyte stimulation, NOX2 is incorporated to the membrane as the granules fuse with the phagosomal or the plasma membrane [78, 81]. This fusion is one of the key events for the microbicidal activity of NOX2. However, NOX2 may also be activated within the granules without a fusion with surface membranes. In this case it is harmful for the neutrophil itself [82, 83]. Neutrophils produce large amounts of $O_2^{\bullet -}$, estimated between approximately 1 and 4 M in the phagosome. However, the steady state concentration has been estimated to be in the µM range because dismutation to H_2O_2 is very rapid (equation 2) [84].

1. Composition of the NADPH oxidase complex

NADPH oxidase is a multi-subunit enzyme complex composed of the membrane-bound flavocytochrome b_{558} (Cyt b_{558}), comprising two subunits (NOX2 also known as gp91^{phox}, and p22^{phox}) and four cytosolic components. The cytosolic components include p47^{phox}, p67^{phox}, p40^{phox}, and a small GTPase Rac1 or Rac2 [85, 86].

NADPH oxidase activity is tightly regulated spatially and temporally, therefore the enzyme exists in two forms, active and inactive, which differ in localization of the subunits in the cell as well as by their structure. In resting phagocytes, the components of the complex exist as separated entities but upon cell activation, the cytosolic subunits undergo posttranslational modifications and migrate to the membrane bound Cyt b_{558} to constitute the activated NADPH oxidase complex [42]. Actually this process involves a complicated set of protein-protein and protein-lipid interactions that will be discussed later.

2. Structure and functions of the membrane subunits

The membrane part of the NADPH oxidase is a transmembrane heterodimer, the flavocytochrome b_{558} that constitutes the catalytic core of the enzyme. It consist of gp91^{phox} and p22^{phox} [6, 17] where both subunits are essential for the stable expression of a functional cytochrome [87, 88].

i. gp91^{phox}

The gp91^{phox} subunit nowadays called NOX2 is a glycoprotein expressed at high levels in phagocytic cells. It is encoded by the CYBB gene located on the chromosome X [89]. It consists of 570 amino acids. The N-terminal (residues 1-290) forms six transmembrane α-helices, responsible for its anchoring in the plasma membrane, its interaction with p22^{phox} and the electron transfer through the membrane from FAD to oxygen thus enabling the production of superoxide anions on the external side of the plasma membrane. This membrane part harbors the two non-identical haem groups of the NADPH oxidase via two histidine pairs [90-92]. The C-terminal cytoplasmic domain (residues 290-570) contains the binding sites for NADPH and FAD and is therefore responsible for the first steps of the electron transfer [93]. NADPH, the electron donor is mainly derived from the pentose phosphate pathway by the oxidation of glucose 6-phosphate [94].

The $gp91^{phox}$ is synthesized as a precursor of 65 kDa partially glycosylated in the endoplasmic reticulum. It is further processed in the Golgi apparatus into a highly glycosylated protein of 91 kDa [87]. This maturation requires the incorporation of both hemes in the precursor 65 kDa and the presence of $p22^{phox}$ protein.

Hence $gp91^{phox}$ contains all cofactors needed for the electron transfer reaction which could take place in four steps: two electrons and one proton are transferred from NADPH to FAD in this model. The first electron is transferred from reduced FAD to the first haem, followed by its transfer to the second haem up to O_2 to form $O_2^{\bullet -}$. In the same way, the second electron is transferred from FAD to the first haem then to the second haem and afterward to oxygen forming superoxide [95-97]. However, the precise mechanism of the electron transfer is not yet known. One can propose the scheme described Figure 5. One can notice that the third and sixth steps in this electron transfer scheme are energetically unfavorable, since the inner haem has a higher midpoint redox potential than the outer haem. That may explain that the presence of oxygen is necessary for rapid electron flow through the NADPH oxidase, as the absence of a terminal electron acceptor will cause electrons to accumulate on the inner haems [98].

There is a need of a production of pure NOX proteins in high amount to identify theses electrons transfer steps and determine the structure of the protein. Two ways are tempted, in our group the production of recombinant proteins in yeast and in Fieschi's group in the production of bacterial homologs.

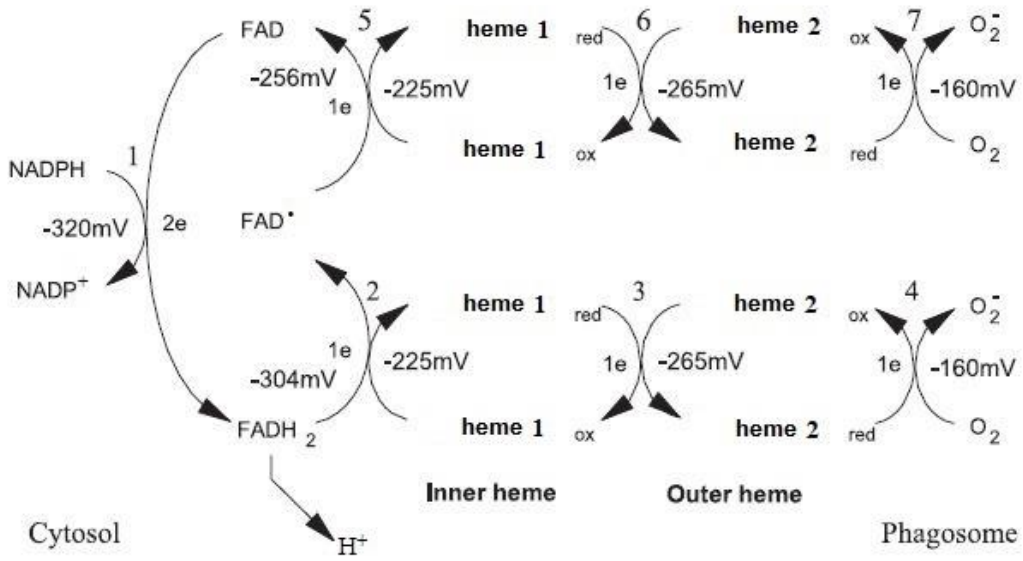

Figure 5: Electron transfer mechanism model catalyzed by flavocytochrome b_{558}

In this model, the electron transfer is carried out in seven oxido-reduction steps with a transfer of two electrons from NADPH to the FAD (1) then the transfer of a first electron via the two haems (2, 3, 4) to a first oxygen and finally the transfer of the second electron from FAD through the haems to a second oxygen (5, 6, 7) (Modified from Cross and Segal 2004) [98].

ii. $p22^{phox}$ protein

$p22^{phox}$ is a membrane protein, which closely associates with $gp91^{phox}$ in a 1:1 ratio [79]. It contains 195 amino acids encoded by the gene CYBA. According to the model proposed, $p22^{phox}$ could contain two transmembrane helices [85, 99]. The C-terminal cytoplasmic portion appears to have a proline-rich region (PRR) that contains a consensus Pro-Xaa-Xaa-Pro motif. This motif is known to be a target of the SH3 (Src homology 3) domains of $p47^{phox}$ [100-102] and this interaction appears to be critical for the activation of NADPH oxidase since a mutation of proline 156 on $p22^{phox}$ blocks the binding of the $p47^{phox}$ protein resulting in a lack of activity NADPH oxidase [103].

$p22^{phox}$ does not possess a catalytic role but remains indispensable. *in vivo*, $p22^{phox}$ has two major functions: 1) a binding to NOX proteins, that results in enzyme stabilization, and 2) a binding to organizer subunits $p47^{phox}$ or NOXO1 [104]. $p22^{phox}$ has also been shown to interact with NOX1 [105, 106], NOX3 [107], and NOX4 [108] [39]. The significance of the $p22^{phox}$ subunit for the phagocyte NADPH oxidase was demonstrated with the identification of CGD patients with mutations in $p22^{phox}$ [109].

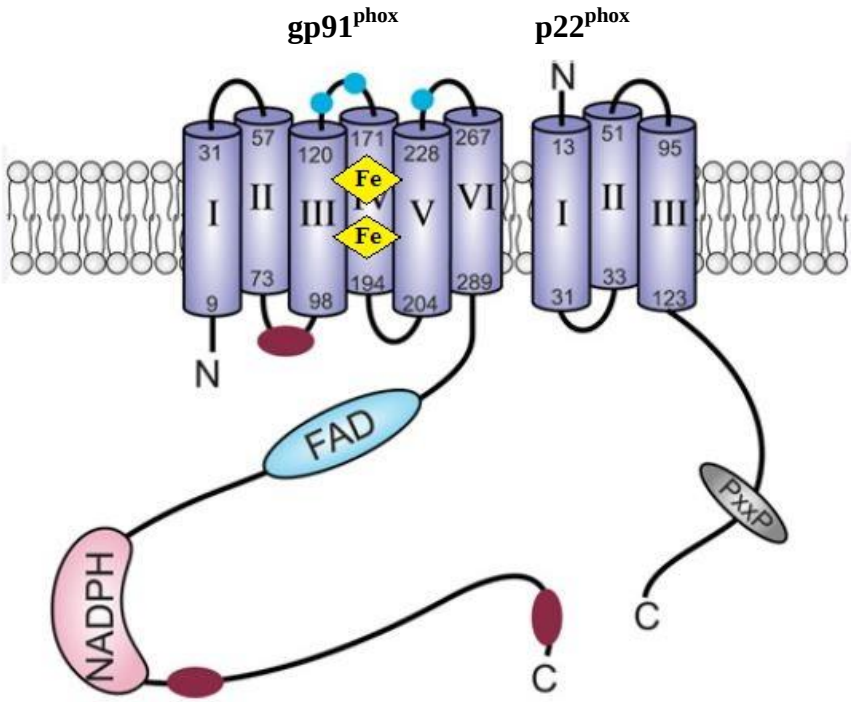

Figure 6: Scheme of cytochrome b_{558}

The transmembrane helices of gp91^{phox} and p22^{phox} are indicated. Glycosylation sites are shown by cyan dots and regions that are expected to interact with p67^{phox} in the active state in red. The FAD and NADPH binding sites in gp91^{phox} are indicated in cyan and pink respectively. The position of the PXXP motif in the cytoplasmic region of p22^{phox} that interacts with p47^{phox} is shown in grey (modified from Groemping 2005).

3. Structure and functions of cytosolic subunits

i. p47^{phox} protein

Description

p47^{phox} is a cytosolic protein encoded by the NCF1 (Neutrophile Cytosolic Factor 1) gene located on chromosome 7 in humans. This protein is composed of 390 amino acids with a molecular weight of 44.7 kDa. p47^{phox} is the protein chiefly responsible for transporting other cytosolic proteins to the Cyt b_{558} to form the active oxidase [110]. *In vitro*, it has been found not to be absolutely indispensable for oxidase activity because at sufficiently high concentrations of p67^{phox} and Rac, superoxide production takes place in the absence of p47^{phox} [111, 112].

However, it is essential in the neutrophil since patients whose neutrophils are deficient in $p47^{phox}$ have CGD [113, 114]. $p47^{phox}$ possesses several distinct functional domains that can either mediate intramolecular interactions or interact with other subunits. Starting from the amino acid N-terminal, $p47^{phox}$ consists of a phox homology (PX) domain that interact with the membrane phospholipids [115], a tandem SH3 domains that interact in the active form with the proline rich region in the C-terminal of $p22^{phox}$ [116], an autoinhibitory region (AIR) that prevents these previous interactions until the protein is phosphorylated [117, 118] and finally a proline rich region (PRR) in the carboxy terminus that interacts with the SH3 domain of $p67^{phox}$ and SH3 domain of $p40^{phox}$ [119, 120]. This interaction is essential for the translocation of $p67^{phox}$ to the Cyt b_{558} (Figure 7).

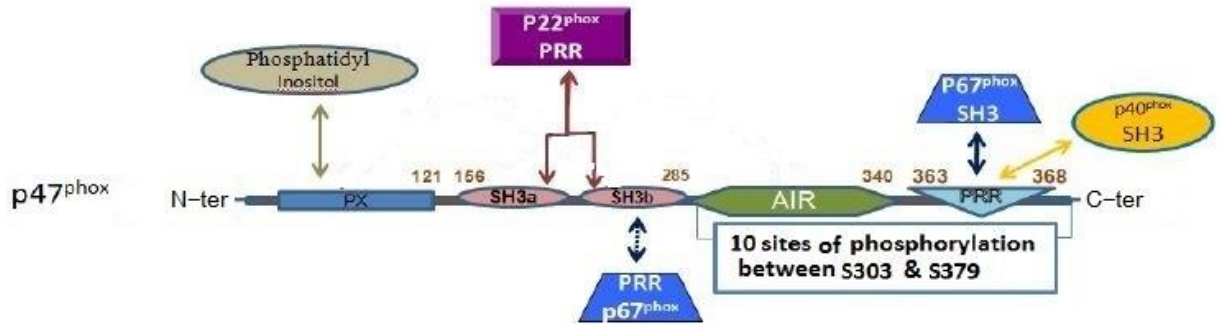

Figure 7: $p47^{phox}$ organization

The arrows represent the different intramolecular and intermolecular interactions that have been identified. The arrow in dotted lines represents interaction that is still under investigations.

Activation of $p47^{phox}$

In the absence of stimulation, $p47^{phox}$ is maintained in a self-inhibited conformation in the neutrophils. Within the PX domain of $p47^{phox}$, the PXXP motif (R_{70}IIPHLPAP$_{78}$) interacts with its SH3 domain [121]. This intramolecular interaction masks the phosphoinositide binding sites of the PX domain of $p47^{phox}$ in resting neutrophils, therefore preventing its membrane association (Figure 8).

Upon neutrophil activation, phosphorylation of several serine residues including S303, S304, S359, and S370 by kinases proteins mediates a conformational change in $p47^{phox}$ [122], unfolding the protein [110]. Phosphorylated $p47^{phox}$ was suggested to increase the binding of $p67^{phox}$ to cytochrome b_{558} by acting as an adapter, bringing $p67^{phox}$ into proximity with

cytochrome b_{558} [123-125]. The exposition of the SH3 domains of p47^{phox} will eventually interact stably with PRR of p22^{phox} [126]. At the same time, the PX domain interacts with specific membrane phospholipids (phosphatidylinositol 3,4-disphosphate (PI(3,4)P2) and phosphatidic acid (PA)) [110]. This opening of p47^{phox} is linked to an increase in hydrophilicity caused by the negative charges provided by the phosphates bound in the serine residues [122]. p47^{phox} is described as organizer subunit of NADPH oxidase complex [127].

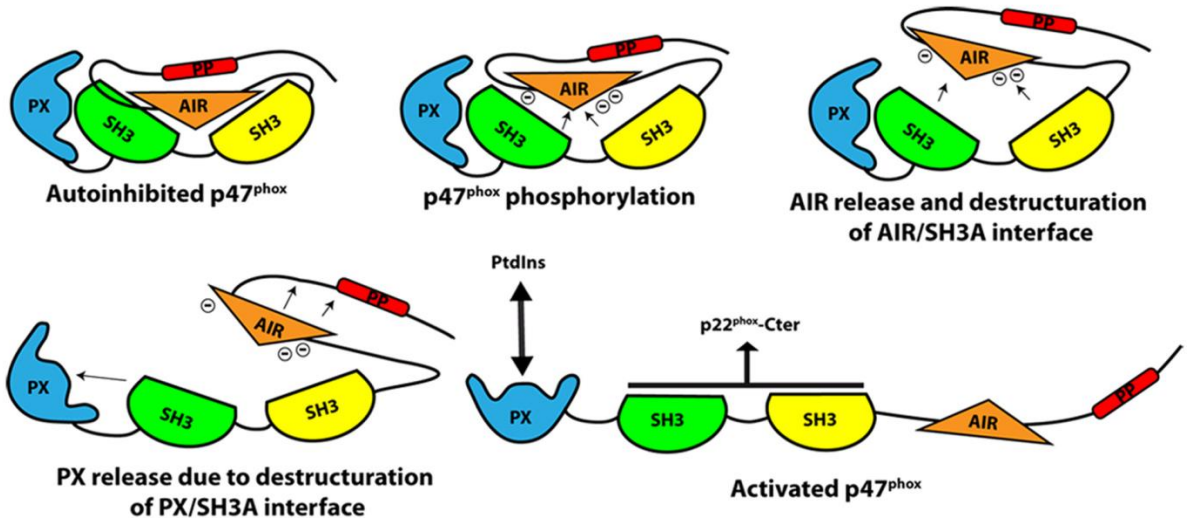

Figure 8: Model of p47^{phox} activation

Both the resting and activated configurations of p47^{phox} are shown (according to Marcoux et al, 2010) [127].

ii. p67^{phox} protein

p67^{phox} is a cytosolic protein encoded by the NCF2 (Neutrophil Cytosolic Factor 2) gene located on chromosome 1 in humans. This protein is composed of 526 amino acids with a molecular weight of 59.8 kDa [128, 129]. Unlike p47^{phox}, p67^{phox} is absolutely required for oxidase activity in cell free system [112]. Additionally, several CGD patients with functionally significant mutations of p67^{phox} have been found [130]. All p67^{phox} mutants responsible for CGD are localized in the half N-terminal part (1-210) [131].

The N- terminal part of p67^{phox} contains a domain of four tetratricopeptide repeat (TPR) motif that is responsible for mediating its interaction with Rac [132, 133] and an activation domain (amino acids 199–210) that has been shown to be essential for $O_2^{\bullet -}$ production in a reconstituted cell free system [134, 135]. It is believed that this region interacts directly with the

flavocytochrome and thereby contributes in the regulation of electron transfer [136]. That is why $p67^{phox}$ is considered as the activator subunit. This domain is followed by a PRR which might interact with the SH3 domain of $p47^{phox}$ and by two SH3 domains that are separated by a PB1 (Phox and Bem1) domain which forms a heterodimer with the PB1 domain of $p40^{phox}$ [137] (Figure 9). The last SH3 domain has been shown to be important for $p67^{phox}$ - $p47^{phox}$ dimerization [105]. Fieschi's group suggests that intramolecular interactions within $p67^{phox}$ may be present [138].

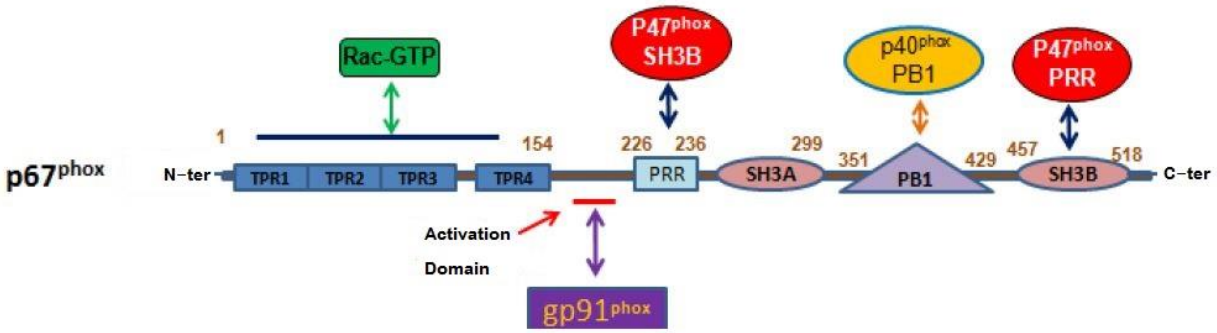

Figure 9: $p67^{phox}$ organization

Although the phosphorylation of $p47^{phox}$ contributes remarkably to the interaction changes, the functional consequences of the phosphorylation of $p67^{phox}$ are less obvious. Distinct sites for ERK2 and p38MAPK-dependent phosphorylation have been found during the activation of neutrophil [139, 140], including the threonine 233 [141, 142] and some serines but the positions of phosphorylated serine are not well determined [143] [140]. Recently, Dang et al. suggested that $p67^{phox}$ undergoes a continual cycle of phosphorylation/dephosphorylation in resting cells and $p67^{phox}$ phosphorylation would be controlled by MEK1/2 and tyrosine kinase [144].

iii. $p40^{phox}$ protein

$p40^{phox}$ is a cytosolic protein encoded by the NCF4 gene located in chromosome 22 in humans, with a molecular weight of 39 kDa. Its sequence contains 336 amino acids. The organization of $p40^{phox}$ domains are described in Figure 10. It consists of a PX domain, a SH3 domain and a PB1 domain. $p40^{phox}$ interacts with $p67^{phox}$ via its PB1 domain [145] while its SH3 domain has been proposed to interact with the PRR of $p47^{phox}$ [146, 147]. However, the affinity between the two proteins is very low (K_d = 5 µM) [120], thus this interaction is very weak in comparison with that between $p47^{phox}$ and $p67^{phox}$ (Kd between 4 and 30 nM) [145, 148, 149].

SH3 domain can also associate with PRR in $p22^{phox}$ [150]. The PX domain of $p40^{phox}$ binds particularly to phosphatidylinositol 3-phosphate (PI(3)P), which accumulates in phagosomal membranes, and could thus facilitate oxidase assembly at this site [151, 152]. A conformation for $p40^{phox}$ at rest was proposed by Ueyama et al. [153]. According to their model, the intramolecular interaction of the PX domain with the PB1 one prevents binding to PI(3)P, thus this interaction must be disrupted to allow binding of $p40^{phox}$ to the membrane (Figure 10). The study of the $p40^{phox}$ deficient CGD patient found by Dinauer group goes in favor of a role of this protein for an assembly of the NADPH oxidase at the phagosome [154].

Compared to the other cytosolic proteins, the overall role of $p40^{phox}$ in oxidase regulation is still controversial, it has been proposed as both activator and inhibitor [155-158]. In fact, after phosphorylation of this protein, it could play a role during the complex activation [119, 159, 160]. It is probably implicated in the stabilization of $p47^{phox}$ /$p67^{phox}$ complex in the cytosol and facilitates its recruitment to the membrane during the activation of NADPH oxidase [161]. It was also reported by Dang et al. that phosphorylated $p40^{phox}$ may induce conformational change that permits $p67^{phox}$ to interact fully with cytochrome b_{558} [125]. Like the previous cytosolic proteins, $p40^{phox}$ undergoes phosphorylation upon oxidase stimulation. These events are produced in correlation with superoxide production [159].

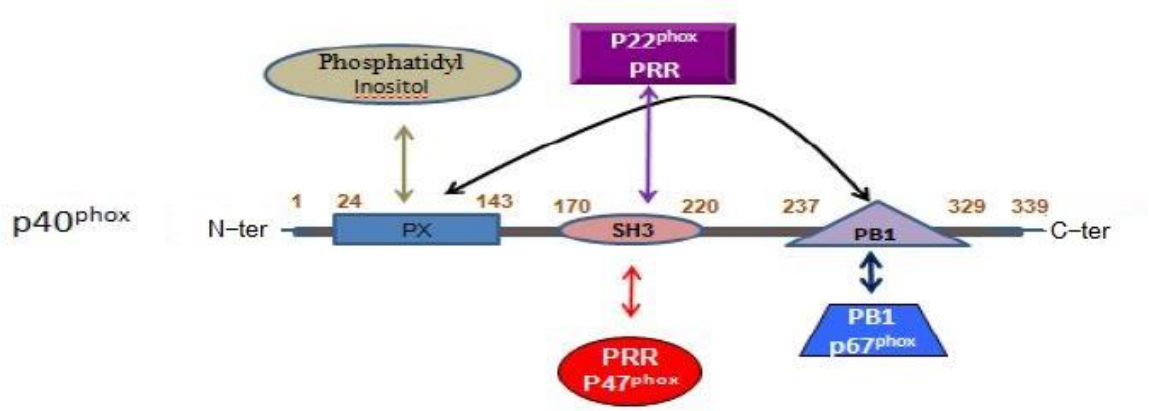

Figure 10: $p40^{phox}$ organization

iv. Rac

Rac protein is a small G-protein of about 21 kDa, composed of 192 amino acids. It exists in two isoforms in phagocytic cells (Rac2 in human neutrophils; Rac1 in human monocytes) and

both share 92% sequence homology [162]. Rac belongs to the Rho-family of small GTPases, which regulate a large variety of signaling pathways. When the neutrophil is at resting state, Rac is in an inactive form, containing a GDP in its binding site and associated to RhoGDI inhibitor (GDP dissociation inhibitor) in 1:1 stoichiometry [162-164]. The conversion between the active and inactive states is tightly controlled by GEFs (guanine-nucleotide-exchange factors) which replace GDP by GTP and allow Rac to be free from RhoGDI inhibitor and to migrate to the membrane. It has been shown that this migration occurs independently of $p47^{phox}$ and $p67^{phox}$ [165] (Figure 11).

Rac protein has an N-terminal domain (RAS effector domain (aa 20-40)) essential for its interaction with the TPR domain of $p67^{phox}$ and for NADPH oxidase activity [133, 166-168]. This interaction takes place when Rac is in the form linked to GTP [132, 169]. Rac undergoes geranylgeranylation at the polybasic region of its C-terminus, which facilitates its association with membranes. Although it has been suggested that Rac solely acts to place the activation domain of $p67^{phox}$ on Cyt b_{558} for regulation of electron transfer and increase the affinity of $p67^{phox}$ to NOX2 [125, 170], there is also notable evidence that Rac itself interacts directly with the Cyt b_{558} to activate the initial electron transfer step from NADPH to FAD [165, 171-173]. *In vivo* and *in vitro*, Rac1 and Rac2 are required for the activation of NADPH oxidase [174-177].

To study the NADPH oxidase activity *in vitro* in a reconstituted system, we used a mutant of Rac, Rac1Q61L, in which the residue Glutamine 61 is substituted by a leucine. The Q61L mutation leads to a constitutively active form of Rac. A study of this mutant showed that Rac1 is more stable and has a greater affinity for $p67^{phox}$ and the complex than the native Rac1 [178].

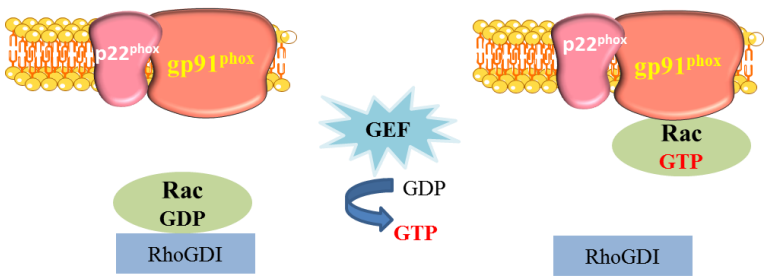

Figure 11: Model of Rac activation

v. Trimera

Studies on binding between the different soluble subunits p47^{phox}, p67^{phox}, p40^{phox} and Rac performed *in vitro* suggested that the cytosolic subunits are preassembled either in heterodimer or in heterotrimer [145, 179, 180]. Different constructions of chimeras were designed, in which individual cytosolic subunits were fused [p47^{phox}-p67^{phox}] [181] or [p67^{phox}-Rac1] [182-186] and supplemented by the missing third subunit (Rac1 and p47^{phox}, respectively), p40^{phox} being not tested since its lack of effect *in vitro*. Another strategy was to construct a trimera, which consists of the PX domain and the two SH3 domains of p47^{phox} (aa 1–286), the tetratricopeptide repeat and activation domains of p67^{phox} (aa 1-212), and full-length Rac1 (aa 1–192) in which the interaction between p47^{phox} and p67^{phox} was replaced by a linker [187] (Figure 12).

Figure 12: Trimera organization

The truncation of p47^{phox} results in the removal of the C-terminal region that keeps the protein in its inhibitory conformation [110], and participates in the prevention of PX domain-phospholipid interaction [188]. Thus, p47^{phox} truncation generates an open conformation of itself, which can react with p22^{phox} [181]. P67^{phox} was truncated right after the end of the activation domain, removing the PRR, the PB1 domain and the two SH3 domains. Rac1 was retained full-length because of the need for an intact polybasic domain for oxidase activation by Rac1 [189]. Further modification was the introduction of Q61L mutation in Rac part, making it constitutively in the GTP-bound form. It ensures that in the trimera an intramolecular bond was built between Rac1 and p67^{phox}, which is essential for the ability of trimera to activate the system [178, 190]. The subsequent change was performed by adding isoprenyl group to the C terminus of Rac1 part, mimicking *in vivo* reality, where Rac is found exclusively in the prenylated form. This last modification was not present in the experiments presented in my thesis.

Trimera was found to act as potent amphiphile-dependent oxidase protein activator upon assembly to native phagocyte membrane or purified Cyt b_{558} [187]. The persistence of a requirement for amphiphile despite the truncation of the p47^{phox} domain provides support for the idea of a direct effect of amphiphile on Cyt b_{558}. Nevertheless, the EC50 activity value measured

with the trimera was 2.5 and 11 times lower than those measured with full-length and truncated individual proteins, respectively [187]. It, thus, appears that procedures replacing the natural association/dissociation cycles between cytosolic subunits by covalent bonds, enhances the half-life of NADPH oxidase complex.

V. Activation of NADPH oxidase complex

1. Physiological activation

The neutrophil NADPH oxidase exists in several states: resting, primed, activated, or inactivated. The resting state is found in circulating blood neutrophils. The primed state can be stimulated by neutrophil adhesion, pro-inflammatory cytokines, lipopolysaccharide and other agents which results in a faster and higher response upon exposure to a second stimulus. The active state is found at the inflammatory or infection site. Activation is induced by the pathogen itself or by pathogen-derived formylated peptides and other agents. Finally, inactivation state can be induced by different anti-inflammatory agents [191] .

Several signal transduction pathways lead to oxidase activation, and various stimuli induce extra and intracellular production of oxygen radicals, showing diversity in the regulating pathways [82, 86, 192]. The signaling pathway activated by phorbol 12-myristate 13-acetate (PMA) involves the serine/threonine protein kinases C (PKC), which are sensitive to phorbol esters [122, 193]. The activation of PKC by PMA activates NADPH-oxidase via the phosphorylation of cytosolic proteins particularly $p47^{phox}$ [110, 194]. Other frequently used stimuli are formylmethionyl-leucyl-phenylalanine (fMLF) [195-197] and the calcium-specific ionophore ionomycin [94, 198] or particulate stimuli such as opsonized bacteria [199, 200]. Phosphatidylinositol 3-kinase (PI 3-kinase) phosphorylates phosphatidylinositol (PI), PI(4)P, and PI(4,5)P2, to form PI(3)P, PI(3,4)P2, and PI(3,4,5)P3, lipids that have been demonstrated to act as second messengers [201]. The PI 3-kinase is also involved in signaling pathways leading to NADPH-oxidase activation [202].

The binding of a fatty acid on the flavocytochrome is not excluded. Phospholipase A2 (PLA2) was reported to play a role in activation of phagocyte NADPH oxidase [203]. The use of inhibitors of PLA2, reduces the production of superoxide ion [124]. Arachidonic acid (AA), the product of phospholipase A2 in activated cells, plays a role in the activation of the NADPH

oxidase, which *in vivo* is still debated. Several mechanisms were proposed by which AA stimulates the respiratory burst. A direct binding of AA to S100 proteins, which regulate the assembly of the NADPH oxidase as well as the activation of signaling molecules was proposed [204]. The activity of the NADPH oxidase induced by AA is comparable to that stimulated with PMA [205] [206]. According to Badwey et al., in their ex vivo system, the rate of production of $O_2^{\bullet-}$ induced by AA in human neutrophils cells is 93.8 ± 12.5 nmol $O_2^{\bullet-}$ / min / 10^7 cells while with PMA is 68.6 ± 14.7 nmol $O_2^{\bullet-}$ / min / 10^7 cells [205]. The intensity and duration of NADPH oxidase activity depend on the present stimuli and its concentration [95, 110, 120, 207].

In resting neutrophil granulocytes, $gp91^{phox}$ and $p22^{phox}$ are shown primarily in the membrane of intracellular vesicles, constitutively as a heterodimer and separated from the cytosolic subunits. The process of translocation and assembly requires posttranslational modifications such as reversible phosphorylation of serine and threonine residues of the cytosolic proteins ($p47^{phox}$, $p67^{phox}$, $p40^{phox}$) [140, 143, 208], as well as the membrane ones ($p22^{phox}$ and $gp91^{phox}$) [110, 209, 210]. Phosphorylation of the cytosolic $p47^{phox}$ subunit leads to conformational changes described above permitting its interaction with $p22^{phox}$ [211, 212]. It has been demonstrated that $p47^{phox}$ organizes the translocation of other cytosolic entities; hence it is known as "organizer subunit." The localization of $p47^{phox}$ to the membrane brings the "activator subunit" $p67^{phox}$ into contact with $gp91^{phox}$ [134] and also brings $p40^{phox}$ to the complex. The activation of Rac which is realized by an exchange of GDP attached against a GTP permits the GTPase Rac to interact with $gp91^{phox}$ via a two-step mechanism involving an initial direct interaction with $gp91^{phox}$ [173] followed by a subsequent interaction with $p67^{phox}$ [85, 133, 209, 213] . A fusion of NOX2-containing vesicles with the plasma membrane or the phagosomal membrane occurs [40]. The active enzyme complex transports electrons from NADPH in the cytosol to the extracellular or phagosomal oxygen in order to produce superoxide anion (Figure 13) [85].

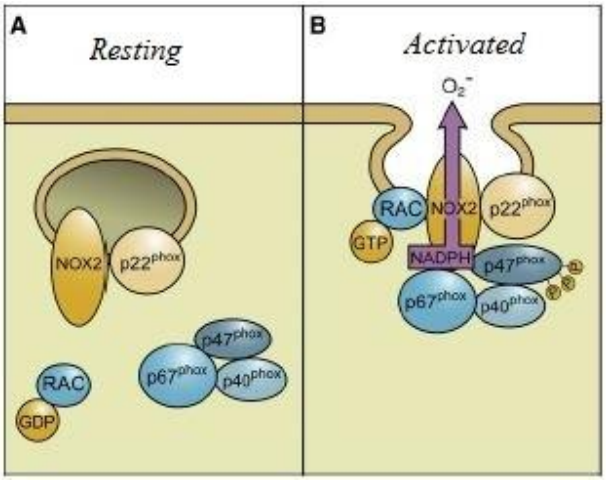

Figure 13: Assembly of the phagocyte NADPH oxidase

The assembly of NOX2 involves a complex series of protein/protein interactions [40]

2. Non physiological activation

The development of a cell-free oxidase activation system was a great help in the understanding of the *in vivo* mechanism of NADPH oxidase activation. This system was designed to mimic *in vivo* oxidase activity under *in vitro* conditions. Additionally, it permits strict quantification of the components of interest, and modifications of membrane composition. In cell-free systems, $gp91^{phox}$, $p22^{phox}$, $p47^{phox}$, $p67^{phox}$ and Rac are incubated together [214]. The presence of $p40^{phox}$ in this system has no effect on the production of superoxide anions, thus this protein is rarely used. For simplicity, there is also possibility to replace the individual cytosolic subunits by trimera [187, 190].

The activation process is bypassed by the introduction of an activator, an amphiphilic molecule, such as sodium dodecyl sulfate (SDS), or an unsaturated fatty acid such as arachidonic acid [215-217]. AA is the most commonly used but other fatty acids such as oleic, linoleic or palmitoleic acid for example, are also effective [19, 218-222]. Direct influence of these lipids on $gp91^{phox}$ was found, leading to conformational changes, which might participate in NADPH oxidase activation [95, 178, 223-226]. The predominant explanation for the oxidase activating ability of these anionic amphiphiles was that they perturbed the intramolecular bonds in $p47^{phox}$ between the polybasic domain and the SH3 tandem mimicking the phosphorylation events that occur in the intact phagocyte, which is a critical step for the assembly of the oxidase complex [211]. A similar effect was seen by phosphorylation of $p47^{phox}$ by protein kinase C *in vitro* [227].

AA was also shown to interact directly with the other cytosolic proteins [124, 227]. Recently Matono et al. showed that AA elicits GDP-to-GTP exchange on Rac and induce direct interaction of Rac-GTP-bound $p67^{phox}$ with the C-terminal cytosolic region of NOX2 in HeLa cells and in cell free system [228].

Our group has brought evidences on the geometrical specificity of *all-cis*-AA configuration to activate the NADPH oxidase in contrast to the *trans* form of AA which is unable to activate the system (unlike the *trans* forms of C18:1 and C18:2) and to give the ability of cytosolic proteins to translocate to the membrane partners [226]. Moreover, we have shown that the *cis* form of AA induces secondary structure changes of $p47^{phox}$ and $p67^{phox}$, while the *trans* one does not affect their conformations, suggesting that the changes observed are of importance for the activation process of these proteins.

VI. Diseases related to the malfunction of the NADPH oxidase

The NADPH oxidase is identified as a key component of human innate host defense and as an important player in other cellular process (Example: signal transduction) due to its capacity to produce superoxide anions which are converted into other ROS. However, excessive or diminished ROS production can disrupt the balance of cell homeostasis, resulting in serious pathologies especially since these enzymes are present in many organ systems. Therefore, regulating the activity of NADPH oxidase is indispensable and ROS generation has to be tightly controlled to make sure they are only produced when and where required [86].

The importance of the functional NADPH-oxidase enzyme to host immunity is clearly highlighted by the human genetic disease, the chronic granulomatous disease (CGD), which happens with an incidence of 1 in 200 000–250 000 [229]. The disease is caused by a mutation in $gp91^{phox}$ (70%), $p47^{phox}$ (25%), $p22^{phox}$ or $p67^{phox}$ (< 5%) that leads to the loss or inactivation of NADPH oxidase [93, 110, 230]. As a result, patients with CGD experience severe recurrent bacterial and fungal infections that lead to the shortage of their life. [100, 231, 232]. Additionally, NOX deficiency may lead to immunosuppression, lack of otoconogenesis, or hypothyroidism [40].

The increased activation of NADPH oxidase and subsequent increase in superoxide anions production are implicated in the pathophysiology of various cardiovascular diseases such as

hypertension, atherosclerosis, diabetes, cardiac hypertrophy, heart failure, and ischemia-reperfusion [233, 234]. NADPH oxidases are also involved in many cardiovascular pathophysiological processes such as endothelial dysfunction, inflammation, hypertrophy, apoptosis, angiogenesis, and vascular and cardiac remodeling. The pathological effects of ROS in the cardiovascular system result simultaneously from their direct actions modifying vascular cell functions and from their ability to scavenge and remove several beneficial vasoprotective compounds such as nitric oxide [235-239]. Increased NADPH oxidase activity is also linked to a large panel of pathologies such as neurodegenerative diseases (Alzheimer's disease and Parkinson's disease) [240], ageing, cancer [241, 242] and immune system disorders [243-245]. Therefore, ROS production has to be well regulated and to be produced for its physiological functions [246]. Consequently, knowledge of the regulation of this system is critical and could help to design better molecules capable of modulating the activity of NADPH oxidase.

VII. Membrane lipids

Clearly, membrane lipids are potential modulator of NADPH oxidase. One of the aims of this work was the study the influence of the composition of the membrane on the functioning of NADPH oxidase.

Lipids are molecules that do not dissolve readily in water but dissolve easily in organic solvents. Lipids constitute about 50% of the mass of most animal cell membranes, nearly all of the remainders are proteins. Membrane phospholipids are a group of molecules that make up the double-layered surface of the cells (lipid bilayer). There are approximately 5×10^6 lipid molecules in a 1μm × 1μm area of lipid bilayer.

They have hydrophilic heads and hydrophobic tails, therefore they are amphiphilic. By constructing a double layer with the polar ends projecting outwards and the nonpolar ends projecting inward, membrane lipids form a 'lipid bilayer', which keeps ions, soluble proteins and other molecules on one side and prevents them from diffusing on the other side of this membrane (Figure 14) [247]. Membrane lipids constitute also a matrix in which membrane proteins reside. Historically lipids were thought to merely have structural roles but later functional roles of membrane lipids were confirmed. They act as regulatory agents in cell growth and adhesion, contribute to biosynthesis of other molecules and play a fundamental role in regulating activities

of some enzymes. The lipid composition of plasma membrane is different among the species and the cells. For example, Table 2 illustrates the lipid composition of plasma membrane in red blood cells. However, the most abundant components of lipids membranes are phospholipids, sphingolipids, glycolipids and sterols [248].

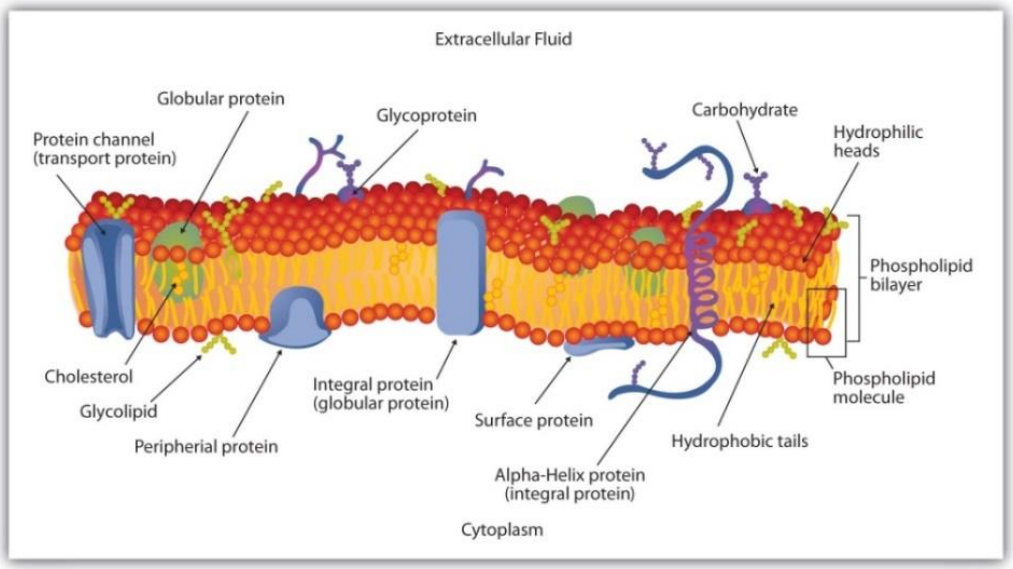

Figure 14: Lipid bilayer with embedded lipid and protein molecules

Table 2: Plasma membrane lipid composition by weight percent of mammalian red blood cells

	species					
lipid	pig	human	cat	rabbit	horse	rat
cholesterol	26.8	26.0	26.8	28.9	24.5	24.7
phosphatidylcholine	13.9	17.5	18.7	22.3	22.0	31.8
sphingomyelin	15.8	16.0	16.0	12.5	7.0	8.6
phosphatidylethanolamine	17.7	16.6	13.6	21.0	12.6	14.4
phosphatidylserine	10.6	7.9	8.1	8.0	9.4	7.2
phosphatidylinositol	1.1	1.2	4.5	1.0	0.2	2.3
phosphatidic acid	0.2	0.6	0.5	1.0	0.2	0.2
lysophosphatidylcholine	0.5	0.9	0.2	0.2	0.9	2.6
glycosphingolipids	13.4	11.0	11.9	5.3	23.5	8.3
Source: From Thomas E. Andreoli et al., *Membrane Physiology* , 2nd ed. (1987), Table I, chapter 27.						

1. Phospholipids

Phospholipids are the major components of cell membranes. The main role of phospholipids in living organism is that they make up the cell membrane. (Figure 15) [249]. Phospholipids are composed of a polar head (glycerol, phosphate group and organic molecules such as choline, serine, glycerol, inositol or ethanolamine.) and two hydrophobic hydrocarbon tails. The tails are usually fatty acids, and they may differ in length (they normally contain between 14 and 24 carbon atoms). One tail usually has one or more cis-double bonds (unsaturated), while the other tail does not (saturated). For example, AA is a polyunsaturated fatty acid present in the phospholipids of membranes of the body's cells. Fatty acids are important sources of fuel because, when metabolized, they give large quantities of ATP [250].

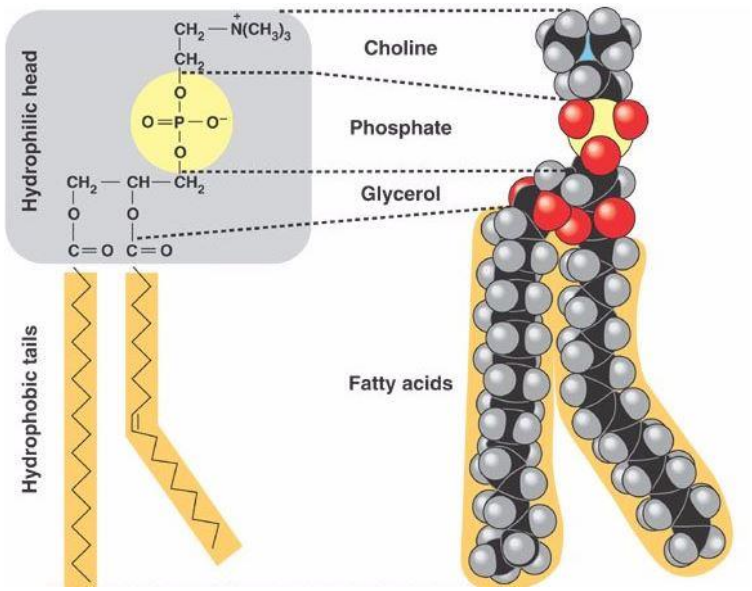

Figure 15: Example of the structure of a phospholipid, the phosphatidylcholine

2. Glycolipids

Glycolipids are lipids with a carbohydrate attached by a glycosidic bond. The simplest glycolipid, called a cerebroside, contains a single sugar residue, either glucose or galactose [251]. They are very abundant in the photosynthetic membranes of algae and plants while we find very rarely these fats in the animal world. They are found exclusively on the outer surface of the cell

membrane, their role is to provide energy and also to act as markers for cellular recognition and cell-to-cell communication (Figure 16) [252].

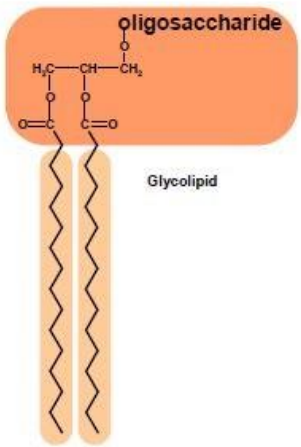

Figure 16: Structure of Glycolipid

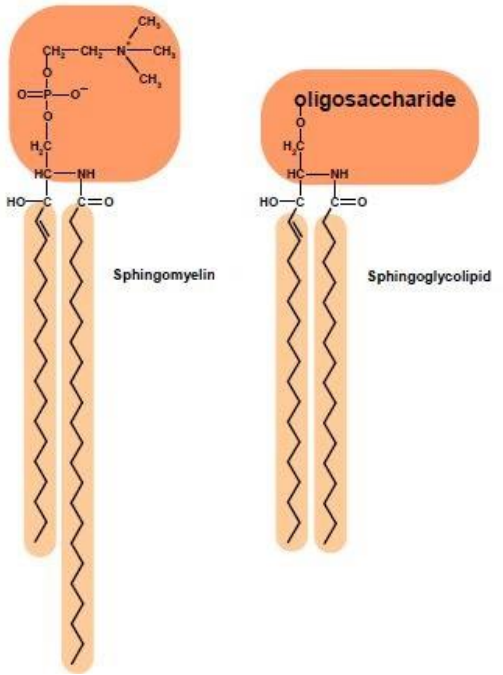

Figure 17: Structure of sphingolipids

3. Sphingolipids

Sphingolipids have a common lipid-based, known as ceramide composed of a long amino alcohol chain (2-amino-1,3-dihydroxy-4-octadecene whose trivial name is sphingosine) (Figure 17). The particularity of this lipid class is to have both hydroxyl and amide groupwhich can be both donor and acceptor of hydrogen bonds, and a carboxyl group which can be hydrogen bond acceptor. These compounds have a structural function in the lipid membranes but also play essential roles in signal transmission, cell recognition and as part of the immune system [248, 253]. In recent years, it has become evident that sphingolipids are involved in the pathophysiology of many diseases including diabetes, cancers, Alzheimer and diseases of the cardiovascular and respiratory systems [251, 254].

4. Sterols

Sterols are a family of lipid derivatives of a sterol nucleus which is made out of alcohol and steroid. They are vital components of all eukaryotic cells and are different depending on the organisms. They occur naturally in plants, animals and fungi. The three families of sterols are illustrated in Figure 18 by their main representatives. Their functions include controlling membrane fluidity and permeability. In some plants, sterols are involved in cell proliferation, signal transduction and modulate the activity of some membrane bound enzymes. The most familiar type of animal sterol is cholesterol [247].

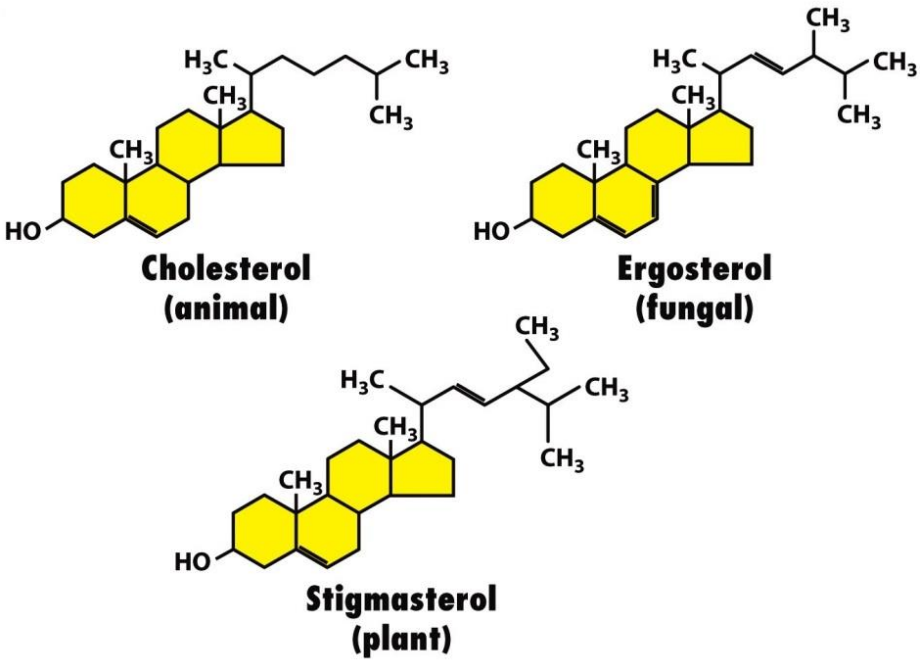

Figure 18: Structure of main sterols

Cholesterol and oxysterols:

The human liver synthesizes about 80% cholesterol and the other 20% comes from daily diet. Cholesterol has a unique structure composed of four linked hydrocarbon rings with hydrocarbon tail linked to the other end to a hydroxyl group [255].

Cholesterol is a key regulator of cell membrane integrity and fluidity. It inserts itself into the bilayers perpendicular to the membrane plane. The hydroxyl group makes hydrogen bonds

with the carbonyl oxygen of phospholipid and sphingolipid head groups while the hydrocarbon tail positions itself in the non-polar region of the bilayer [256]. Small amount of cholesterol may also be found on the membrane of some other organelles, such as the mitochondria and the endoplasmic reticulum. Cholesterol cannot dissolve in the blood. It has to be transported within the cells by carriers called lipoproteins. Low-density lipoprotein (LDL) and very low-density lipoprotein (VLDL) are known as the "bad" cholesterols because they can build up on the walls of the arteries and contributes to plaque formation while high-density lipoprotein (HDL) is known as "good" cholesterol as it helps carry LDL cholesterol away from the arteries and back to the liver,

Cholesterol is vital to all animals; it serves as a cofactor for signaling molecules and a precursor for the biosynthesis of steroid hormones, including vitamin D and the sex hormones testosterone, estrogen and cortisone. It also plays an important role in assisting the liver in the manufacture of bile acids, which is essential for digestion and absorption of fat soluble vitamins such as vitamin A, D, E and K [257]. Cholesterol also plays an essential role in our nervous system. It promotes our learning ability and memory. Actually, one of the reasons that sleep is beneficial to our learning and memory is because it enables our brain to synthesize more cholesterol. The absence of cholesterol may result in loss of memory and difficulty in focusing [258, 259]. On the other hand, high cholesterol level is linked to an elevated risk of cardiovascular disease, which involves coronary heart disease, stroke, and peripheral vascular disease [260-262]. High cholesterol has also been associated with diabetes and high blood pressure [263, 264].

Oxysterols are structurally similar to cholesterol, but with one or more additional oxygen containing functional groups (such as alcohol, carbonyl or epoxide groups), they are intermediates or even end products in cholesterol excretion pathways. Because they can pass cell membranes and the blood brain barrier at a faster rate than cholesterol itself, they are also important as transport forms of cholesterol. The wide diversity of oxysterols implicated in human health and disease vary in their origin, either enzymatic or non-enzymatic (Figure 19), their effects and functions. Some are known to be damaging since they are involved in apoptosis, necrosis, inflammation, immunosuppression, and development of atherosclerosis and Alzheimer disease [265-268], whereas others may play essential physiological roles as intermediates in bile

acid synthesis, in sterol transport between tissues and in the regulation of cholesterol homeostasis and gene expression. Under normal conditions, oxysterols involved in these processes are retained at very low and controlled levels, usually in the presence of a large excess of cholesterol (10^3 fold). Relatively high levels of oxysterols are present in some food, particularly cholesterol-rich foods such as meat, eggs and dairy products. These are probably produced non-enzymatically during cooking, processing and storage [269, 270].

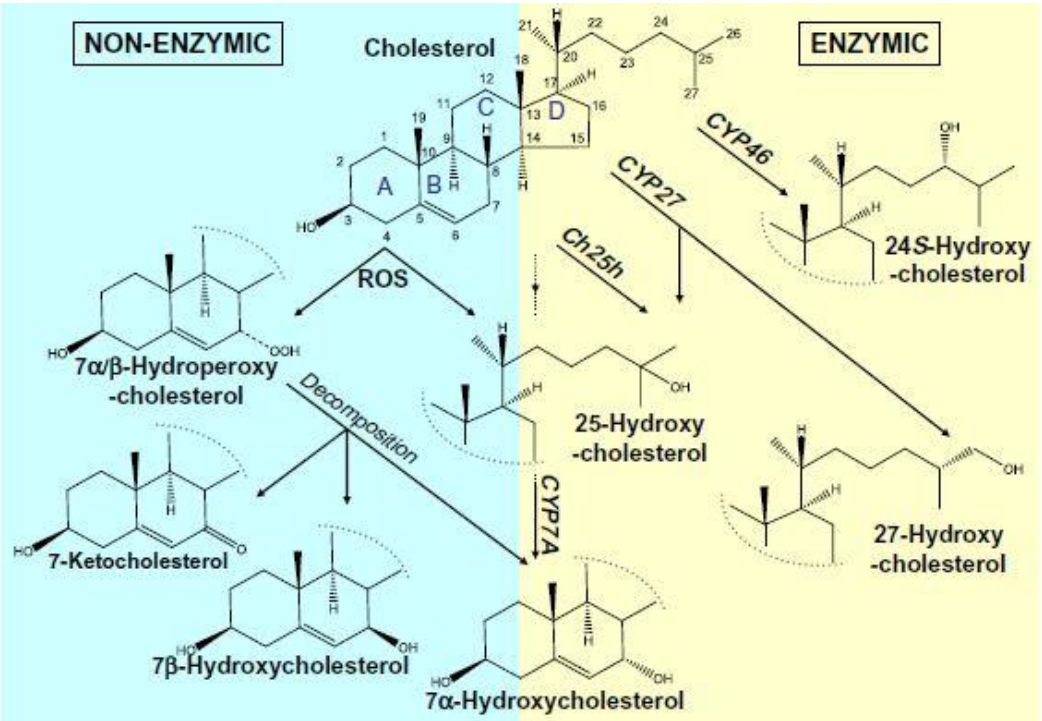

Figure 19: Structures and sources of selected oxysterols

(According to Jessup [270])

VIII. Lipid rafts

Lipid rafts (LRs) are distinct, dynamic, detergent-resistant cell membrane microdomains highly enriched in cholesterol and sphingolipids and harbor different assortment of proteins (Figure 20) [271]. It has been reported that LRs contain 3 to 5 fold the amount of cholesterol found in the surrounding bilayer. Also, LRs are enriched in sphingolipids such as sphingomyelin, which is typically raised by 50% compared to the plasma membrane [272]. LRs are more ordered and tightly packed than the surrounding bilayer, but float freely in the membrane bilayer. In fact, it has been demonstrated that tight packing between sterols and sphingolipids is the driving force for raft formation [273]. Furthermore, cholesterol exerts a

stabilizing role in LRs by filling the void space between sphingolipids and making hydrogen bonds with them [274, 275]. Even if LRs are more common in plasma membrane, they have also been shown in other parts of the cell, such as Golgi and lysosomes.

These specialized membrane microdomains play different vital roles such as organizing centers for the assembly of signaling molecules, influencing membrane fluidity and membrane protein trafficking, and regulating neurotransmission and receptor trafficking [276, 277]. On the other hand, researchers are started to link LRs with various diseases, including AIDS, Alzheimer's, anthrax, and atherosclerosis [274, 278, 279].

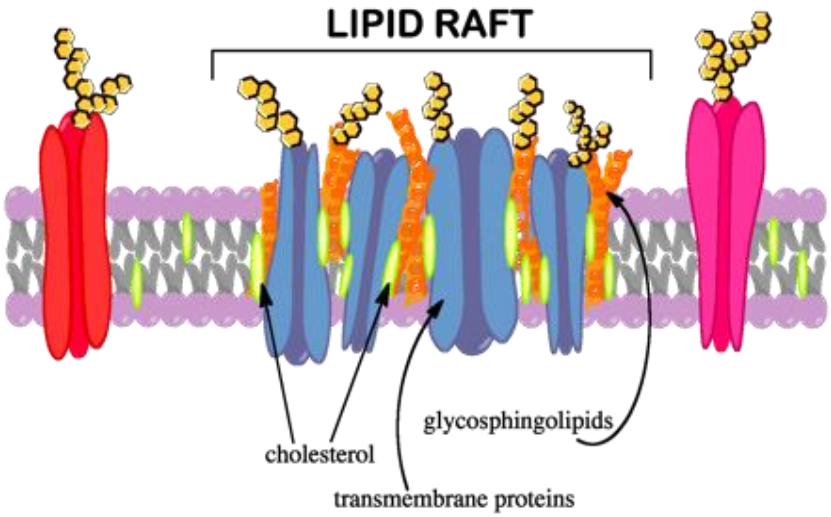

Figure 20: Scheme of lipid rafts

Lipid rafts are cholesterol and sphingolipid rich domains of plasma membrane where is localized a variety of signaling and transport proteins.

IX. NADPH oxidase and lipids

Regulation of the phagocyte NADPH oxidase is not fully understood. Lipids are one of the important modulators of this enzyme complex, through protein-lipid interactions, activation by arachidonic acid and the localization of the NADPH oxidase in lipid rafts.

The role of membrane lipids in oxidase assembly has been widely studied in the last decades [42, 85, 280]. Phosphoinositides (PI) are considered as important regulators of NADPH oxidase activation. They serve as sites for specific localization of cytosolic proteins [281]. It has been shown that direct or indirect interactions of PI with $p40^{phox}$ and $p47^{phox}$ constitute an

essential mechanism to orchestrate the assembly of the cytoplasmic components at the phagosomal membrane [282, 283]. These two proteins contain a lipid binding domain, a PX domain which binds to PI with a strong specificity. The PX domain of $p40^{phox}$ interacts selectively with phosphatidyl-inositol 3-phosphate, (PI(3)P) [152, 284], while the PX domain of $p47^{phox}$ preferentially recognizes phosphatidylinositol 3,4-disphosphate (PI(3,4)P2) [121, 152, 285]. The fixation of $p47^{phox}$ to the lipids is crucial for its translocation and for the production of superoxide anions [123]. Fixation to anionic phospholipids (phosphatidylserine and phosphatidic acid) or membrane phosphoinositides of $p40^{phox}$ and $p47^{phox}$ stabilizes their connections with the Cyt b_{558} [286]. Furthermore, the polybasic C-terminal domain of Rac develops links with anionic phospholipids which is also vital for NADPH functionality [287].

Activation of phospholipase A_2 (PLA_2) seems to be important for the activity of NADPH oxidase [288], but its role is not yet fully clarified. PLA_2 may be translocated to the membrane and catalyze the production of AA in the stimulated human neutrophils [288-290]. As said in paragraph IV, studies in human neutrophil suggest that AA affects the N-terminal domain of $gp91^{phox}$ by inducing conformational changes [223]. Other studies realized in cell free system, report that AA promotes conformational changes in $p47^{phox}$ and $p67^{phox}$ necessary for the activation of the NADPH oxidase [124, 291].

Interestingly, NADPH oxidases have been found in LR. Cytoplasmic proteins are efficiently recruited to the raft-associated Cyt b_{558} upon activation to reconstitute the active complex [292]. Moreover, distribution and regulation of NADPH oxidase in LRs were reported in murine microglial cells, bovine aortic endothelial and coronary arterial endothelial cells and in human neutrophils[293-297]. In particular, it has been demonstrated that NADPH oxidase was assembled and activated in LR of neutrophils, producing $O_2^{\bullet -}$, causing respiratory bursts and killing bacteria [292, 298].

The preincubation of cells with methyl-β-cyclodextrin (MβCD) for cholesterol depletion leads to the breakdown of LRs as it suppresses the glue effect of cholesterol on sphingolipids [299, 300]. In addition to that, removal of raft-cholesterol leads to dissociation of most proteins from the rafts, rendering them nonfunctional [274].

Pedruzzi et al. showed that 7-ketocholesterol induces oxidative stress and/or apoptotic events in human aortic smooth muscle cells (SMCs). They observed that 7-ketocholesterol

induces ROS production by upregulation of Nox-4 specifically [301]. It was also demonstrated that 7-ketocholesterol induce activation of NADPH oxidase by stimulate translocation of $p47^{phox}$ from the cytosol to the cell's plasma membrane, forming an active NADPH-oxidase complex [302].

X. Nanoparticles

In the last decades Nanoparticles (NPs) have been widely used however relatively little is known about the interaction of nanoscale objects with biomolecules. In this work we aimed to study the enzymatic behavior of NADPH oxidase in the presence of different NPs.

1. Generalities

NPs are objects with at least one of their three dimensions in the range of 1 to 100 nanometers. NPs generally possess different properties compared to the fine particles (FPs) of the same composition. NPs have a greater surface area per weight than FPs which makes them more reactive [303]. Their bioactivities are different from that of the fine size analogue due to quite different surface properties from the interior states, such as energy levels, electronic structure, and reactivity. Nanotechnology is one of the key technologies of the current decades which responds to a wide variety of novel applications in domestic, industrial and biomedical fields [304]. Use of nanotechnology has known exponential growth in the areas of health care, consumer products such as clothes and electronics. This is attributed to their unique chemical, mechanical, optical, magnetic, and biological properties [305, 306].

The particle size of nanomaterials is small enough to enter almost in all areas of living bodies, including cells and organelles; therefore, nanomaterials are convenient for both *in vivo* biomedical research and applications. The use of materials in nanoscale gives freedom to adjust essential properties such as solubility, diffusivity, blood circulation half-life, drug release characteristics, and immunogenicity. In the last two decades, a number of nanoparticle-based therapeutic and diagnostic agents have been improved for the treatment of cancer, diabetes, pain, asthma, allergy and infections. [307-309].

Many advantages of nanoparticle-based drug delivery have been realized. It enhances the solubility of poorly water-soluble drugs, extends the half-life of drug, releases drugs at a sustained rate or in an environmentally responsive way and thus reduces the frequency of

administration, transports drugs in a target manner to decrease systemic side effects, and delivers two or more drugs simultaneously for combination therapy to produce a synergistic effect and suppress drug resistance [310]. As a result, a few nanoparticle-based therapeutic products have been presented into the pharmaceutical market, and numerous other products are currently under clinical investigation [308, 311]. For example, Doxil® was the first liposomal drug formulation approved by the Food and Drug Administration (FDA) for the treatment of AIDS associated with Kaposi's sarcoma. Doxil® has prolonged doxorubicin (anticancer drug) circulation half-life and enhanced drug deposition in the tumor tissue [312]. For diagnostic applications, nanoparticles permit detection at the molecular scale; they help detect abnormalities such as fragments of viruses, precancerous cells, and disease markers that cannot be identified with traditional diagnostics [313]. For example, organic and inorganic nanoparticles were suggested as intravascular probes for diagnostics. They can be used for molecular imaging, cell or DNA labeling, immunohistochemistry, and tumor vessel imaging [314, 315]. Nanoparticle-based imaging contrast agents have also been reported to improve the sensitivity and specificity of magnetic resonance imaging [316]. For example, the intense scattering of gold nanoparticles makes them promising probes for biological imaging applications and cancer detection [317]

Nanotechnology offers a new approach in the fight against cancer, high surface to volume ratio permitting many functional groups to be attached to a nanoparticle, which can seek out and destruct the diseased cells. Some nanomaterials can absorb the laser light and transfer it into localized heat energy. They are being used for cancer cell destruction (photothermal therapy) in order to replace surgery or chemotherapy [318-320]. Recently, a combination of radiotherapy with NPs has been suggested as a new alternative to improve protocols of cancer treatment [321, 322]. One of the most promising techniques in cancer therapy is hadron therapy (or proton therapy), where fast carbon (or proton) ions are used as an alternative to hard x-rays [323].The treatment by fast ions opens new perspectives for an efficient and less traumatic eradication of cancers. Fast ion irradiation in presence of high-Z NPs was shown as a very promising method for future advances in cancer therapy [321].

2. Titanium dioxide nanoparticles

Metal oxide NPs, such as TiO_2, ZnO, CeO_2 and Al_2O_3 NPs are now being produced in large quantities and commercialized for several purposes. Among these, TiO_2 NPs are utilized in many commercial products [324]. TiO_2 is chemically inert, semiconducting material that also possesses photocatalytic activity in the presence of light with energy equal to or higher than its band-gap energy. Crystalline TiO_2 exists naturally in four polymorphs: anatase (tetragonal), brookite (orthorhombic), rutile (tetragonal), and TiO2 (B) (monoclinic) with anatase being more chemically reactive [325].

TiO_2 NPs are produced abundantly because of their high stability and low cost, for example, they are present in papers, pigments, inks, cosmetics, pharmaceutical additives, toothpastes, plastics industry, optics and electronics. Over the last two decades, environmental and energy applications of TiO_2 NPs including photocatalytic treatment of wastewater, pesticide degradation and water splitting to produce hydrogen have been widely investigated [326, 327]. Furthermore, they are approved as a food and pharmaceutical additive (E171). In the United States it is included in the Food and Drug Administration (FDA) Inactive Ingredients Guide for dental paste, oral capsules, suspensions, tablets and dermal preparations [328]. In nanomedicine, TiO_2 NPs are under investigation as useful tools in advanced imaging and nanotherapy [329]. TiO_2 NPs are being explored in cancer diagnosis and bring benefits in cancer therapy by absorbing near infrared light [330], and thus are considered as potential photosensitizers for photodynamic therapy [331]. Very promising is the finding that photo-activated nanostructured TiO_2 exhibited selective cytotoxicity against breast epithelial cancer cells [332]. Furthermore, the physical properties of TiO_2 NPs make them interesting products for a use in various skin care and cosmetic products such as sunscreens [333]. TiO_2 NPs are under investigation as novel treatments for acne vulgaris, atopic dermatitis, hyperpigmented skin lesions, and other nondermatologic diseases [334, 335].

Despite their presence in everyday life, modest research effort has been made in studying their potential adverse effects on living bodies and environment. TiO_2 NPs can be absorbed into the human body by inhalation, ingestion, and dermal penetration, then they can be distributed to vital organs, including lymph, brain, lung, liver, and kidney [336-338]. TiO_2 NPs can enter not only in cells, but also mitochondria and nuclei [339]. Oxidative stress is thought to be a key

mechanism responsible for adverse biological effects exerted by NPs. Most work to date has reported that TiO_2 NPs toxicity is strongly related to ROS and oxidative products generation (i.e., lipid peroxidation), as well as the depletion of cellular antioxidants.[340-344]. TiO_2 NP-mediated ROS generation has been reported to orchestrate a series of pathological events leading to genotoxicity, immunotoxicity, neurotoxicity and carcinogenicity [328, 345]. The International Agency for Research on Cancer (IARC), therefore, has classified TiO_2 as a Group 2B carcinogen (possibly carcinogenic to humans) [346]. Pulmonary studies support the carcinogenicity of TiO_2 NPs in intratracheal and inhalation exposure. However, exposure modes such as intragastric or dermal exposure do not show a carcinogenic consequence [345]. The precise mechanisms of TiO_2 NPs-induced carcinogenesis are not clear. Limited data indicate that ROS production, oxidative stress, as well as, cell signaling of carcinogenic genes alterations may play an important role in the etiology of their carcinogenesis.at relatively high doses. Neutrophils are quickly recruited to titanium implantation areas [347]. Moreover, NPs has been shown to activate immune cells including macrophages and neutrophils that contribute to ROS production [348, 349].

3. Platinum nanoparticles

Platinum (Pt) is one of the rarest and most expensive metals. Noble metal NPs and, in particular, Pt NPs at the oxidation state 0 have shown to be efficient catalysts for chemical reactions such as hydrogenation, hydration and oxidation. Pt NPs are utilized in a number of industrial applications, including catalysis, plastics, nanofibers, textiles, cosmetics and dietary supplements [350].

In medicine, Rosenberg et al. published a report in 1965 on the inhibition of Escherichia coli division by platinum electrolysis products [351]. Later, Rosenberg et al. revealed that cisplatin is highly effective against rat sarcomas [352]. As a novel aspect, recent reports recommended the use of Pt NPs in cancer therapies through different strategies [353]. It was, for example, demonstrated that Pt NPs cause significant DNA strand breaks in human colon carcinoma cells (HT29) [354]. Furthermore, it was shown that Pt NPs in combination with hadron therapy lead to an enhancement of strongly lethal DNA damage caused by double-strand breaks. The mechanism causing the DNA damage might be attributed to the auto-amplification of the radiation effect by NPs that are directly associated with the DNA. It would result in the

generation of hydroxyl radicals leading to DNA strand breaks [321]. These effects could be mediated by the release of Pt^{2+} ions from the NPs due to the generation of H_2O_2 [355, 356]. However, other reports have shown that the strand-breaking properties of Pt NPs were not associated with the induction of oxidative stress, since neither a formation of ROS nor an oxidative DNA damage were observed [356]. Additionally, there is evidence that Pt NPs are effective in the photothermal treatment of neuro cancer cells [357]. Clearly the use of Pt NPs is beneficial in cancer therapy but the mechanism is not fully understood.

Pt NPs have also been demonstrated to possess antioxidative properties and inhibit pulmonary inflammation caused by exposure to cigarette smoke [358-361]**.** Other contradictory reports suggested that Pt NPs can induce inflammation, hepatotoxicity, acute and chronic nephrotoxicity in mice [362-364]. Taken together, these data indicate that the biological effects of Pt NPs remain poorly understood and a full understanding of the toxic and beneficial effects induced by Pt NPs is fundamental.

Objectives

"Goals are the fuel in the furnace of achievement."

Brian Tracy

During these three years of my PhD work, I have worked on NADPH oxidase enzyme, an enzyme presents in a wide variety of cells and involved in the immune defense but also in certain pathological diseases like cardiovascular disease. I attempted to study the influence of different parameters; lipids and nanoparticles on phagocyte NADPH oxidase (NOX2).

My research work was divided into four parts:

The first part was to purify, characterize and optimize the conditions for trimera in order to validate its use for the next experiments. For simplification we replaced the cytosolic proteins with the trimera. The challenge of this part of work was to get trimera in sufficient quantity and quality. Then, we wanted to confirm that trimera is functionally comparable to the separated cytosolic proteins and to determine eventual structural changes of trimera when activated.

In the second part, we aimed to better understand how the activity of NADPH oxidase can be regulated by some lipids. We first examined the role of natural cholesterol present in neutrophils on NADPH oxidase activity. It was also important to determine whether cholesterol and oxysterol themselves can have activator effect on NADPH oxidase. We were interested in the influence of cholesterol and oxysterols on the functionality of the enzyme. We also tried to understand the mechanism of action and the target sites of cholesterol in NADPH oxidase and finally the structural effects of cholesterol on NADPH oxidase.

The third part focused on understanding the enzymatic behavior of NADPH oxidase in the presence of TiO_2 NPs and to check if NADPH oxidase could be a pathway involved in ROS generation by TiO_2 NPs as it has been suggested. We were interested on the effect of TiO_2 NPs on the function of NADPH oxidase in cell free system and in human neutrophils but also their effects on proteins conformations.

Finally, in the fourth part, we initiated the study of Pt NPs on NADPH oxidase to demonstrate if they are involved in any oxidative stress toxicity. We were interested to know if Pt-NPs alone can provoke the production of ROS via NADPH oxidase and if they can influence AA-induced NADPH oxidase activity. Since the combination of NPs and radiation was suggested as a promising therapy for cancer, we were particularly interested to study the consequences of Pt-NPs and NADPH oxidase proteins irradiation on the functionality of the enzyme.

Materials & Methods

"Great scientific contributions have been techniques."

B. F. Skinner

I. Preparation of proteins

In this work, the functional study of NADPH oxidase complex has been performed *in vitro*. This requires the assembly of the different soluble and membranous proteins of the enzyme complex. To do this, the different proteins that constitute the complex must be produced and purified separately in advance. In this chapter the purification protocols of every cytosolic proteins and membrane fraction will be described.

1. Preparation of membrane fractions

The neutrophils were prepared from human blood from healthy donors (ESF Paris, France) as described in [365]. 500 ml of blood are gently mixed with an equal volume of saline (NaCl 0.9%) containing 2% dextran, in a sterile polypropylene cylinder of 1 L. The mixture was left until having two separated phases, the red blood cells precipitate largely and the lighter upper part is removed and centrifuged 8 min, at 400 g at room temperature. PBS was added to the pellets and then deposited on 0.5 volume Ficoll in order to separate lymphocytes and monocytes from neutrophil. 30 min centrifugation at 400 g allowed obtaining a pellet containing PMNs and some red blood cells. The erythrocytes are then lysed by osmotic shock by addition of 12 ml of cold water and stopped after 40 seconds by addition of 4 ml of cold KCl 0.6M. The volume is brought to 50 ml by addition of cold PBS in order to put the cells in appropriate buffer. The red cells are eliminated after their lysis by centrifugation 8 min, at 400 g and 4 °C. For activity measurement on neutrophils, the cells are then resuspended in Hank's buffer. For membrane preparation, the pellet is resuspended in a lysis buffer (10 ml PBS pH 7.4 supplemented with 340 mM sucrose, 7 mM magnesium sulphate, 1 mM PMSF, 200 µM leupeptin). The solution is usually at around 10^8 cells /mL. Neutrophils are broken by a series of six sonications in the 50% pulse mode at power pulses (3) in an ice-cooled beaker during 10 s with interval of 1 min between the sonications (sonicator XL, Misonixinc.), followed by a centrifugation during 12 min, at 10,000 g, at 6 °C to separate the unbroken cells and debris (pellet) from the membranes and the soluble proteins (supernatant). The separation of the neutrophil membrane fractions from the cytosol is done by a second centrifugation of the supernatant 1h30, at 200 000 g, at 6 °C. The membrane fractions are resuspended in few milliliters of lysis buffer, aliquoted and stored at -80

°C. Routinely 10^9 cells were purified from 0.5 L of blood and 3 ml of membrane at 4 mg/ml of total proteins were extracted from these cells.

The concentration of flavocytochrome b_{558} in membrane fractions (MF) is calculated from the absorption spectrum of the solution. The element which absorbs the most in this protein is the heme group. The absorbance spectra of a solution containing 50 µL of MF diluted 4 times with PBS (total volume 200 µL) is measured between 350 and 600 nm. The reduced form is obtained by adding 1 mg of sodium dithionite in the measure cuvette, the reference cuvette containing the oxidized form. Cyt b_{558} concentration is obtained by measuring the absorbance of the Soret band at 427 *minus* 411 nm of the difference spectrum (reduced *minus* oxidized) using an extinction coefficient of 200 $mM^{-1}.cm^{-1}$ [366] (Figure 21).

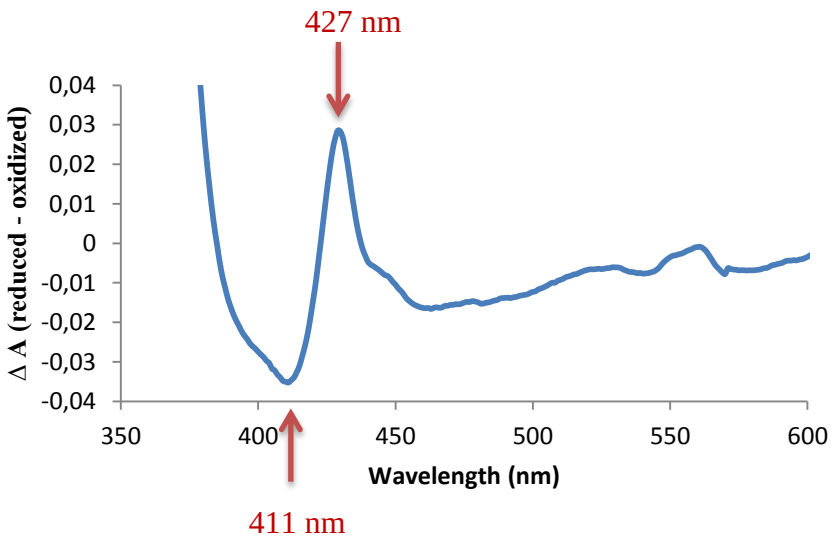

Figure 21: Absorption difference spectrum of Cyt b_{558}.

Absorption difference spectrum (reduced *minus* oxidized) of membrane fraction of neutrophils. 50 µL of the MF are diluted in 150 µL of PBS buffer.

2. Expression and purification of cytosolic proteins

i. Culture of bacteria expressing cytosolic proteins in *E.coli*

The protocols of expression and purification of recombinant cytosolic proteins have been previously established in the laboratory [367]. The plasmids coding for the human cytosolic

proteins, pET15b-His p67^{phox}, pET15b-His p47^{phox} and pGEX2T-GST Rac1Q61L were provided by Dr. M.C. Dagher (Laboratoire TheREx, TIMC-IMAG, Grenoble, France). The GTP like form of Rac1which is a constitutively active form of Rac was obtained by the mutation Q61L and was used in all the experiments presented in this work. The plasmid of the trimera (p47^{phox} aa 1-286, p67^{phox} aa 1-212, and RacQ61L full length) was a generous gift from Pr. E. Pick. All the plasmids were checked for their sequence and used for transformation of *Escherichia coli BL21-(DE)3*. A DNA sequence coding either for a histidine tag (His-tag) or Glutathione-S-Transferase tag (GST-tag) is present at the N-terminal of the genes for facilitating protein purification by chromatography affinity.

A relatively standard culture protocol was used for the majority of the strains. A stock culture of *E. coli* (glycerated, stored at – 80 °C) expressing the protein of interest is used to inoculate a Petri dish of Luria Bertani (LB) medium in presence of the appropriate antibiotics (ampicillin (Rac and p47^{phox}), ampicillin and chloramphenicol (p67^{phox}), kanamycin and chloramphenicol (trimera)). The Petri dishes are incubated at 37 °C for 16 h. A colony is then cultured in 60 mL of LB medium supplemented with the suitable antibiotic (50 mg/L of ampicillin (Rac and p47^{phox}), 50 mg/L of ampicillin and 34 mg/L of chloramphenicol (p67^{phox}), 50 mg/L of kanamycin and 34 mg/L of chloramphenicol (trimera)). The culture is then incubated at 37 °C under stirring for 16 h. 20 mL of this culture are added to 1.5 L of Terrific Broth medium (TB) supplemented with the relevant antibiotic in the same way as the LB medium. The flask is incubated in shaking condition at 37 °C until it reaches an absorbance of 0.9 at 600 nm, then 0.5 mM IPTG is added to induce the synthesis of protein and the culture is incubated overnight at 30 °C. The culture is pelleted and placed in the freezer at -20 °C until use.

ii. Extraction of proteins

The bacterial pellet (18-25 g) containing the proteins obtained previously, is dissolved in 20-30 mL of solubilizing buffer containing 50 mM HEPES, 200 mM NaCl and 1 mM ethylenediaminetetraacetic acid (EDTA) (pH 7.5) to which is added 1 mg of DNase (DNA hydrolysis), 1 mM phenylmethylsulfonyl fluoride (PMSF, serine protease inhibitor), 1 mM DTT (reduction of disulfide bonds) and 1 mM benzamidine (serine protease inhibitor). The mixture is homogenized using a manual homogenizer, then sonicated to break the membranes and to release the contents of the bacteria (cytosol) including soluble proteins. The sonication is carried out 4

times for 2 minutes in a 50% pulse mood at power pulses (6) in an ice- cooled beaker with pauses of 2 minutes to avoid overheating. The bacterial lysate is centrifuged 1h30, at 160 000 g, at 6 °C. Cell debris and membranes are found in the pellet and the proteins of interest are in the supernatant (35 mL). The cleared cell-free supernatant is filtered to remove all traces of debris and bacteria and diluted twice by the addition of the equilibration buffer of the chromatography column that will be used.

Liquid chromatography columns are linked to a system "AKTA prime" (GE Healthcare) which permits controlling the chromatography in automatic way. The purifications are carried out in a cold room with this fully automated system comprising a pump, valves, mixers, a UV detector and a fraction collector. All the cytosolic NADPH oxidase proteins are found to be preferred targets for proteases; several inhibitors such as leupeptin, glutamic acid, arginine or a cocktail of inhibitors have been tested. The most effective one is found to be PMSF (specific for serine proteases). The best way to protect the proteins is to maintain the solutions at temperatures below 5 °C and to perform the purification as quickly as possible. We have chosen to purify the proteins mainly in two steps, an ion exchange chromatography which allows the separation of proteins from a large number of other molecules including DNA, then an affinity chromatography is performed since all the proteins are tagged with either a histidine or a GST tag.

iii. Purification of $p47^{phox}$

Step 1: Chromatography on sulfopropyl sepharose resin (SP-Sepharose)

Ion exchange chromatography separates proteins based on their net charge. The separation is based on the formation of ionic bonds between the charged groups of proteins and an ion-exchange gel carrying the opposite charge (Figure 22).

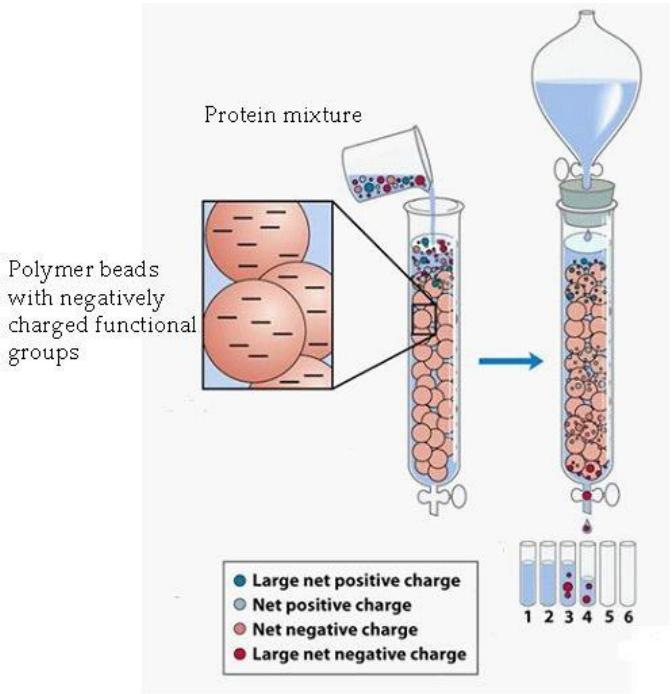

Figure 22: Separation of proteins of various charges by ion exchange chromatography

The isoelectric point of $p47^{phox}$ is 9.2 so a cation exchange resin such as SP-Sepharose (GE Healthcare) which contains a resin negatively charged at pH 7.5, can be used. This column allows a good separation because large majority of the cytosolic proteins are negatively charged at this pH. The column is equilibrated with 200 mL of equilibration buffer (20 mM HEPES, 100 mM NaCl at pH 7.5 and 1 mM PMSF). The column is then loaded with the sample. The elimination of negatively charged proteins, DNA and other molecules is done by washing the column with 150 mL of equilibration buffer. $p47^{phox}$ is then eluted by passing 100 mL of equilibration buffer supplemented with 400 mM NaCl. The column is then washed with 100 mL of buffer containing a high concentration of NaCl (20 mM HEPES, 1 M NaCl at pH 7.5).

Step 2: Chromatography on affinity column:

Affinity chromatography is based on a highly specific interaction such as that between antigen and antibody, enzyme and substrate, or receptor and ligand (Figure 23). As mentioned,

p47^{phox} that I used has a histidine tag. A nickel-sepharose column (GE Healthcare) has been used to purify the proteins.

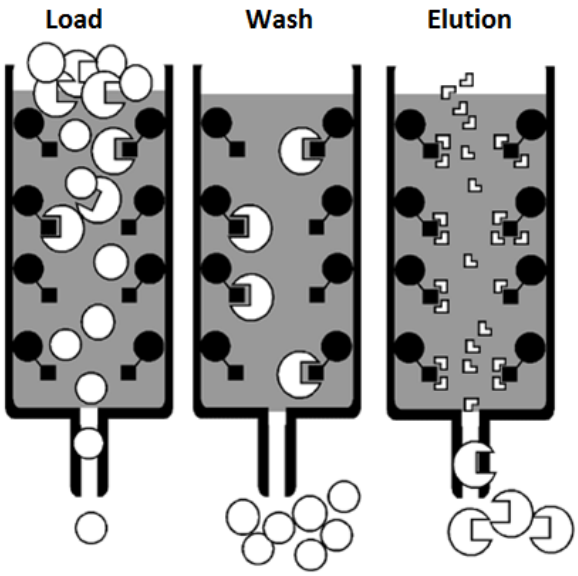

Figure 23: Principle of proteins separation by affinity chromatography

The column is equilibrated with 100 mL of equilibration buffer (0.7 M NaCl, 30 NaH_2PO_4, 30 mM imidazole, pH 7.5) then the sample (diluted twice with the equilibration buffer + 1mM PMSF) is loaded for 1.5 hour. The column is then washed with 80 mL of washing buffer (0.1 M NaCl, 30 mM NaH_2PO_4, 10 mM imidazole, pH 7.5) also in the presence of 1 mM PMSF. The proteins are then eluted with the elution buffer (150 mM imidazole, 0.1 M NaCl, 30 mM NaH_2PO_4, pH 7.5), this high concentration of imidazole allows the elution of p47^{phox} protein. Once the proteins are eluted, they are dialyzed against the dialysis buffer (30 mM NaH_2PO_4, 100 mM NaCl, pH 7.5) in the cold room which allows removing small molecules such as imidazole and storing all the proteins in a buffer close to the one used for the experiments.

iv. Purification of p67^{phox} and Rac1Q61L

Step 1: Chromatography on an anion exchange column

The isoelectric points of p67^{phox} and Rac1Q61L are respectively 6.3 and 7.8. We chose to purify p67^{phox} on a quaternary amine sepharose resin (Q Sepharose, GE Healthcare) and on the SP sepharose for Rac1Q61L. In the case of Rac1Q61L, chromatography was performed at pH 7.0

which makes this protein predominantly in positively charged form. The protocol and the buffer applied to these columns are those described previously for $p47^{phox}$.

Step 2: Affinity chromatography

The second purification step is carried out on a nickel sepharose column for $p67^{phox}$ and on a glutathione sepharose column for Rac1Q61L. For the nickel sepharose column, the protocol is identical to the one used for $p47^{phox}$. Rac1Q61L bearing a GST tag it is purified on a glutathione sepharose column (GE Healthcare). The column is equilibrated with 100 mL of PBS. The sample is then diluted twice in this buffer and loaded on the column. Afterwards, it is washed with 100 mL of PBS buffer. Finally, the protein is eluted by passage of 50 mL of elution buffer (50 mM Tris-HCl, 10 mM reduced glutathione, pH 8.0). The sample is dialyzed against the dialysis buffer (30 mM NaH_2PO_4, 100 mM NaCl, pH 7.5) and stored at -80 °C.

v. Purification of trimera

Step 1: Affinity chromatography

The trimera is expressed as N-terminal His-tagged fusion protein. Thus it is purified in the same way than $p47^{phox}$ His-tag on a nickel sepharose column. The solution is applied to the nickel column after being diluted twice with buffer (0.5M NaCl, 30 mM Na_2HPO_4, 20 mM imidazole, pH 7.4) in the presence of 1 mM PMSF. The mixture is loaded for 1.5 hour so that the proteins of interest effectively cling to the nickel resin. Then the column is washed with the same buffer to remove unwanted bound proteins. The bound proteins are eluted from the resin with the elution buffer (0.1M NaCl, 30 mM Na_2HPO_4 and 300 mM imidazole, pH 7.4).

Step 2: Size exclusion chromatography

Exclusion gel-filtration chromatography is carried out to separate the proteins based upon their different sizes. Small proteins penetrate the pores of the gel particles and are retarded relative to the large proteins which do not penetrate it. The large proteins move faster through the column, they are less retarded than the small ones. Therefore, they come out first (Figure 24).

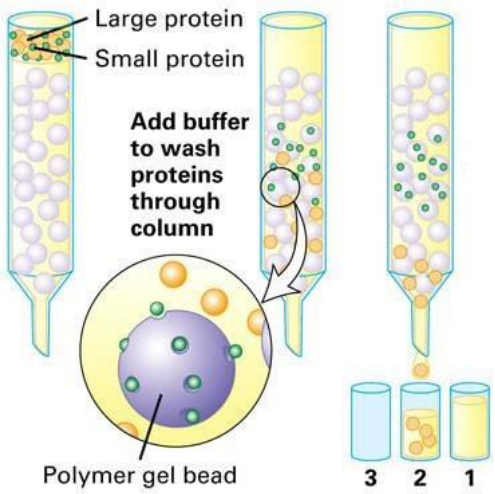

Figure 24: Separation of proteins of various sizes on a gel filtration column

The proteins of interest from the previous nickel sepharose column are injected in superdex 75 Hiload 16/60 column. This column allows the separation of proteins ranging in size from 3000 to 90000 Da. The protocol that we used is the following: The column is run at 4 °C with a flow rate of 0.5 ml/min and equilibrated with 600 mL buffer (30 mM Na_2HPO_4 pH 7.4). The proteins are eluted with the same phosphate buffer to which 1 mM PMSF is added. Then, all the fractions corresponding to the different peaks are deposited on SDS gel. The fractions containing the trimera are generally concentrated using VIVASPIN concentrators

II. Proteins analysis

1. Determination of proteins concentration

Proteins concentration was determined using two methods. Measuring the absorbance at 280 nm using the NanoDrop2000 spectrophotometer, (Thermo Scientific, France) provides a very fast and very cheap (2µl of protein solution) detection way of protein concentration from the extinction coefficient of the protein of interest (obtained by the ExPASy website-ProtParam tool). In the case of the trimera, the ε_{280} is 124 mM^{-1} cm^{-1}. This method is very useful to follow the evolution of the samples after different chromatography steps and dialysis. It also shows whether DNA is present or not in the solution by following the absorbance between 250 and 290 nm.

Since it is based on absorption measurements, it is relevant only for soluble proteins and if no other molecules absorbing at 280 nm are present.

The colorimetric assay by the bicinchoninic acid (BCA) is used for determining the total concentration of protein in a solution, in mg/ml. The BCA assay depends on two reactions. First, the peptide bonds in protein reduce Cu^{2+} to Cu^{+}. Next, bicinchoninic acid chelates with each Cu^{+} ion forming a purple-colored product that strongly absorbs light at a wavelength of 562 nm. The intensity of the color is proportional to the protein concentration in the sample. Bovine serum albumin (BSA) is used to perform a concentration range of 5 to 40 µg/ml that allows correlating the absorbance at 562 nm to the protein concentration. This protocol is the standard protocol provided by the manufacturer. This method has been used for the determination of the protein concentration of the membrane fraction of the neutrophils.

2. Evaluation of protein purification by SDS-PAGE

Gel electrophoresis separate proteins in function of their charge and/or size. One uses often SDS-PAGE (sodium dodecyl sulfate polyacrylamide gel electrophoresis) in which the native structure of proteins that are run within the gel is not maintained. The proteins are denatured with an anionic detergent, SDS (sodium dodecyl sulfate: CH3 $(CH2)_{11}OSO_3Na$) which binds in large amount on the surface of proteins, in particular on their hydrophobic portions while keeping their tertiary structure. The net charge of all the proteins is thus negative and proportional to their surface. The proteins then migrate according to their molecular weights (Figure 25).

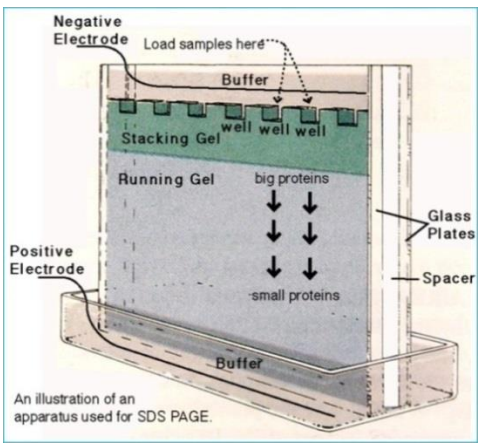

Figure 25: Schematic representation of the migration of SDS PAGE

The progress of the purity of the protein solutions obtained after each purification step is followed by the migration of aliquots of the peaks observed during the chromatography on SDS PAGE. We used a polyacrylamide gel (10% Bis Tris Nupage, Invitrogen) which allows good separation of the bands for proteins having a molecular weight between 20 and 150 kDa. The samples are prepared by mixing 10 µl of the sample with 10 µL of Laemmli SDS Buffer and 1µL of 2-Mercaptoethanol. The Dual Color (Biorad) is the molecular weight marker that was used. The prepared samples are placed in the wells and the migration is done for 45 minutes at 175 V. After migration, the gel is incubated in a fixation buffer (10% acetic acid, 20% ethanol) for 30 min. Afterwards, the fixation solution is replaced by a staining buffer (0.25% Coomassie blue, 7% acetic acid, 40% ethanol) and then by a washing buffer (10% ethanol and 7% acetic acid). The gel is photographed and recorded using a Syngene unit.

III. Functional study of NADPH oxidase proteins

1. Measurement of superoxide anion production rate

Absorption spectroscopy allows us to measure the activity of NADPH oxidase by determining the rate of superoxide anion production. In most of the experiments presented in my thesis, the measurements were done in cell free or *in vitro* system. The functional NADPH oxidase complex was reconstituted from membrane fractions of neutrophils containing the Cyt b_{558} and recombinant purified cytosolic proteins. None of the protein of the NADPH oxidase complex produces superoxide anion until the enzyme is assembled and activated. Therefore, it had been necessary to find a way to assemble all the components of the NADPH oxidase and activate them. This protocol was first proposed by [368]. In the reaction mixture, (3-5) nM Cyt *b558*, 470 nM $p67^{phox}$, 450 nM $p47^{phox}$ and 560 nM Rac or 200 nM trimera instead of the three separated subunits are incubated for 4 min at 25 °C in the presence of the optimal concentration of the activator which is AA. The reactional volume 0.5 mL was adjusted with the activity buffer (PBS, 10 mM $MgSO_4$, pH 7.5). After incubation, 50 µM of cyt *c* are added and the reaction is initiated by adding NADPH (250 µM).

The superoxide anions produced by Cyt *b558* (equation 1) are indirectly quantified thanks to their capacity to reduce cyt *c* (equation 6). The cyt c reduction is followed at 550 nm, the

wavelength at which the molar extinction coefficient of cyt *c* reduced minus oxidized is equal to 21 $mM^{-1}cm^{-1}$ [369].

$$NADPH + 2\,O_2 \longrightarrow NADP^+ + H^+ + 2\,O_2^{\bullet-} \qquad \textbf{Equation (1)}$$

$$cyt\ c\ Fe^{3+} + O_2^{\bullet-} \longrightarrow O_2 + cyt\ c\ Fe^{2+} \qquad \textbf{Equation (6)}$$

$$O_2^{\bullet-} + HO_2^{\bullet} + H^+ \longrightarrow O_2 + H_2O_2 \qquad \textbf{Equation (2)}$$

The reduction of cyt *c* was followed at 550 nm using a Thermo evolution 500 Spectrophotometer for 60 s. The initial slope of the curve is equal to the rate of superoxide anion formation. However, as cyt *c* may be reduced by other reducers than superoxide anion. The same experiment was repeated in the presence of 50 µg/ml superoxide dismutase (SOD). SOD transforms $O_2^{-\bullet}$ into H_2O_2 (equation 2) which is unable to reduce cyt *c*. Thus, a regular control of a true production of $O_2^{-\bullet}$ was done by the addition of SOD. An example of kinetics is given in Figure 26. The rates being given in mole of $O_2^{-\bullet}$ produced s^{-1} mole Cyt b_{558} $^{-1}$, they correspond to the turnover or specific activity of the enzyme.

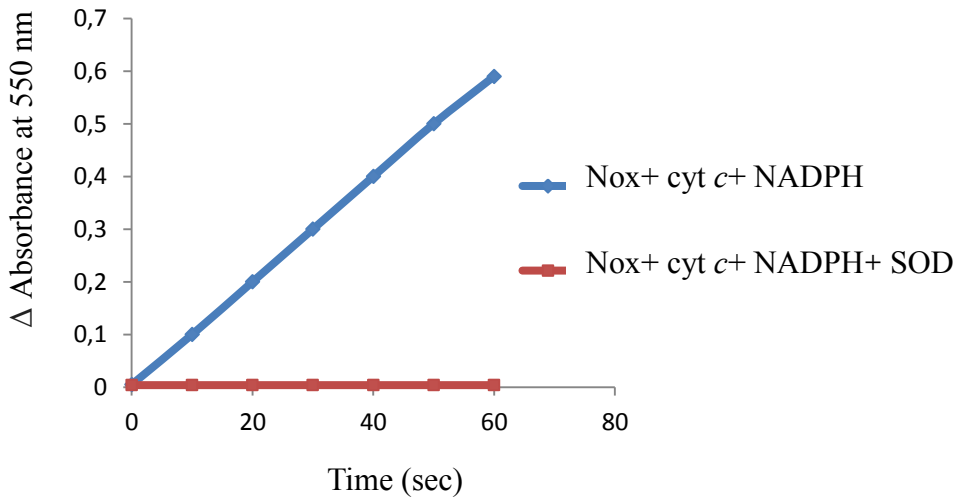

Figure 26: Example of kinetics of superoxide anion production

In a 0.5 mL cuvette containing buffer (PBS, 10 mM $MgSO_4$, pH 7.5), 3 nM Cyt b_{558} , 200 nM trimera are added. Then, the solution is mixed and 40 µM AA is added to activate complex. After incubation for 4 min at 25 °C, 50 µM of cyt *c* are added and the reaction is initiated by adding NADPH (250 µM). The zero time corresponds to the addition of the addition of NADPH. The rate is measured at 550 nm for 60 s. Control of $O_2^{-\bullet}$ is done by the addition of 50 µg/ml superoxide dismutase (SOD).

2. Determination of enzymatic parameters

The enzymatic parameters EC50 and V_{max} were calculated by non-linear least square fitting of the curves of superoxide rate of production vs. protein concentration using Michaelis-Menten equation 7.

$$v = \frac{v_{max}[P]}{EC50 + [P]} \qquad \textbf{Equation (7)}$$

Where [P] is the concentration of the considered protein. V_{max} represents the maximum rate of $O_2^{-\bullet}$ produced by NADPH oxidase, at maximum protein concentrations. EC50 is the protein concentration at which the reaction rate is half of V_{max} (Figure 27). Plotting and calculation were performed using Graph Pad Prism Version 6.

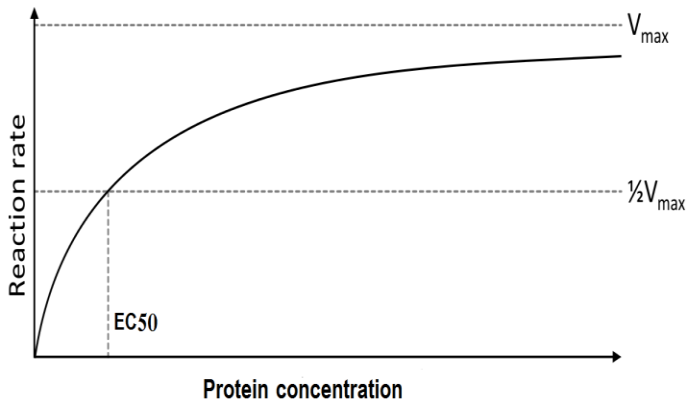

Figure 27: Michaelis–Menten curve for an enzyme reaction showing the relation between the protein concentration and reaction rate.

IV. Neutrophil cell activity measurement

Two cuvettes of 1 ml each contains 100 µM of cyt *c* in Hank's was incubated at 37 ° C for 2 min with 25 U /ml SOD in the reference cuvette. Then 10 µL of freshly isolated human neutrophil cell suspension at 10^8 cells/ ml was added to each cuvette. After another 2 min, 10 µL of PMA 166 µM (0.1 mg/ml in DMSO) was added to each cuvette. The reduction of cyt *c* was followed at 550 nm for 5 min. The more linear slope of the curve is equal to the rate of superoxide anion formation.

V. Structural study of NADPH oxidase proteins

1. Intrinsic fluorescence Assays

Fluorescence of protein is the sum of the fluorescence from individual aromatic residues. Most of the intrinsic fluorescence emissions of a protein are due to excitation of tryptophan residues, with some emissions due to tyrosine and phenylalanine. We used the sensitivity of the tryptophan fluorescence to the environment to probe the effect of molecules on the cytosolic proteins.

Steady-state fluorescence spectra were performed on Fluorolog3- Horiba Spectrofluorimeter at 25 °C. Various concentrations of tested molecules were added to a final volume of 3 mL of buffer (PBS supplemented with 10 mM $MgSO_4$) containing the trimera in a quartz cuvette. The tryptophan fluorescence emission spectra of proteins were obtained by exciting the samples at 290 nm (2 nm bandwidth) and recorded between 300 to 550 nm (5 nm bandwidth). The excitation wavelength was chosen at 290 nm to optimize the signal to noise ratio and to reduce the contribution of tyrosine residues to the signal [227]. 3 mL of buffer was used as baseline.

2. Circular dichroism

Circular Dichroism (CD) is an absorption technique based on the differential absorbance of left and right circularly polarized light by chiral molecules. It is a technique used to study the structure of proteins and to have information on the interaction between protein and other molecules. The CD spectra in the far UV (180-260 nm) for proteins arises from n-π^* and π-π^* transition of the amide group in the polypeptide backbone.

Synchrotron radiation circular dichroism (SRCD) spectra were measured at the synchrotron radiation SOLEIL, Gif/Yvette, France on the DISCO beamline which delivers photons of energy of 1-20 ev, covering near UV to VUV region [370]. The principle of Circular Dichroism spectrophotometer set-up is shown below (Figure 28).

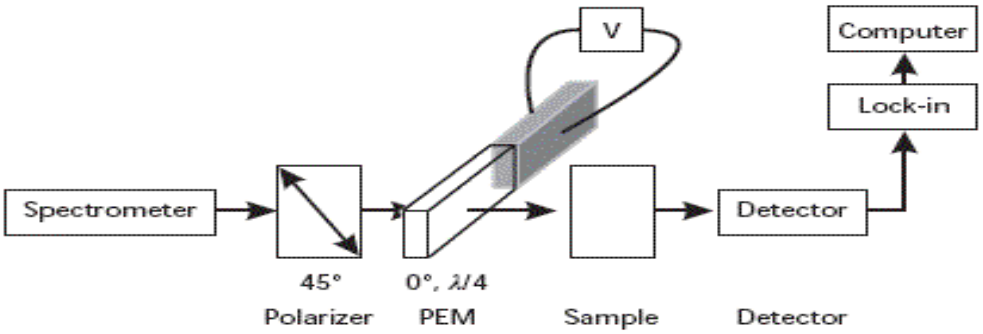

Figure 28: Schematic representation of Circular Dichroism spectrophotometer

A CaF_2 cell was used for the experiment. The sample was loaded between two cell plates. The assembled cell was then placed in the cell holder. Two Teflon rings were positioned on the top of the cell plates to prevent the cell from rotating. The cell holder was then placed in the sample chamber and the spectrum was recorded. The calibration was made using a solution of camphorsulphonic acid (CSA). Spectra were measured over the wavelength range from 170 to 260 nm. Three scans were measured and averaged for the samples and the baseline. The averaged baseline was subtracted from the samples and the curves obtained smoothed. SRCD spectra were recorded at 25 °C. The solutions contained the selected protein were prepared in 100 mM sodium fluoride; 10 mM sodium phosphate pH 7.0. Spectra are expressed in delta epsilon units, calculated using mean residue weights of trimera 82,681 Da. Depending on the composition of the solution that we studied, the baseline was done with the corresponding buffer alone or in the presence of the solvent. In order to compare the spectra, a same volume of the solvent of the tested molecule was present in each sample. BeStSel software was used to assess the percentage of the different types of secondary structure conformation of the trimera (α helices, β sheets and disordered structures) and the changes in protein conformation while it is in contact with other molecules [370].

VI. Cholesterol measurements

1. Quantification of intrinsic cholesterol in neutrophil membrane fractions

Intrinsic cholesterol concentration in human neutrophil membrane fractions was measured by the Amplex Red Cholesterol Assay Kit purchased from (Invitrogen; A12216). It is a fluorometric method for a sensitive quantitation of cholesterol using a fluorescence microplate

reader. The assay depends on an enzymatic reaction that detects both free cholesterol and cholesteryl esters. Cholesteryl esters are hydrolyzed by cholesterol esterase into cholesterol, which is then oxidized by cholesterol oxidase to give H_2O_2 and the corresponding ketone product. The hydrogen peroxide is then detected using 10-acetyl-3,7-dihydroxyphenoxazine (Amplex® Red reagent), a highly sensitive and stable probe for H_2O_2. In the presence of horseradish peroxidase (HRP), Amplex® Red reagent reacts with H_2O_2 with a 1:1 stoichiometry to make highly fluorescent resorufin [371, 372] (Figure 29). The absorption and fluorescence emission maximum of Resorufin is approximately 571 nm and 585 nm respectively (Figure 30).

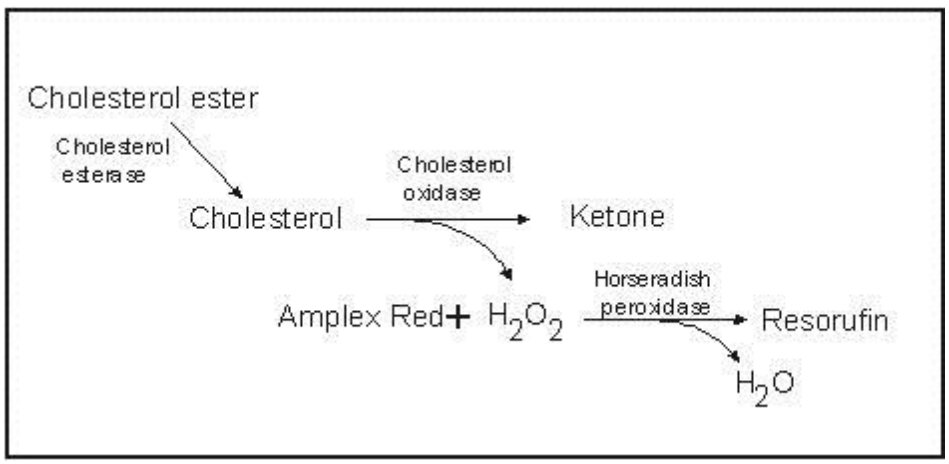

Figure 29: Enzymatic Reaction for Cholesterol Quantitation.

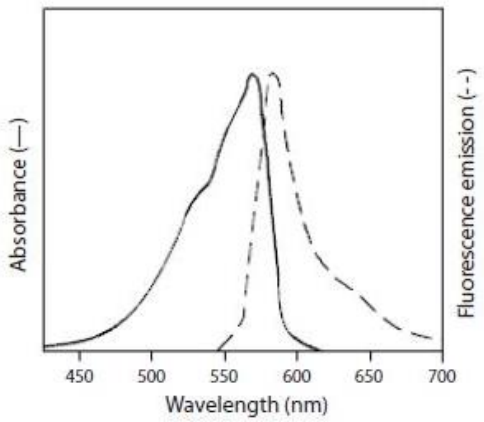

Figure 30: Normalized absorption and fluorescence emission spectra of resorufin

The Amplex® Red cholesterol assay can measure cholesterol at a concentration of 200 nM or lower and can accurately detect the cholesterol content in a solution containing 0.01 µL of human serum. A cholesterol standard curve was prepared by diluting the appropriate amount of 5.17 mM cholesterol reference standard into the reaction Buffer (0.1 M potassium phosphate, pH 7.4, 0.25 M NaCl, 25 mM cholic acid, 0.1% Triton® X-100) to produce cholesterol concentrations of 0 to ~20 µM (Figure 31). Reaction Buffer without cholesterol was used as a negative control. Cholesterol containing samples were diluted in the reaction Buffer. 50 µL of the diluted samples and controls (standard points) were pipetted into separate wells of a microplate. The reactions were started by adding 50 µL of 300 µM Amplex® Red reagent containing 2 U/mL horseradish peroxidase (HRP), 2 U/mL cholesterol oxidase, and 0.2 U/mL cholesterol esterase working solution to each microplate well containing the samples and controls. Reactions were incubated at 37°C for 30 minutes. Fluorescence was measured with a fluorescence microplate reader using excitation at 560 ± 10 nm and fluorescence detection at 590 ± 10 nm. The intrinsic cholesterol concentration was estimated by three independent measurements from different blood donors.

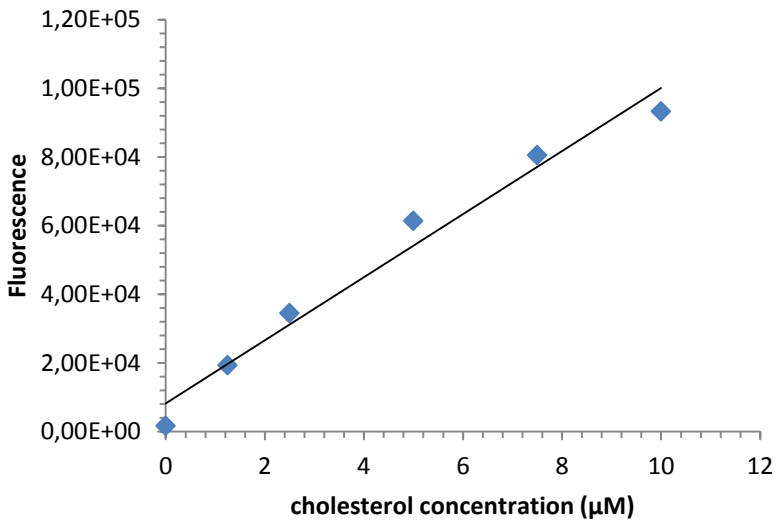

Figure 31: Detection of cholesterol using the Amplex® Red reagent–based assay

Each reaction contained 150 µM Amplex® Red reagent, 1 U/mL HRP, 1 U/mL cholesterol oxidase, 0.1 µM cholesterol esterase and the indicated amount of the cholesterol in 1X reaction buffer. All the reagents came from cholesterol assay kit (Invitrogen; A12216). Reactions were incubated at 37°C for 30 minutes. Fluorescence was measured with a fluorescence microplate reader using excitation at 560 ± 10 nm and fluorescence detection at 590 ± 10 nm.

2. Depletion of cholesterol

Cyclodextrins (CDs) are cyclic oligosaccharides consisting of α (1–4)-linked D-glycopyranose units. CDs contain a number of glucose monomers ranging from six to eight units in a ring (Figure 32):

- α (alpha)-cyclodextrin: 6-membered sugar ring molecule
- β (beta)-cyclodextrin: 7-membered sugar ring molecule
- γ (gamma)-cyclodextrin: 8-membered sugar ring molecule

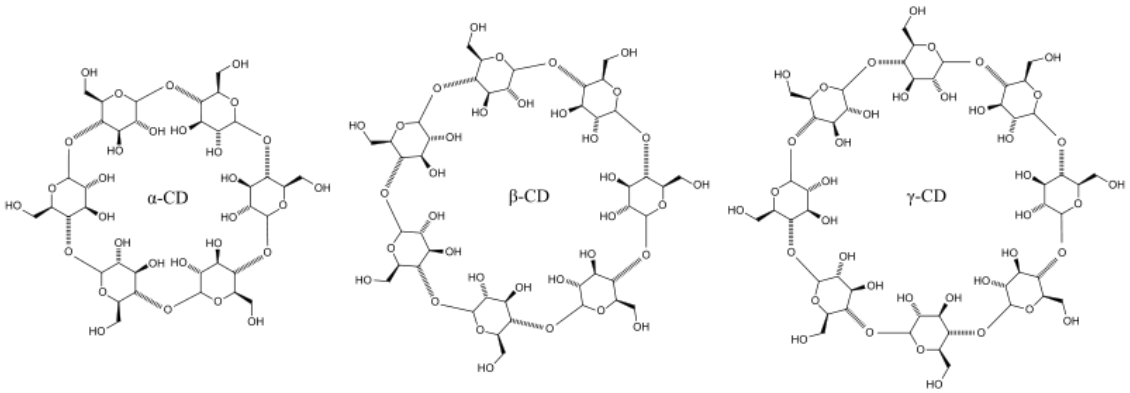

Figure 32: Structural representations of α, β and γ cyclodextrin

These compounds are known as strong carriers for hydrophobic molecules because they contain a hydrophobic cavity which can encapsulate hydrophobic substances. MβCD is a well-established cholesterol depleting reagent of phospholipidic membranes without affecting their permeability and it is the most commonly used reagent [373-376]. methyl-β-cyclodextrin (MβCD) was used to extract cholesterol from the neutrophil membranes according to the following protocol. The neutrophil membranes were incubated for 1 hour, at 4 °C in presence of 10 mM MβCD. The mixture was centrifuged at 148 000 g for 1h30 at 4 °C. Neutrophil membranes were found in the pellet and the cyclodextrin-cholesterol complexes were in the supernatant. The neutrophil membranes were resolubilised in PBS.

VII. Quantification of H_2O_2 produced upon NADPH oxidase activation

H_2O_2 produced upon NADPH oxidase activation was measured similar to cholesterol using the Amplex red assay kit (Figure 29). H_2O_2 standard curve was prepared by diluting the appropriate amount of 20 mM H_2O_2 reference standard into the reaction buffer to produce H_2O_2

concentrations of 0 to ~20 µM. NADPH oxidase was activated in cell free system by AA as mentioned in section (III-1) except that cyt c was not added. After addition of NADPH, 50 µL of the activated samples were added to 50 µL of 300 µM Amplex® Red reagent containing 2 U/mL horseradish peroxidase (HRP). Reactions were incubated at 37°C for 30 minutes. Fluorescence was measured as indicated in section (VI-1).

VIII. Nanoparticles characterization

1. Dynamic light scattering measurement

Light scattering is a characteristic property of objects of size less than one micrometer. The diffusion phenomenon is observed when the wavelength of the light is much longer than the size of the considered object, is mainly due to Rayleigh scattering. It is an elastic diffusion; it means that the electromagnetic wave retains the same energy during the diffusion. In fact, suspended particles are subjected to Brownian mobility and the resulting light interference contains information on their speed of movement. This speed is intrinsically linked to the particle size, small particles moving faster than larger ones. DLS spectroscopic analysis technique measures hydrodynamic radius of the nanoparticles in suspension in a liquid. The measured hydrodynamic radius which should obey to Stokes-Einstein equation (equation 8) is the radius of a theoretical sphere including the nanoparticle, plus functionalization and solvation spheres [377].

$$\mathbf{R_H} = \frac{K_B T}{6\pi\eta D} \qquad \textbf{Equation (8)}$$

Where K_B is Boltzmann constant in $m^2.Kg.s^{-2}.K^{-1}$, T is the temperature in Kelvin; η is the fluid viscosity in Kg. $m^{-1}.s^{-1}$ and D is the diffusion coefficient in $m^2.s^{-1}$.

DLS measurements were performed at room temperature on a Malvern ZetaSizer ZEN 3600 equipped with a 633 nm laser. Data were collected with a scattering angle of 173°. 500 µL of each solution was prepared in disposable cuvette (Visible cuvette, brand). The measurement was performed at the center of the cuvette to minimize edge effects. A range between 2 and 60 µg/mL of TiO_2 NPs suspensions prepared in PBS or water were tested. The size of 20 µg/mL TiO_2 NPs in presence of MF (0.5µg/mL cyt b_{558}) or trimera 18 µg/mL was evaluated. 1 mM Pt-

naked Pt-PEG NPs +/- 200 nM trimera suspensions were prepared in water or PBS were also characterized.

2. Transmission electron microscopy

Transmission electron microscopy (TEM) is used to produce images from a sample by illuminating the sample with electrons within a high vacuum, and detecting the electrons that are transmitted through the sample. The TEM uses a beam of highly energetic electrons instead of light. On the way through the sample some parts of the sample stop or deflect electrons more than other parts. The electrons are collected from below the sample onto a phosphorescent screen or by a CCD camera. In the regions where electrons do not pass through the sample the image is dark. Where electrons are unscattered, the image is brighter, and there are a range of greys depending on how many electrons interact with and are scattered by the sample [378]. TEMs are capable of imaging at a significantly higher resolution than light microscopes, owing to the small de Broglie wavelength of electrons. TEM is used to reveal the finest details of the internal structure even as small as a single atom.

The morphology and size of NPs were determined by TEM. The solutions contained either 1 mM Pt-naked or Pt-PEG NPs or 0.5 mg/mL TiO_2 NPs +/-50 µg/mL trimera and +/-1 mg/mL membrane proteins containing 25µg/mL cyt *b*$_{558}$. 4 µL of the suspension was deposited onto glow-discharged carbon-coated copper grids and after 1 minute of interaction, the excess of solution was removed with a filter paper (Whatman). As a result, the sample wass dried onto the support. Zero-loss (20 eV window) images of TiO_2 NPs were acquired on field emission gun transmission electron microscope operating at 200 kV (JEOL 2200FS, JEOL LTD®). The size of nanoparticles was measured from the images obtained using the software ImageJ 1.47v.

IX. Gamma irradiations

Ionizing radiation is composed of particles that individually have sufficient energy to remove an electron from an atom or molecule. This ionization generates free radicals that are atoms or molecules containing unpaired electrons which tend to be chemically reactive. High energy ionizing radiation is used to initiate free radical reactions. High energy irradiation sources can be divided into two groups: the first one consists of sources from natural and artificial

radioisotopes like radium, cesium-137 and cobalt-60. The second group includes X-ray generator and electron accelerators. The most common gamma radiation source is cobalt-60.

Cobalt-60 decays mainly by emission of β particles to give an excited state of Nickel-60. Nickel-60 in the excited state instantly loses energy by emitting two γ photons with energies of 1.173 and 1.33 MeV, to reach a stable state [379]. Those two highly energetic gamma photons lose the majority of their energy through their interaction with irradiated samples. The different states involved in the disintegration of cobalt-60 are explained in figure 33.

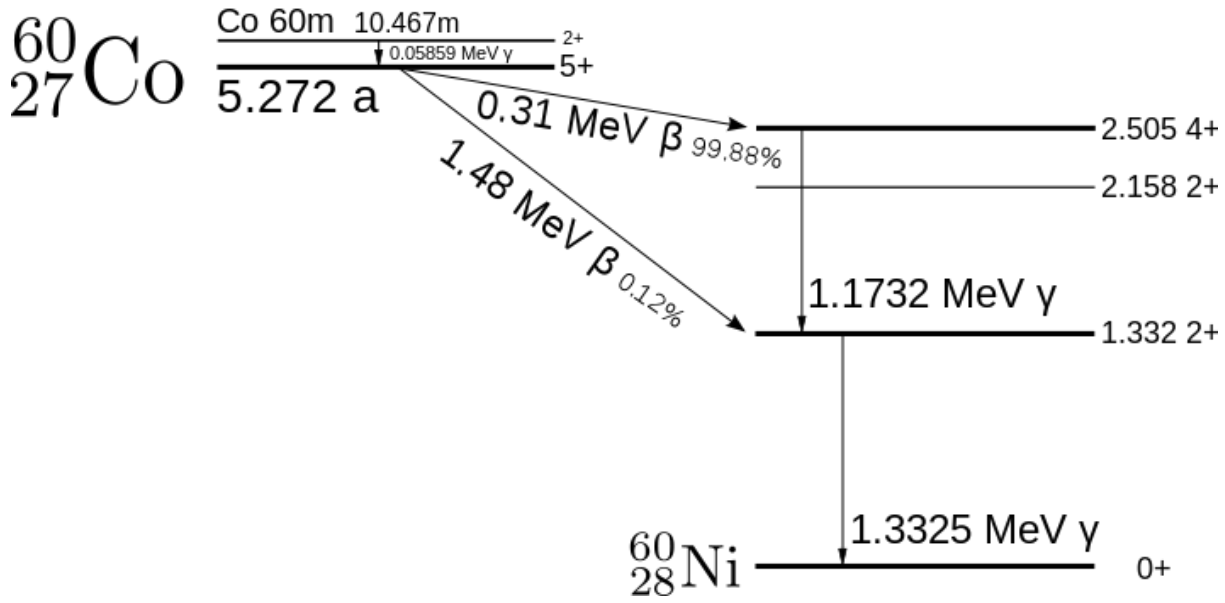

Figure 33: Radioactive decay of cobalt-60

Products of water radiolysis after 100ns for Gamma radiation:

$$H_2O \rightarrow e^-_{aq}, H^\bullet, {}^\bullet OH, H_2, H_2O_2, H_3O^+ \qquad \textbf{Equation (9)}$$

We have tested the sensitivity of NADPH oxidase proteins to free radicals formed by water radiolysis upon γ-irradiation to mimic oxidative stress conditions. In air atmosphere and without the help of any other scavenger, Reactions (10) and (11) take place. As a consequent, the solution contains hydroxyl radicals ($^\bullet OH$), hydrogen peroxide (H_2O_2) and superoxide anions ($O_2^{\bullet-}$) which

are the most important ones. The chemical yields are: $G(^{\bullet}OH)= 0.28$, $G(H_2O_2)= 0.073$, $G(O_2^{\bullet-})= 0.342$. Hydroxyl radicals $^{\bullet}OH$ are one of the most reactive oxidants in organisms due to their high redox potential $E°\ (OH^{\bullet}/OH^{-}) = 1.9$ V and $E°\ (H^{+}, OH^{\bullet}/H_2O) = 2.72$ V [380]. They react almost with every type of biomolecules in a non-selective way. Superoxide anions are also formed via one electron reduction of O_2. Hydrogen peroxide H_2O_2 is stronger oxidant than $O_2^{\bullet-}$.

$$\mathbf{e^{-}_{aq} + O_2 \rightarrow O_2^{\bullet-};\ k_{11} = 1.9 \times 10^{10}\ M^{-1}s^{-1}} \qquad \textbf{Equation (10)}$$

$$\mathbf{H^{\bullet} + O_2 \rightarrow O_2^{\bullet-} + H^{+};\ k_{12} = 1.2 \times 10^{10}\ M^{-1}s^{-1}} \qquad \textbf{Equation (11)}$$

γ-irradiation were carried out using the panoramic ^{60}Co γ source IL60OPL Cis-Bio International (France) at the University Paris-Sud (Orsay, France). The dose rate was measured by Fricke dosimetry [381]. All irradiations were performed at room temperature and under aerobic conditions. The solutions to be irradiated contained the chosen protein (trimera, $p47^{phox}$) or membrane fractions, alone or with Pt NPs in water. Experiments were done in triplicate.

Results & Discussion

"The aim of discussion should not be victory, but progress."

Joseph Joubert

CHAPTER 1: CHARACTERIZATION OF TRIMERA

I. Introduction

The development of a cell-free oxidase activation system was a great help in the identification and characterization of the components of the NADPH oxidase complex, the understanding of the mechanism of NADPH oxidase activation, the search for inhibitory drugs, and the diagnosis of various forms of chronic granulomatous disease (CGD) [382].

Cell-free assays consist of a mixture of the individual components of the NADPH oxidase complex, derived from resting phagocytes or in the form of purified recombinant proteins. This system was designed to mimic *in vivo* oxidase activity under *in vitro* conditions. In cell-free systems, the activation process is realized by the introduction of an activator, an anionic amphiphile such as arachidonic acid (AA) or other fatty acids or surfactants. This activating property of AA had been deduced from the observation that phospholipase A2 inhibitors decreased NADPH oxidase activity [218, 219]. Activation is commonly quantified by measuring the primary product of the reaction, $O_2^{\cdot -}$, trapped immediately after its production by an appropriate acceptor in a kinetic assay, allowing the calculation of the rate of $O_2^{\cdot -}$ production [19, 218-222]. Our group took advantage of this system and developed a cell-free system, which permits quantification of the components of interest, modifications of membrane composition, testing and identifying the potential effects of different molecules in various steps of oxidase activation [148, 149, 367]. Studies of the assembly process of the cytosolic proteins on the Cyt b_{558} had shown that the sequence of addition of the proteins and the time between each addition had an impact on the activity [149]. So for our studies of effects of various additives, it seemed important to have a system in which we got rid of this problem. Therefore it was sensible to use a construction [$p47^{phox}$ (aa 1–286), $p67^{phox}$ (aa 1-212) and a full length Rac1 (aa 1-192)] created by Pr. Edgar Pick, that we called trimera. In order to validate the use of the trimera, different experiments were performed with the three separated proteins and with the trimera.

II. Characterization and assessing the validity of the trimera as a replacement of the cytosolic proteins

As described in the introduction section, the trimera consisted of only the domains necessary for Cyt b_{558} activation, $p47^{phox}$ (aa 1–286), $p67^{phox}$ (aa 1-212) and the full length Rac1 (aa 1-192). These domains were fused to constitute a kind of chimera [187, 190]. A precondition

for using the trimera was to ascertain that it was functionally comparable to the separated cytosolic subunits. Different experiments were performed to characterize the trimera and to validate its use instead of separated cytosolic proteins for our next experiments. We studied the activation of NADPH oxidase by AA with trimera compared to separate proteins, the structural effects of AA on trimera and the rate of production of superoxide anions at two temperatures. Furthermore, H_2O_2 production by the enzyme complex was measured and consequently the effect of H_2O_2 and ROS on NADPH oxidase was tested.

1. Purification of trimera

The expression and purification of the trimera were described in Materials and Methods section. The purity of trimera solution was checked by migration on 10% BisTris-NuPAGE SDS gels (Invitrogen), stained with Coomassie Brilliant Blue. The purification was generally successful and trimera appeared as a double band as many cytosolic NADPH oxidase proteins, at a molecular weight around 82 kDa (Figure 34).

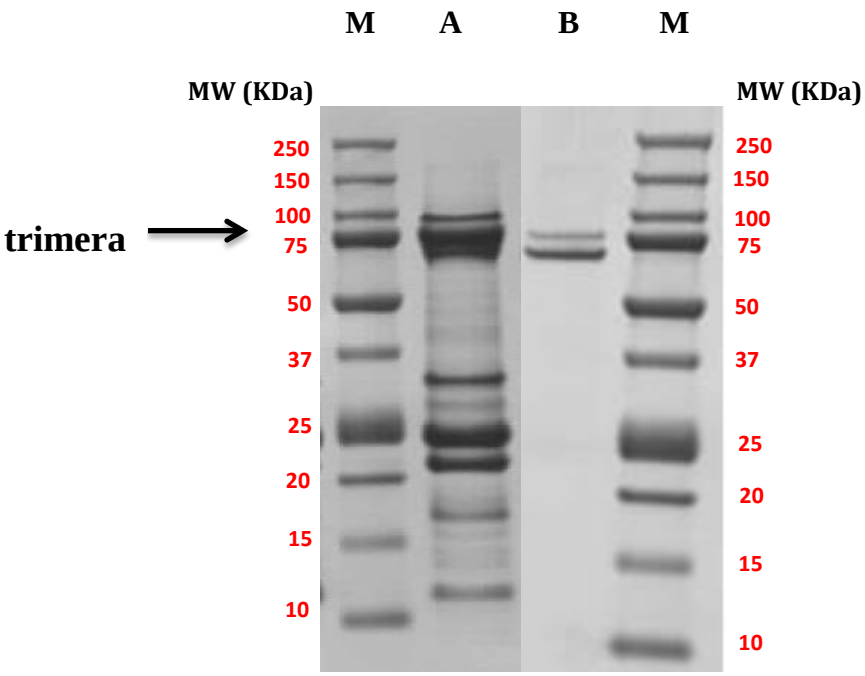

Figure 34: SDS–PAGE of trimera solutions after Ni column and gel filtration chromatography.

Each lane was loaded with 10 µL of proteins. (A) Protein eluted after nickel affinity chromatography; (B) Elution of trimera after gel filtration chromatography; (M) molecular weight marker (dual-color, Biorad).

2. Optimization of AA activation with the trimera

Arachidonic acid is known to be an excellent activator of all components of the NADPH oxidase *in vitro* but also *in vivo* [124, 383]. In our laboratory, AA is used as a formal activator in the cell-free system studies. The aim of this experiment was to determine the optimal concentration of *cis*-AA that led to the maximum activity with the separated subunits and with the trimera. Different concentrations of AA (0- 160 µM) were incubated with human neutrophil membrane fractions (3 nM Cyt b_{558}) and with either separated proteins ($p67^{phox}$ 470 nM, $p47^{phox}$ 450 nM and Rac 560 nM) or trimera 200 nM.. The rate of superoxide anion production was measured upon increasing concentrations of AA.

As for separate proteins, no activity was measured in the absence of AA as shown in Figure 35. A bell shape curve in agreement with the usual findings is observed [226, 384]. By increasing AA concentrations, the activity increases and then decreases. The maximum was obtained for a *cis*-AA concentration of 52 µM.

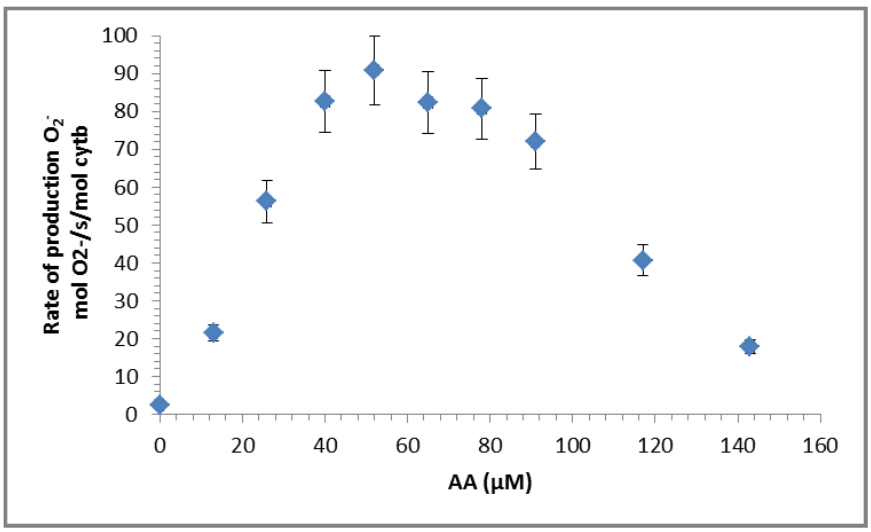

Figure 35: Superoxide anion production in function of AA concentrations for separate proteins

The superoxide production was measured spectrophotometry following cyt *c* reduction at 550 nm as mentioned in the Materials and Methods section. Variable concentrations of AA were incubated with human neutrophil membrane fractions (3 nM Cyt b_{558}) and the cytosolic subunits $p67^{phox}$ 470 nM, $p47^{phox}$ 450 nM and Rac 560 nM at 25°C. The reaction was initiated by the addition of 250 µM NADPH in the presence of 50 µM cyt *c*. The data are the average of 3 independent measurements.

Figure 36 shows that the NADPH oxidase activity with trimera is AA concentration dependent until a concentration of 50 µM and then reaches a pseudo-plateau instead of a more pronounced inhibition with the cytosolic proteins. No significant difference of the maximal activity values induced by AA has been observed when trimera or cytosolic proteins were used. We chose to use a concentration for *cis*-AA of 40 µM for all the next experiments since it gave nearly the maximum of activity for both.

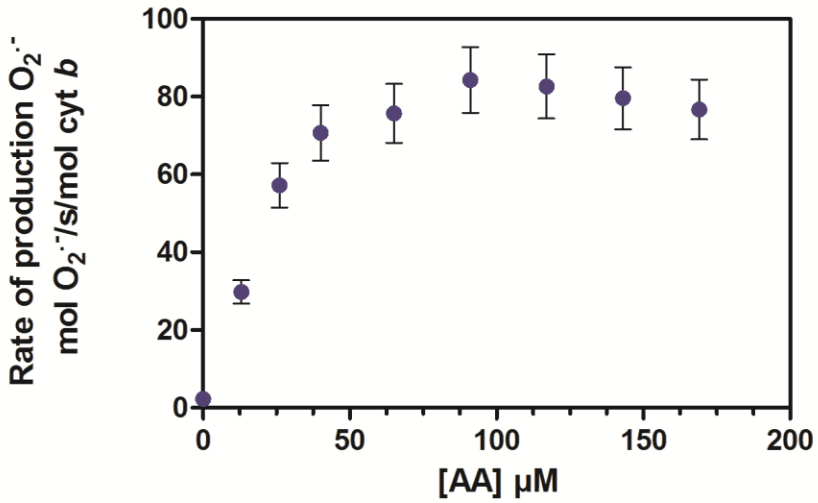

Figure 36: Arachidonic acid dependence of NADPH oxidase activity with the trimera.

Trimera (200 nM) and neutrophil membrane fractions (3 nM Cyt b_{558}) were incubated with variable concentrations of AA at 25°C. The superoxide production was measured spectrophotometry following cyt *c* reduction at 550 nm as mentioned in the Materials and Methods section. The data are the average of 3 independent measurements.

Different concentrations of cyt *c* (50, 100, and 150 µM) have been tested. The initial rate of superoxide anion production was similar. Thus, we chose to do all the next experiments with 50 µM cyt *c*.

3. Structural effects of AA

i. Effect of AA on soluble and membrane proteins

To evaluate the sensitivity of each component to AA, superoxide anion production rate was measured after pre-incubation of 10 s of membrane components or of the trimera or of both, with AA (Fig.37). After 10 s of separate pre-incubations of the membrane and of the trimera, both solutions were mixed and left for a second incubation for 4 min. We chose a pre-incubation time of 10 s because a longer one (30 s) led to a drastic decrease of the activity. This was also observed in the case of separated subunits [149].

First, when both membrane fractions and trimera were preincubated 10 s separately with AA, and then incubated 4 min together, the activity was maintained to about 95% of the observed one in standard conditions. The same level of activity (95%) was measured when AA was incorporated only to the membrane fractions. On the other hand, when AA was added only to the trimera, the activity dropped to 73% (Figure 37). It is known that AA has an indispensable effect on Cyt b_{558}. We show that, like for separate subunits, addition of AA on the trimera is not sufficient.

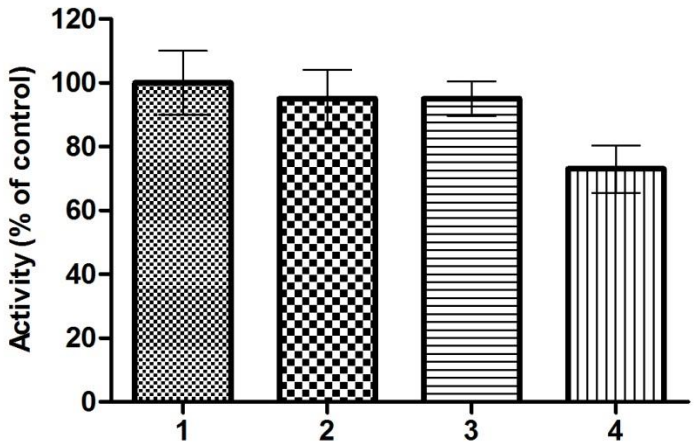

Figure 37: Effect of AA activation of membrane fraction and trimera.

(1) In the control experiment membrane fraction and the trimera were incubated together during 4 min in the presence of 40 µM AA. The rate obtained corresponds to the 100% value (75 mol $O_2^{\cdot-}$ /s/mol cyt b_{558}). (2-4) Membrane fractions (MF) and trimera were separately preincubated during 10 s and mixed together for 4 min as follow: (2) both were preincubated with 40 µM AA, (3)

only MF was preincubated with 40 µM AA, (4) only the trimera were preincubated with 40 µM AA.

ii. Effect of AA on the secondary structure of the trimera

It was interesting to measure the SRCD spectrum of trimera to gain information about the modifications of the secondary structures that might or might not occur when it is activated by AA. We recorded SRCD spectra of trimera (18µM) with increasing AA concentration (0-500 µM). As baseline, SRCD of AA solution was measured. The SRCD spectrum of trimera displays a positive band at 195 nm and a large negative band near 215 nm (Figure 38). The secondary structure of trimera remained unchanged in the presence of AA for the whole range of concentrations tested, in contrast to what our group observed with $p47^{phox}$ and $p67^{phox}$ (Bizouarn et al. submitted). However these AA-dependent secondary structure modifications seemed principally to occur in the truncated regions of $p47^{phox}$ and $p67^{phox}$, which is in agreement with our observations on the trimera.

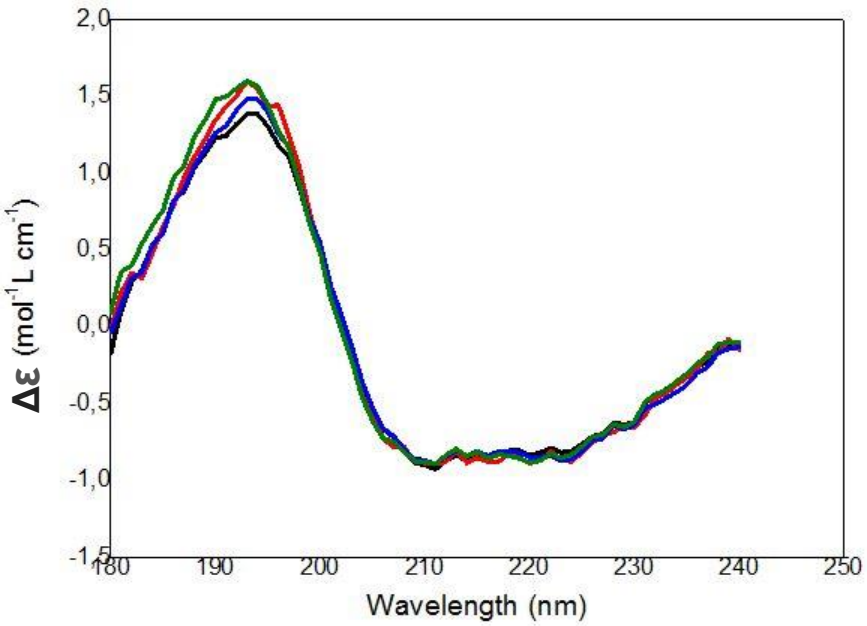

Figure 38: SR-CD spectra of trimera in the presence of increasing amounts of AA

SRCD spectra of the trimera (18 µM) alone (black) and in the presence of AA 100 µM (blue); 200 µM (red); 500 µM (green). The buffer was NaF 100 mM, NaPi 10 mM pH 7, 25°C.

iii. Effect of AA on the tryptophan intrinsic fluorescence of the trimera

To complete the study, we followed the variation of intrinsic tryptophan fluorescence spectra upon addition of AA (Figure 39). Trimera contains a total of thirteen tryptophan residues. It was previously shown that addition of AA to the cytosolic subunits $p67^{phox}$ and $p47^{phox}$ induced measurable decreases of the intrinsic tryptophan fluorescence levels [227, 385].

By increasing AA concentration up to 140 µM, the fluorescence yield of the trimera underwent a concentration dependent decrease (Fig. 39). A small blue shift up to 5 nm was also observed, consistent with a slightly more hydrophobic tryptophan environment. The quenching of fluorescence of the endogenous tryptophans of the trimera indicates that at least one of the locations of AA is probably close to one or several Trp residues like in separated cytosolic proteins.

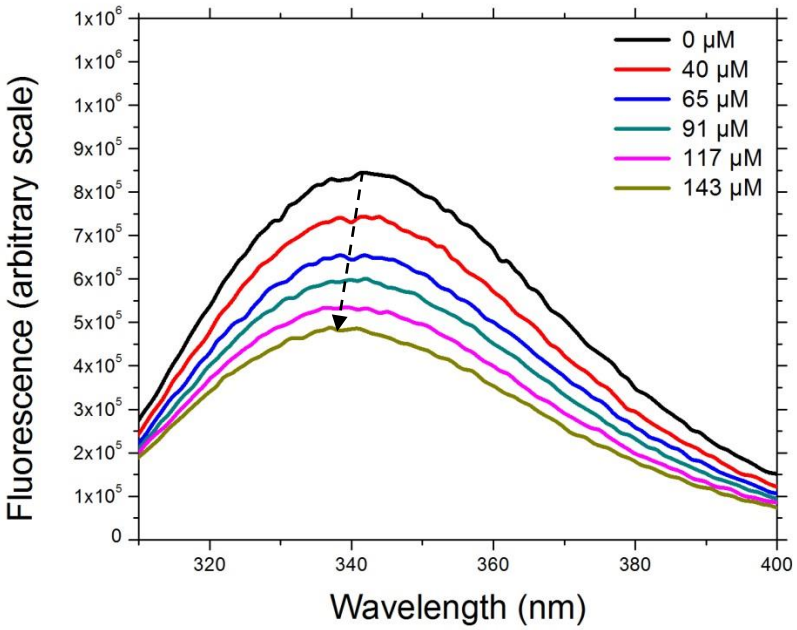

Figure 39: Fluorescence of trimera treated with AA.

The emission spectrum was measured using an excitation wavelength of 290 nm as described in the Materials and Methods section. Results are representative of at least three independent experiments. trimera 60 nM, AA as stated in the figure legend.

4. Kinetic parameters of superoxide anion production in the presence of trimera

The rate of superoxide production stimulated by AA for increasing concentrations of trimera was measured (Figure 40). This dependence could always be fitted using a Michaelis-Menten -like equation (equation 7, see Materials and Methods) and from the curve one could determine EC_{50} and V_{max} values. The data in Fig 40 reveal that the dose-response curve obtained with trimera was hyperbolic in agreement with Pick's results [187]. Oxidase activation by AA with trimera exhibited a V_{max} of 70.3±2 mol $O_2^{\bullet-}$/s/ mol cyt *b*$_{558}$ and EC_{50} of 48.6±3 nM, which is respectively 1.5 times higher and 6.8 times lower than those measured with trimera activated by LiDS. That might be explained by the fact that different amphiphiles have slightly different activation mechanism of NADPH oxidation, consequently, kinetic parameters are different. The EC_{50} values of the separated subunits were determined previously by our group [149] (Table 3). One can notice that EC_{50}(p47) < EC_{50}(p67) < EC_{50}(trimera)≪EC_{50}(Rac). Thus trimera and p67^{phox} have closer affinity for the complex than the other proteins. This might be attributed to their similar roles as activator of NADPH oxidase complex.

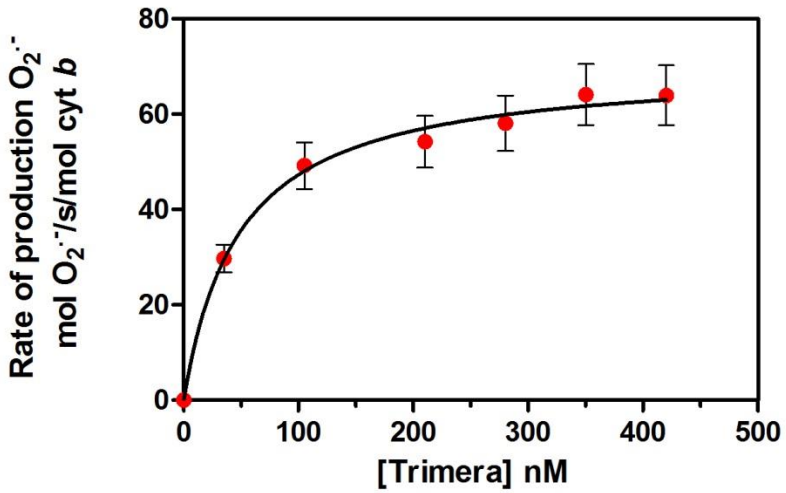

Figure 40: NADPH oxidase activity dependence on trimera concentration

The assays mixtures consisted of trimera at varying concentrations (from 0 to 420 nM) and membrane fractions of human neutrophils (3 nM Cyt *b*$_{558}$) to which were added 40 µM AA. The superoxide formation was measured as indicated in Materials and Methods. The values are an average of three independent measurements ± SEM.

Protein used for the titration:	Other cytosolic proteins present in CFS	EC_{50} (nM)
trimera	-	48.6±3
$p67^{phox}$	$p47^{phox}$ +Rac	30±4
$p47^{phox}$	$p67^{phox}$ +Rac	7 .7±3.1
Rac	$P67^{phox}$ + $p47^{phox}$	152±52

Table 3: Kinetics parameters for cytosolic proteins using Michaelis-Menten equation in presence of AA

The EC_{50} values for the separated subunits were measured previously by our group [149]. The concentrations of the proteins except those used for the titration were as following: $p67^{phox}$ (250 nM), $p47^{phox}$ (200 nM), Rac (500 nM).

5. Assembly of NADPH oxidase in the presence of trimera

The kinetics of assembly with separate cytosolic proteins is complex. In the absence of incubation period, a lag period of 20 sec is observed with the separated cytosolic proteins to reach a stationary activity of the oxidase. Conversely, the maximal rate of formation of superoxide is obtained only if the system is allowed to assemble during 4 min. It was assumed to reflect a necessity of assembly of the Nox complex. [149]. As said previously, in the trimera, the inhibitory region of $p47^{phox}$ is absent, $p47^{phox}$ and $p67^{phox}$ are already linked to each other and Rac is already in its active form. For this reason, trimera is assumed to be in a form very close to the active one. Thus two sets of kinetic measurements were performed (Figure 41). The first one was achieved with the standard procedure in which the membrane fractions and the trimera were mixed with AA, and allowed to incubate for 4 min before the addition of cyt *c* and NADPH. In the second one the same components were mixed but there was no incubation period.

We noticed that similar superoxide ion rates of production were reached with or without incubation time. These results show that the use of trimera nearly suppresses the need of incubation period. It suggests that the lag effectively corresponds to important conformation changes induced by AA on the cytosolic components and not on Cyt $b_{558,}$

In what follows, we have kept this 4 min incubation time for the separate cytosolic proteins and for the trimera, to make both assays comparable.

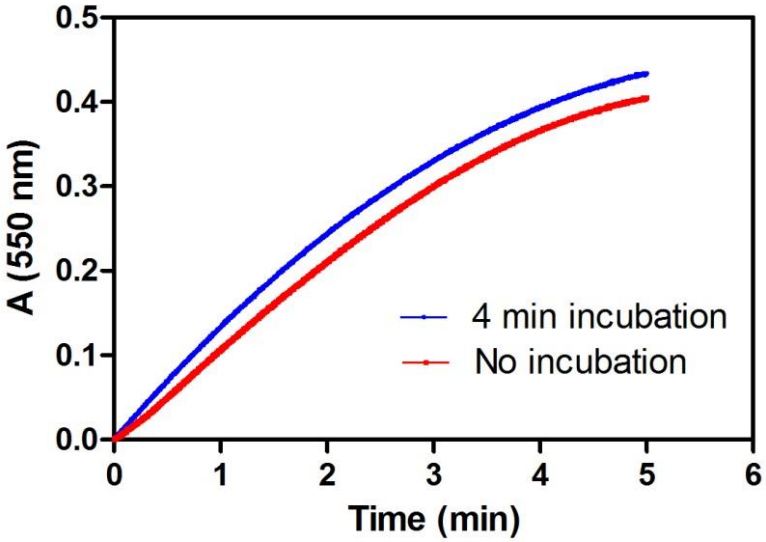

Figure 41: Time course of the superoxide anion production catalyzed by the NADPH oxidase complex.

(blue) control assay involving membrane fraction of human neutrophils (3 nM Cyt *b*$_{558}$), trimera (200 nM) and AA (40 µM) with 4 min incubation, (red) The same components as (blue) but no incubation was performed, the activity measurement was done directly after the addition of cyt c, red. 0 min corresponds to the addition of NADPH.

6. Quantification of H_2O_2 produced upon NADPH oxidase activation

Superoxide anions formed by NADPH oxidase can rapidly dismutate to hydrogen peroxide and dioxygen either spontaneously, particularly at low pH, or catalyzed by superoxide dismutase (SOD). H_2O_2 can react with biological systems, thus it was important to measure its quantity coming from NADPH oxidase activity and to compare this production when either the trimera or the separated subunits were used. The protocol is explained in Material and Methods. We found that 30 µM and 35 µM H_2O_2 were produced when either separated proteins or trimera were used respectively. Thus the cell free system in the presence of either the separated subunits or the trimera is capable to produce H_2O_2 in similar concentrations.

7. Effect of H_2O_2 addition during the assembly phase

In active neutrophils, high concentrations of H_2O_2 have been measured in the vicinity of NADPH complex [84, 386]. Hydrogen peroxide is rather stable and is likely to diffuse including through the membrane to distant targets. Our results also showed that H_2O_2 was produced in cell free system. Therefore, it was of special interest to analyze the effect of H_2O_2 addition on the oxidase activity. In particular, we examined whether hydrogen peroxide had an effect on oxidase activity during the assembly process, which takes place during the incubation time in our cell free system. Hydrogen peroxide at two concentrations (9 or 900 μM) was added at several times during the 4-min phase of assembly, the system was then allowed to finish assembling until the end of 4 min, and then NADPH was added to trigger the reaction (Figure 42).

We observed that the activity was lowered upon addition of 9 and of 900 μM hydrogen peroxide to about 65 and 55% of its initial value, respectively when the addition occurred at the start of the incubation. A slightly greater sensitivity of the system appeared 1 min after addition of AA and some protection could be noticed when hydrogen peroxide was added 3 min after addition of AA. This behavior had been seen with the separated cytosolic subunits and in a greater extent using the mixture $\bullet OH + O_2^{\bullet -}$ in the place of H_2O_2 [148]. This suggested that, the system went through a sensitive substate 1 min after addition of AA. During this intermediate state, some regions of the proteins would be more exposed. When the assembly is over, the exposed surface would have decreased, enabling protection. However, in the case of trimera, the protection was not total, catalytically important regions seem still accessible to H_2O_2. This shows that even if the maximum rate of production of superoxide is obtained immediately, some long rearrangements occur after mixing. It justifies the incubation time of 4 min. Then a tighter assembly substate can take place.

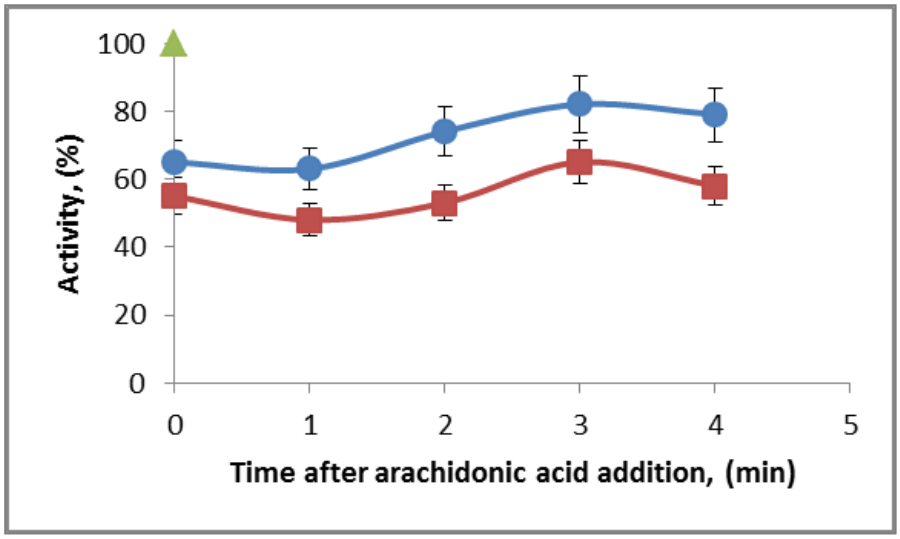

Figure 42: Effect of H_2O_2 on NADPH-oxidase activity.

Membrane fractions (3 nM Cyt *b*$_{558}$), trimera 200 nM, and AA 40 µM were mixed as described in Materials and methods. H_2O_2 was added at various times after addition of AA. Results are expressed as percentages of the control activity: without H_2O_2 (▲), 9 µM H_2O_2 (●), 900 µM H_2O_2 (■).

8. Sensitivity of cytosolic proteins to free radicals

The trimera being composed of domains that are believed to interact less with each other than the separated proteins, it was conceivable that this protein was more open so more sensitive to ROS. We aimed to determine the sensitivity of the protein to oxygen free radicals, thus to test the accessibility of residues important for the activity to free radicals. Aqueous solutions of trimera 25 µM or $p47^{phox}$ 30 µM in phosphate buffer solutions were exposed to γ-rays under aerobic conditions for different time intervals (6, 10, 15, 20, 30 min) with the same dose rate (10 Gy/min). Therefore the doses were equal to 60, 100, 150, 200, 300 Gy. Non-irradiated samples were kept in the same conditions for 30 min. After irradiation of trimera and of $p47^{phox}$, they were used in cell free assays containing the other non-irradiated oxidase components. The production rates of superoxide were measured as usual (Figure 43).

Although in these experiments the doses were very high, whatever the irradiated protein, the oxidase activity of the reconstituted system was slightly lowered and not annihilated. In the case of $p47^{phox}$, 100 % of the oxidase activity was preserved up to 150 Gy. For an irradiation with 300 Gy, $p47^{phox}$ led to 85% of the NADPH oxidase activity while the trimera led to 75% of the

activity. The results point out that both trimera and $p47^{phox}$ exhibited resistance behaviors and are not sensitive toward free radicals produced by γ-irradiation.

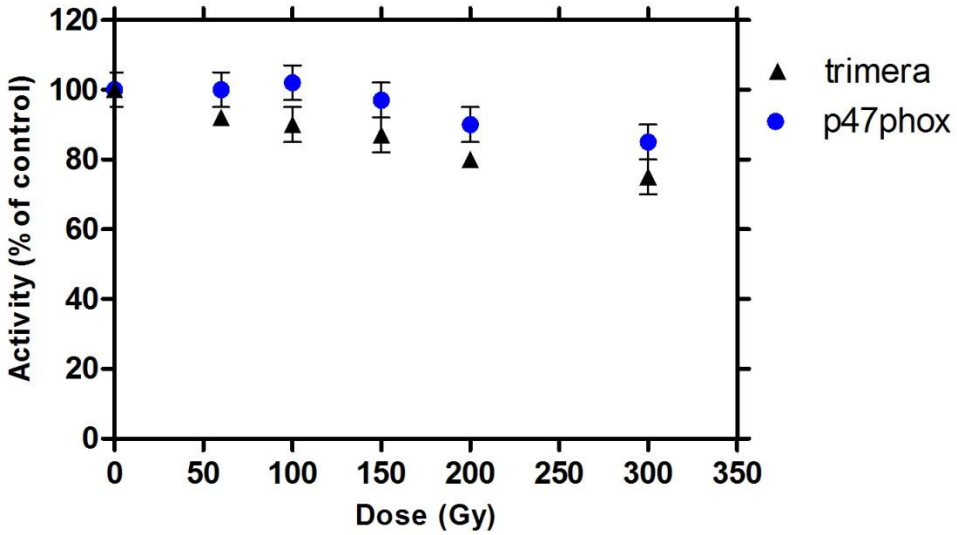

Figure 43: Activity measurement in presence of irradiated $p47^{phox}$ or trimera

Aqueous solutions containing $p47^{phox}$ (30 µM) and trimera (25 µM) were irradiated separately at different irradiation time 6, 10, 15, 20, 30 min, which corresponds to 60, 100, 150, 200, 300 Gy. Non-irradiated samples were kept for 30 min at room temperature. After irradiation of trimera or of $p47^{phox}$, they were reconstituted in the cell free assay containing the other non-irradiated oxidase proteins. Then, NADPH oxidase activity was measured after activation by AA 40 µM. The superoxide rate of formation was measured as indicated in Materials and Methods. Each irradiation condition was done in triplicate and the results are the averages of these three independent measurements.

9. Influence of temperature on the activity of NADPH oxidase

During kinetic experiments, it was observed that a small change of the incubation temperature led to a difference of the activity of NADPH oxidase complex, which showed a need for tight control of this parameter in experiments. The variation of the rate as function of the temperature gives also access to important thermodynamic parameters.

The rates of production of superoxide in presence of the trimera at various temperatures were measured (Figure 44). As expected, the rate of superoxide anion production increased with the temperature. Effectively, even a small increase of temperature led to a significant increase in

the rate of production in the range studied. Similar results were also found with separated subunits [387].

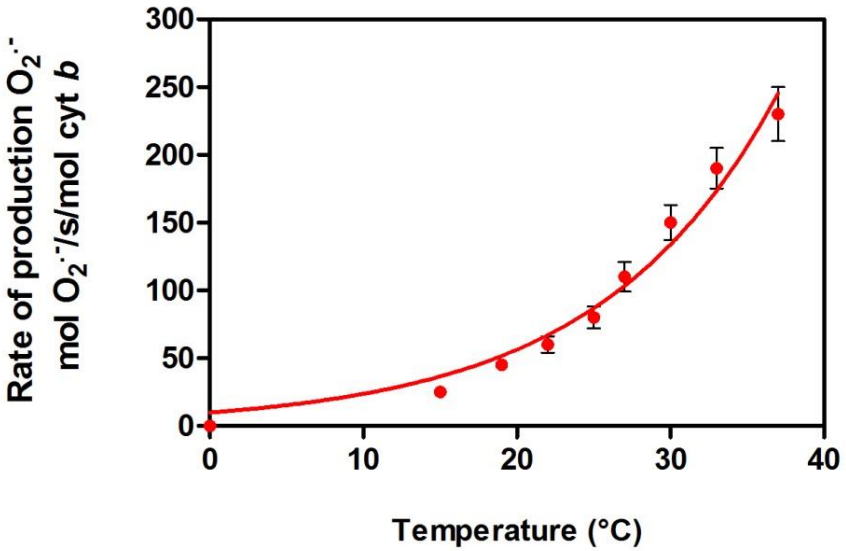

Figure 44: Dependence of NADPH oxidase activity as a function of temperature

Neutrophil membrane fractions and trimera were incubated together in the presence of 40 µM AA at different temperatures. Superoxide production was initiated by addition of NADPH (250 µM) and the rate of $O_2^{\cdot -}$ was quantified by the reduction of cyt c (50 µM). The values are an average of 3 independent measurements ±SEM.

If we assume that the assembly process has been identical for all the temperature studied, the activation energy can be calculated. This dependence should follow the Arrhenius law.

$$k = A \exp(E_a/RT) \qquad \text{(equation 12)}$$

Arrhenius' equation gives the dependence of the rate constant k of a chemical reaction on the absolute temperature T (in kelvins), where A is the pre-exponential factor , E_a is the activation energy ($J.mol^{-1}$), and R is the universal gas constant ($R= 8.314\ J.mol^{-1}.K^{-1}$).

Transforming the Arrhenius law using the logarithm of each member becomes:

$$\ln(k) = \ln(A)\ (-E_a/RT) \qquad \text{(equation 13)}$$

So, when a reaction has a rate constant that obeys Arrhenius' equation, a plot of ln(k) versus 1/T gives a straight line, whose gradient can be used to determine E_a .

To check that the Arrhenius law is followed here and to determine the thermodynamic parameters of NADPH oxidation, Arrhenius plot was constructed (Figure 45). A linear behavior on the whole range of tested temperatures with activation energy of 74.1±3 kJ.mol^{-1} was found. It is interesting to notice that this value is close to the activation energy of NADPH oxidase determined for membrane fractions of bovine (79.5 kJ.mol^{-1}) [387] and for eosinophils (104.6 kJ.mol^{-1}) [388]. So, the formed catalytic center seems thermodynamically similar for both complexes.

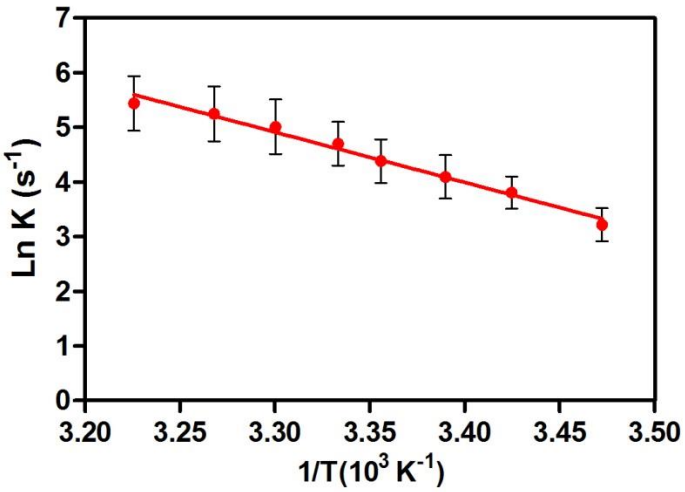

Figure 45: Arrhenius plot of NADPH oxidase activity

The curve was plotted according to equation 13 and the activation energy was calculated from the slope .

In practice, in all experiments presented in the thesis, incubations and measurements were performed at 25 °C to avoid eventual protein denaturation due to higher temperature and a better control of the experimental conditions.

III. Discussion: trimera instead of separated proteins

The construction of trimera by Pick et al. [187] was chosen based on the accumulated information concerning the involvement of certain domains of $p47^{phox}$, $p67^{phox}$, and Rac in oxidase assembly [85, 280, 389]. The concept was to fuse crucial parts of the three cytosolic proteins $p47^{phox}$, $p67^{phox}$ and Rac to bypass the need for protein-protein interaction between $p47^{phox}$ and $p67^{phox}$ and between $p67^{phox}$ and Rac, resulting in a single protein. The trimera was shown to form a highly stable complex with cytochrome b_{558}, in contrast to the liability of complexes formed with three individual subunits, whether full-length or truncated. It even can ensure a right stoichiometry of cytosolic components on Cyt b_{558} which is not totally verified with the separated cytosolic. The trimera was designed to possess several advantages: (a) $p47^{phox}$ segment is free of an autoinhibitory region; (b) Rac constitutively in the GTP-bound form and (c) the C terminus has the potential to be prenylated [187].

1. On the role of AA with trimera

In vitro activation of the NADPH oxidase complex is commonly performed by the sole presence of AA. However, the exact role of AA on the activation of each components of NADPH oxidase is not completely understood. The predominant explanation for the oxidase activating ability of AA was that it perturbs the intramolecular bond in $p47^{phox}$ between the polybasic domain and the SH3 tandem mimicking the phosphorylation events that occur in the intact phagocyte [211]. A similarity of action between AA and $p47^{phox}$ phosphorylation was observed by the fluorescence measurement of its endogenous tryptophans (same percent reduction), which led to the proposal that AA has the ability to produce the same structural changes on $p47^{phox}$ induced by phosphorylation [227]. Similarly, Shiose et al, showed that the addition of AA (50-100 µM) allowed $p47^{phox}$ to bind to C-ter of $p22^{phox}$ as permitted by the mutation S303-304-328E [124, 127].

Trimera showed dependence on AA in agreement with the finding of Pick's group where they demonstrated that using trimera, no oxidase activation is elicited in the absence of LiDS [187]. It seemed surprising, at first, because of the absence of the autoinhibitory region in the $p47^{phox}$ segment and because of the results presented by Sumimoto's group where AA was not needed anymore with the C-ter deleted $p47^{phox}$ (aa 1-286) and $p67^{phox}$ (aa 1-212)[291] and the finding that $p47^{phox}$-$p67^{phox}$ chimeras supplemented with Rac1-GTP are active with a Cyt b_{558}

preparation in the absence of amphiphile [181]. However, the latter finding can be explained by the fact that Cyt b_{558} preparation was relipidated with a mixture rich in anionic phospholipids. The requirement for amphiphile despite the truncation of the p47^{phox} segment in the trimera provides support for the idea of a direct effect of AA on Cyt b_{558} [223]. In fact, it was shown that the best superoxide production took place when the membranes and cytosolic subunits were simultaneously in contact with AA [225]. Direct effect of AA on gp91^{phox} leads to conformational changes which might also participate in NADPH oxidase activation [95] [390]. Clearly, AA acts on several sites on both cytosolic and membranous proteins.

2. On the structural effect of AA on trimera

When AA was preincubated 10 s with both components or with the membrane part, 95% of the activity was conserved but when it was preincubated with the trimera, only 73% of superoxide production was conserved. This result strengthens the idea of some direct activation effect of AA on Cyt b_{558}.

AA dependent activations of cytosolic proteins p47^{phox}, p67^{phox} and trimera were investigated at the level of their secondary structure using SR-CD independently for each protein (Bizouarn et al. 2016). We have shown that AA modifies the SR-CD spectrum of p47^{phox} and p67^{phox} when entire. It is likely that AA targets the C-terminus part of the protein since no modification of the spectra was observed for p47^{phox}ΔC-ter and trimera (Figure 38) by the presence of AA. This is in agreement with previous work demonstrating that the C-terminal region of p47^{phox} is the primary target of the conformational change during the activation of NADPH oxidase [135, 226]. The results on the trimera bring additional evidences that the perturbation in the intramolecular bond in p47^{phox} between the polybasic domain and the SH3 tandem implies modifications of the secondary structure of C-terminal part (probably PRR).

We have shown recently that AA modified the environment of tryptophan residues in the separated cytosolic subunits: both p47^{phox}and p67^{phox} underwent a strong fluorescence decrease, which would be related to structural modifications necessary for their interaction with Cyt b_{558} [226, 227]. A similar tryptophan fluorescence decrease was observed for the trimera upon addition of AA. This observation suggests that AA is inserted close to tryptophan residues of

trimera and that fluorescence changes of p47^{phox}and p67^{phox} may not reflect necessarily conformational changes but only changes on tryptophan environment.

3. On the comparison between separated proteins and trimera

A precondition for using the trimera was to ascertain that it is functionally comparable with the separate cytosolic subunits. We have verified that the rates of production of superoxide anions and hydrogen peroxide were similar and that the dependences of the activity in function of AA concentration were also comparable with the cytosolic fractions and the trimera. Furthermore, affinity of trimera to Cyt b_{558} is similar to p67^{phox} where both are activator of the complex.

It is well known that, if no incubation takes place before the measurement of activity, in other words if NADPH is added immediately after AA, a lag of around 20 sec is observed on kinetics before a stationary activity of the oxidase is reached [149, 391]. Conversely, no lag period was observed when trimera was incorporated instead of the separated proteins (Figure 41). This lag period, attributed to structure changes that should happen on separate subunits, was bypassed when trimera was used. It seems that activation of Cyt b_{558} by AA and the binding of trimera to the membrane fractions are fast and that an efficient complex is formed rapidly between the two parts.

The assembly is a dynamic process permitting certain subunits to be exchanged during the 4-min incubation time. In a previous study our group has shown that the process leading to the assembly, which takes place during the incubation period, involves at least two major phases. The presence of two phases in the assembly process, a sensitive one followed by a resistant one against ROS damages, observed with the separate cytosolic subunits was also found to a lesser extent with the trimera [148]. Despite the fact that the use of trimera suppresses the need for incubation time, our results indicate that during the first phase 1 min after addition of AA, important targets of free radicals are still reachable. But once the complex is more tightly assembled it is less accessible to ROS.

Both trimera and p47^{phox} showed resistance behavior toward free radicals produced by γ-irradiation. Such results were unexpected because usually irradiation of enzymes with high doses leads to inactivation. Probably, the important residues of the proteins where not damaged by irradiation, thus the proteins can still work. In contrast to my results, our group showed

previously that each subunit behaved differently. When $p47^{phox}$ from bovine was subjected to irradiation with doses higher than 200 Gy, this protein behaved as if it were no longer able to play a role in the NADPH-oxidase complex, with a remaining activity equivalent to that measured in its absence [148]. It is known that irradiation has different effects on proteins depending on their origin. It seems that human proteins are more resistant to irradiation effects than the bovine ones.

In conclusion, we have demonstrated that trimera is functionally comparable with the separated subunits, which makes it a very interesting tool. Consequently, we have chosen to perform our experiments with the trimera instead of the separated subunits $p67^{phox}$, $p47^{phox}$ and Rac in order to diminish the number of independent parameters to consider and to facilitate the interpretations of our results.

CHAPTER 2: EFFECT OF CHOLESTEROL ON NADPH OXIDASE

I. Introduction

The damaging role of ROS in cardiovascular diseases (atherosclerosis, vascular inflammation, endothelial dysfunction) leading to coronary heart disease, stroke or *angina pectoris* has been extensively shown [392, 393]. Due to its strong activity and its presence in many cells, NOX2 is one of the major actors at the origin of oxidative stress. Actually NOX2 is one of the main isomers involved in the cardiovascular field [394]. On the other hand, high cholesterol level is linked to an elevated risk of cardiovascular diseases [260], through high concentration of LDL-cholesterol in blood [261, 262]. High cholesterol amount has also been associated with diabetes and high blood pressure [263, 264].

Interestingly, NADPH oxidases have been found in lipid rafts (LR), which are dynamic, detergent-resistant plasma membrane microdomains highly enriched in cholesterol and sphingolipids [395, 396]. Nox cytoplasmic proteins are efficiently recruited to these raft-associated flavocytochromes b_{558} upon activation to reconstitute the active complex [292]. These facts prompted us to study the effect of cholesterol and oxysterols on the functioning of NADPH oxidase. In this chapter, we investigated the consequences of the presence of cholesterol and oxysterols on the production of ROS by NADPH oxidase and we studied the structural effect of cholesterol on NADPH oxidase cytosolic protein. The results of this chapter are the subject of paper I.

II. Intrinsic cholesterol concentration and effect of cholesterol depletion by Methyl-β-cyclodextrin on superoxide production rate

We first measured the intrinsic cholesterol concentration in human neutrophil membrane fractions. We found 3±1 µM cholesterol in the final reaction volume of cell free system assay containing 40 µg/ml membrane proteins (2 nM Cyt b_{558}) in three independent measurements. Then to investigate the role of cholesterol that is naturally present in the neutrophil membrane on NADPH oxidase, 10 mM MβCD was used to disrupt lipid rafts by removing cholesterol from membranes [374, 397, 398]. The rate was measured as described in Material and Methods. We found that cholesterol depletion decreased superoxide production rate relative to the non-treated membrane neutrophil to (44 ±7) %.

In the following studies, the level of cholesterol was increased to a range corresponding to hypercholesterolemia (up to 33% of the normal concentration) and above, to enlighten the effects of such increase.

III. Cholesterol as a Nox-activating molecule?

We aimed at determining whether cholesterol could have an activator effect on NADPH oxidase. The results expressed as percentages of NADPH oxidase activity as a function of cholesterol are displayed in Figure 46. Addition of cholesterol in the range 0.2-1 µM (7 to 33% increase compared to the intrinsic value) provoked slight but significant activation of NADPH oxidase complex, but still far from an equivalent level to AA. The rate of production of $O_2^{\bullet-}$ stayed at around 13% of the rate value obtained with AA for concentrations above 1 µM. Comparable results were obtained using the separated subunits where a maximum activity of (20± 2) % of AA- dependent activity was reached.

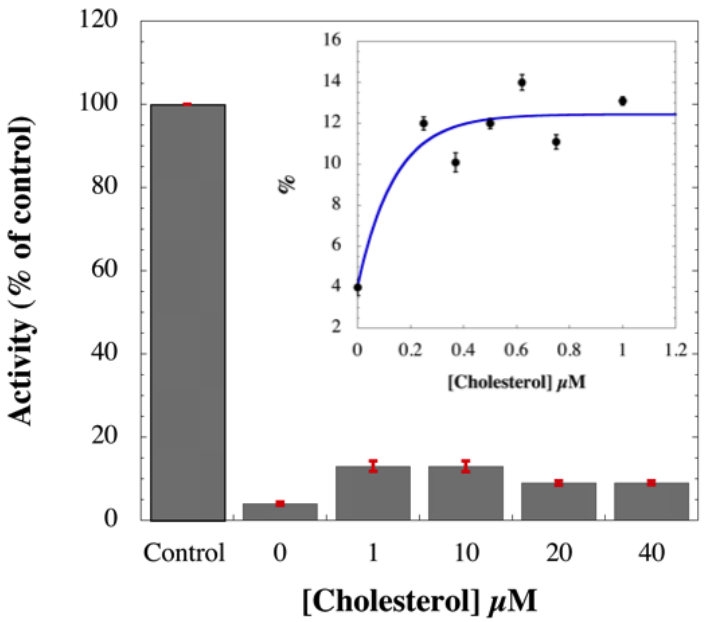

Figure 46: Dependence of NADPH oxidase activity as a function of cholesterol concentration in the absence of arachidonic acid.

Membrane fractions (2 nM Cyt *b*$_{558}$) with trimera 200 nM were incubated 4 min in presence of different concentrations of cholesterol. Control experiment representing 100 % (68 mol $O_2^{\bullet-}$/s/ mol cyt *b*$_{558}$) of the activity was realized in presence of 40 µM AA and in absence of cholesterol. The rates of superoxide production were measured as described in Materials and Methods. The data are the average of 3 independent measurements ± SEM.

Oxysterols are intermediates or even end products in cholesterol excretion pathways, thus it was interesting to check if oxysterols could have a different effect on NADPH oxidase from that of cholesterol. 25-hydroxycholesterol (Figure 47A) and 5a, 6a-epoxycholesterol that can be produced by enzymatic and non-enzymatic pathways of cholesterol (Figure 47B) were tested. Again slight activation of NADPH oxidase was achieved by the presence of oxysterols in a similar way to cholesterol. Thus we decided to focus on the influence of cholesterol on NADPH oxidase for the next experiments.

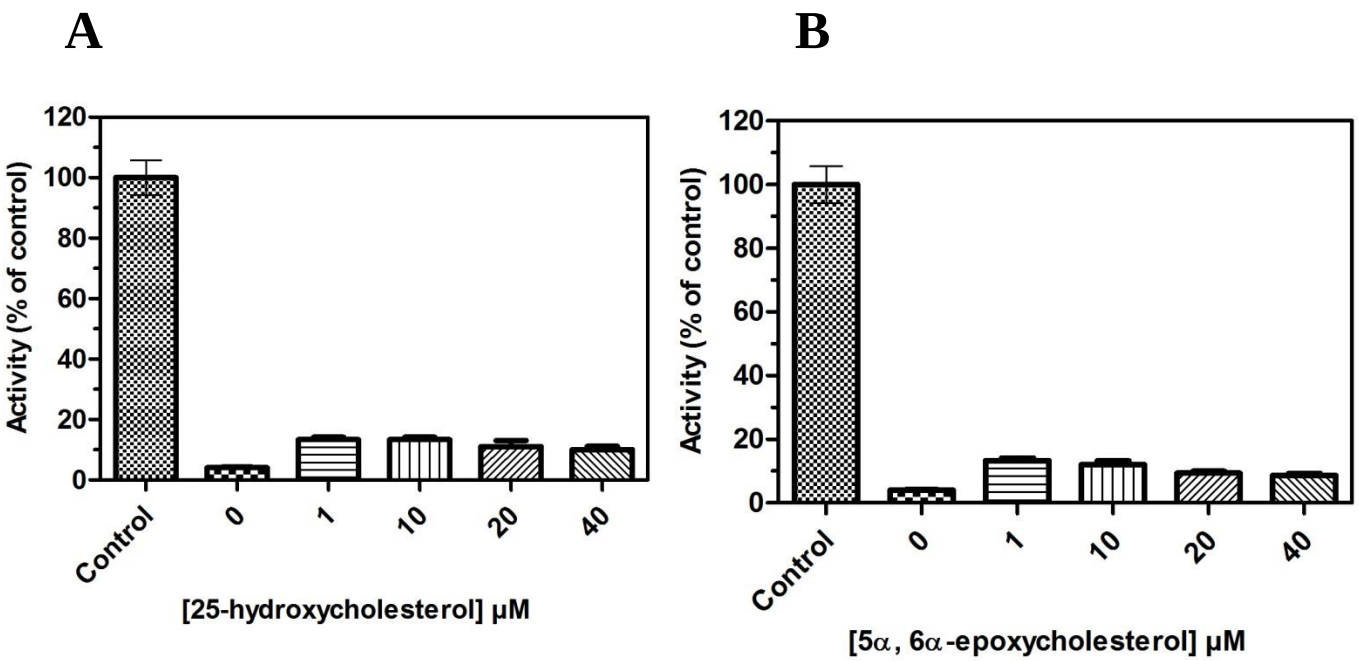

Figure 47: Dependence of NADPH oxidase activity as a function of oxysterols concentration in the absence of arachidonic acid.

Membrane fractions (3 nM Cyt *b*$_{558}$) with trimera 200 nM were incubated 4 min in presence of different concentrations of oxycholesterol (A) 25-hydroxycholesterol (B) 5a, 6a-epoxycholesterol. Control experiment representing 100 % (76 mol $O_2^{\bullet -}$/s/ mol Cyt *b*$_{558}$) of the activity was realized in presence of 40 µM AA and in absence of cholesterol. The rates of superoxide production were measured as described in Materials and Methods. The data are the average of 3 independent measurements ± SEM.

Pedruzzi et al. showed that 7-ketocholesterol induces oxidative stress and/or apoptotic events in human aortic smooth muscle cells (SMCs). They observed that 7-ketocholesterol induces ROS production by upregulation of Nox-4 specifically [301]. Different oxysterols can lead to different effect on NADPH oxidases other than NOX2.

IV. Superoxide production in the presence of AA and added cholesterol

1. The addition of cholesterol inhibits NADPH oxidase activity

Since cholesterol alone does not activate NADPH oxidase, we tested the cholesterol effect on the Nox-activation by AA. 20 mM stock solution of cholesterol was prepared in ethanol. Further dilutions were done in ethanol to get stocks of AA 65 mM supplemented with cholesterol at a concentration range of (0.1-16 mM), in order to keep the same amount of ethanol in all assay conditions. 3µL of each mixture were added in the cuvette to finally have in the cell free system, cholesterol at concentrations between 0.25-40 µM and AA at 40 µM. The AA induced NADPH-oxidase activity was followed upon increasing concentrations of cholesterol (Figure 48). The rate of production with AA alone was considered as 100%. Surprisingly, when membrane fractions and trimera were incubated together at 25°C with 0.25 µM cholesterol and 40 µM AA, the activity dropped to about 86 ± 5%. The AA-induced NADPH oxidase activity was thus reduced by addition of less than 10% of the intrinsic cholesterol amount. Then a second inhibition phase appeared for higher concentration of cholesterol. This decrease of the activity could be fitted by a two inhibitory sites equation and the parameters of the fit are given in Table 4.

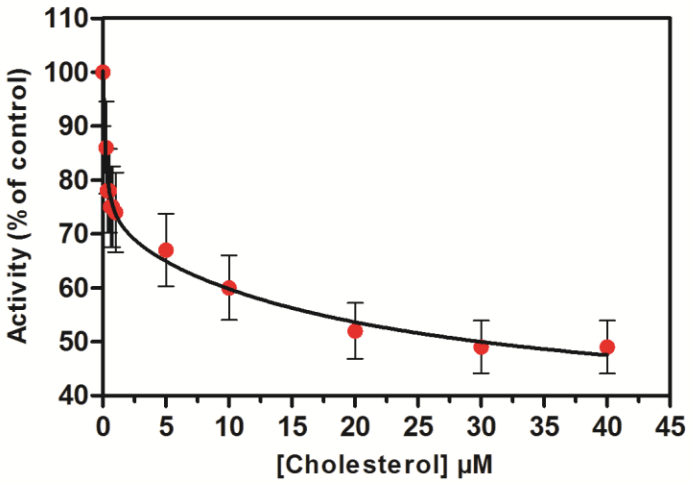

Figure 48: NADPH-oxidase activity inhibition by cholesterol

Neutrophil membrane fractions and trimera were incubated together in the presence of a mixture of 40 µM AA plus varied cholesterol concentration at 25°C. The oxidase activity was expressed as the percent of activity measured in the absence of cholesterol (79 mol $O_2^{\cdot-}$/s/mol cyt *b*$_{558}$) as described in Materials and Methods. The values are an average of 3 independent measurements ±SEM.

$$* \; Y = Y_{min} + \frac{Y_1}{\left(1 + [chol]/K_{i_1}\right)} + \frac{Y_2}{\left(1 + [chol]/K_{i_2}\right)}$$

	Value	error
Y_{min}(%)	35	9.6
Y_1 (%)	30	4.6
K_{i_1}(µM)	0.19	0.09
Y_2 (%)	35	7.3
K_{i_2} (µM)	21.2	16.7

Table 4: kinetic parameters of the fit by a two inhibitory sites equation.

This result had to be validated with the separated proteins. Thus, the same experiment was performed with separated subunits p67^{phox}, p47^{phox} and Rac instead of trimera. The AA-cholesterol-inhibition curves in the presence of trimera or of the cytosolic proteins were very close to each other (Figure 49). This shows that again the inhibition of NADPH oxidase observed with the trimera is not an artefact but takes place also with the more physiological proteins p67^{phox}, p47^{phox} and Rac.

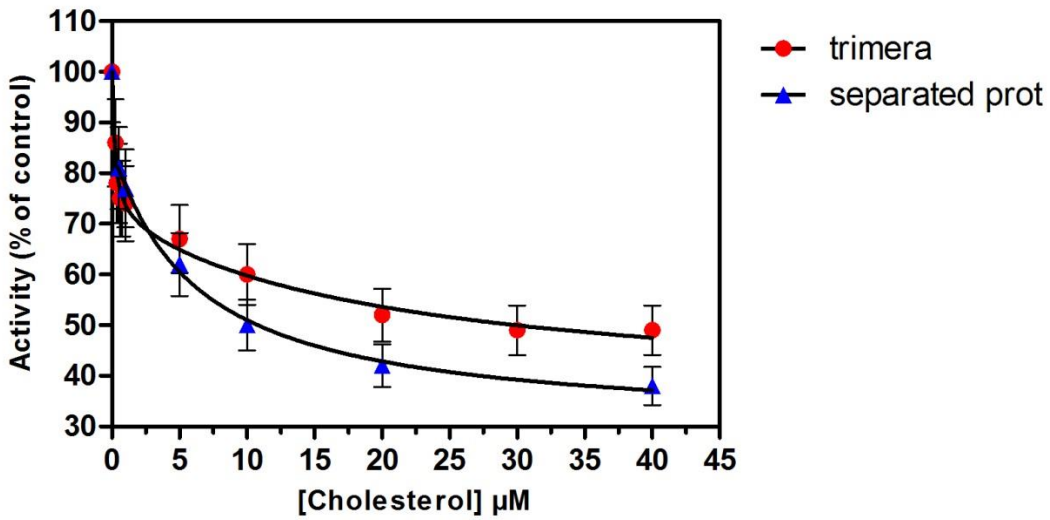

Figure 49: NADPH-oxidase activity inhibition by cholesterol in the presence of separated cytosolic proteins.

Neutrophil membrane fractions and the cytosolic subunits p67^{phox} 470 nM, p47^{phox} 450 nM and Rac 560 nM or trimera were incubated together in the presence of a mixture of 40 µM AA plus cholesterol at 25°C. The oxidase activity was expressed as the percent of activity measured in the absence of cholesterol (75 mol $O_2^{\cdot -}$/s/mol Cyt b_{558}) as described in Materials and Methods. The values are an average of 3 independent measurements ±SEM.

It was also important to check if the same inhibitory effect takes place at the physiological temperature 37 °C. Thus we incubate the trimera and membrane fractions with cholesterol 0.25-40 µM in a mixture with 40µM AA, at 37 °C. Again, a similar inhibitory effect of cholesterol on NADPH oxidase was observed (Figure 50).

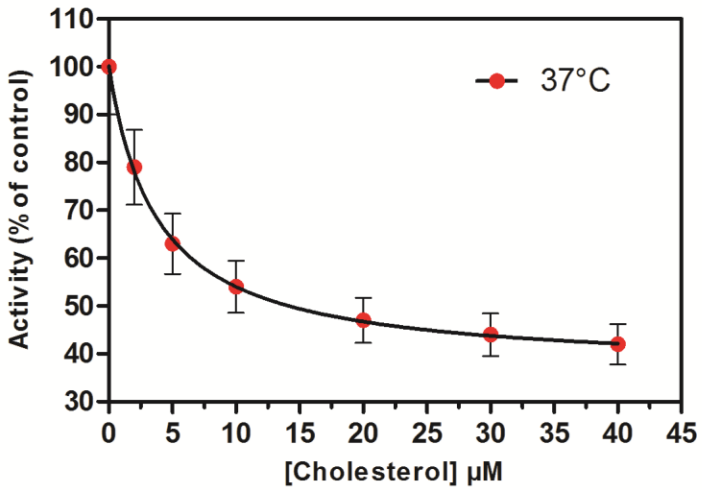

Figure 50: NADPH-oxidase activity inhibition by cholesterol at 37 °C

Neutrophil membrane fractions and trimera were incubated together in the presence of a mixture of 40 µM AA plus cholesterol at 37°C. The oxidase activity was expressed as the percent of activity measured in the absence of cholesterol (219 mol $O_2^{\cdot-}$/s/mol cyt *b*$_{558}$) at 37°C. The values are an average of 3 independent measurements ±SEM.

Finally, since this study is to better understand the events that could happen to Nox2 following hypercholesterolemia, we have explored the behavior of the phagocyte NADPH oxidase from hypercholesteremic donor. The AA-induced NADPH oxidase activity was also reduced by addition of cholesterol to the neutrophil membrane fractions in a similar way to the one from control donor (Figure 51).

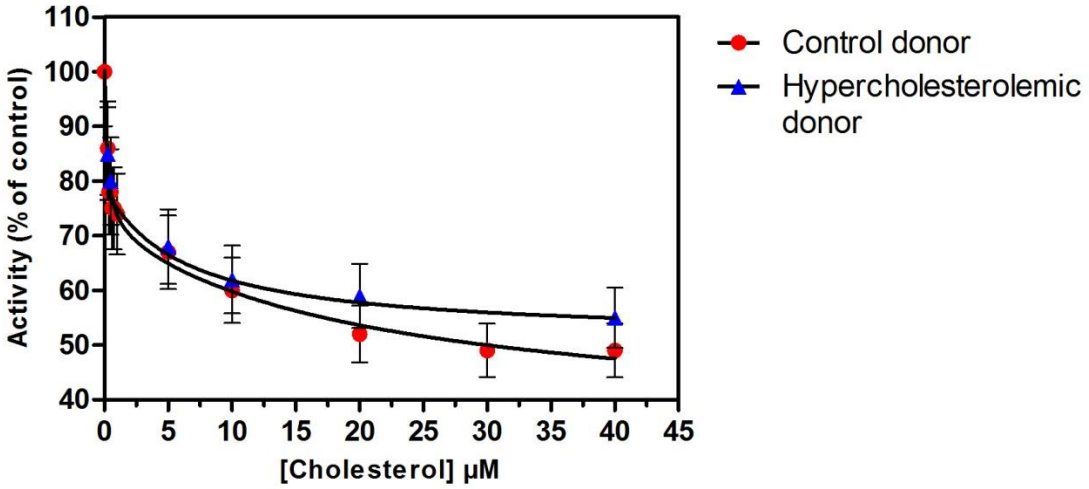

Figure 51: NADPH-oxidase activity inhibition by addition of cholesterol to neutrophil membrane fractions from hypercholesteremic donor

Neutrophil membrane fractions either from normal or hypercholesteremic donor were incubated together with trimera in the presence of a mixture of 40 µM AA plus cholesterol at 25°C. The oxidase activity was expressed as the percent of activity measured in the absence of cholesterol (92 mol $O_2^{\cdot-}$/s/mol cyt *b*$_{558}$) at 25°C. The values are an average of 3 independent measurements ±SEM.

The intrinsic cholesterol concentration in the human neutrophil membrane fractions from the hypercholesteremic donor was found to be 3.5 ± 1 µM of cholesterol for 25 µg/ml membrane proteins (5 nM Cyt *b*$_{558}$), which is 16% higher than the level of the "normal" donors. However unfortunately we know nothing about the level of cholesterol of the "normal" donors.

2. Effect of cholesterol on AA activation profile

To probe the effect of cholesterol on the NADPH activation profile by AA, we performed titrations of the activity *vs.* AA concentration in the absence and in the presence of two concentrations of cholesterol (0.5 and 20 µM). In this experiment, cholesterol was added at the same time as arachidonic acid (Figure 52).

In the presence of cholesterol, the $O_2^{\bullet-}$ production was lower on the full range of concentrations of AA, which confirms the inhibitory effect of cholesterol in a concentration-dependent manner. However the maximum activity was achieved with the same AA concentration and the bell-shape was kept.

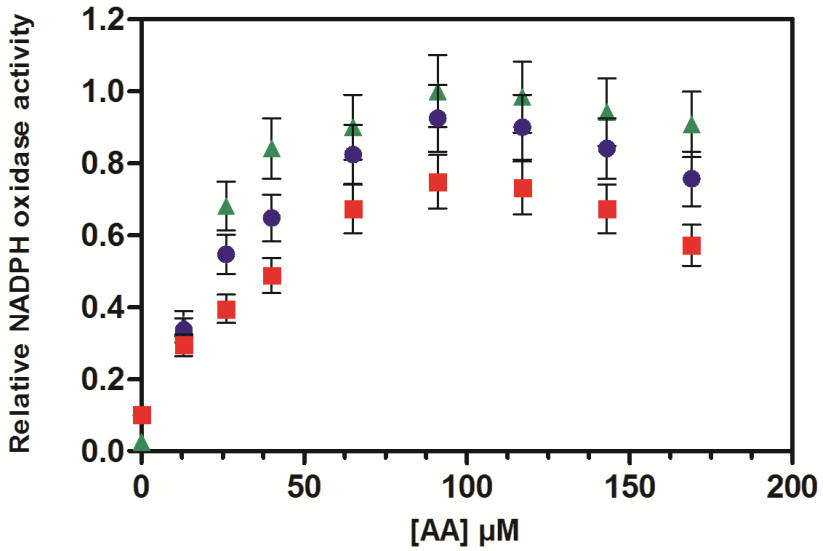

Figure 52: Effect of cholesterol on the AA-dependent activation profile.

Neutrophil membrane fractions and trimera were incubated together in the presence of a mixture of varying amounts of AA plus cholesterol. The cholesterol concentration was as follow, ▲: no cholesterol; ●: 0.5 µM cholesterol; ■: 20 µM cholesterol. Oxidase activities were expressed relative to the maximum activity (119 ± 12 mol $O_2^{\bullet-}$/s/mol Cyt *b*$_{558}$).The rate of $O_2^{\bullet-}$ production was achieved as described in Materials and Methods.

3. Modification of kinetic parameters in the presence of added cholesterol

The absence of effect of cholesterol on the AA activation profile described above raised the question of the mechanism by which addition of cholesterol decreases the activity of the complex. In that purpose, the rate of superoxide production for increasing concentrations of trimera with and without cholesterol was determined. This dependence could be fitted using a Michaelis-Menten-like equation (Equation 7, see Materials and Methods) and from each curve one could determine EC_{50} and V_{max} values. As expected, there was a marked loss in the oxidase activity in the presence of cholesterol for the whole range of concentrations of trimera, with important variations for both the EC_{50} and V_{max} values (Figure 53). In the presence of cholesterol, the complex exhibited 1.5 times lower V_{max} value and the EC_{50} was 1.6 times higher than its

values measured in absence of cholesterol (Table 5), which reflects a decrease of affinity of trimera for the Cyt*b*$_{558}$.

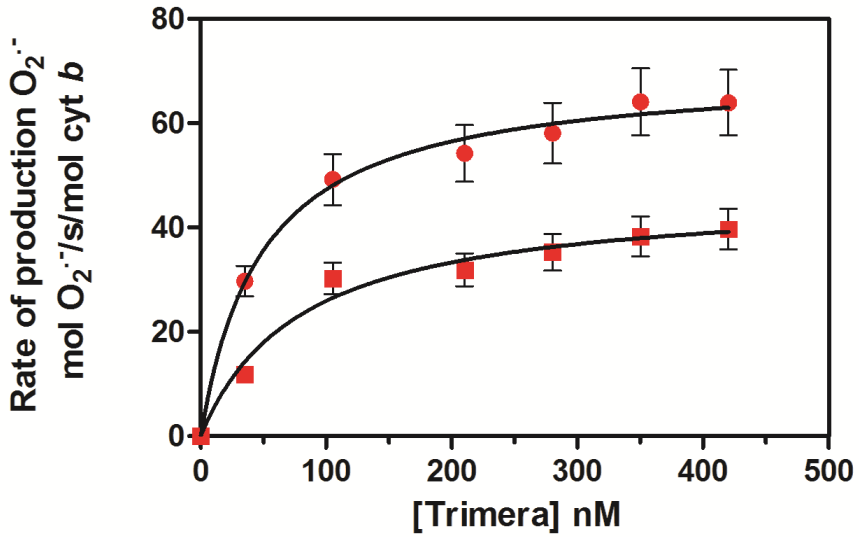

Figure 53: Effect of cholesterol on the trimera dependence NADPH oxidase activity

The assays mixtures consisted of trimera at varying concentrations (from 0 to 420 nM) and membrane fractions of human neutrophils (3 nM Cyt *b*$_{558}$) to which were added ●40 µM AA or ■ a mixture of 40 µM AA and 10 µM cholesterol. The superoxide formation was measured as indicated in Materials and Methods. The values are an average of three independent measurements ±SEM.

Kinetic parameters of NADPH oxidase activation by trimera		
Assay supplemented with:	**V_{max}** **mol $O_2^{\cdot-}$/s/mol cytb**	**EC_{50} (nM trimera)**
AA 40 µM	**70.3±2**	**48.6±3**
AA 40 µM, cholesterol 10µM	**46.6±6**	**79.8±19**

Table 5: Values of the parameters of the fit by Michaelis-Menten equation are shown

Each curve was fitted by Michaelis-Menten like equation using a Marquardt algorithm, leading to the determination of the EC_{50} and V_{max} values related to the trimera.

4. Effect of cholesterol addition during the assembly phase

To examine whether cholesterol had an effect on the oxidase assembly process, 10 µM of cholesterol were added at different times during the 4-min phase of incubation (Figure 54). Depending on the time at which cholesterol was added, various levels of inhibition were noticed. $O_2^{\bullet-}$ production was drastically lowered to ~66% of the control when cholesterol was added immediately after all the NADPH-oxidase components. The inhibition was less and less important (up to no inhibition) in function of the time of addition. If cholesterol addition took place 4 min after the mixing, the oxidase activity was comparable to that of the control. Again the same dependence was observed when the trimera or the cytosolic subunits were used. These results (Figures 53 and 54) suggest that cholesterol interferes with the interactions between the cytosolic proteins and Cyt *b*$_{558}$. There is little chance that this time dependence reflects a low rate of interaction between cholesterol and proteins because of the highly hydrophobic character of cholesterol. Its insertion in hydrophobic domains is immediate.

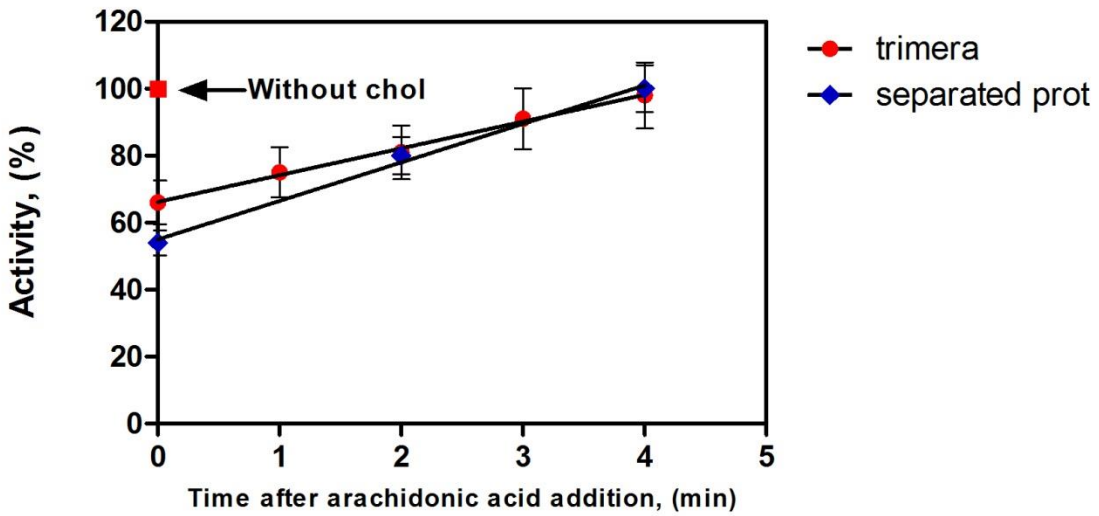

Figure 54: Effect of the addition time of cholesterol on NADPH-oxidase activity.

Membrane fractions and cytosolic subunits p67^{phox} 470 nM, p47^{phox} 450 nM and Rac 560 nM or trimera 200 nM and 40 µM AA were incubated 4 min in reaction buffer. 10 µM cholesterol were added at various times after the addition of AA. Conditions are as described under Materials and methods. Results are expressed as percentages of the control activity (without cholesterol addition). The values represent the means ± SEM of three independent experiments.

V. Structural effects of added cholesterol

1. Effect of cholesterol on water-soluble and membrane proteins

To evaluate the sensitivity of each component to cholesterol, superoxide anion production rate was measured after a pre-incubation of 10 s of membrane components or trimera or both, either with AA alone (Figure 55A) or with a mixture of cholesterol and AA (Figure 55B), before the 4 min incubation.

First, as said in the previous chapter, when both membrane fractions and trimera were preincubated 10 s separately with AA, and then incubated 4 min together, the activity was maintained to about 95% of the observed one in standard conditions. The same level of activity (95%) was measured when AA was incorporated only to the membrane fractions. On the other hand, when AA was added only to the trimera, the activity dropped to 73% (Figure 55A).

The experiment with AA (Figure 55A) served as control for the ones with cholesterol. In all cases, addition of cholesterol +AA either to the membrane or to the trimera or to both separately led to a decreased rate of superoxide production (Figure 55B). Incorporating cholesterol +AA only to the membrane fractions or only to the trimera gave comparable effect, indicating that cholesterol could act on both partners. When cholesterol was added to both counterparts, the activity drop was more important, in this case the addition of 5 µM or more of cholesterol led to a decrease of the activity down to ~50%. The rate of production of superoxide anions always decreased by increasing cholesterol concentration. This decrease was quasi linear when one component only was incubated with cholesterol and appeared biphasic when both components were in contact with the lipid, in agreement with the results presented Figure 48.

A

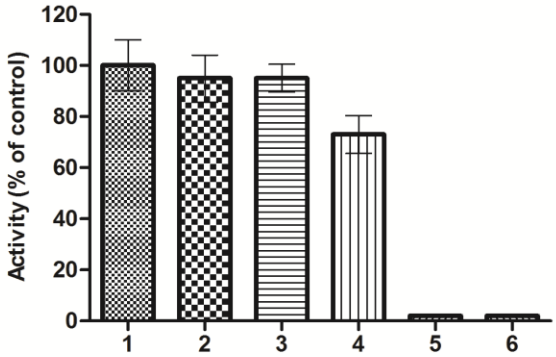

B

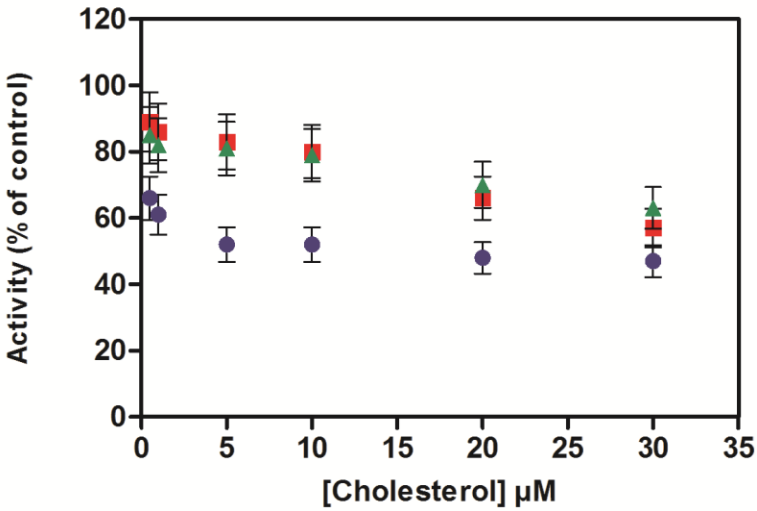

Figure 55: Effect of cholesterol on AA activation of membrane fraction and trimera.

(A) AA activation of membrane fraction and trimera. (1) In the control experiment membrane fraction and the trimera were incubated together during 4 min in the presence of 40 µM AA. The rate obtained corresponds to the 100% value (75 mol $O_2^{\cdot-}$/s/mol Cyt b_{558}). (2-4) Membrane fractions (MF) and trimera were separately preincubated during 10 s and mixed together for 4 min as follow: (2) both were preincubated with 40 µM AA, (3) only MF was preincubated with 40 µM AA, (4) only the trimera were preincubated with 40 µM AA. (5) The rate was measured in absence of trimera. (6) The rate was measured in absence of MF.
(B) Membrane fractions (MF) and trimera were separately preincubated during 10 s and mixed together for 4 min as follow: ■ only MF was preincubated with 40 µM AA plus cholesterol as indicated, ▲only the trimera was preincubated with 40 µM AA plus cholesterol as indicated and ● both were preincubated with 40 µM AA plus cholesterol. Activities in fig. 6B were expressed as the percent of activities measured of fig. 6A corresponding to each state to assess the cholesterol effect only.

2. Effect of cholesterol on the tryptophan intrinsic fluorescence of the trimera

To probe the effect of cholesterol on the trimera conformational state, we followed the variation of intrinsic tryptophan fluorescence spectra upon addition of cholesterol and/or AA (Figure 56). Surprisingly, the addition of cholesterol had no effect on the fluorescence yield of the trimera but a blue shift up to 5 nm was detected by increasing cholesterol concentration to 50 µM (Figure 56A), indicating that addition of cholesterol does not induce major conformational changes in the trimera, as AA does (Figure 39). When cholesterol was added to the trimera treated with 40 µM AA, the initial quenching of 25% due to the presence of AA still was visible, but there was no further lowering due to cholesterol (Figure 56B). In addition the blue shift up to 5 nm was still observed after the addition of both AA and cholesterol.

A

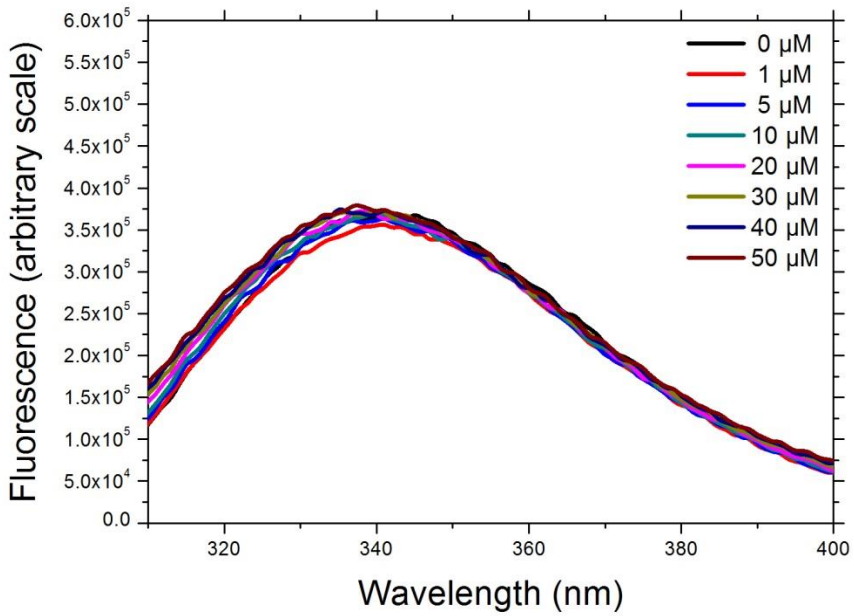

B

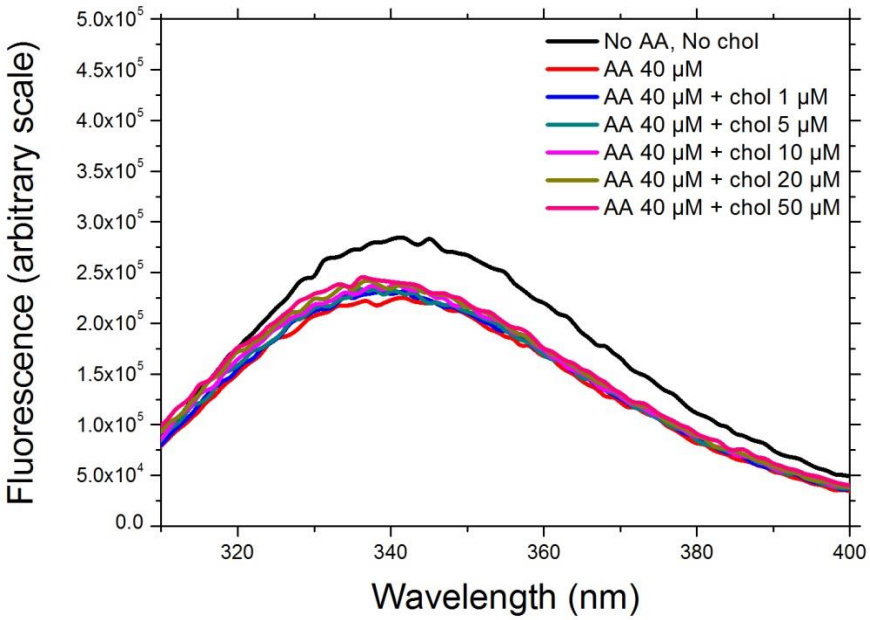

Figure 56: Fluorescence of trimera treated with cholesterol or/and AA.

The emission spectrum was measured using an excitation wavelength of 290 nm as described in the Materials and Methods section. Results are representative of at least three independent experiments. A: trimera 60 nM, cholesterol as stated in the figure legend. B: trimera 60 nM, AA 40µM, cholesterol as stated in the figure legend.

3. Effect of cholesterol on the secondary structure of the trimera

We aimed to study the possible secondary structure modifications of trimera that can be induced by cholesterol. We measured SRCD spectra of trimera (18 µM) with increasing cholesterol concentration (10-50 µM). As baseline, SRCD of cholesterol solution was measured. The secondary structure of trimera remained unchanged in the presence of cholesterol at the three concentrations tested (Figure 57). These results indicate that cholesterol cannot contribute to major secondary structures modifications and can explain the ineffectiveness of cholesterol to activate NADPH oxidase complex. At least the inhibition does not come from a secondary structural change of the cytosolic protein.

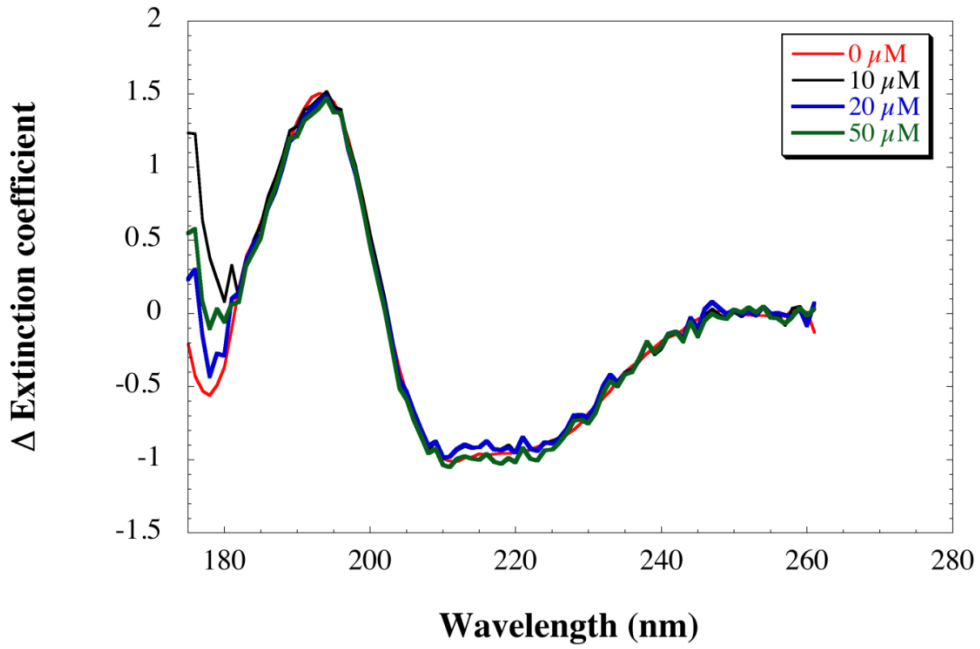

Figure 57: Effect of cholesterol on the SRCD spectra of trimera.

CD spectra of trimera (18µM) in the presence of increasing cholesterol concentration (10-50µM) are shown. The solvent was NaF 100mM /NaPi 10 mM pH 7, 25°C. Curves are fits using BeStSel.

VI. Discussion on the effect of lipids on NADPH oxidase

In this work we have explored the effect of added lipids and particularly cholesterol on the activity of the phagocyte NADPH oxidase. This study is related to events that could happen to Nox2 following hypercholesterolemia. It is also related to the hypothesis of modulation of NADPH oxidase activity by the membrane composition, in particular when inserted in lipid rafts rich in cholesterol. In fact, some studies have reported a distribution and regulation of Nox proteins and oxidase subunits in LRs, (most of the studies were performed in non-human cells [294-297] except those two in human neutrophils [292, 298]). Given that, NADPH oxidase activation demands many partners to work together, LRs can provide a useful platform for Nox2 and its subunits to aggregate and then function as an active enzyme complex that produces $O_2^{\bullet-}$ [296, 297, 399-403]. Studies in neutrophils showed that active NADPH oxidase would preferentially assemble in lipid rafts [298, 404]. The integrity of LRs would play an important

role in the regulation of NADPH oxidase activity and cholesterol would be an essential component for NADPH oxidase as shown in previous reports [294, 405].

1. On the required cholesterol presence in neutrophils

The regulatory role of LR was rationalized by the fact that cholesterol exerts a stabilizing role by filling the void space between sphingolipids and forming hydrogen bonds with them. Thus, cholesterol depletion by MβCD would lead to the breakdown of LRs as it suppresses the glue effect of cholesterol on sphingolipids [299, 300]. In addition to that, removal of raft-cholesterol leads to dissociation of most proteins from the rafts, rendering them nonfunctional [274].

Shao et al. showed that incubation of the cells with MβCD resulted in a loss of association of $gp91^{phox}$ with the LR fractions [292] while Vilhardt et al. reported that cholesterol depletion by MβCD reduced significantly $O_2^{\bullet-}$ production in both intact cells and a cell-free reconstituted system. MβCD effect was joined with a parallel reduction of the translocation of cytosolic components to the membrane [294]. Later, Fuhler et al. further demonstrated that treatment of neutrophils with the MβCD, abrogated fMLP-induced ROS production and activation of protein kinases ERK1/2 and B/Akt in both unprimed and primed neutrophils, further assisting the opinion that LR-associated NADPH oxidase produces ROS and contributes importantly to the onset of phagocytic respiratory bursts [406]. Malla et al. also observed that incubation of breast carcinoma cells with MβCD resulted in disruption of LRs and down-regulation of NADPH oxidase subunits [405]. Similarly, in bovine aortic resting endothelial cells where NADPH oxidase proteins were found preassembled and functional in membrane rafts, the enzyme activity was decreased by sequestering cholesterol [407]. Our results about removal of cholesterol by MβCD are in agreement with the preceding findings since the oxidase activity was decreased to 44±7 %. However, one study by Han et al. showed the opposite, they observed that lipid rafts maintained NADPH oxidase in the inactive state in human renal cells and cholesterol depletion translocated NADPH oxidase subunits out of LRs and increased oxidase activity [293]. It is possible that this effect depends on cell type.

2. On the target sites of cholesterol

The search of the cholesterol recognition/interaction amino acid consensus (CRAC) formulated as **L/V**-$(X)_{1-5}$-**Y**-$(X)_{1-5}$-**R/K-**, where X represents one to five of any amino acid, described for cholesterol binding site [408] revealed that $gp91^{phox}$ possessed five possible consensus sequence. However, only two CRAC sequences are located in the transmembrane domains (the first and sixth) of $gp91^{phox}$. In $p22^{phox}$, two CRAC sequences have been identified in the assumed transmembrane domains. The presence of cholesterol-binding motifs on transmembrane helices of $gp91^{phox}$ and $p22^{phox}$ would permit interactions between cholesterol and the Cyt b_{558} complex and may explain NADPH oxidase activity sensitivity to cholesterol.

Our results indicated slight but significant activation of NADPH oxidase complex in cell free system by addition of cholesterol alone at physiological concentrations (10-20% above the normal level), which is actually in the physiological uncertainty (3±1µM). Conversely, addition of cholesterol in this range had an inhibitory effect on AA activation of NADPH oxidase activity. This inhibition was observed when either trimera or separated proteins were tested. Similar amplitude was also observed at 37°C corresponding to physiological temperature. NADPH oxidase of neutrophils extracted from hypercholesteremic donors showed similar behavior. Finally, the inhibitory effect of cholesterol did not interfere with the action of AA (same profile), indicating different binding sites for both lipidic compounds.

Several facts indicate the presence of two independent inhibitory binding sites. Effectively, in Figure 48, the curve could be fitted only with a two-site inhibition equation. In addition, cholesterol inhibitory effect was observed when it was preincubated either with the membrane or with the trimera alone. When 10 µM cholesterol was added to one component (membrane or trimera) 20% inhibition was observed, but when both components were preincubated with the same concentration, a higher inhibition was measured (~50%). It strengthens the idea that cholesterol affects not only the membrane fraction but also the cytosolic one and that he effects are additive.

The kinetic parameters in the presence of cholesterol revealed that V_{max} for trimera is lower while EC_{50} is higher, which suggests a cholesterol binding site on the trimera and/or a less stable and imperfect assembly of the complex. Furthermore, cholesterol acts before assembly (Figure 53), which might reflect that, one of the cholesterol binding sites is in the interaction region

between membrane and cytosolic components, in the region hindered after assembly. Indeed, once the complex is formed, cholesterol cannot have access to it and makes no inhibitory effect. This effect has to be related to the observation that the depletion of cholesterol by MβCD also reduced the translocation of cytosolic proteins [293]. The decreases of activity observed when cholesterol is either depleted or added suggest strongly that the cholesterol concentration found in membrane neutrophil is optimal for NADPH oxidase activity and/or that added cholesterol does not reach the LRs but instead is inserted in proteins.

3. On the conformation of the cytosolic partner

We have shown recently that AA modified the environment of tryptophan residues in the separate cytosolic subunits: both $p47^{phox}$ and $p67^{phox}$ underwent fluorescence decrease, which would be related to structural modifications necessary for their interaction with Cyt b_{558} [226, 227]. Opposite to AA, cholesterol has no effect on the fluorescence of trimera. It has also no significant effect on the secondary structure of the trimera, as shown by the CD spectra. These results indicate that cholesterol cannot adapt the protein confirmation to the membrane subunit as AA does.

CHAPTER 3: EFFECT OF TITANUM DIOXIDE NANOPARTICLES ON NADPH OXIDASE

I. Introduction

TiO_2 NPs are metal oxide NPs commercialized for many uses in everyday life, however their toxicity has been poorly investigated. Most work to date has demonstrated that TiO_2 NPs toxicity is strongly related to ROS production and consequent oxidative stress. On the other hand, little information about TiO_2 NPs immunotoxicity is known. The photo-activation of these NPs is well known and has many applications [409, 410]. However, *in vivo,* the photocatalytic activity of TiO_2 is unlikely. UV and visible light are absorbed and no activation of TiO_2 NPs photo-catalysis of cellular components can take place, except in the skin [411]. Recently described effects of TiO_2 NPs on mammalian neutrophils and inflammation include the capacity of neutrophils to phagocyte and absorb TiO_2 NPs [412]. In addition, TiO_2 NPs were shown to activate neutrophils by phosphorylation of p38 mitogen-activated protein kinase (MAPK) and extracellular signal-regulated kinases -1/2 (Erk-1/2) [413]. Cellular internalization of NPs has been shown to activate macrophages and neutrophils that contribute to superoxide anion production by the NADPH oxidase complex [348, 349] thus it was important to investigate the influence of TiO_2 NPs on the behavior of the NADPH oxidase and to check if NADPH oxidase is one of the pathways involved in ROS generation by TiO_2 NPs.

In this chapter, we studied not only the effect of anatase TiO_2 NPs on the function of NADPH oxidase in cell free system and in human neutrophils but we also examined their effects on the cytosolic proteins conformation by different methods (fluorescence, synchrotron radiation circular dichroism (SRCD), transmission electron microscope (TEM), dynamic light scattering (DLS)). The use of these combined methods has provided a broad view of how TiO_2 NPs influence NADPH oxidase functioning and hypotheses about the origin of TiO_2 NPs toxicity. The results of this chapter are the subject of paper II.

II. TiO_2 NPs size characterization

Anatase TiO_2 NPs were a generous gift of Dr. Hynd Remita. They were suspended in deionized water (1 mg/mL) and sonicated in an ultra-sound bath for 10 min before use. The experiments were performed in PBS buffer. It is known that TiO_2 NPs are affected by the buffer and especially by phosphate ions and we chose this buffer to be as close as possible to living medium [414].

The hydrodynamic size of TiO_2 NPs in water and PBS was estimated by DLS. The average size of the NPs aggregates in water was about 350 ± 50 nm for the concentration range of 2-80 µg/mL of TiO_2. This NP aggregate population was the only one (100 %) for TiO_2 NPs concentrations lower than 20 µg/mL but another population of larger agglomerates whose sizes were estimated to about ~2000 nm (5 %) appeared when TiO_2 NPs concentration was higher than 20 µg/mL. We noticed also that the size of the NP aggregates in a physiological medium, such as PBS, was similar (460 ± 50 nm) to that in water. By TEM we could also observe particle aggregation (Figure 58A). From these techniques, we showed that the aggregates are constituted by particles of about 30± 5 nm (Figure 58B). These results are in accordance with those in the literature where it was shown that TiO_2 NPs tend to associate to form relatively strongly bonded aggregates or soft agglomerates [328]. TEM images also showed that when mixed with the membrane fractions, TiO_2 NPs are in contact with the vesicles (Figure 58C), and that aggregation of TiO_2 NPs was similar in absence and in presence of membrane fractions (Figure 58C). Likewise, DLS measurements showed that the size of TiO_2 NPs aggregates did not change when MF (0.5µg/mL Cyt b_{558}) or trimera 18 µg/mL were added to 20 µg/mL TiO_2 NPs, a concentration comparable to what was used in the cell free system assays for the measurements of NADPH oxidase activities. In conclusion, the presence of the cytosolic or membrane proteins did not change the state of the NPs.

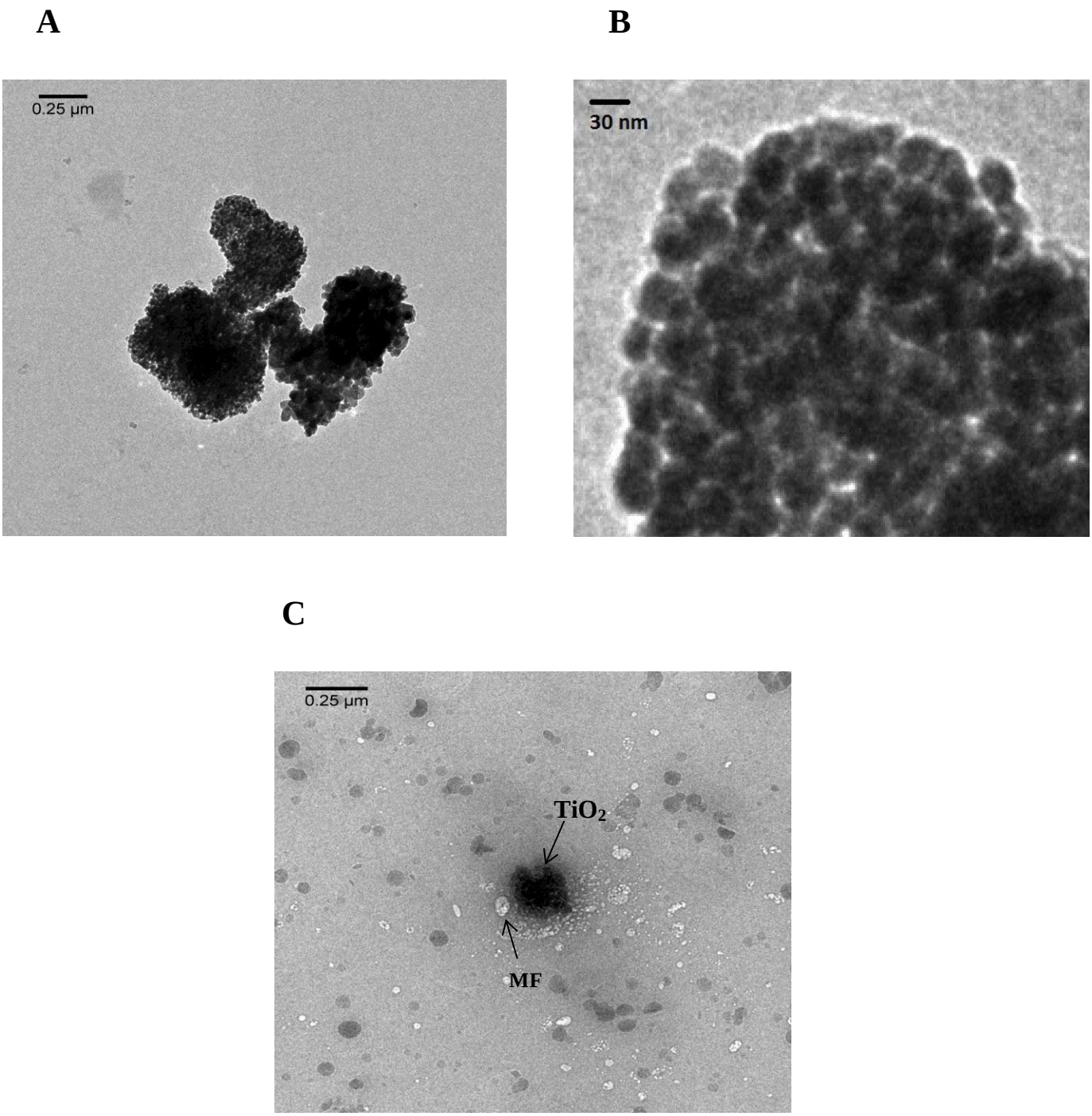

Figure 58: TEM images of TiO_2 NPs alone and with proteins

TEM images of (A) 0.5 mg/mL TiO_2 NPs alone; (B) enlarged view of the cluster; (C) 0.5 mg/mL TiO_2 NPs with MF (25µg/mL cyt *b558*) and 50 µg/mL trimera.

III. Structural effects

1. Tryptophan fluorescence of the trimera in the presence of TiO_2 NPs

The possibility of conformation changes of the trimera were evaluated by measuring the intrinsic fluorescence spectrum of tryptophan residues of the protein, before and after addition of TiO_2 NPs. Trimera contains a total of thirteen tryptophan residues (seven, four and two in the $p47^{phox}$, $p67^{phox}$ and Rac portions, respectively). The amplitude of the emission spectrum decreased linearly by the addition of TiO_2 NPs without any change of the wavelength at the maximum (340 nm) (Figure 59, 60). The decrease of fluorescence intensity indicates a quenching probably due to proximity of TiO_2 NPs and some tryptophan residues without change in the surrounding of these residues. The intensity of the shoulder at around 440 nm increased concomitantly with the decrease of the intensity of the 340 nm band, which might be due to energy transfer between the NPs and trimera (Figure 61).

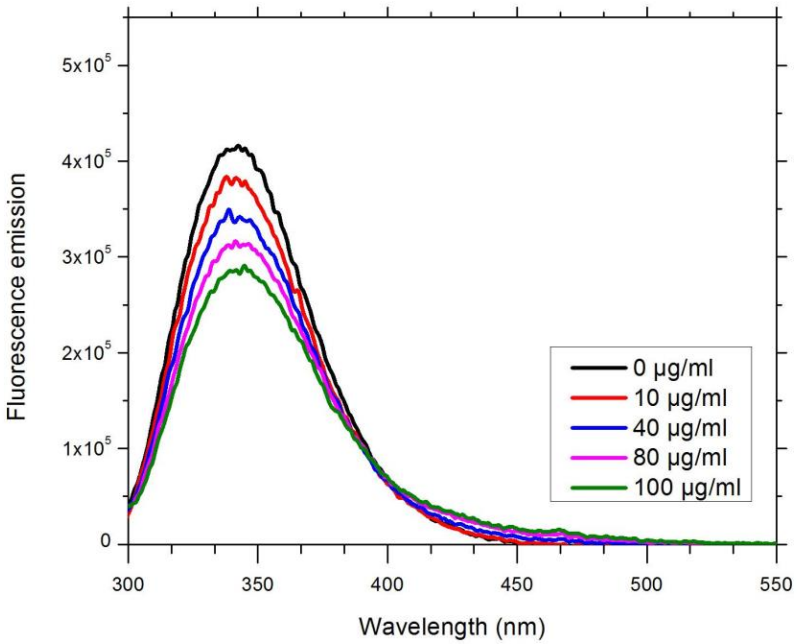

Figure 59: Fluorescence spectrum of trimera in the presence and absence of TiO_2 NPs.

The solution containing 5 µg/mL (60 nM) trimera and TiO_2 at the concentrations of 0, 10, 40, 80 and 100 µg/mL in a final volume of 3 mL of buffer (PBS supplemented with 10 mM $MgSO_4$,). The emission spectra were measured using an excitation wavelength of 290 nm as described in the Materials and Methods section. Results are representative of at least three independent experiments.

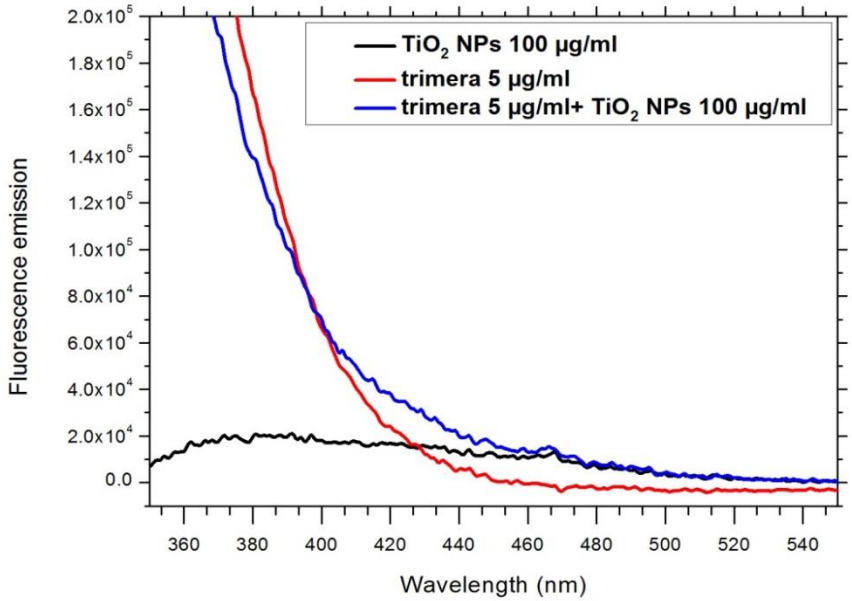

Figure 60: Enlargement of the fluorescence spectrum in the region 360-500 nm.

The spectrum of TiO_2 nanoparticles alone in solution is compared to that of trimera in the presence and absence of TiO_2. The solvent was PBS buffer supplemented with 10 mM $MgSO_4$.

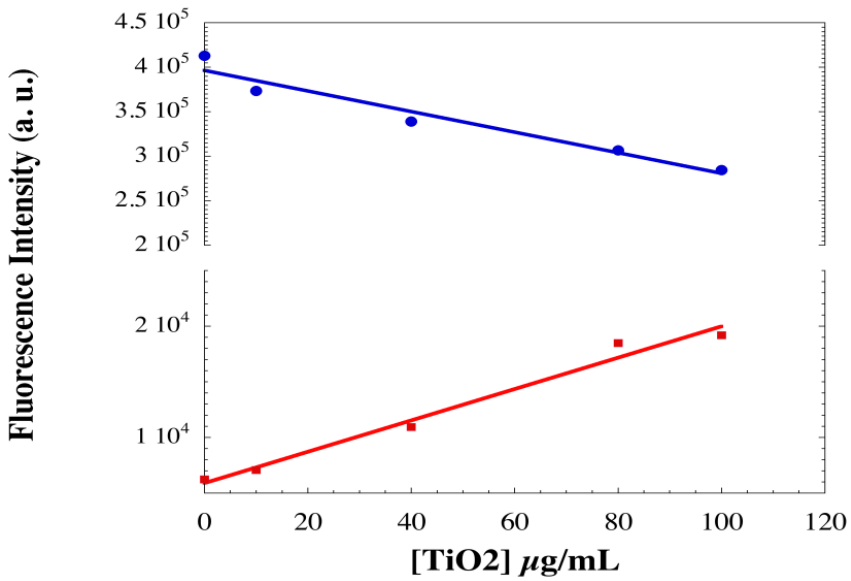

Figure 61: Variation of the emission fluorescence intensity of the trimera-TiO_2 NP suspensions

(A) at 340 nm, (B) at 440 nm. The mixture contained 5 µg/ml (60 nM) trimera and TiO_2 concentrations of 0, 10, 40, 80 and 100 µg/ml in a final volume of 3 mL of buffer (PBS supplemented with 10 mM $MgSO_4$). The emission spectra were measured using an excitation wavelength of 290 nm as described in the Materials and Methods section. Results are representative of at least three independent experiments.

As a control experiment, we have also checked the effect of TiO_2 NPs on the fluorescence of tryptophan (Trp) amino acid in solution. The quenching of Trp amino acid in solution by the NPs appears different in amplitude: the environment of the amino acids seems to be modified (shift of the maximum to the red) (Figure 62). This indicates some affinity between Trp and TiO_2 NPs.

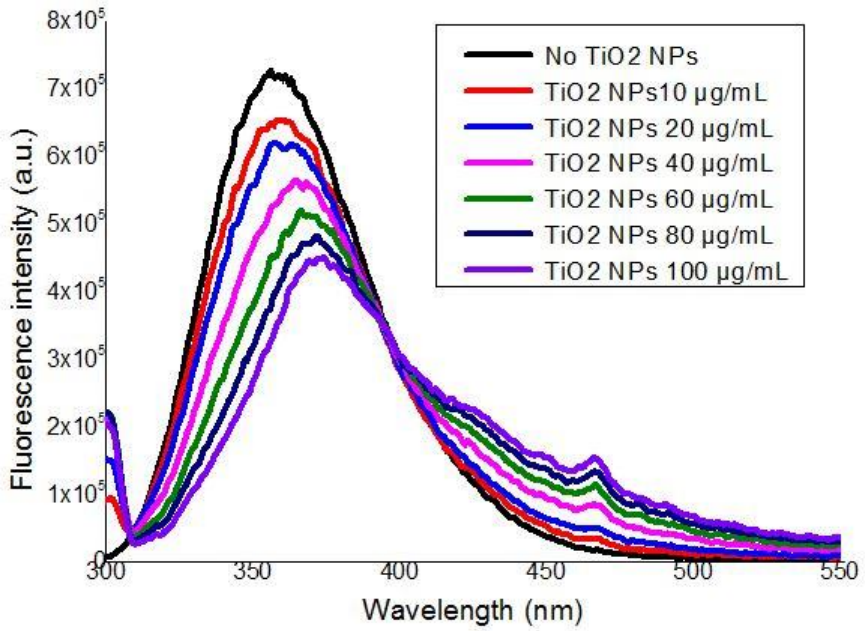

Figure 62: Fluorescence spectrum of Trp in the presence and absence of TiO_2 NPs.

Fluorescence emission spectra of the Tryptophan residues - TiO_2 NPs suspensions containing 8 µM Trp and TiO_2 concentrations of 0, 10, 20, 40, 60, 80 and 100 µg/mL in a final volume of 3 mL of buffer (PBS supplemented with 10 mM $MgSO_4$,). The emission spectra were measured using an excitation wavelength of 290 nm as described in the Materials and Methods section.

2. Effect of TiO_2 NPs on the secondary structure of the trimera

The eventual changes of the secondary structure due to the NPs were investigated by SRCD spectroscopy. We have recorded the SRCD spectra of 1.5 mg/mL (18µM) trimera in the absence and in the presence of 60 µg/mL TiO_2 NPs and 300 µM AA (Figure 63). In Table 5 are gathered the percentages of α-helices and β-sheets obtained by fitting the spectra with the BestSel software [370]. Analysis of the SRCD spectra of the trimera suggests that this chimeric

protein would be mostly composed of random coil (40 %) and that the content of helices would be very low (3-4%) which is surprising regarding the known structures of $p47^{phox}$, $p67^{phox}$ and Rac (Table 6). No major changes in the secondary structure are observed either with NPs or with AA. Altogether these results show that the interaction between NPs and trimera, indicated by fluorescence quenching, have no big consequence on the secondary structure of the protein.

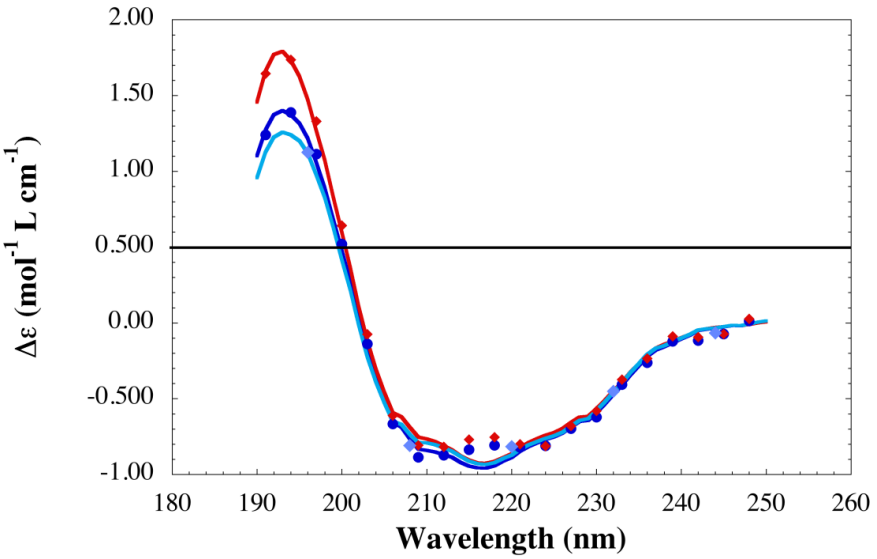

Figure 63: SRCD spectra of trimera alone and with either TiO_2 NPs or AA

SRCD spectra of the trimera (18 µM) alone (dark blue), in the presence of TiO_2 nanoparticles (60 µg/mL) (sky blue) and AA (300µM) (red). The solvent was NaF 100mM /NaPi 10 mM pH 7, 25°C. The points are experimental, the curves are the fits using BeStSel [370].

Assay enriched with	α-helix	β-sheets	Turns	Other
Trimera	4.1	40.5	13.8	41.7
Trimera + AA 300µM	2.5	42.0	13.7	41.8
Trimera + TiO_2 NPs	3.1	40.1	13.9	42.9

Table 6: Analysis of the SRCD spectra of trimera alone, with AA and with TiO_2 NPs, using BestSel software.

IV. Effects on the functionality

1. Effects of TiO_2 NPs on the NADPH oxidase activity

First, we have checked that TiO_2 NPs alone did not reduce cyt *c*, and/or that in these conditions, NPs by themselves did not produce superoxide anions. In order to investigate the effect of NPs on the NADPH oxidase, the rate of superoxide anion production was measured upon addition of TiO_2 NPs in the cell free assay conditions previously optimized with trimera [415] (Figure 64). The initial slope of the curve is equal to the rate of superoxide anion formation. This rate was faster in the presence of TiO_2 NP. The identification of $O_2^{-\bullet}$ was performed by addition of 50 µg/mL SOD.

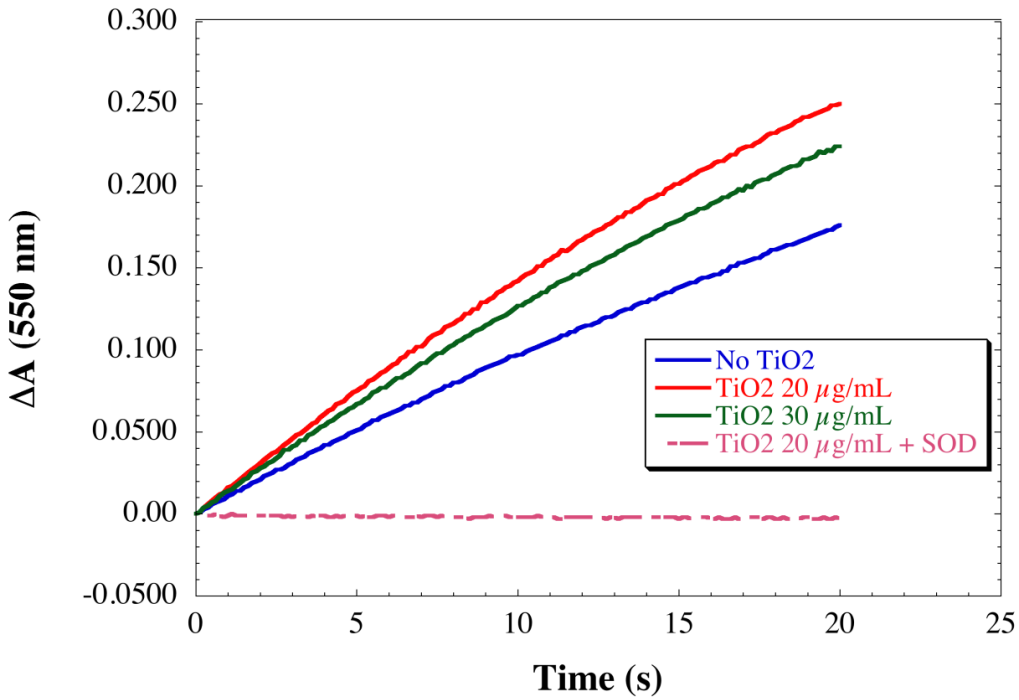

Figure 64: Kinetics of superoxide anion production in presence of TiO_2

Neutrophil membrane fractions (5 nM Cyt b_{558}) and trimera 200 nM were incubated together in the presence of 40 µM AA and (0, 20, 30 µg/mL) TiO_2 NPs. The production was initiated by addition of NADPH (250 µM) and the rate of $O_2^{-\bullet}$ was quantified by the reduction of cyt c (50 µM). Control (dotted red line) was performed by the addition of 50 µg/mL SOD. (on the fig: 20µg/mL TiO2 in presence of SOD). The initial rates of production of superoxide are the following: 92.0±0.3, 134.0±0.5, 119.2±0.4 mol O_2^{-}/s/mol Cyt b_{558} for TiO_2 NPs 0, 20, 30 µg/ml respectively.

The TiO_2 NPs dependence of the activity of the complex was investigated in parallel with either the trimera or the mix of cytosolic proteins $p47^{phox}$, $p67^{phox}$ and Rac. All components were incubated together with TiO_2 NPs (2-60) µg/mL and 40 µM AA (Figure 65). The rate of superoxide anion production in the absence of NPs was considered as 100% of NADPH oxidase activity. No difference was noticed between the trimera and the cytosolic proteins. In both cases we clearly observed an increase in the NADPH oxidase activity in the presence of NPs. The curves of Figure 65 exhibit a bell shape profile with a maximum (140% of the reference) at around 20 µg/mL of TiO_2 NPs. For higher concentrations of TiO_2 NPs (> 20 µg/mL), the rate returned close to the activation level of the control. This result indicates that TiO_2 NPs potentiate the NADPH oxidase activity. The activity remained constant for concentrations higher than 40 µg/mL probably due to some aggregations of NPs at higher concentrations.

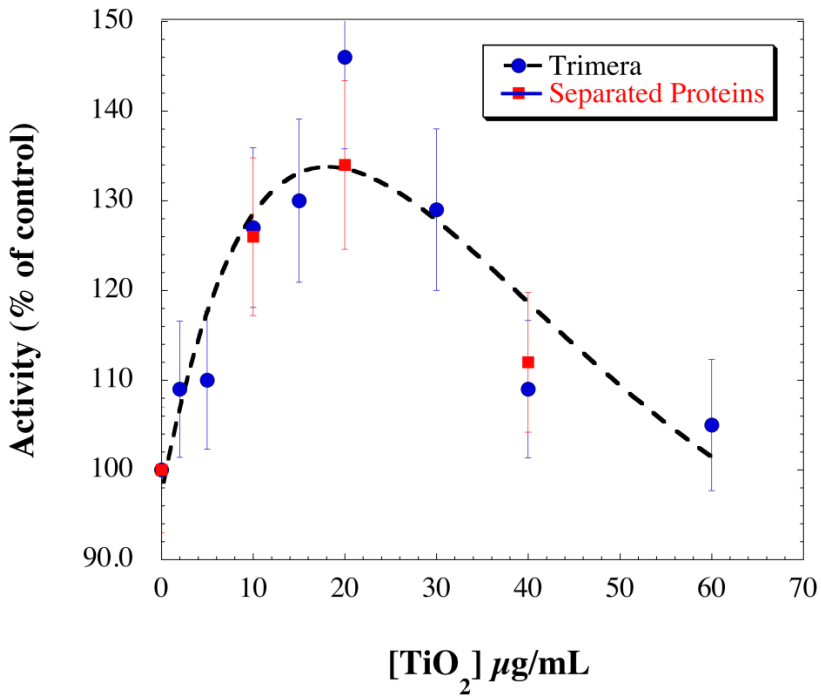

Figure 65: Dependence of NOX activity as a function of TiO_2 NPs concentration

Neutrophil membrane fractions (5 nM Cyt b_{558}) and trimera 200 nM (●) or the cytosolic subunits ($p67^{phox}$ 200 nM, $p47^{phox}$ 260 nM and Rac 580 nM) (■) were incubated together in the presence of 40 µM AA and TiO_2 NPs. Oxidase activity was expressed as the percent of activity measured in the absence of TiO_2 NPs (90 mol $O_2^{\cdot-}$/s/mol Cyt b_{558}), as described in Materials and Methods. Points are an average of 3 independent measurements. The dotted curve is a visual fit for both systems.

Thus, we further questioned whether TiO_2 NPs alone (20 or 40 µg/mL) could activate the NADPH oxidase complex and thus replace AA as activator (Figure 66). Almost no NADPH oxidase activity (5 ± 2 %) was detected with NPs instead of AA (control). Comparable results were obtained using the separated subunits where an activity of 4 ± 2 % of AA- dependent activity was reached, a value close to the negative control, in absence of AA and NPs.

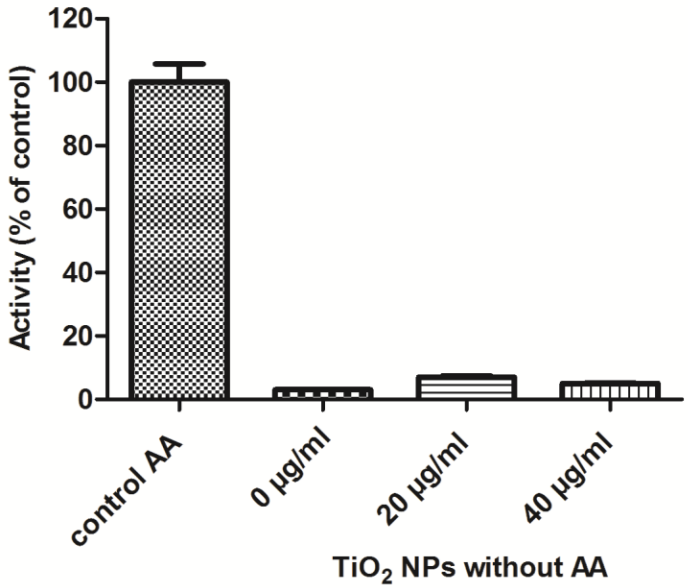

Figure 66: Dependence of NADPH oxidase activity as a function of TiO_2 NPs concentrations in the absence of arachidonic acid.

Membrane fractions (4 nM Cyt b_{558}) with trimera 200 nM were incubated 4 min in the presence of 0, 20 or 40 µg/mL TiO_2 NPs. Control experiment representing 100 % (83 mol $O_2^{\bullet-}$/s/ mol Cyt b_{558}) of the activity was realized in presence of 40 µM AA and in absence of TiO_2 NPs. The rates of superoxide production were measured as described in Materials and Methods. Data are the average of 3 independent measurements.

Since TiO_2 NPs cannot be considered as activating molecules, the significant increase in the rate of $O_2^{\bullet-}$ production with NPs might be due to an indirect effect, for example by interacting with AA. We therefore investigated the effect of TiO_2 NPs on the AA activation profile. To probe this effect, we performed titrations of the oxidase activity vs. AA concentration in the absence and in the presence of 20 µg/mL TiO_2 NPs added after arachidonic acid (Figure 67). The rate of production with 40 µM AA alone was considered as 100%. In agreement with the above-

mentioned results, in the presence of TiO_2 NPs, the $O_2^{\bullet-}$ production rate was higher on the full range of AA concentrations. Both curves exhibited bell-shapes as usual but the optimal concentration of AA was lower (62 µM) in the presence than in the absence (90 µM) of NPs.

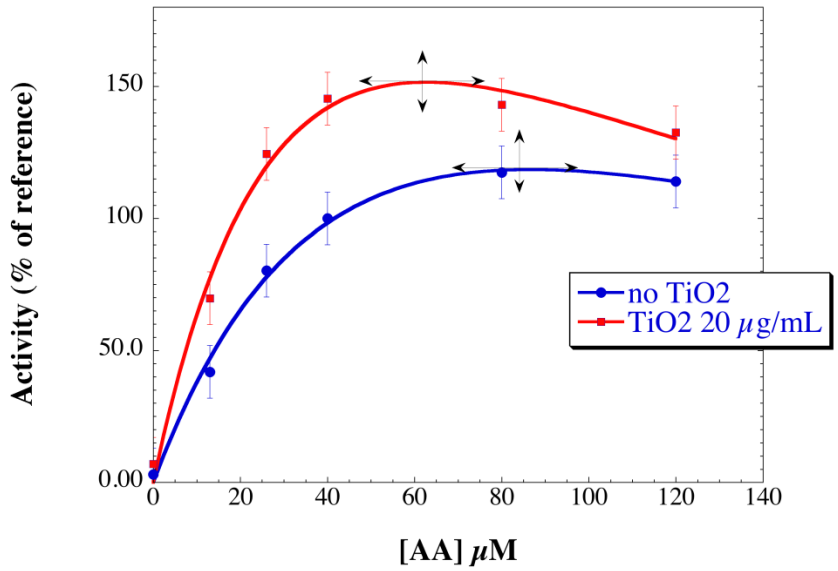

Figure 67: Effect of TiO_2 NPs on the AA-dependent activation profile.

Neutrophil membrane fractions and trimera were incubated together in the presence of varying concentration of AA. The TiO_2 NPs concentration was as follow, (●): no TiO_2 NPs; (■): 20 µg/mL TiO_2 NPs. Oxidase activities were expressed as the percent of activity measured in the presence of 40 µM AA (85 mol $O_2^{\bullet-}$/s/mol Cyt b_{558}). The curves are visual fits of the experimental points. The rate of $O_2^{\bullet-}$ production was measured as described in Materials and Methods.

2. Effect of TiO_2 NPs addition at different sequences of cell free system assay

To examine whether TiO_2 NPs have an effect on specific steps of the assembly, several concentration of TiO_2 NPs (10, 20, 40 µg/mL) were added at different times: (i) to the membrane fractions alone before mixing to the cytosolic subunits; (ii) to mixed membrane fractions and trimera; (iii) to the membrane fractions plus trimera plus AA (Figure 68). Regardless the stages at which TiO_2 NPs were added, the rates of production of superoxide were the same within

uncertainty. The highest $O_2^{\bullet-}$ production was still observed when 20 µg/mL TiO_2 NPs were incorporated in the system whatever the sequence of addition of NPs.

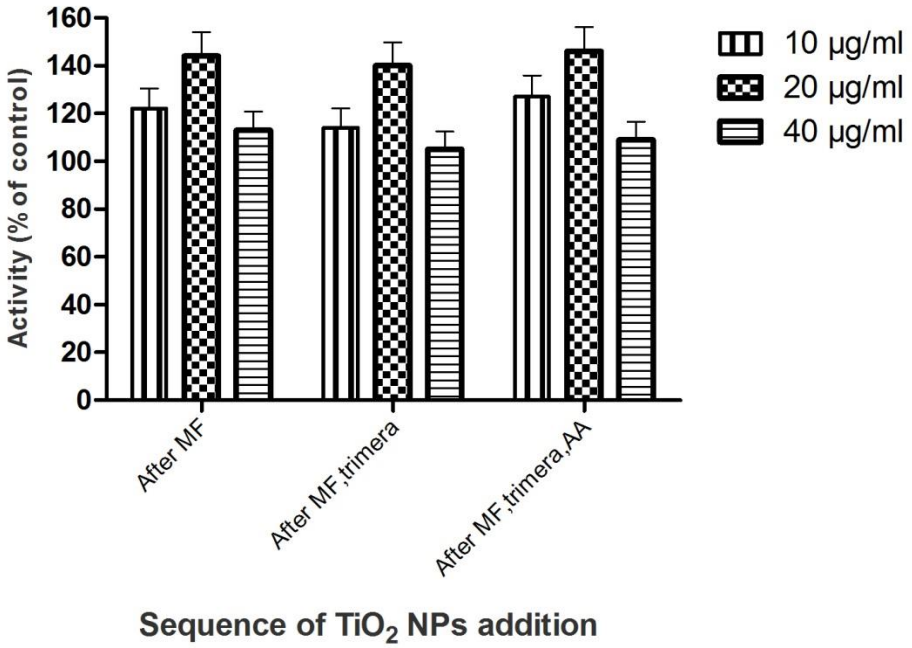

Figure 68: Effect of TiO_2 NPs as a function of its sequence of addition in the cell free system.

Neutrophil membrane fractions (4 nM cyt *b558*) and 200 nM trimera were incubated together in the presence of 40 µM AA and TiO_2 NPs (10, 20, 40 µg/mL). TiO_2 NPs was added to the solution either after the membrane fractions or after the membrane fractions and trimera or after the membrane fractions, trimera and AA. Oxidase activity was expressed as the percent of activity measured in the absence of TiO_2 NPs (84 mol $O_2^{\bullet-}$/s/mol cyt *b558*) as described in Materials and Methods. Points are an average of 3 independent measurements.

3. TiO_2 NPs effect on neutrophil cells

Neutrophil cells can be stimulated to produce superoxide anions by addition of PMA, which activates NADPH-oxidase through a signaling pathway leading to activation of PKC. To investigate the influence of TiO_2 NPs on neutrophil, cells were incubated either with 1.66 µM PMA alone or with 20 µg /ml TiO_2 NPs alone or both. The rates of superoxide anion production are reported in Table 6. No activity was observed in the absence of PMA. The rate of production of $O_2^{\bullet-}$ induced by PMA was 52.1 ± 10.5 nmol $O_2^{\bullet-}$/ min /10^7 cells. Interestingly, no NADPH oxidase activity was detected with TiO_2 NPs alone. TiO_2 NPs could not induce higher NADPH

oxidase activity in neutrophil cells when it was incubated with PMA in opposite to what we observed in cell free system (table 7).

Assay incubated with:	Rate of $O_2^{\cdot-}$ production (nmol $O_2^{\cdot-}$/min/10^7 cells)
PMA 0 µM	0
PMA 1.66 µM	52.1 ± 10.5
TiO_2 NPs 20 µg /ml	0.3
PMA 1.66 µM, TiO_2 NPs 20 µg /ml	53.4 ± 10

Table 7: Rates of superoxide anion production in neutrophil cells

V. Discussion on the effect of TiO_2 NPs

Oxide nanoparticles are widely used and their toxicity levels seem to be quite different in function of the metal albeit always related to induction of oxidative stress [416]. Some work has been done on the toxicity of ZnO NPs. A ROS formation enhancement was observed in ZnO-treated liver cells [417-419] and on ZnO-treated-macrophages from wt mice, whereas this formation was impaired in the treated macrophages from the $p47^{phox-/-}$ animals. To our knowledge, this is the only work that has been done on NADPH oxidase. [417]. The use of TiO_2 NPs has become widespread including in situations where they can be absorbed by living bodies. The photocatalytic activity of TiO_2 is well known [420], however UVA and visible light do not penetrate inside the body. Thus there is no light exposure and no activation of TiO_2 NPs by photo-catalysis.

The toxic effects of TiO_2 NPs seem to be mainly due to indirect production of ROS and therefore to induction of oxidative stress. One of the first studies about interaction between NPs and neutrophils was done in 1988; Hedenborg demonstrated that TiO_2 induced the production of ROS by human neutrophils [421]. Goncalves et al showed that TiO_2-induced change in cellular

morphology in a concentration-dependent manner in neutrophils, indicating a capacity to activate neutrophils [413, 422]. It was also reported that TiO_2 NPs increased respiratory burst of fish PMNs [423]. Additionally, TiO_2 NPs were shown to induce oxidative damage to human bronchial epithelial cells in the absence of photoactivation [424]. They are known to enhance superoxide production in osteoblasts [344]. TiO_2 NPs were shown to interact with proteins and enzymes in hepatic tissues, interfering with antioxidant defenses mechanisms and leading to generation of ROS [425]. Since NADPH oxidase is a major actor of oxidative stress by producing superoxide ions, it was evident that investigating the effect of TiO_2 NPs on this enzyme constitutes a relevant issue.

Our TEM images showed that NPs remain in the aggregation state even when they are in contact with the proteins. It was demonstrated that phagocytes are able to phagocytose particles when they are bigger than100 nm [426]. Additionally, it was reported that NPs enhance the ability of human neutrophils to exert phagocytosis by a Syk-dependent mechanism [427]. Thus, TiO_2 NPs in our case can enter the cell by phagocytosis and may lead consequently to activation of NADPH oxidase. TiO_2 NPs aggregates are known to interact with neutrophils. Recent work by Scanning electron microscope [347] showed increasing stiffness of the membrane and cell morphology alteration. Our present results indicate that this stiffness might not impede the NADPH oxidase functioning.

In vivo, it was shown that proteins adsorb on TiO_2 NPs. In some cases, these NPs induced conformational changes in proteins and affected their functions [339, 428, 429]. The Trp fluorescence intensity of fibrinogen is quenched, resulting from its interaction with TiO_2 NPs. Furthermore, CD experiments showed that fibrinogen secondary structure was slightly disturbed by TiO_2 NPs. Finally, Wang et al. proposed that exposure to TiO_2 NPs may have effect on human health by activating or inactivating functional proteins [430]. It is well known that the cytosolic proteins must undergo conformational changes to lead to active enzymes. Indeed, the lack of change of the CD spectra (Fig 18) suggests that TiO_2 NPs have no significant effect on the secondary structure of the trimera. Nevertheless, the quenching of fluorescence of the endogenous tryptophans of the trimera induced by the presence of NPs indicates that the NPs are probably close to the protein. Similarly, TEM images showed that membrane fractions are close to TiO_2 NPs. Taken all together, on one hand NADPH oxidase proteins possibly adsorb on the

NPs through the formation of a complex NPs- cytosolic and membranous proteins. On the other hand this does not prevent their assembly and the formation of an active NADPH oxidase.

In the case of NADPH oxidase, we do not observe any ROS production in absence of PMA, in contrast to Jovanovic's group finding where TiO_2 NPs increased respiratory burst when incubated with fish PMNs alone [423]. The different effects of TiO_2 NPs can be explained by the fact that neutrophils of aquatic vertebrates are different from those of human.

Surprisingly, the presence of TiO_2 NPs increased the rate of superoxide anion production of AA-induced NADPH oxidase in cell free system (up to 140% of its value without NPs), this effect being dependent on the NPs concentration. Differently, 20 µg/ml TiO_2 NPs cannot induce PMA over-activation of NADPH oxidase in neutrophil neither inhibits the activation by PMA. It is possible that 20 µg/ml NPs are not enough to over stimulate the neutrophils or that they could not penetrate into the cells.

TiO_2 NPs do not interact at a specific step of activation, indicating that their targets are not specifically the membrane fraction or the cytosolic proteins and that it does not prevent the complex formation but rather target the entire complex assembled and active. Since the presence of TiO_2 NPs modifies the AA-dependent activation profile of the enzyme as shown in Figure 61, one can suggest that NPs induce changes, which are important for the activity. We can postulate that a more efficient structure of the NADPH oxidase complex is attained in the presence of NPs. We can exclude a consequence of AA availability due to NPs since the higher NADPH oxidase activity is observed at lower concentration of AA in the presence of NPs than in their absence. This phenomenon cannot be attributed only to an interaction with the sole membrane fraction since the sequence of addition of the NP had no effect on it. It is likely that NPs sustain the entire active complex. Taken together, these facts indicate that the secondary structure may be conserved and at the same time other modifications must have happened to lead to hyperactivation.

CHAPTER 4: EFFECT OF PLATINUM NANOPARTICLES ON NADPH OXIDASE

I. Introduction

Our aim in this chapter is to evaluate the possibility that NADPH oxidase is one of the pathways involved in ROS generation by Pt NPs which can lead to the effective damage in cancer cells or the undesired oxidative stress in the adjacent healthy cells [364, 431]. Therefore we investigated the influence of platinum nanoparticles (Pt NPs) on the behavior of NADPH oxidase, present in the neutrophil phagocytes.

The study is focused on the effect of Pt NPs on the enzymatic behavior of NADPH oxidase. In addition to studying the effect of Pt NPs on the function of NADPH oxidase we have also examined their effects on proteins conformations by different techniques (fluorescence, TEM, DLS). The use of these combined techniques gave us some answers to the preceding questions. We also investigated the potential impact of Pt NPs on NADPH oxidase proteins under gamma irradiation as these NPs were proposed for the enhancement of the anticancer therapeutical protocol where NPs are associated with radiotherapy.

II. Synthesis and characterization of platinum nanoparticles

The synthesis of platinum nanoparticles performed by Daniela Salado Leza (ISMO, Paris-Sud University) was mediated by γ -ray water radiolysis. The hydrated electrons and the reducing radicals (H·) formed during water radiolysis induce homogeneous reduction and nucleation [321]. The main advantage of this method is to synthesize nanoparticles in water, which is compatible with the use of biological systems. Polyethylene glycol PEG (Mw= 1000) was used to stabilize and control NPs growth during synthesis. PEG is a commonly used stabilizer for biomedical applications (FDA approved) due to its physico-chemical characteristics and biological compatibility [432]. Pt NPs were characterized first by their size (diameter) and found to be in the nanoscale range. TEM imaging and the size distribution histogram revealed that the particle diameter of 1 mM platinum nanoparticles stabilized by PEG is estimated to be 4±2 nm (Figure 69A, Figure 70A), which corresponds approximately to 1000 platinum atoms in a particle, while the size of a naked platinum nanoparticles at 1 mM is 30± 10 nm ((Figure 69B, Figure 70B). Size measurements from TEM imaging showed that solutions of PEG-coated nanoparticles stored twenty days remain stable (5± 2 nm) (Figure 69C).

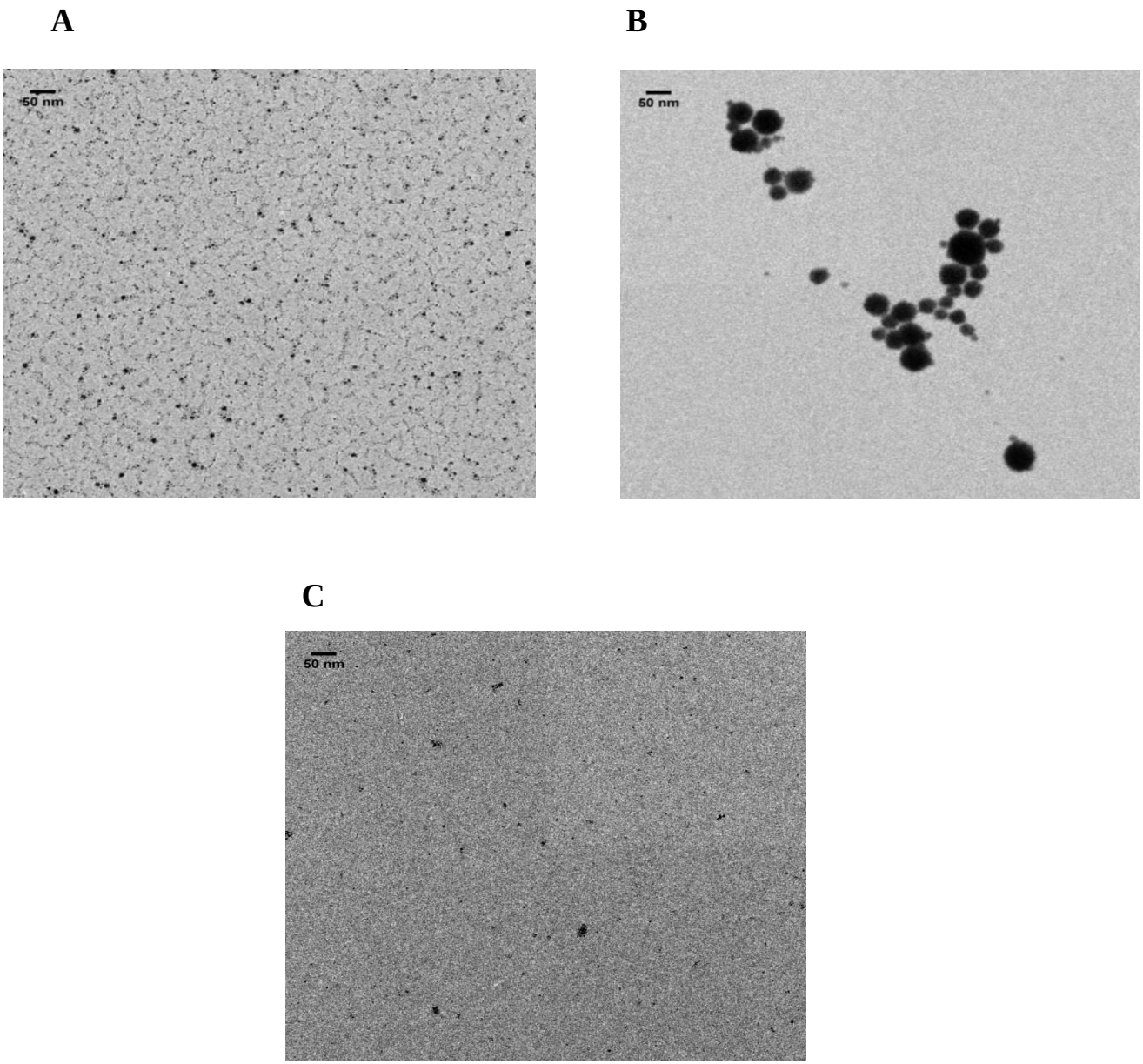

Figure 69: Characterization of platinum nanoparticles by transmission electron microscope

TEM of 1 mM (A) Pt NPs coated with PEG, (B) naked Pt NPs. (C) Pt NPs coated with PEG stored for twenty days.

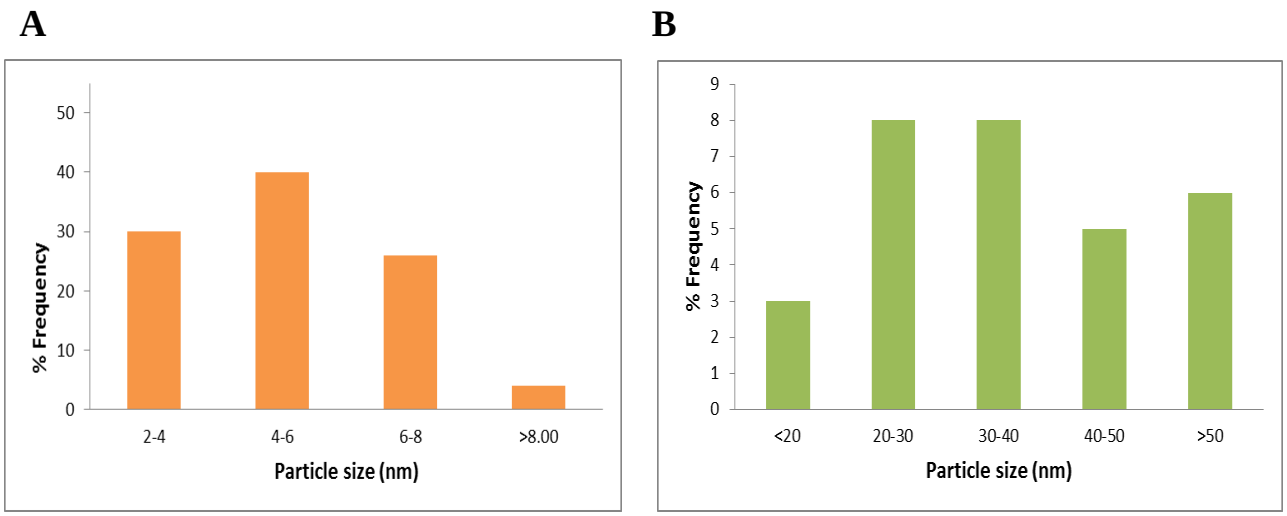

Figure 70: Size distribution histogram generated using TEM for (A) Pt PEG NPs, (B) naked Pt NPs.

The average hydrodynamic size of Pt NPs in water and PBS was estimated by DLS. We found that 1 mM PEG-coated Pt NPs had a size of 8.5± 2 nm while the size of 1 mM naked Pt NPs is 108± 5 nm both in water and PBS. The size estimated by DLS was bigger since it measures not only the NPs core but also the solvent shells around. The size of Pt naked NPs is largely increased, they are probably aggregated. Then the size of Pt PEG NPs was estimated by DLS in presence of the cytosolic proteins of NADPH oxidase. We found that the hydrodynamic size of Pt PEG NPs increases up to 13 nm in the presence of 200 nM trimera, which suggests that Pt PEG NPs interact with the proteins.

III. Interaction of Pt NPs with the trimera determined by fluorescence emission

Since DLS showed that Pt PEG NPs and trimera are in contact, it was necessary to check if NPs can cause any conformational modifications of the trimera. The intrinsic fluorescence emission spectrum of trimera, which contains 13 tryptophan residues, was recorded between 300 and 500 nm, in absence of NPs and with different concentrations of Pt PEG NPs (0.1-2µM). The amplitude of the emission spectrum of trimera decreased in the presence of Pt PEG NPs with a small shift in the maximum wavelength (340 nm) (Figure 71). The fluorescence quenching was observed even with the smallest concentration of NPs (0.1µM) used and increased slightly with

the concentration of NPs. This decrease of fluorescence intensity indicates again proximity of Pt PEG NP and trimera. Differently, no energy transfer between Pt NPs and trimera was measured opposite to what seemed to happen in the case of TiO_2 NPs.

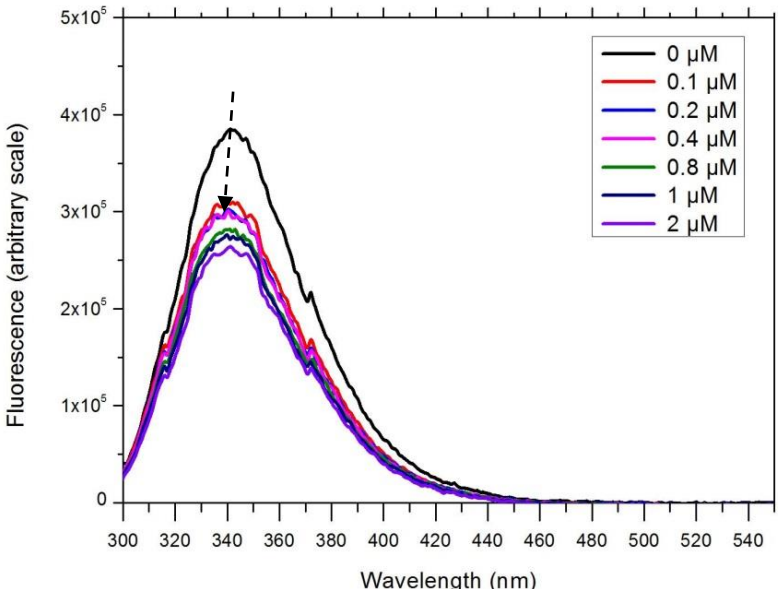

Figure 71: Fluorescence emission spectra of the trimera-Pt PEG NPs solutions

The solutions contain 60 nM trimera and Pt PEG NPs at the indicated concentrations in a final volume of 3 mL of buffer (PBS supplemented with 10 mM $MgSO_4$,). The emission spectra were measured using an excitation wavelength of 290 nm as described in the Materials and Methods section.

IV. Effects on the functionality of NADPH oxidase

1. Pt PEG NPs as an activating molecule?

We aimed at determining whether Pt PEG NPs alone (200, 400 nM) could activate the NADPH oxidase complex and the production of superoxide anions as our formal activator AA does (Figure 72). Interestingly almost no NADPH oxidase activity (3 ± 1 %), equivalent to zero within uncertainty, was detected in presence of Pt PEG NPs instead of AA (control = 100 %). Comparable results were observed when naked Pt NPs were tested and similar results were obtained using the separated subunits $p47^{phox}$, $p67^{phox}$ and Rac, where no activity was measured (data not shown).

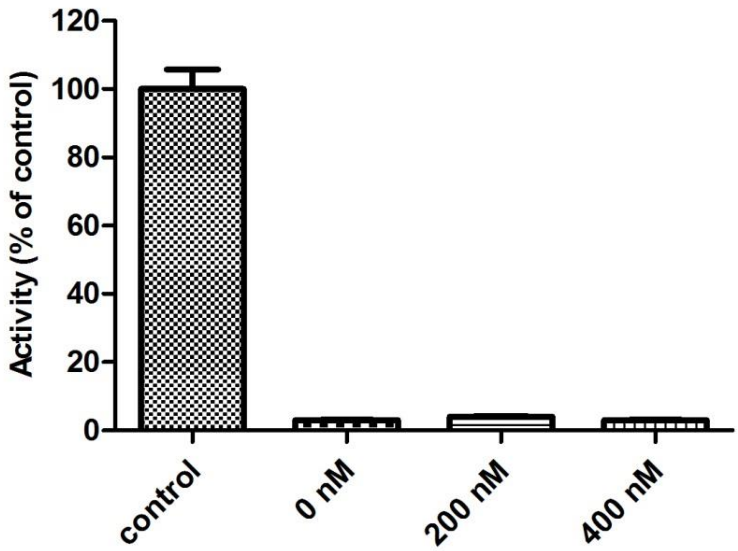

Figure 72: Dependence of NADPH oxidase activity as a function of Pt PEG NPs concentrations in the absence of arachidonic acid.

Membrane fractions (4 nM Cyt b_{558}) with trimera 200 nM were incubated 4 min in presence of 0, 200, 400 nM Pt PEG NPs. Control experiment representing 100 % (95 mol $O_2^{\bullet -}$/s/ mol Cyt *b558*) of the activity was realized in presence of 40 µM AA and in absence of NPs. The rates of superoxide production were measured as described in Materials and Methods. Data are the average of 3 independent measurements ± SEM.

2. NADPH oxidase activation by AA in the presence of Pt-NPs

Since Pt NPs alone do not activate NADPH oxidase, we have estimated their effect on the enzyme activated by AA. The AA-induced NADPH oxidase activity was measured upon increasing concentrations of Pt NPs (Figure 73). The effect was investigated in parallel with either the PEG NPs or the naked NPs. Both Nox components were incubated with Pt PEG NPs (100-400 nM) or Pt naked NPs (0.1-3.2 µM) and 40 µM AA (Figure 73). The rate of superoxide anion production in the absence of NPs was considered as 100% of NADPH oxidase activity. Similar rates of superoxide production were measured in the presence or absence of Pt PEG NPs or Pt naked NPs for the whole range of tested NPs concentrations. No significant activation or inhibition of NADPH oxidase activity was observed even with the highest concentrations of Pt PEG NPs. A very small inhibition, within uncertainty, is observed with Pt naked NPs (Figure 73B). These results indicate that Pt NPs have no important effect on AA-induced NADPH oxidase activity.

A

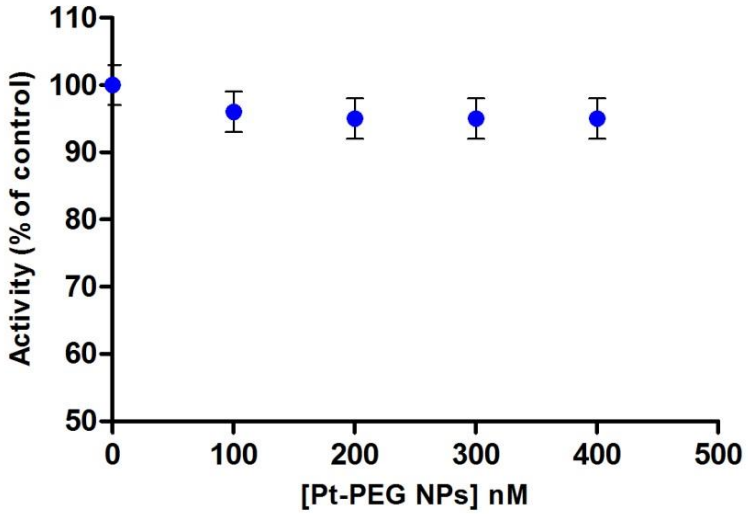

B

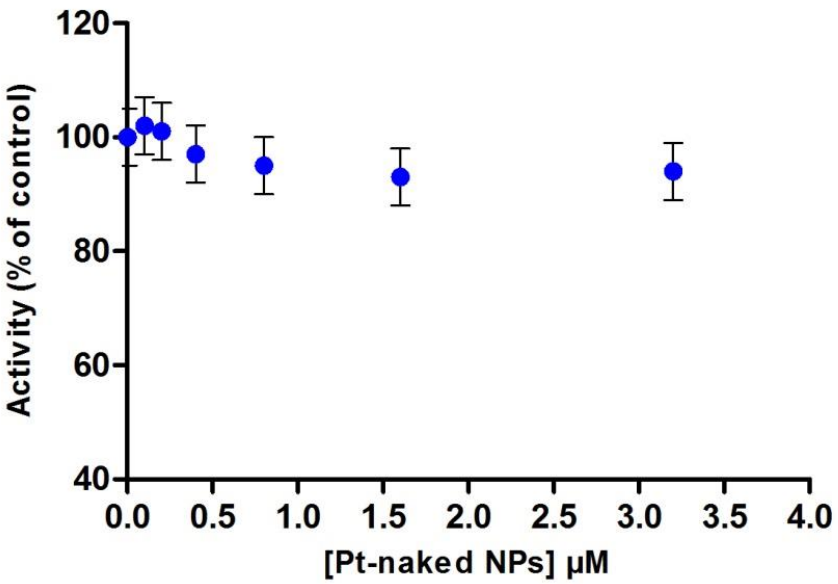

Figure 73: Dependence of Nox activity as a function of Pt NPs concentration

Neutrophil membrane fractions (5 nM Cyt *b558*) and trimera 200 nM were incubated together in the presence of 40 µM AA and (A) Pt PEG NPs (100-400 nM) or (B) Pt naked NPs (0.1-3.2 µM). Oxidase activity was expressed as the percent of activity measured in the absence of Pt NPs (92 mol $O_2^{\cdot-}$/s/mol cyt *b558*) as described in Materials and Methods. Points are an average of 3 independent measurements ±SEM.

3. Effect of Pt PEG NPs on the AA-dependent activation profile

We further questioned whether Pt NPs had an effect on the NADPH activation profile by AA. To test this possibility, we performed titrations of the oxidase activity vs. AA concentration in the absence and in the presence of 200 nM Pt PEG NPs added after arachidonic acid (Figure 74). The rate of production with 40 µM AA alone (the concentration used as reference), was considered as 100%. In agreement with the above -mentioned results, the $O_2^{\bullet-}$ production rate was similar on the full range of AA concentrations in the presence and in the absence of Pt PEG NPs, which confirms the absence of any Pt NPs effect on the AA activation of NADPH oxidase.

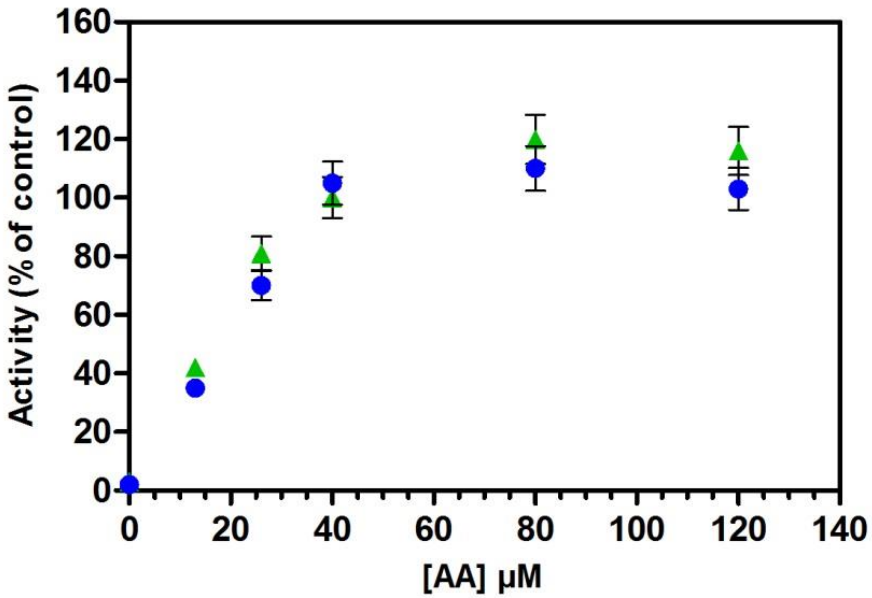

Figure 74: Effect of Pt PEG NPs on the AA-dependent activation profile

Neutrophil membrane fractions and trimera were incubated together in the presence of varying concentration of AA, in absence of Pt PEG NPs (▲) or in presence of 200 nM Pt PEG NPs (●). Oxidase activities were expressed as the percent of activity measured in the presence of 40 µM AA (88 mol $O_2^{\cdot-}$/s/mol cyt b_{558}). The rate of $O_2^{\bullet-}$ production was measured as described in Materials and Methods.

4. Pt PEG NPs effect on neutrophil cells

The absence of Pt NPs effect on AA-induced NADPH oxidase activity in cell-free system, prompted us to check if they can have an effect on NADPH oxidase in living neutrophils cells.

To investigate the influence of Pt PEG NPs on neutrophils, cells were incubated either with 1.66 µM PMA alone or with 1.66 µM Pt PEG NPs alone or both. The rates of superoxide anion production are reported in Table 7.No superoxide anion production of neutrophils was measured in the absence of PMA. Neutrophils were stimulated only when they were exposed to PMA. Interestingly, no NADPH oxidase activity was detected when neutrophils were incubated with Pt PEG NPs alone. Clearly, Pt PEG NPs could not induce NADPH oxidase activation in neutrophil cells. Meanwhile, PMA-induced NADPH-oxidase activity was neither significantly inhibited nor activated by the presence of Pt PEG NPs (Table 8).

Assay incubated with:	**Rate of $O_2^{\cdot -}$ production (nmol $O_2^{\cdot -}$/min/10^6cells)**
PMA 0 µM	**0**
PMA 1.66 µM	**52.1 ± 10.5**
Pt-PEG NPs 1.66 µM	**0.6**
PMA 1.66 µM plus Pt-PEG NPs 1.66 µM	**43.8± 10**

Table 8: Rates of superoxide anion production in neutrophil cells

5. Influence of gamma irradiation on the functioning of the cell free system

Since the combination of radiotherapy with platinum coated NPs was proposed as a cancer therapy protocol, it was necessary to check NADPH oxidase activity when NOX proteins and Pt PEG NPs were irradiated by γ-rays. Membrane fractions (70 nM Cyt b_{558}), trimera (2.5 µM), +/- Pt-PEG NPs (2.5 µM) were mixed in water in a final volume of 170 µl and exposed to γ-rays under aerobic conditions for different time intervals 1, 2, 3, 4 min. The dose rate was 8 Gy/min at the desired position. Non-irradiated samples were kept in the same conditions for 4 min. After irradiation of Nox proteins +/- Pt PEG NPs, the components were reconstituted and activated by AA for a cell free assay. The production rate of superoxide was measured as usual. As seen Figure 75, NADPH oxidase activity of the reconstituted system was decreased to 70 % of the initial activity at the maximum irradiation dose (4 min) when Nox proteins were irradiated.

Oxidase activity in the presence of the irradiated Pt PEG NPs was also slightly diminished for the whole range of irradiation doses. These results point out that NADPH oxidase activity was not extensively affected by the γ-irradiation of both proteins and Pt PEG NPs. Moreover, irradiated Pt PEG NPs did not induce ROS formation by NADPH oxidase.

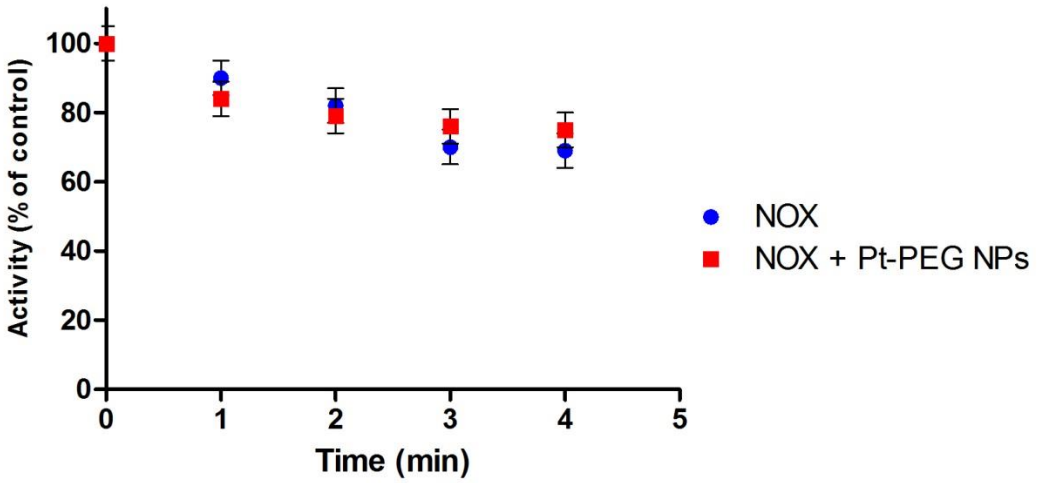

Figure 75: Influence of Gamma irradiation of Nox proteins and Pt PEG NPs on NADPH oxidase activity.

170 µl aqueous solutions containing neutrophil membrane fractions (70 nM cyt *b*$_{558}$) and trimera (2.5 µM) were irradiated together at different irradiation time 1, 2, 3, 4 min. Pt PEG NPs concentration was as follow, ●: no Pt PEG NPs; ■: 2.5 µM Pt-PEG NPs. Non-irradiated samples were kept for 4 min at room temperature. Then, NADPH oxidase activity of the irradiated proteins alone or with the irradiated NPs was measured after activation by AA 40 µM. The superoxide formation was measured as indicated in Materials and Methods. Each irradiation condition was done in triplicate and the results are the averages of these three independent measurements.

V. Discussion on the effect of Pt NPs

Platinum based nanomaterials such as cisplatin, oxaliplatin, and carboplatin were shown to be useful as anticancer drugs [433, 434]. Novel platinum analog were developed to allow controlled release and specific accumulation in the targeted disease tissue [435-437]. However, there are few reports on the physiological effects of platinum nanoparticles, especially with respect to their potential toxicity. It was shown that Pt NPs could induce inflammation hepatotoxicity, acute and chronic nephrotoxicity in mice [362-364].

In this study, we have tested the hypothesis that Pt NPs can induce inflammation through NADPH oxidase activation. When human endothelial and lung epithelial cells were exposed to Pt NPs, they were not found to induce cytotoxicity or oxidative stress in both cell type [431]. Similarly, our results clearly showed that Pt PEG NPs and naked Pt NPs cannot activate NADPH oxidase and initiate the subsequent production of superoxide anion either in cell free system or in neutrophil cells. Although, Pt PEG NPs are in contact with the cytosolic proteins as shown by the tryptophan fluorescence emission change of trimera and the DLS measurements, they are probably not able to induce the conformational changes necessary for NADPH oxidase activation as AA does. In addition, our results suggest that, Pt PEG NPs themselves do not provoke inflammation status in neutrophil cells, they are unable to activate the signaling pathways of the neutrophils leading to activation of the enzyme.

Pt NPs were shown to scavenge ROS such as superoxide anion, hydrogen peroxide and hydroxyl radical in a size-dependent manner *in vitro* and *in vivo* [359, 438, 439]. However, our current study demonstrated that the superoxide anion production was neither inhibited nor stimulated in the presence of both Pt PEG NPs and naked Pt NPs even at micromolar concentrations in cell free system. This was observed in the whole range of concentration of AA. The amount of superoxide scavenged by cyt c was not modified, indicating that the rate constant of reaction of Pt NPs with $O_2^{\bullet -}$ is probably lower than that of cyt c. In conclusion, Pt NPs do not interfere with $O_2^{\bullet -}$ production, they have no influence on the effect of AA, they do not disturb the conformational changes known to be induced by AA to activate NADPH oxidase and they do not interfere in the reactions of cyt c.

The combination of radiotherapy and Pt NPs was proposed in the last decades for the enhancement of cancer treatment [353, 354], Porcel et al. suggested that Pt NPs could be used for enhanced radiosensitization [321]. Therefore, we checked NADPH oxidase activity when Nox proteins and Pt NPs were irradiated by γ-rays. Our results demonstrated that NADPH oxidase activity was not largely affected by the γ-irradiation of a mixture containing membrane and cytosolic proteins of NOX (70 % of NADPH oxidase initial activity was measured for the maximum dose of radiation). Moreover there was no sensitization by Pt PEG NPs, since the remaining rate of production of $O_2^{\bullet -}$ was not modified in their presence. In conclusion, our findings suggest that there is no radio-sensitization when irradiation is made with γ-rays. In addition, they probably do not initiate oxidative stress conditions in normal cells.

Conclusions & Perspectives

"The danger which threatens researchers today would be to conclude that there is nothing more to discover."

Pierre Joliot

The aim of my thesis was to study the influence on NADPH oxidase activity, of molecules coming from food and from modern life known to be involved in increase of oxidative stress. In this work, we studied the NADPH oxidase functioning in an *in vitro* system. I was interested in the influence of two types of oxidative stress participants: cholesterol and some of its oxidized forms and two kinds of metal nanoparticles.

For these studies, it was of importance to use a reproducible model system, thus we replaced the cytosolic proteins by a fusion called trimera, which ensures the right stoichiometry of cytosolic proteins. Different chromatographic techniques were used to purify the trimera. This working technical part was long and stressful but necessary to obtain the best purified trimera. We showed that trimera was functionally comparable to the separate cytosolic subunits. In particular, the activity of NADPH oxidase with Trimera showed dependence on AA like separate cytosolic proteins, which demonstrated that AA acts on several sites on both trimera and membranous proteins. The rates of production of $O_2^{\bullet -}$, the dependence of the activity on temperature and the sensitivity of NADPH oxidase to free radicals were comparable when either trimera or separate subunits were used. Thus, trimera was a good tool to study the interaction of cytochrome b_{558} with the membrane environment and with other molecules. However, further investigation on the mechanism of the assembly of the complex is needed which may give information for developing new inhibitors for therapeutic uses.

I investigated the consequences of the addition of cholesterol on NADPH oxidase, on the production of ROS. The results presented here show that while the presence of cholesterol at physiological concentration (e.g. in lipid rafts) is important for the NADPH oxidase function, an addition of cholesterol might have several consequences: i) a slight but significant activity in the absence of the usual pro-inflammatory signals such as AA with the possibility of a permanent mild inflammatory state; ii) an inhibition of the activity of NADPH oxidase in the presence of pro-inflammatory signals. In both cases there would be a modification of the response to the signaling regulation. In other words, we showed that the cholesterol already inserted in the phagocyte membrane is optimal for the function of NADPH oxidase. Further research on other NOX must be considered to determine whether this is a universal effect of cholesterol lowering the capacity of all NOX to produce ROS. Cholesterol would make them less efficient in the defence against pathogens but also in their other functions such as cellular signaling, regulation

of gene expression and cell differentiation. Moreover, this work opens up numerous perspectives on the possibility to study the roles of other lipids. Phospholipids, sphingolipids and Omega 3 are good candidates, which might have influence on NADPH oxidase. The reconstitution of the system in liposome should bring more information about the interaction of lipids with NADPH oxidase complex.

The third part of this work dealt with the interactions between nanoparticles and NOX2. Different techniques (TEM, DLS, CD) were used and various collaborations (ISMO, Institut Curie, synchrotron Soleil) were established which gave me a good opportunity to learn new methods and to better evaluate NPs effect on NOX2. This study for the first time highlights that NADPH oxidase hyper-activation and the subsequent increase in ROS production in the presence of TiO_2 NPs could be one of the pathways involved in ROS generation by these NPs, thus participating in inflammatory status and oxidative stress damage, which might make them toxic. Since TiO_2 NPs are used in many applications, it would clearly be of interest to extend our investigation of TiO_2 NPs on other cells to better evaluate their participation in oxidative stress, for example on pulmonary cells where TiO_2 NPs are highly absorbed. On the other hand, our results clearly show that Pt NPs do not induce inflammation status via NADPH oxidase complex and suggest that they are not stimulant of reactive oxygen species production thus they are probably not implicated in oxidative stress damage. However, further investigation is needed to elucidate their effect on other molecular functions and to better evaluate their toxicity. Different metal NPs have different effects on NOX2, thus it would be interesting to study other nanomaterials for example nanodiamonds which is now started to be used widely in nanomedicine.

References

"If you steal from one author it's plagiarism; if you steal from many it's research."

Wilson Mizner

[1]. Baldridge, C. W. & Gerard, R. W. (1932) *The extra respiration of phagocytosis*
[2]. Sbarra, A. J. & Karnovsky, M. L. (1959) The biochemical basis of phagocytosis. I. Metabolic changes during the ingestion of particles by polymorphonuclear leukocytes, *The Journal of biological chemistry.* **234**, 1355-62.
[3]. Iyer, G., Islam, M. & Quastel, J. (1961) Biochemical aspects of phagocytosis.
[4]. Rossi, F. & Zatti, M. (1964) Biochemical aspects of phagocytosis in poly-morphonuclear leucocytes. NADH and NADPH oxidation by the granules of resting and phagocytizing cells, *Experientia.* **20**, 21-23.
[5]. Babior, B., Curnutte, J. & Kipnes, B. (1975) Pyridine nucleotide-dependent superoxide production by a cell-free system from human granulocytes, *Journal of Clinical Investigation.* **56**, 1035.
[6]. Segal, A. W. & Jones, O. T. (1978) Novel cytochrome b system in phagocytic vacuoles of human granulocytes, *Nature*. **276**, 515-7.
[7]. Segal, A., Jones, O. G., Webster, D. & Allison, A. (1978) Absence of a newly described cytochrome b from neutrophils of patients with chronic granulomatous disease, *The Lancet.* **312**, 446-449.
[8]. McCord, J. M. & Fridovich, I. (1969) Superoxide dismutase. An enzymic function for erythrocuprein (hemocuprein), *The Journal of biological chemistry.* **244**, 6049-55.
[9]. Babior, B. M., Kipnes, R. S. & Curnutte, J. T. (1973) Biological defense mechanisms. The production by leukocytes of superoxide, a potential bactericidal agent, *Journal of Clinical Investigation.* **52**, 741.
[10]. Berendes, H., Bridges, R. & Good, R. (1957) A fatal granulomatosus of childhood: the clinical study of a new syndrome, *Minnesota medicine.* **40**, 309-312.
[11]. Quie, P., White, J., Holmes, B. & Good, R. (1967) In vitro bactericidal capacity of human polymorphonuclear leukocytes: diminished activity in chronic granulomatous disease of childhood, *Journal of clinical investigation.* **46**, 668.
[12]. Baehner, R. L. & Nathan, D. G. (1967) Leukocyte oxidase: defective activity in chronic granulomatous disease, *Science (New York, NY).* **155**, 835-836.
[13]. Holmes, B., Page, A. R. & Good, R. A. (1967) Studies of the metabolic activity of leukocytes from patients with a genetic abnormality of phagocytic function, *Journal of Clinical Investigation.* **46**, 1422.
[14]. Royer-Pokora, B., Kunkel, L. M., Monaco, A. P., Goff, S. C., Newburger, P. E., Baehner, R. L., Cole, F. S., Curnutte, J. T. & Orkin, S. H. (1986). Cloning the gene for the inherited disorder chronic granulomatous disease on the basis of its chromosomal location. Paper presented at the *Cold Spring Harbor symposia on quantitative biology*.
[15]. Teahan, C., Rowe, P., Parker, P., Totty, N. & Segal, A. W. (1987) The X-linked chronic granulomatous disease gene codes for the β-chain of cytochrome b− 245.
[16]. Dinauer, M. C., Orkin, S. H., Brown, R., Jesaitis, A. J. & Parkos, C. A. (1987) The glycoprotein encoded by the X-linked chronic granulomatous disease locus is a component of the neutrophil cytochrome b complex.
[17]. Parkos, C. A., Dinauer, M. C., Walker, L. E., Allen, R. A., Jesaitis, A. J. & Orkin, S. H. (1988) Primary structure and unique expression of the 22-kilodalton light chain of human neutrophil cytochrome b, *Proceedings of the National Academy of Sciences of the United States of America.* **85**, 3319-23.
[18]. Segal, A. W. (1987) Absence of both cytochrome b− 245 subunits from neutrophils in X-linked chronic granulomatous disease.

[19]. Bromberg, Y. & Pick, E. (1985) Activation of NADPH-dependent superoxide production in a cell-free system by sodium dodecyl sulfate, *The Journal of biological chemistry.* **260**, 13539-45.
[20]. Heyneman, R. & Vercauteren, R. (1984) Activation of a NADPH oxidase from horse polymorphonuclear leukocytes in a cell-free system, *Journal of leukocyte biology.* **36**, 751-759.
[21]. Nunoi, H., Rotrosen, D., Gallin, J. I. & Malech, H. L. (1988) Two forms of autosomal chronic granulomatous disease lack distinct neutrophil cytosol factors, *Science (New York, NY).* **242**, 1298-1301.
[22]. Volpp, B. D., Nauseef, W. M. & Clark, R. A. (1988) Two cytosolic neutrophil oxidase components absent in autosomal chronic granulomatous disease, *Science (New York, NY).* **242**, 1295-1297.
[23]. Abo, A., Pick, E., Hall, A., Totty, N., Teahan, C. G. & Segal, A. W. (1991) Activation of the NADPH oxidase involves the small GTP-binding protein p21rac1, *Nature.* **353**, 668-670.
[24]. Knaus, U. G., Heyworth, P. G., Evans, T., Curnutte, J. T. & Bokoch, G. M. (1991) Regulation of phagocyte oxygen radical production by the GTP-binding protein Rac 2, *Science (New York, NY).* **254**, 1512-1515.
[25]. Wientjes, F., Hsuan, J., Totty, N. & Segal, A. W. (1993) p40phox, a third cytosolic component of the activation complex of the NADPH oxidase to contain src homology 3 domains, *Biochem J.* **296**, 557-561.
[26]. Krause, K. H. (2004) Tissue distribution and putative physiological function of NOX family NADPH oxidases, *Japanese journal of infectious diseases.* **57**, S28-9.
[27]. Lambeth, J. D. & Neish, A. S. (2014) Nox enzymes and new thinking on reactive oxygen: a double-edged sword revisited, *Annual Review of Pathology: Mechanisms of Disease.* **9**, 119-145.
[28]. Banfi, B., Maturana, A., Jaconi, S., Arnaudeau, S., Laforge, T., Sinha, B., Ligeti, E., Demaurex, N. & Krause, K. H. (2000) A mammalian H+ channel generated through alternative splicing of the NADPH oxidase homolog NOH-1, *Science (New York, NY).* **287**, 138-42.
[29]. Suh, Y.-A., Arnold, R. S., Lassegue, B., Shi, J., Xu, X., Sorescu, D., Chung, A. B., Griendling, K. K. & Lambeth, J. D. (1999) Cell transformation by the superoxide-generating oxidase Mox1, *Nature.* **401**, 79-82.
[30]. Shiose, A., Kuroda, J., Tsuruya, K., Hirai, M., Hirakata, H., Naito, S., Hattori, M., Sakaki, Y. & Sumimoto, H. (2001) A novel superoxide-producing NAD (P) H oxidase in kidney, *Journal of Biological Chemistry.* **276**, 1417-1423.
[31]. Geiszt, M., Kopp, J. B., Varnai, P. & Leto, T. L. (2000) Identification of renox, an NAD(P)H oxidase in kidney, *Proceedings of the National Academy of Sciences of the United States of America.* **97**, 8010-4.
[32]. Cheng, G., Cao, Z., Xu, X., Van Meir, E. G. & Lambeth, J. D. (2001) Homologs of gp91phox: cloning and tissue expression of Nox3, Nox4, and Nox5, *Gene.* **269**, 131-140.
[33]. De Deken, X., Wang, D., Many, M. C., Costagliola, S., Libert, F., Vassart, G., Dumont, J. E. & Miot, F. (2000) Cloning of two human thyroid cDNAs encoding new members of the NADPH oxidase family, *The Journal of biological chemistry.* **275**, 23227-33.
[34]. Banfi, B., Molnar, G., Maturana, A., Steger, K., Hegedus, B., Demaurex, N. & Krause, K. H. (2001) A Ca(2+)-activated NADPH oxidase in testis, spleen, and lymph nodes, *The Journal of biological chemistry.* **276**, 37594-601.
[35]. Dupuy, C., Ohayon, R., Valent, A., Noel-Hudson, M. S., Deme, D. & Virion, A. (1999) Purification of a novel flavoprotein involved in the thyroid NADPH oxidase. Cloning of the porcine and human cdnas, *The Journal of biological chemistry.* **274**, 37265-9.

[36]. Sumimoto, H., Miyano, K. & Takeya, R. (2005) Molecular composition and regulation of the Nox family NAD(P)H oxidases, *Biochemical and biophysical research communications.* **338**, 677-86.
[37]. Takeya, R., Ueno, N., Kami, K., Taura, M., Kohjima, M., Izaki, T., Nunoi, H. & Sumimoto, H. (2003) Novel human homologues of p47phox and p67phox participate in activation of superoxide-producing NADPH oxidases, *Journal of Biological Chemistry.* **278**, 25234-25246.
[38]. Geiszt, M., Lekstrom, K., Brenner, S., Hewitt, S. M., Dana, R., Malech, H. L. & Leto, T. L. (2003) NAD (P) H oxidase 1, a product of differentiated colon epithelial cells, can partially replace glycoprotein 91phox in the regulated production of superoxide by phagocytes, *The Journal of Immunology.* **171**, 299-306.
[39]. Martyn, K. D., Frederick, L. M., von Loehneysen, K., Dinauer, M. C. & Knaus, U. G. (2006) Functional analysis of Nox4 reveals unique characteristics compared to other NADPH oxidases, *Cellular signalling.* **18**, 69-82.
[40]. Bedard, K. & Krause, K. H. (2007) The NOX family of ROS-generating NADPH oxidases: physiology and pathophysiology, *Physiological reviews.* **87**, 245-313.
[41]. Drummond, G. R., Selemidis, S., Griendling, K. K. & Sobey, C. G. (2011) Combating oxidative stress in vascular disease: NADPH oxidases as therapeutic targets, *Nature reviews Drug discovery.* **10**, 453-71.
[42]. Sumimoto, H. (2008) Structure, regulation and evolution of Nox-family NADPH oxidases that produce reactive oxygen species, *FEBS Journal.* **275**, 3249-3277.
[43]. Opitz, N., Drummond, G. R., Selemidis, S., Meurer, S. & Schmidt, H. H. (2007) The 'A's and 'O's of NADPH oxidase regulation: a commentary on "Subcellular localization and function of alternatively spliced Noxo1 isoforms", *Free radical biology & medicine.* **42**, 175-9.
[44]. Bedard, K., Jaquet, V. & Krause, K. H. (2012) NOX5: from basic biology to signaling and disease, *Free radical biology & medicine.* **52**, 725-34.
[45]. Banfi, B., Tirone, F., Durussel, I., Knisz, J., Moskwa, P., Molnar, G. Z., Krause, K. H. & Cox, J. A. (2004) Mechanism of Ca2+ activation of the NADPH oxidase 5 (NOX5), *The Journal of biological chemistry.* **279**, 18583-91.
[46]. Ameziane-El-Hassani, R., Morand, S., Boucher, J. L., Frapart, Y. M., Apostolou, D., Agnandji, D., Gnidehou, S., Ohayon, R., Noel-Hudson, M. S., Francon, J., Lalaoui, K., Virion, A. & Dupuy, C. (2005) Dual oxidase-2 has an intrinsic Ca2+-dependent H2O2-generating activity, *The Journal of biological chemistry.* **280**, 30046-54.
[47]. Cheng, G., Cao, Z., Xu, X., van Meir, E. G. & Lambeth, J. D. (2001) Homologs of gp91phox: cloning and tissue expression of Nox3, Nox4, and Nox5, *Gene.* **269**, 131-40.
[48]. El-Benna, J., Dang, P. M. & Gougerot-Pocidalo, M. A. (2007) Role of the NADPH oxidase systems Nox and Duox in host defense and inflammation, *Expert review of clinical immunology.* **3**, 111-5.
[49]. Karlsson, A. & Dahlgren, C. (2002) Assembly and activation of the neutrophil NADPH oxidase in granule membranes, *Antioxidants & redox signaling.* **4**, 49-60.
[50]. Paffenholz, R., Bergstrom, R. A., Pasutto, F., Wabnitz, P., Munroe, R. J., Jagla, W., Heinzmann, U., Marquardt, A., Bareiss, A., Laufs, J., Russ, A., Stumm, G., Schimenti, J. C. & Bergstrom, D. E. (2004) Vestibular defects in head-tilt mice result from mutations in Nox3, encoding an NADPH oxidase, *Genes & development.* **18**, 486-91.
[51]. Banfi, B., Malgrange, B., Knisz, J., Steger, K., Dubois-Dauphin, M. & Krause, K. H. (2004) NOX3, a superoxide-generating NADPH oxidase of the inner ear, *The Journal of biological chemistry.* **279**, 46065-72.

[52]. El Hassani, R. A., Benfares, N., Caillou, B., Talbot, M., Sabourin, J. C., Belotte, V., Morand, S., Gnidehou, S., Agnandji, D., Ohayon, R., Kaniewski, J., Noel-Hudson, M. S., Bidart, J. M., Schlumberger, M., Virion, A. & Dupuy, C. (2005) Dual oxidase2 is expressed all along the digestive tract, *American journal of physiology Gastrointestinal and liver physiology.* **288**, G933-42.
[53]. Ris-Stalpers, C. (2006) Physiology and pathophysiology of the DUOXes, *Antioxidants & redox signaling.* **8**, 1563-72.
[54]. Ohye, H. & Sugawara, M. (2010) Dual oxidase, hydrogen peroxide and thyroid diseases, *Experimental biology and medicine (Maywood, NJ).* **235**, 424-33.
[55]. Halliwell, B. & Gutteridge, J. M. (1999) *Free radicals in biology and medicine*, Oxford university press Oxford.
[56]. Figueira, T. R., Barros, M. H., Camargo, A. A., Castilho, R. F., Ferreira, J. C., Kowaltowski, A. J., Sluse, F. E., Souza-Pinto, N. C. & Vercesi, A. E. (2013) Mitochondria as a source of reactive oxygen and nitrogen species: from molecular mechanisms to human health, *Antioxidants & redox signaling.* **18**, 2029-74.
[57]. Fransen, M., Nordgren, M., Wang, B. & Apanasets, O. (2012) Role of peroxisomes in ROS/RNS-metabolism: implications for human disease, *Biochimica et biophysica acta.* **1822**, 1363-73.
[58]. Dickinson, B. C. & Chang, C. J. (2011) Chemistry and biology of reactive oxygen species in signaling or stress responses, *Nat Chem Biol.* **7**, 504-511.
[59]. Fantone, J. C. & Ward, P. A. (1982) Role of oxygen-derived free radicals and metabolites in leukocyte-dependent inflammatory reactions, *The American journal of pathology.* **107**, 395-418.
[60]. Reeves, E. P., Nagl, M., Godovac-Zimmermann, J. & Segal, A. W. (2003) Reassessment of the microbicidal activity of reactive oxygen species and hypochlorous acid with reference to the phagocytic vacuole of the neutrophil granulocyte, *Journal of medical microbiology.* **52**, 643-51.
[61]. Brawn, K. & Fridovich, I. (1980) *Superoxide radical and superoxide dismutases: threat and defense*, Springer.
[62]. Bielski, B. H., Cabelli, D. E., Arudi, R. L. & Ross, A. B. (1985) Reactivity of HO2/O− 2 radicals in aqueous solution, *Journal of Physical and Chemical Reference Data.* **14**, 1041-1100.
[63]. Klebanoff, S. J. (2005) Myeloperoxidase: friend and foe, *Journal of leukocyte biology.* **77**, 598-625.
[64]. Michelson, A. M., McCord, J. M. & Fridovich, I. (1977). Superoxide and superoxide dismutases. Paper presented at the *EMBO Workshop on Superoxide and Superoxide Dismutases 1976: Banyuls, France)*.
[65]. Fenton, H. J. H. (1894) LXXIII.-Oxidation of tartaric acid in presence of iron, *Journal of the Chemical Society, Transactions.* **65**, 899-910.
[66]. Gutteridge, J. & Bannister, J. V. (1986) Copper+ zinc and manganese superoxide dismutases inhibit deoxyribose degradation by the superoxide-driven Fenton reaction at two different stages. Implications for the redox states of copper and manganese, *Biochem J.* **234**, 225-228.
[67]. Weiss, S. J. (1989) Tissue destruction by neutrophils, *The New England journal of medicine.* **320**, 365-76.
[68]. Rubbo, H., Darley-Usmar, V. & Freeman, B. A. (1996) Nitric oxide regulation of tissue free radical injury, *Chemical research in toxicology.* **9**, 809-20.

[69]. Dupre-Crochet, S., Erard, M. & Nubetae, O. (2013) ROS production in phagocytes: why, when, and where?, *Journal of leukocyte biology.* **94**, 657-70.
[70]. Lambeth, J. D. (2004) NOX enzymes and the biology of reactive oxygen, *Nature reviews Immunology.* **4**, 181-9.
[71]. Poli, G., Leonarduzzi, G., Biasi, F. & Chiarpotto, E. (2004) Oxidative stress and cell signalling, *Current medicinal chemistry.* **11**, 1163-82.
[72]. Fridovich, I. (1989) Superoxide dismutases. An adaptation to a paramagnetic gas, *The Journal of biological chemistry.* **264**, 7761-7764.
[73]. Frenkel, K. (1992) Carcinogen-mediated oxidant formation and oxidative DNA damage, *Pharmacology & therapeutics.* **53**, 127-66.
[74]. Cohen, G. & Hochstein, P. (1963) Glutathione peroxidase: The primary agent for the elimination of hydrogen peroxide in erythrocytes *Biochemistry.* **2**, 1420-8.
[75]. Valko, M., Leibfritz, D., Moncol, J., Cronin, M. T., Mazur, M. & Telser, J. (2007) Free radicals and antioxidants in normal physiological functions and human disease, *The international journal of biochemistry & cell biology.* **39**, 44-84.
[76]. Sies, H. (1997) Oxidative stress: oxidants and antioxidants, *Experimental Physiology.* **82**, 291-295.
[77]. Witko-Sarsat, V., Rieu, P., Descamps-Latscha, B., Lesavre, P. & Halbwachs-Mecarelli, L. (2000) Neutrophils: molecules, functions and pathophysiological aspects, *Laboratory investigation; a journal of technical methods and pathology.* **80**, 617-53.
[78]. Borregaard, N., Heiple, J. M., Simons, E. R. & Clark, R. A. (1983) Subcellular localization of the b-cytochrome component of the human neutrophil microbicidal oxidase: translocation during activation, *J Cell Biol.* **97**, 52-61.
[79]. Huang, J., Hitt, N. D. & Kleinberg, M. E. (1995) Stoichiometry of p22-phox and gp91-phox in phagocyte cytochrome b558, *Biochemistry.* **34**, 16753-7.
[80]. Kjeldsen, L., Sengelov, H., Lollike, K., Nielsen, M. H. & Borregaard, N. (1994) Isolation and characterization of gelatinase granules from human neutrophils, *Blood.* **83**, 1640-9.
[81]. Garcia, R. C. & Segal, A. W. (1984) Changes in the subcellular distribution of the cytochrome b-245 on stimulation of human neutrophils, *Biochemical Journal.* **219**, 233-242.
[82]. Lundqvist, H., Follin, P., Khalfan, L. & Dahlgren, C. (1996) Phorbol myristate acetate-induced NADPH oxidase activity in human neutrophils: only half the story has been told, *Journal of leukocyte biology.* **59**, 270-9.
[83]. Vaissiere, C., Le Cabec, V. & Maridonneau-Parini, I. (1999) NADPH oxidase is functionally assembled in specific granules during activation of human neutrophils, *Journal of leukocyte biology.* **65**, 629-34.
[84]. Hampton, M. B., Kettle, A. J. & Winterbourn, C. C. (1998) Inside the neutrophil phagosome: oxidants, myeloperoxidase, and bacterial killing, *Blood.* **92**, 3007-3017.
[85]. Groemping, Y. & Rittinger, K. (2005) Activation and assembly of the NADPH oxidase: a structural perspective, *Biochem J.* **386**, 401-416.
[86]. El-Benna, J., Dang, P. M., Gougerot-Pocidalo, M. A. & Elbim, C. (2005) Phagocyte NADPH oxidase: a multicomponent enzyme essential for host defenses, *Archivum immunologiae et therapiae experimentalis.* **53**, 199-206.
[87]. Yu, L., Zhen, L. & Dinauer, M. C. (1997) Biosynthesis of the phagocyte NADPH oxidase cytochrome b558. Role of heme incorporation and heterodimer formation in maturation and stability of gp91phox and p22phox subunits, *The Journal of biological chemistry.* **272**, 27288-94.
[88]. Burritt, J. B., DeLeo, F. R., McDonald, C. L., Prigge, J. R., Dinauer, M. C., Nakamura, M., Nauseef, W. M. & Jesaitis, A. J. (2001) Phage display epitope mapping of human neutrophil

flavocytochrome b558. Identification of two juxtaposed extracellular domains, *The Journal of biological chemistry.* **276**, 2053-61.
[89]. Royer-Pokora, B., Kunkel, L. M., Monaco, A. P., Goff, S. C., Newburger, P. E., Baehner, R. L., Cole, F. S., Curnutte, J. T. & Orkin, S. H. (1986) Cloning the gene for an inherited human disorder--chronic granulomatous disease--on the basis of its chromosomal location, *Nature.* **322**, 32-8.
[90]. Biberstine-Kinkade, K. J., Yu, L., Stull, N., LeRoy, B., Bennett, S., Cross, A. & Dinauer, M. C. (2002) Mutagenesis of p22(phox) histidine 94. A histidine in this position is not required for flavocytochrome b558 function, *The Journal of biological chemistry.* **277**, 30368-74.
[91]. Biberstine-Kinkade, K. J., DeLeo, F. R., Epstein, R. I., LeRoy, B. A., Nauseef, W. M. & Dinauer, M. C. (2001) Heme-ligating Histidines in Flavocytochromeb 558 identification of specific histidines gp91 phoxI, *Journal of Biological Chemistry.* **276**, 31105-31112.
[92]. Yu, L., Quinn, M. T., Cross, A. R. & Dinauer, M. C. (1998) Gp91phox is the heme binding subunit of the superoxide-generating NADPH oxidase, *Proceedings of the National Academy of Sciences.* **95**, 7993-7998.
[93]. Debeurme, F., Picciocchi, A., Dagher, M. C., Grunwald, D., Beaumel, S., Fieschi, F. & Stasia, M. J. (2010) Regulation of NADPH oxidase activity in phagocytes: relationship between FAD/NADPH binding and oxidase complex assembly, *The Journal of biological chemistry.* **285**, 33197-208.
[94]. Dahlgren, C. & Karlsson, A. (1999) Respiratory burst in human neutrophils, *Journal of immunological methods.* **232**, 3-14.
[95]. Doussière, J., Gaillard, J. & Vignais, P. V. (1996) Electron transfer across the O2-generating flavocytochrome b of neutrophils. Evidence for a transition from a low-spin state to a high-spin state of the heme iron component, *Biochemistry.* **35**, 13400-13410.
[96]. Isogai, Y., Iizuka, T. & Shiro, Y. (1995) The mechanism of electron donation to molecular oxygen by phagocytic cytochrome b558, *Journal of Biological Chemistry.* **270**, 7853-7857.
[97]. Koshkin, V., Lotan, O. & Pick, E. (1997) Electron transfer in the superoxide-generating NADPH oxidase complex reconstituted in vitro, *Biochimica et Biophysica Acta (BBA)-Bioenergetics.* **1319**, 139-146.
[98]. Cross, A. R. & Segal, A. W. (2004) The NADPH oxidase of professional phagocytes--prototype of the NOX electron transport chain systems, *Biochimica et biophysica acta.* **1657**, 1-22.
[99]. Campion, Y., Jesaitis, A. J., Nguyen, M. V. C., Grichine, A., Herenger, Y., Baillet, A., Berthier, S., Morel, F. & Paclet, M.-H. (2009) New p22-phox monoclonal antibodies: identification of a conformational probe for cytochrome b558, *Journal of innate immunity.* **1**, 556-569.
[100]. Dinauer, M. C., Pierce, E. A., Erickson, R. W., Muhlebach, T. J., Messner, H., Orkin, S. H., Seger, R. A. & Curnutte, J. T. (1991) Point mutation in the cytoplasmic domain of the neutrophil p22-phox cytochrome b subunit is associated with a nonfunctional NADPH oxidase and chronic granulomatous disease, *Proceedings of the National Academy of Sciences of the United States of America.* **88**, 11231-5.
[101]. Leto, T. L., Adams, A. G. & de Mendez, I. (1994) Assembly of the phagocyte NADPH oxidase: binding of Src homology 3 domains to proline-rich targets, *Proceedings of the National Academy of Sciences of the United States of America.* **91**, 10650-4.
[102]. Sumimoto, H., Kage, Y., Nunoi, H., Sasaki, H., Nose, T., Fukumaki, Y., Ohno, M., Minakami, S. & Takeshige, K. (1994) Role of Src homology 3 domains in assembly and

activation of the phagocyte NADPH oxidase, *Proceedings of the National Academy of Sciences of the United States of America.* **91**, 5345-9.
[103]. Leusen, J. H., Bolscher, B. G., Hilarius, P. M., Weening, R. S., Kaulfersch, W., Seger, R. A., Roos, D. & Verhoeven, A. J. (1994) 156Pro-->Gln substitution in the light chain of cytochrome b558 of the human NADPH oxidase (p22-phox) leads to defective translocation of the cytosolic proteins p47-phox and p67-phox, *The Journal of experimental medicine.* **180**, 2329-34.
[104]. Dahan, I., Issaeva, I., Gorzalczany, Y., Sigal, N., Hirshberg, M. & Pick, E. (2002) Mapping of functional domains in the p22(phox) subunit of flavocytochrome b(559) participating in the assembly of the NADPH oxidase complex by "peptide walking", *The Journal of biological chemistry.* **277**, 8421-32.
[105]. Takeya, R., Ueno, N., Kami, K., Taura, M., Kohjima, M., Izaki, T., Nunoi, H. & Sumimoto, H. (2003) Novel human homologues of p47phox and p67phox participate in activation of superoxide-producing NADPH oxidases, *The Journal of biological chemistry.* **278**, 25234-46.
[106]. Laude, K., Cai, H., Fink, B., Hoch, N., Weber, D. S., McCann, L., Kojda, G., Fukai, T., Schmidt, H. H., Dikalov, S., Ramasamy, S., Gamez, G., Griendling, K. K. & Harrison, D. G. (2005) Hemodynamic and biochemical adaptations to vascular smooth muscle overexpression of p22phox in mice, *American journal of physiology Heart and circulatory physiology.* **288**, H7-12.
[107]. Ueno, N., Takeya, R., Miyano, K., Kikuchi, H. & Sumimoto, H. (2005) The NADPH oxidase Nox3 constitutively produces superoxide in a p22phox-dependent manner: its regulation by oxidase organizers and activators, *The Journal of biological chemistry.* **280**, 23328-39.
[108]. Ambasta, R. K., Kumar, P., Griendling, K. K., Schmidt, H. H., Busse, R. & Brandes, R. P. (2004) Direct interaction of the novel Nox proteins with p22phox is required for the formation of a functionally active NADPH oxidase, *The Journal of biological chemistry.* **279**, 45935-41.
[109]. Parkos, C. A., Dinauer, M. C., Jesaitis, A. J., Orkin, S. H. & Curnutte, J. T. (1989) Absence of both the 91kD and 22kD subunits of human neutrophil cytochrome b in two genetic forms of chronic granulomatous disease, *Blood.* **73**, 1416-20.
[110]. El-Benna, J., Dang, P. M., Gougerot-Pocidalo, M. A., Marie, J. C. & Braut-Boucher, F. (2009) p47phox, the phagocyte NADPH oxidase/NOX2 organizer: structure, phosphorylation and implication in diseases, *Experimental & molecular medicine.* **41**, 217-25.
[111]. Koshkin, V., Lotan, O. & Pick, E. (1996) The cytosolic component p47(phox) is not a sine qua non participant in the activation of NADPH oxidase but is required for optimal superoxide production, *The Journal of biological chemistry.* **271**, 30326-9.
[112]. Freeman, J. L. & Lambeth, J. D. (1996) NADPH oxidase activity is independent of p47phox in vitro, *The Journal of biological chemistry.* **271**, 22578-82.
[113]. Babior, B. M. (2004) NADPH oxidase, *Current Opinion in Immunology.* **16**, 42-47.
[114]. Babior, B. M. (1999) NADPH oxidase: an update, *Blood.* **93**, 1464-76.
[115]. Ago, T., Kuribayashi, F., Hiroaki, H., Takeya, R., Ito, T., Kohda, D. & Sumimoto, H. (2003) Phosphorylation of p47phox directs phox homology domain from SH3 domain toward phosphoinositides, leading to phagocyte NADPH oxidase activation, *Proceedings of the National Academy of Sciences of the United States of America.* **100**, 4474-9.
[116]. (1994) SH3-dependent assembly of the phagocyte NADPH oxidase, *The Journal of experimental medicine.* **180**, 2011-2015.
[117]. Ago, T., Nunoi, H., Ito, T. & Sumimoto, H. (1999) Mechanism for phosphorylation-induced activation of the phagocyte NADPH oxidase protein p47(phox). Triple replacement of serines 303, 304, and 328 with aspartates disrupts the SH3 domain-mediated intramolecular

interaction in p47(phox), thereby activating the oxidase, *The Journal of biological chemistry.* **274**, 33644-53.
[118]. Durand, D., Cannella, D., Dubosclard, V., Pebay-Peyroula, E., Vachette, P. & Fieschi, F. (2006) Small-angle X-ray scattering reveals an extended organization for the autoinhibitory resting state of the p47(phox) modular protein, *Biochemistry.* **45**, 7185-93.
[119]. Grizot, S., Grandvaux, N., Fieschi, F., Faure, J., Massenet, C., Andrieu, J. P., Fuchs, A., Vignais, P. V., Timmins, P. A., Dagher, M. C. & Pebay-Peyroula, E. (2001) Small angle neutron scattering and gel filtration analyses of neutrophil NADPH oxidase cytosolic factors highlight the role of the C-terminal end of p47phox in the association with p40phox, *Biochemistry.* **40**, 3127-33.
[120]. Massenet, C., Chenavas, S., Cohen-Addad, C., Dagher, M. C., Brandolin, G., Pebay-Peyroula, E. & Fieschi, F. (2005) Effects of p47phox C terminus phosphorylations on binding interactions with p40phox and p67phox. Structural and functional comparison of p40phox and p67phox SH3 domains, *The Journal of biological chemistry.* **280**, 13752-61.
[121]. Ago, T., Takeya, R., Hiroaki, H., Kuribayashi, F., Ito, T., Kohda, D. & Sumimoto, H. (2001) The PX domain as a novel phosphoinositide- binding module, *Biochemical and biophysical research communications.* **287**, 733-8.
[122]. Inanami, O., Johnson, J. L., McAdara, J. K., Benna, J. E., Faust, L. R., Newburger, P. E. & Babior, B. M. (1998) Activation of the leukocyte NADPH oxidase by phorbol ester requires the phosphorylation of p47PHOX on serine 303 or 304, *The Journal of biological chemistry.* **273**, 9539-43.
[123]. Ago, T., Kuribayashi, F., Hiroaki, H., Takeya, R., Ito, T., Kohda, D. & Sumimoto, H. (2003) Phosphorylation of p47phox directs phox homology domain from SH3 domain toward phosphoinositides, leading to phagocyte NADPH oxidase activation, *Proceedings of the National Academy of Sciences.* **100**, 4474-4479.
[124]. Shiose, A. & Sumimoto, H. (2000) Arachidonic acid and phosphorylation synergistically induce a conformational change of p47phox to activate the phagocyte NADPH oxidase, *The Journal of biological chemistry.* **275**, 13793-801.
[125]. Dang, P. M., Cross, A. R. & Babior, B. M. (2001) Assembly of the neutrophil respiratory burst oxidase: a direct interaction between p67PHOX and cytochrome b558, *Proceedings of the National Academy of Sciences of the United States of America.* **98**, 3001-5.
[126]. Fontayne, A., Dang, P. M., Gougerot-Pocidalo, M. A. & El-Benna, J. (2002) Phosphorylation of p47phox sites by PKC alpha, beta II, delta, and zeta: effect on binding to p22phox and on NADPH oxidase activation, *Biochemistry.* **41**, 7743-50.
[127]. Marcoux, J., Man, P., Petit-Haertlein, I., Vives, C., Forest, E. & Fieschi, F. (2010) p47phox molecular activation for assembly of the neutrophil NADPH oxidase complex, *The Journal of biological chemistry.* **285**, 28980-90.
[128]. Volpp, B. D., Nauseef, W. M. & Clark, R. A. (1988) Two cytosolic neutrophil oxidase components absent in autosomal chronic granulomatous disease, *Science (New York, NY).* **242**, 1295-7.
[129]. Nunoi, H., Rotrosen, D., Gallin, J. I. & Malech, H. L. (1988) Two forms of autosomal chronic granulomatous disease lack distinct neutrophil cytosol factors, *Science (New York, NY).* **242**, 1298-301.
[130]. Leusen, J. H., de Klein, A., Hilarius, P. M., Ahlin, A., Palmblad, J., Smith, C. I., Diekmann, D., Hall, A., Verhoeven, A. J. & Roos, D. (1996) Disturbed interaction of p21-rac with mutated p67-phox causes chronic granulomatous disease, *The Journal of experimental medicine.* **184**, 1243-9.

[131]. Grizot, S., Fieschi, F., Dagher, M. C. & Pebay-Peyroula, E. (2001) The active N-terminal region of p67phox. Structure at 1.8 A resolution and biochemical characterizations of the A128V mutant implicated in chronic granulomatous disease, *The Journal of biological chemistry.* **276**, 21627-31.
[132]. Diekmann, D., Abo, A., Johnston, C., Segal, A. W. & Hall, A. (1994) Interaction of Rac with p67phox and regulation of phagocytic NADPH oxidase activity, *Science (New York, NY).* **265**, 531-3.
[133]. Koga, H., Terasawa, H., Nunoi, H., Takeshige, K., Inagaki, F. & Sumimoto, H. (1999) Tetratricopeptide repeat (TPR) motifs of p67(phox) participate in interaction with the small GTPase Rac and activation of the phagocyte NADPH oxidase, *The Journal of biological chemistry.* **274**, 25051-60.
[134]. Han, C. H., Freeman, J. L., Lee, T., Motalebi, S. A. & Lambeth, J. D. (1998) Regulation of the neutrophil respiratory burst oxidase. Identification of an activation domain in p67(phox), *The Journal of biological chemistry.* **273**, 16663-8.
[135]. Han, C. H. & Lee, M. H. (2000) Activation domain in P67phox regulates the steady state reduction of FAD in gp91phox, *Journal of veterinary science.* **1**, 27-31.
[136]. Li, X. J., Fieschi, F., Paclet, M. H., Grunwald, D., Campion, Y., Gaudin, P., Morel, F. & Stasia, M. J. (2007) Leu505 of Nox2 is crucial for optimal p67phox-dependent activation of the flavocytochrome b558 during phagocytic NADPH oxidase assembly, *Journal of leukocyte biology.* **81**, 238-49.
[137]. Wilson, M. I., Gill, D. J., Perisic, O., Quinn, M. T. & Williams, R. L. (2003) PB1 domain-mediated heterodimerization in NADPH oxidase and signaling complexes of atypical protein kinase C with Par6 and p62, *Molecular cell.* **12**, 39-50.
[138]. Durand, D., Vives, C., Cannella, D., Perez, J., Pebay-Peyroula, E., Vachette, P. & Fieschi, F. (2010) NADPH oxidase activator p67(phox) behaves in solution as a multidomain protein with semi-flexible linkers, *Journal of structural biology.* **169**, 45-53.
[139]. Ahmed, S., Prigmore, E., Govind, S., Veryard, C., Kozma, R., Wientjes, F. B., Segal, A. W. & Lim, L. (1998) Cryptic Rac-binding and p21(Cdc42Hs/Rac)-activated kinase phosphorylation sites of NADPH oxidase component p67(phox), *The Journal of biological chemistry.* **273**, 15693-701.
[140]. Dang, P. M., Morel, F., Gougerot-Pocidalo, M. A. & El Benna, J. (2003) Phosphorylation of the NADPH oxidase component p67(PHOX) by ERK2 and P38MAPK: selectivity of phosphorylated sites and existence of an intramolecular regulatory domain in the tetratricopeptide-rich region, *Biochemistry.* **42**, 4520-6.
[141]. Dusi, S., Della Bianca, V., Grzeskowiak, M. & Rossi, F. (1993) Relationship between phosphorylation and translocation to the plasma membrane of p47phox and p67phox and activation of the NADPH oxidase in normal and Ca(2+)-depleted human neutrophils, *The Biochemical journal.* **290 (Pt 1)**, 173-8.
[142]. Forbes, L. V., Truong, O., Wientjes, F. B., Moss, S. J. & Segal, A. W. (1999) The major phosphorylation site of the NADPH oxidase component p67phox is Thr233, *The Biochemical journal.* **338 (Pt 1)**, 99-105.
[143]. Benna, J. E., Dang, P. M., Gaudry, M., Fay, M., Morel, F., Hakim, J. & Gougerot-Pocidalo, M. A. (1997) Phosphorylation of the respiratory burst oxidase subunit p67(phox) during human neutrophil activation. Regulation by protein kinase C-dependent and independent pathways, *The Journal of biological chemistry.* **272**, 17204-8.
[144]. Dang, P. M., Raad, H., Derkawi, R. A., Boussetta, T., Paclet, M. H., Belambri, S. A., Makni-Maalej, K., Kroviarski, Y., Morel, F., Gougerot-Pocidalo, M. A. & El-Benna, J. (2011)

The NADPH oxidase cytosolic component p67phox is constitutively phosphorylated in human neutrophils: Regulation by a protein tyrosine kinase, MEK1/2 and phosphatases 1/2A, *Biochemical pharmacology.* **82**, 1145-52.
[145]. Lapouge, K., Smith, S. J., Groemping, Y. & Rittinger, K. (2002) Architecture of the p40-p47-p67phox complex in the resting state of the NADPH oxidase. A central role for p67phox, *The Journal of biological chemistry.* **277**, 10121-8.
[146]. Wientjes, F. B., Hsuan, J. J., Totty, N. F. & Segal, A. W. (1993) p40phox, a third cytosolic component of the activation complex of the NADPH oxidase to contain src homology 3 domains, *The Biochemical journal.* **296 (Pt 3)**, 557-61.
[147]. Fuchs, A., Dagher, M. C. & Vignais, P. V. (1995) Mapping the domains of interaction of p40phox with both p47phox and p67phox of the neutrophil oxidase complex using the two-hybrid system, *The Journal of biological chemistry.* **270**, 5695-7.
[148]. Ostuni, M. A., Gelinotte, M., Bizouarn, T., Baciou, L. & Houee-Levin, C. (2010) Targeting NADPH-oxidase by reactive oxygen species reveals an initial sensitive step in the assembly process, *Free radical biology & medicine.* **49**, 900-7.
[149]. Karimi, G., Houee Levin, C., Dagher, M. C., Baciou, L. & Bizouarn, T. (2014) Assembly of phagocyte NADPH oxidase: A concerted binding process?, *Biochimica et biophysica acta.* **1840**, 3277-83.
[150]. Tamura, M., Shiozaki, I., Ono, S., Miyano, K., Kunihiro, S. & Sasaki, T. (2007) p40phox as an alternative organizer to p47phox in Nox2 activation: a new mechanism involving an interaction with p22phox, *FEBS letters.* **581**, 4533-8.
[151]. Ellson, C. D., Gobert-Gosse, S., Anderson, K. E., Davidson, K., Erdjument-Bromage, H., Tempst, P., Thuring, J. W., Cooper, M. A., Lim, Z. Y., Holmes, A. B., Gaffney, P. R., Coadwell, J., Chilvers, E. R., Hawkins, P. T. & Stephens, L. R. (2001) PtdIns(3)P regulates the neutrophil oxidase complex by binding to the PX domain of p40(phox), *Nature cell biology.* **3**, 679-82.
[152]. Kanai, F., Liu, H., Field, S. J., Akbary, H., Matsuo, T., Brown, G. E., Cantley, L. C. & Yaffe, M. B. (2001) The PX domains of p47phox and p40phox bind to lipid products of PI(3)K, *Nature cell biology.* **3**, 675-8.
[153]. Ueyama, T., Tatsuno, T., Kawasaki, T., Tsujibe, S., Shirai, Y., Sumimoto, H., Leto, T. L. & Saito, N. (2007) A regulated adaptor function of p40phox: distinct p67phox membrane targeting by p40phox and by p47phox, *Molecular biology of the cell.* **18**, 441-54.
[154]. Chen, J., He, R., Minshall, R. D., Dinauer, M. C. & Ye, R. D. (2007) Characterization of a mutation in the Phox homology domain of the NADPH oxidase component p40phox identifies a mechanism for negative regulation of superoxide production, *The Journal of biological chemistry.* **282**, 30273-84.
[155]. Kuribayashi, F., Nunoi, H., Wakamatsu, K., Tsunawaki, S., Sato, K., Ito, T. & Sumimoto, H. (2002) The adaptor protein p40(phox) as a positive regulator of the superoxide-producing phagocyte oxidase, *The EMBO journal.* **21**, 6312-20.
[156]. Lopes, L. R., Dagher, M. C., Gutierrez, A., Young, B., Bouin, A. P., Fuchs, A. & Babior, B. M. (2004) Phosphorylated p40PHOX as a negative regulator of NADPH oxidase, *Biochemistry.* **43**, 3723-30.
[157]. Sathyamoorthy, M., de Mendez, I., Adams, A. G. & Leto, T. L. (1997) p40(phox) down-regulates NADPH oxidase activity through interactions with its SH3 domain, *The Journal of biological chemistry.* **272**, 9141-6.
[158]. Cross, A. R. (2000) p40(phox) Participates in the activation of NADPH oxidase by increasing the affinity of p47(phox) for flavocytochrome b(558), *The Biochemical journal.* **349**, 113-7.

[159]. Fuchs, A., Bouin, A. P., Rabilloud, T. & Vignais, P. V. (1997) The 40-kDa component of the phagocyte NADPH oxidase (p40phox) is phosphorylated during activation in differentiated HL60 cells, *European journal of biochemistry / FEBS.* **249**, 531-9.
[160]. Someya, A., Nunoi, H., Hasebe, T. & Nagaoka, I. (1999) Phosphorylation of p40-phox during activation of neutrophil NADPH oxidase, *Journal of leukocyte biology.* **66**, 851-7.
[161]. Roos, D., van Bruggen, R. & Meischl, C. (2003) Oxidative killing of microbes by neutrophils, *Microbes and infection / Institut Pasteur.* **5**, 1307-15.
[162]. Kwong, C. H., Malech, H. L., Rotrosen, D. & Leto, T. L. (1993) Regulation of the human neutrophil NADPH oxidase by rho-related G-proteins, *Biochemistry.* **32**, 5711-5717.
[163]. Pick, E., Gorzalczany, Y. & Engel, S. (1993) Role of the rac1 p21-GDP-dissociation inhibitor for rho heterodimer in the activation of the superoxide-forming NADPH oxidase of macrophages, *European journal of biochemistry / FEBS.* **217**, 441-55.
[164]. Grizot, S., Faure, J., Fieschi, F., Vignais, P. V., Dagher, M. C. & Pebay-Peyroula, E. (2001) Crystal structure of the Rac1-RhoGDI complex involved in nadph oxidase activation, *Biochemistry.* **40**, 10007-13.
[165]. Heyworth, P. G., Bohl, B. P., Bokoch, G. M. & Curnutte, J. T. (1994) Rac translocates independently of the neutrophil NADPH oxidase components p47phox and p67phox. Evidence for its interaction with flavocytochrome b558, *The Journal of biological chemistry.* **269**, 30749-52.
[166]. Dusi, S., Donini, M. & Rossi, F. (1996) Mechanisms of NADPH oxidase activation: translocation of p40phox, Rac1 and Rac2 from the cytosol to the membranes in human neutrophils lacking p47phox or p67phox, *The Biochemical journal.* **314 (Pt 2)**, 409-12.
[167]. Quinn, M. T., Evans, T., Loetterle, L. R., Jesaitis, A. J. & Bokoch, G. M. (1993) Translocation of Rac correlates with NADPH oxidase activation. Evidence for equimolar translocation of oxidase components, *The Journal of biological chemistry.* **268**, 20983-7.
[168]. Freeman, J. L., Kreck, M. L., Uhlinger, D. J. & Lambeth, J. D. (1994) Ras effector-homolog region on Rac regulates protein associations in the neutrophil respiratory burst oxidase complex, *Biochemistry.* **33**, 13431-13435.
[169]. Nisimoto, Y., Freeman, J. L., Motalebi, S. A., Hirshberg, M. & Lambeth, J. D. (1997) Rac binding to p67(phox). Structural basis for interactions of the Rac1 effector region and insert region with components of the respiratory burst oxidase, *The Journal of biological chemistry.* **272**, 18834-41.
[170]. Abo, A., Webb, M. R., Grogan, A. & Segal, A. W. (1994) Activation of NADPH oxidase involves the dissociation of p21rac from its inhibitory GDP/GTP exchange protein (rhoGDI) followed by its translocation to the plasma membrane, *The Biochemical journal.* **298 Pt 3**, 585-91.
[171]. Kao, Y. Y., Gianni, D., Bohl, B., Taylor, R. M. & Bokoch, G. M. (2008) Identification of a conserved Rac-binding site on NADPH oxidases supports a direct GTPase regulatory mechanism, *The Journal of biological chemistry.* **283**, 12736-46.
[172]. Miyano, K. & Sumimoto, H. (2007) Role of the small GTPase Rac in p22phox-dependent NADPH oxidases, *Biochimie.* **89**, 1133-44.
[173]. Diebold, B. A. & Bokoch, G. M. (2001) Molecular basis for Rac2 regulation of phagocyte NADPH oxidase, *Nature immunology.* **2**, 211-5.
[174]. Gabig, T. G., Crean, C. D., Mantel, P. L. & Rosli, R. (1995) Function of wild-type or mutant Rac2 and Rap1a GTPases in differentiated HL60 cell NADPH oxidase activation, *Blood.* **85**, 804-11.

[175]. Dorseuil, O., Vazquez, A., Lang, P., Bertoglio, J., Gacon, G. & Leca, G. (1992) Inhibition of superoxide production in B lymphocytes by rac antisense oligonucleotides, *The Journal of biological chemistry.* **267**, 20540-2.
[176]. Knaus, U. G., Heyworth, P. G., Evans, T., Curnutte, J. T. & Bokoch, G. M. (1991) Regulation of phagocyte oxygen radical production by the GTP-binding protein Rac 2, *Science (New York, NY).* **254**, 1512-5.
[177]. Abo, A., Pick, E., Hall, A., Totty, N., Teahan, C. G. & Segal, A. W. (1991) Activation of the NADPH oxidase involves the small GTP-binding protein p21rac1, *Nature.* **353**, 668-70.
[178]. Miyano, K., Fukuda, H., Ebisu, K. & Tamura, M. (2003) Remarkable stabilization of neutrophil NADPH oxidase using RacQ61L and a p67phox-p47phox fusion protein, *Biochemistry.* **42**, 184-90.
[179]. Wientjes, F. B., Panayotou, G., Reeves, E. & Segal, A. W. (1996) Interactions between cytosolic components of the NADPH oxidase: p40phox interacts with both p67phox and p47phox, *The Biochemical journal.* **317 (Pt 3)**, 919-24.
[180]. Fuchs, A., Dagher, M. C., Faure, J. & Vignais, P. V. (1996) Topological organization of the cytosolic activating complex of the superoxide-generating NADPH-oxidase. Pinpointing the sites of interaction between p47phoz, p67phox and p40phox using the two-hybrid system, *Biochimica et biophysica acta.* **1312**, 39-47.
[181]. Ebisu, K., Nagasawa, T., Watanabe, K., Kakinuma, K., Miyano, K. & Tamura, M. (2001) Fused p47phox and p67phox truncations efficiently reconstitute NADPH oxidase with higher activity and stability than the individual components, *The Journal of biological chemistry.* **276**, 24498-505.
[182]. Alloul, N., Gorzalczany, Y., Itan, M., Sigal, N. & Pick, E. (2001) Activation of the superoxide-generating NADPH oxidase by chimeric proteins consisting of segments of the cytosolic component p67(phox) and the small GTPase Rac1, *Biochemistry.* **40**, 14557-66.
[183]. Miyano, K., Ogasawara, S., Han, C. H., Fukuda, H. & Tamura, M. (2001) A fusion protein between rac and p67phox (1-210) reconstitutes NADPH oxidase with higher activity and stability than the individual components, *Biochemistry.* **40**, 14089-97.
[184]. Mizrahi, A., Berdichevsky, Y., Ugolev, Y., Molshanski-Mor, S., Nakash, Y., Dahan, I., Alloul, N., Gorzalczany, Y., Sarfstein, R., Hirshberg, M. & Pick, E. (2006) Assembly of the phagocyte NADPH oxidase complex: chimeric constructs derived from the cytosolic components as tools for exploring structure-function relationships, *Journal of leukocyte biology.* **79**, 881-95.
[185]. Sarfstein, R., Gorzalczany, Y., Mizrahi, A., Berdichevsky, Y., Molshanski-Mor, S., Weinbaum, C., Hirshberg, M., Dagher, M. C. & Pick, E. (2004) Dual role of Rac in the assembly of NADPH oxidase, tethering to the membrane and activation of p67phox: a study based on mutagenesis of p67phox-Rac1 chimeras, *The Journal of biological chemistry.* **279**, 16007-16.
[186]. Gorzalczany, Y., Alloul, N., Sigal, N., Weinbaum, C. & Pick, E. (2002) A prenylated p67phox-Rac1 chimera elicits NADPH-dependent superoxide production by phagocyte membranes in the absence of an activator and of p47phox: conversion of a pagan NADPH oxidase to monotheism, *The Journal of biological chemistry.* **277**, 18605-10.
[187]. Berdichevsky, Y., Mizrahi, A., Ugolev, Y., Molshanski-Mor, S. & Pick, E. (2007) Tripartite chimeras comprising functional domains derived from the cytosolic NADPH oxidase components p47phox, p67phox, and Rac1 elicit activator-independent superoxide production by phagocyte membranes: an essential role for anionic membrane phospholipids, *The Journal of biological chemistry.* **282**, 22122-39.

[188]. Marcoux, J., Man, P., Castellan, M., Vives, C., Forest, E. & Fieschi, F. (2009) Conformational changes in p47(phox) upon activation highlighted by mass spectrometry coupled to hydrogen/deuterium exchange and limited proteolysis, *FEBS letters.* **583**, 835-40.
[189]. Kreck, M. L., Freeman, J. L., Abo, A. & Lambeth, J. D. (1996) Membrane association of Rac is required for high activity of the respiratory burst oxidase, *Biochemistry.* **35**, 15683-92.
[190]. Mizrahi, A., Berdichevsky, Y., Casey, P. J. & Pick, E. (2010) A prenylated p47phox-p67phox-Rac1 chimera is a Quintessential NADPH oxidase activator: membrane association and functional capacity, *The Journal of biological chemistry.* **285**, 25485-99.
[191]. El-Benna, J., Dang, P. M. & Gougerot-Pocidalo, M. A. (2008) Priming of the neutrophil NADPH oxidase activation: role of p47phox phosphorylation and NOX2 mobilization to the plasma membrane, *Seminars in immunopathology.* **30**, 279-89.
[192]. Dahlgren, C. (1987) Difference in extracellular radical release after chemotactic factor and calcium ionophore activation of the oxygen radical-generating system in human neutrophils, *Biochimica et biophysica acta.* **930**, 33-8.
[193]. Cox, J. A., Jeng, A. Y., Sharkey, N. A., Blumberg, P. M. & Tauber, A. I. (1985) Activation of the human neutrophil nicotinamide adenine dinucleotide phosphate (NADPH)-oxidase by protein kinase C, *The Journal of clinical investigation.* **76**, 1932-8.
[194]. El-Benna, J., Faust, L. P. & Babior, B. M. (1994) The phosphorylation of the respiratory burst oxidase component p47phox during neutrophil activation. Phosphorylation of sites recognized by protein kinase C and by proline-directed kinases, *The Journal of biological chemistry.* **269**, 23431-6.
[195]. Marasco, W. A., Phan, S. H., Krutzsch, H., Showell, H. J., Feltner, D. E., Nairn, R., Becker, E. L. & Ward, P. A. (1984) Purification and identification of formyl-methionyl-leucyl-phenylalanine as the major peptide neutrophil chemotactic factor produced by Escherichia coli, *The Journal of biological chemistry.* **259**, 5430-9.
[196]. Fu, H., Bylund, J., Karlsson, A., Pellme, S. & Dahlgren, C. (2004) The mechanism for activation of the neutrophil NADPH-oxidase by the peptides formyl-Met-Leu-Phe and Trp-Lys-Tyr-Met-Val-Met differs from that for interleukin-8, *Immunology.* **112**, 201-10.
[197]. Hurtado-Nedelec, M., Makni-Maalej, K., Gougerot-Pocidalo, M. A., Dang, P. M. & El-Benna, J. (2014) Assessment of priming of the human neutrophil respiratory burst, *Methods in molecular biology (Clifton, NJ).* **1124**, 405-12.
[198]. Dahlgren, C. & Karlsson, A. (2002) Ionomycin-induced neutrophil NADPH oxidase activity is selectively inhibited by the serine protease inhibitor diisopropyl fluorophosphate, *Antioxidants & redox signaling.* **4**, 17-25.
[199]. DeLeo, F. R., Allen, L. A., Apicella, M. & Nauseef, W. M. (1999) NADPH oxidase activation and assembly during phagocytosis, *Journal of immunology (Baltimore, Md : 1950).* **163**, 6732-40.
[200]. Makni-Maalej, K., Chiandotto, M., Hurtado-Nedelec, M., Bedouhene, S., Gougerot-Pocidalo, M. A., Dang, P. M. & El-Benna, J. (2013) Zymosan induces NADPH oxidase activation in human neutrophils by inducing the phosphorylation of p47phox and the activation of Rac2: involvement of protein tyrosine kinases, PI3Kinase, PKC, ERK1/2 and p38MAPkinase, *Biochemical pharmacology.* **85**, 92-100.
[201]. Carpenter, C. L. & Cantley, L. C. (1996) Phosphoinositide kinases, *Current opinion in cell biology.* **8**, 153-8.
[202]. Vossebeld, P. J., Homburg, C. H., Schweizer, R. C., Ibarrola, I., Kessler, J., Koenderman, L., Roos, D. & Verhoeven, A. J. (1997) Tyrosine phosphorylation-dependent activation of

phosphatidylinositide 3-kinase occurs upstream of Ca2+-signalling induced by Fcgamma receptor cross-linking in human neutrophils, *Biochemical Journal.* **323**, 87-94.
[203]. Dana, R., Leto, T. L., Malech, H. L. & Levy, R. (1998) Essential Requirement of Cytosolic Phospholipase A2for Activation of the Phagocyte NADPH Oxidase, *Journal of Biological Chemistry.* **273**, 441-445.
[204]. Hii, C. S. & Ferrante, A. (2007) Regulation of the NADPH oxidase activity and anti-microbial function of neutrophils by arachidonic acid, *Archivum immunologiae et therapiae experimentalis.* **55**, 99-110.
[205]. Badwey, J. A., Curnutte, J. T. & Karnovsky, M. L. (1981) cis-Polyunsaturated fatty acids induce high levels of superoxide production by human neutrophils, *The Journal of biological chemistry.* **256**, 12640-3.
[206]. Hardy, S. J., Robinson, B. S., Ferrante, A., Hii, C. S., Johnson, D. W., Poulos, A. & Murray, A. W. (1995) Polyenoic very-long-chain fatty acids mobilize intracellular calcium from a thapsigargin-insensitive pool in human neutrophils. The relationship between Ca2+ mobilization and superoxide production induced by long- and very-long-chain fatty acids, *The Biochemical journal.* **311 (Pt 2)**, 689-97.
[207]. Vignais, P. (2002) The superoxide-generating NADPH oxidase: structural aspects and activation mechanism, *CMLS, Cell Mol Life Sci.* **59**, 1428-1459.
[208]. Belambri, S. A., Dang, P. M. & El-Benna, J. (2014) Evaluation of p47phox phosphorylation in human neutrophils using phospho-specific antibodies, *Methods in molecular biology (Clifton, NJ).* **1124**, 427-33.
[209]. Raad, H., Paclet, M. H., Boussetta, T., Kroviarski, Y., Morel, F., Quinn, M. T., Gougerot-Pocidalo, M. A., Dang, P. M. & El-Benna, J. (2009) Regulation of the phagocyte NADPH oxidase activity: phosphorylation of gp91phox/NOX2 by protein kinase C enhances its diaphorase activity and binding to Rac2, p67phox, and p47phox, *FASEB journal : official publication of the Federation of American Societies for Experimental Biology.* **23**, 1011-22.
[210]. Regier, D. S., Greene, D. G., Sergeant, S., Jesaitis, A. J. & McPhail, L. C. (2000) Phosphorylation of p22 phox Is Mediated by Phospholipase D-dependent and-independent Mechanisms CORRELATION OF NADPH OXIDASE ACTIVITY AND p22 phox PHOSPHORYLATION, *Journal of Biological Chemistry.* **275**, 28406-28412.
[211]. Groemping, Y., Lapouge, K., Smerdon, S. J. & Rittinger, K. (2003) Molecular basis of phosphorylation-induced activation of the NADPH oxidase, *Cell.* **113**, 343-55.
[212]. Sumimoto, H., Hata, K., Mizuki, K., Ito, T., Kage, Y., Sakaki, Y., Fukumaki, Y., Nakamura, M. & Takeshige, K. (1996) Assembly and activation of the phagocyte NADPH oxidase. Specific interaction of the N-terminal Src homology 3 domain of p47phox with p22phox is required for activation of the NADPH oxidase, *The Journal of biological chemistry.* **271**, 22152-8.
[213]. Lapouge, K., Smith, S. J., Walker, P. A., Gamblin, S. J., Smerdon, S. J. & Rittinger, K. (2000) Structure of the TPR domain of p67phox in complex with Rac.GTP, *Molecular cell.* **6**, 899-907.
[214]. Bromberg, Y., Sha'ag, D., Shpungin, S. & Pick, E. (1986) Activation of the superoxide forming NADPH oxidase in a macrophage-derived cell-free system by fatty acids and detergents, *Advances in prostaglandin, thromboxane, and leukotriene research.* **16**, 153-63.
[215]. McPhail, L. C., Clayton, C. C. & Snyderman, R. (1984) A potential second messenger role for unsaturated fatty acids: activation of Ca2+-dependent protein kinase, *Science (New York, NY).* **224**, 622-5.

[216]. McPhail, L. C., Clayton, C. C. & Snyderman, R. (1984) A potential second messenger role for arachidonic acid: activation of Ca2+-dependent protein kinase, *Transactions of the Association of American Physicians.* **97**, 222-31.
[217]. Rossary, A., Arab, K., Goudable, J. & Steghens, J. P. (2007) [Fatty acids regulate NOX activity], *Annales de biologie clinique.* **65**, 33-40.
[218]. Bromberg, Y. & Pick, E. (1984) Unsaturated fatty acids stimulate NADPH-dependent superoxide production by cell-free system derived from macrophages, *Cellular immunology.* **88**, 213-21.
[219]. Curnutte, J. T. (1985) Activation of human neutrophil nicotinamide adenine dinucleotide phosphate, reduced (triphosphopyridine nucleotide, reduced) oxidase by arachidonic acid in a cell-free system, *The Journal of clinical investigation.* **75**, 1740-3.
[220]. Heyneman, R. A. & Vercauteren, R. E. (1984) Activation of a NADPH oxidase from horse polymorphonuclear leukocytes in a cell-free system, *Journal of leukocyte biology.* **36**, 751-9.
[221]. McPhail, L. C., Shirley, P. S., Clayton, C. C. & Snyderman, R. (1985) Activation of the respiratory burst enzyme from human neutrophils in a cell-free system. Evidence for a soluble cofactor, *The Journal of clinical investigation.* **75**, 1735-9.
[222]. Qualliotine-Mann, D., Agwu, D. E., Ellenburg, M. D., McCall, C. E. & McPhail, L. C. (1993) Phosphatidic acid and diacylglycerol synergize in a cell-free system for activation of NADPH oxidase from human neutrophils, *The Journal of biological chemistry.* **268**, 23843-9.
[223]. Foubert, T. R., Burritt, J. B., Taylor, R. M. & Jesaitis, A. J. (2002) Structural changes are induced in human neutrophil cytochrome b by NADPH oxidase activators, LDS, SDS, and arachidonate: intermolecular resonance energy transfer between trisulfopyrenyl-wheat germ agglutinin and cytochrome b(558), *Biochimica et biophysica acta.* **1567**, 221-31.
[224]. Taylor, R. M., Riesselman, M. H., Lord, C. I., Gripentrog, J. M. & Jesaitis, A. J. (2012) Anionic lipid-induced conformational changes in human phagocyte flavocytochrome b precede assembly and activation of the NADPH oxidase complex, *Archives of biochemistry and biophysics.* **521**, 24-31.
[225]. Doussiere, J., Bouzidi, F., Poinas, A., Gaillard, J. & Vignais, P. V. (1999) Kinetic study of the activation of the neutrophil NADPH oxidase by arachidonic acid. Antagonistic effects of arachidonic acid and phenylarsine oxide, *Biochemistry.* **38**, 16394-406.
[226]. Souabni, H., Thoma, V., Bizouarn, T., Chatgilialoglu, C., Siafaka-Kapadai, A., Baciou, L., Ferreri, C., Houee-Levin, C. & Ostuni, M. A. (2012) trans Arachidonic acid isomers inhibit NADPH-oxidase activity by direct interaction with enzyme components, *Biochimica et biophysica acta.* **1818**, 2314-24.
[227]. Swain, S. D., Helgerson, S. L., Davis, A. R., Nelson, L. K. & Quinn, M. T. (1997) Analysis of activation-induced conformational changes in p47phox using tryptophan fluorescence spectroscopy, *The Journal of biological chemistry.* **272**, 29502-10.
[228]. Matono, R., Miyano, K., Kiyohara, T. & Sumimoto, H. (2014) Arachidonic acid induces direct interaction of the p67(phox)-Rac complex with the phagocyte oxidase Nox2, leading to superoxide production, *The Journal of biological chemistry.* **289**, 24874-84.
[229]. Bylund, J., Goldblatt, D. & Speert, D. P. (2005) Chronic granulomatous disease: from genetic defect to clinical presentation, *Advances in experimental medicine and biology.* **568**, 67-87.
[230]. Winkelstein, J. A., Marino, M. C., Johnston, R. B., Jr., Boyle, J., Curnutte, J., Gallin, J. I., Malech, H. L., Holland, S. M., Ochs, H., Quie, P., Buckley, R. H., Foster, C. B., Chanock, S. J. &

Dickler, H. (2000) Chronic granulomatous disease. Report on a national registry of 368 patients, *Medicine.* **79**, 155-69.
[231]. Dinauer, M. C. & Orkin, S. H. (1988) Chronic granulomatous disease. Molecular genetics, *Hematology/oncology clinics of North America.* **2**, 225-40.
[232]. Seger, R. A. (2010) Chronic granulomatous disease: recent advances in pathophysiology and treatment, *The Netherlands journal of medicine.* **68**, 334-40.
[233]. Cave, A. C., Brewer, A. C., Narayanapanicker, A., Ray, R., Grieve, D. J., Walker, S. & Shah, A. M. (2006) NADPH oxidases in cardiovascular health and disease, *Antioxidants & redox signaling.* **8**, 691-728.
[234]. Brandes, R. P. & Kreuzer, J. (2005) Vascular NADPH oxidases: molecular mechanisms of activation, *Cardiovascular research.* **65**, 16-27.
[235]. Varga, Z. V., Kupai, K., Szucs, G., Gaspar, R., Paloczi, J., Farago, N., Zvara, A., Puskas, L. G., Razga, Z., Tiszlavicz, L., Bencsik, P., Gorbe, A., Csonka, C., Ferdinandy, P. & Csont, T. (2013) MicroRNA-25-dependent up-regulation of NADPH oxidase 4 (NOX4) mediates hypercholesterolemia-induced oxidative/nitrative stress and subsequent dysfunction in the heart, *Journal of molecular and cellular cardiology.* **62**, 111-21.
[236]. Li, H., Horke, S. & Förstermann, U. (2013) Oxidative stress in vascular disease and its pharmacological prevention, *Trends in Pharmacological Sciences.* **34**, 313-319.
[237]. Lassegue, B. & Griendling, K. K. (2010) NADPH oxidases: functions and pathologies in the vasculature, *Arteriosclerosis, thrombosis, and vascular biology.* **30**, 653-61.
[238]. Griendling, K. K., Sorescu, D. & Ushio-Fukai, M. (2000) NAD(P)H oxidase: role in cardiovascular biology and disease, *Circulation research.* **86**, 494-501.
[239]. Drummond, G. R. & Sobey, C. G. (2014) Endothelial NADPH oxidases: which NOX to target in vascular disease?, *Trends in Endocrinology & Metabolism.* **25**, 452-463.
[240]. Sorce, S. & Krause, K. H. (2009) NOX enzymes in the central nervous system: from signaling to disease, *Antioxidants & redox signaling.* **11**, 2481-504.
[241]. Waris, G. & Ahsan, H. (2006) Reactive oxygen species: role in the development of cancer and various chronic conditions, *Journal of carcinogenesis.* **5**, 14.
[242]. Kamata, T. (2009) Roles of Nox1 and other Nox isoforms in cancer development, *Cancer science.* **100**, 1382-8.
[243]. Račková, L. (2013) Cholesterol load of microglia: Contribution of membrane architecture changes to neurotoxic power?, *Archives of biochemistry and biophysics.* **537**, 91-103.
[244]. Lambeth, J. D., Kawahara, T. & Diebold, B. (2007) Regulation of Nox and Duox enzymatic activity and expression, *Free radical biology & medicine.* **43**, 319-31.
[245]. Carnevale, R., Loffredo, L., Sanguigni, V., Plebani, A., Rossi, P., Pignata, C., Martire, B., Finocchi, A., Pietrogrande, M. C., Azzari, C., Soresina, A. R., Martino, S., Cirillo, E., Martino, F., Pignatelli, P. & Violi, F. (2014) Different degrees of NADPH oxidase 2 regulation and in vivo platelet activation: lesson from chronic granulomatous disease, *Journal of the American Heart Association.* **3**, e000920.
[246]. Nunes, P., Demaurex, N. & Dinauer, M. C. (2013) Regulation of the NADPH oxidase and associated ion fluxes during phagocytosis, *Traffic (Copenhagen, Denmark).* **14**, 1118-31.
[247]. Vance, J. E. & Vance, D. E. (2008) *Biochemistry of lipids, lipoproteins and membranes*, Elsevier.
[248]. Tristram-Nagle, S. & Nagle, J. F. (2004) Lipid bilayers: thermodynamics, structure, fluctuations, and interactions, *Chemistry and physics of lipids.* **127**, 3-14.
[249]. Chaffey, N. (2003) Alberts, B., Johnson, A., Lewis, J., Raff, M., Roberts, K. and Walter, P. Molecular biology of the cell. 4th edn, *Annals of Botany.* **91**, 401.

[250]. Ruxton, C., Reed, S. C., Simpson, M. & Millington, K. (2004) The health benefits of omega-3 polyunsaturated fatty acids: a review of the evidence, *Journal of Human Nutrition and Dietetics.* **17**, 449-459.
[251]. Russo, S., Ross, J. & Cowart, L. (2013) *Sphingolipids in obesity, type 2 diabetes, and metabolic disease,* Springer.
[252]. Nagle, J. F. & Tristram-Nagle, S. (2000) Structure of lipid bilayers, *Biochimica et biophysica acta.* **1469**, 159-95.
[253]. Bartke, N. & Hannun, Y. A. (2009) Bioactive sphingolipids: metabolism and function, *Journal of lipid research.* **50**, S91-S96.
[254]. Gulbins, E. & Petrache, I. (2013) *Sphingolipids in disease*, Springer.
[255]. Yeagle, P. L. (1985) Cholesterol and the cell membrane, *Biochimica et Biophysica Acta (BBA) - Reviews on Biomembranes.* **822**, 267-287.
[256]. Ohvo-Rekilä, H., Ramstedt, B., Leppimäki, P. & Slotte, J. P. (2002) Cholesterol interactions with phospholipids in membranes, *Progress in lipid research.* **41**, 66-97.
[257]. Hanukoglu, I. (1992) Steroidogenic enzymes: Structure, function, and role in regulation of steroid hormone biosynthesis, *The Journal of Steroid Biochemistry and Molecular Biology.* **43**, 779-804.
[258]. Schreurs, B. G. (2010) The Effects of Cholesterol on Learning and Memory, *Neuroscience and biobehavioral reviews.* **34**, 1366-1379.
[259]. Pfrieger, F. W. (2003) Cholesterol homeostasis and function in neurons of the central nervous system, *CMLS, Cell Mol Life Sci.* **60**, 1158-1171.
[260]. James C. E. Underwood, S. S. C. (2009) *General and Systematic Pathology,* London: Churchhill livingstone.
[261]. Brown, M. S. & Goldstein, J. L. (1984) How LDL receptors influence cholesterol and atherosclerosis, *Scientific American.* **251**, 58-66.
[262]. Bhatnagar, D., Soran, H. & Durrington, P. N. (2008) Hypercholesterolaemia and its management, *BMJ (Clinical research ed).* **337**, a993.
[263]. Crall, F. V., Jr. & Roberts, W. C. (1978) The extramural and intramural coronary arteries in juvenile diabetes mellitus: analysis of nine necropsy patients aged 19 to 38 years with onset of diabetes before age 15 years, *The American journal of medicine.* **64**, 221-30.
[264]. Selby, J. V., Friedman, G. D. & Quesenberry, C. P., Jr. (1990) Precursors of essential hypertension: pulmonary function, heart rate, uric acid, serum cholesterol, and other serum chemistries, *American journal of epidemiology.* **131**, 1017-27.
[265]. Bjorkhem, I. & Diczfalusy, U. (2002) Oxysterols: friends, foes, or just fellow passengers?, *Arteriosclerosis, thrombosis, and vascular biology.* **22**, 734-42.
[266]. Olkkonen, V. M. & Lehto, M. (2004) Oxysterols and oxysterol binding proteins: role in lipid metabolism and atherosclerosis, *Annals of medicine.* **36**, 562-72.
[267]. Brown, A. J. & Jessup, W. (1999) Oxysterols and atherosclerosis, *Atherosclerosis.* **142**, 1-28.
[268]. Vaya, J. & Schipper, H. M. (2007) Oxysterols, cholesterol homeostasis, and Alzheimer disease, *Journal of Neurochemistry.* **102**, 1727-1737.
[269]. Antonchik, A. V., Zhabinskii, V. N. & Khripach, V. A. (2007) [Oxysterols: genesis and basic functions], *Bioorganicheskaia khimiia.* **33**, 297-309.
[270]. Brown, A. J. & Jessup, W. (2009) Oxysterols: Sources, cellular storage and metabolism, and new insights into their roles in cholesterol homeostasis, *Molecular aspects of medicine.* **30**, 111-22.

[271]. London, E. (2002) Insights into lipid raft structure and formation from experiments in model membranes, *Current Opinion in Structural Biology.* **12**, 480-486.
[272]. Anchisi, L., Dessi, S., Pani, A. & Mandas, A. (2013) Cholesterol homeostasis: A key to prevent or slow down neurodegeneration, *Frontiers in Physiology.* **3**.
[273]. Silvius, J. R. (2003) Role of cholesterol in lipid raft formation: lessons from lipid model systems, *Biochimica et Biophysica Acta (BBA) - Biomembranes.* **1610**, 174-183.
[274]. Jin, S., Zhou, F., Katirai, F. & Li, P. L. (2011) Lipid raft redox signaling: molecular mechanisms in health and disease, *Antioxidants & redox signaling.* **15**, 1043-83.
[275]. Simons, K. & Ehehalt, R. (2002) Cholesterol, lipid rafts, and disease, *The Journal of clinical investigation.* **110**, 597-603.
[276]. Korade, Z. & Kenworthy, A. K. (2008) Lipid rafts, cholesterol, and the brain, *Neuropharmacology.* **55**, 1265-1273.
[277]. Tsui-Pierchala, B. A., Encinas, M., Milbrandt, J. & Johnson Jr, E. M. (2002) Lipid rafts in neuronal signaling and function, *Trends in Neurosciences.* **25**, 412-417.
[278]. Fantini, J., Garmy, N., Mahfoud, R. & Yahi, N. (2002) Lipid rafts: structure, function and role in HIV, Alzheimer's and prion diseases, *Expert reviews in molecular medicine.* **4**, 1-22.
[279]. Michel, V. & Bakovic, M. (2007) Lipid rafts in health and disease, *Biology of the Cell.* **99**, 129-140.
[280]. Nauseef, W. (2004) Assembly of the phagocyte NADPH oxidase, *Histochem Cell Biol.* **122**, 277-291.
[281]. Brechard, S., Plancon, S. & Tschirhart, E. J. (2013) New insights into the regulation of neutrophil NADPH oxidase activity in the phagosome: a focus on the role of lipid and Ca(2+) signaling, *Antioxidants & redox signaling.* **18**, 661-76.
[282]. Seet, L.-F. & Hong, W. (2006) The Phox (PX) domain proteins and membrane traffic, *Biochimica et Biophysica Acta (BBA) - Molecular and Cell Biology of Lipids.* **1761**, 878-896.
[283]. Stahelin, R. V., Burian, A., Bruzik, K. S., Murray, D. & Cho, W. (2003) Membrane binding mechanisms of the PX domains of NADPH oxidase p40phox and p47phox, *The Journal of biological chemistry.* **278**, 14469-79.
[284]. Bravo, J., Karathanassis, D., Pacold, C. M., Pacold, M. E., Ellson, C. D., Anderson, K. E., Butler, P. J., Lavenir, I., Perisic, O., Hawkins, P. T., Stephens, L. & Williams, R. L. (2001) The crystal structure of the PX domain from p40(phox) bound to phosphatidylinositol 3-phosphate, *Molecular cell.* **8**, 829-39.
[285]. Karathanassis, D., Stahelin, R. V., Bravo, J., Perisic, O., Pacold, C. M., Cho, W. & Williams, R. L. (2002) Binding of the PX domain of p47(phox) to phosphatidylinositol 3,4-bisphosphate and phosphatidic acid is masked by an intramolecular interaction, *The EMBO journal.* **21**, 5057-5068.
[286]. Tamura, M., Ogata, K. & Takeshita, M. (1993) Phosphatidic Acid-Induced Superoxide Generation in Electropermeabilized Human Neutrophils, *Archives of biochemistry and biophysics.* **305**, 477-482.
[287]. Ugolev, Y., Molshanski-Mor, S., Weinbaum, C. & Pick, E. (2006) Liposomes comprising anionic but not neutral phospholipids cause dissociation of Rac(1 or 2) x RhoGDI complexes and support amphiphile-independent NADPH oxidase activation by such complexes, *The Journal of biological chemistry.* **281**, 19204-19.
[288]. Hazan, I., Dana, R., Granot, Y. & Levy, R. (1997) Cytosolic phospholipase A2 and its mode of activation in human neutrophils by opsonized zymosan. Correlation between 42/44 kDa mitogen-activated protein kinase, cytosolic phospholipase A2 and NADPH oxidase, *The Biochemical journal.* **326 (Pt 3)**, 867-76.

[289]. Rubin, B. B., Downey, G. P., Koh, A., Degousee, N., Ghomashchi, F., Nallan, L., Stefanski, E., Harkin, D. W., Sun, C., Smart, B. P., Lindsay, T. F., Cherepanov, V., Vachon, E., Kelvin, D., Sadilek, M., Brown, G. E., Yaffe, M. B., Plumb, J., Grinstein, S., Glogauer, M. & Gelb, M. H. (2005) Cytosolic phospholipase A2-alpha is necessary for platelet-activating factor biosynthesis, efficient neutrophil-mediated bacterial killing, and the innate immune response to pulmonary infection: cPLA2-alpha does not regulate neutrophil NADPH oxidase activity, *The Journal of biological chemistry.* **280**, 7519-29.
[290]. Shmelzer, Z., Haddad, N., Admon, E., Pessach, I., Leto, T. L., Eitan-Hazan, Z., Hershfinkel, M. & Levy, R. (2003) Unique targeting of cytosolic phospholipase A(2) to plasma membranes mediated by the NADPH oxidase in phagocytes, *The Journal of Cell Biology.* **162**, 683-692.
[291]. Hata, K., Ito, T., Takeshige, K. & Sumimoto, H. (1998) Anionic amphiphile-independent activation of the phagocyte NADPH oxidase in a cell-free system by p47phox and p67phox, both in C terminally truncated forms. Implication for regulatory Src homology 3 domain-mediated interactions, *The Journal of biological chemistry.* **273**, 4232-6.
[292]. Shao, D., Segal, A. W. & Dekker, L. V. (2003) Lipid rafts determine efficiency of NADPH oxidase activation in neutrophils, *FEBS letters.* **550**, 101-6.
[293]. Han, W., Li, H., Villar, V. A., Pascua, A. M., Dajani, M. I., Wang, X., Natarajan, A., Quinn, M. T., Felder, R. A., Jose, P. A. & Yu, P. (2008) Lipid rafts keep NADPH oxidase in the inactive state in human renal proximal tubule cells, *Hypertension.* **51**, 481-7.
[294]. Vilhardt, F. & van Deurs, B. (2004) The phagocyte NADPH oxidase depends on cholesterol-enriched membrane microdomains for assembly, *The EMBO journal.* **23**, 739-48.
[295]. Yang, B., Oo, T. N. & Rizzo, V. (2006) Lipid rafts mediate H2O2 prosurvival effects in cultured endothelial cells, *FASEB journal : official publication of the Federation of American Societies for Experimental Biology.* **20**, 1501-3.
[296]. Zhang, A. Y., Yi, F., Zhang, G., Gulbins, E. & Li, P. L. (2006) Lipid raft clustering and redox signaling platform formation in coronary arterial endothelial cells, *Hypertension.* **47**, 74-80.
[297]. Zuo, L., Ushio-Fukai, M., Hilenski, L. L. & Alexander, R. W. (2004) Microtubules regulate angiotensin II type 1 receptor and Rac1 localization in caveolae/lipid rafts: role in redox signaling, *Arteriosclerosis, thrombosis, and vascular biology.* **24**, 1223-8.
[298]. Guichard, C., Pedruzzi, E., Dewas, C., Fay, M., Pouzet, C., Bens, M., Vandewalle, A., Ogier-Denis, E., Gougerot-Pocidalo, M. A. & Elbim, C. (2005) Interleukin-8-induced priming of neutrophil oxidative burst requires sequential recruitment of NADPH oxidase components into lipid rafts, *The Journal of biological chemistry.* **280**, 37021-32.
[299]. Bollinger, C. R., Teichgraber, V. & Gulbins, E. (2005) Ceramide-enriched membrane domains, *Biochimica et biophysica acta.* **1746**, 284-94.
[300]. Gulbins, E. & Li, P. L. (2006) Physiological and pathophysiological aspects of ceramide, *American journal of physiology Regulatory, integrative and comparative physiology.* **290**, R11-26.
[301]. Pedruzzi, E., Guichard, C., Ollivier, V., Driss, F., Fay, M., Prunet, C., Marie, J. C., Pouzet, C., Samadi, M., Elbim, C., O'Dowd, Y., Bens, M., Vandewalle, A., Gougerot-Pocidalo, M. A., Lizard, G. & Ogier-Denis, E. (2004) NAD(P)H oxidase Nox-4 mediates 7-ketocholesterol-induced endoplasmic reticulum stress and apoptosis in human aortic smooth muscle cells, *Molecular and cellular biology.* **24**, 10703-17.

[302]. Rosenblat, M. & Aviram, M. (2002) Oxysterol-induced activation of macrophage NADPH-oxidase enhances cell-mediated oxidation of LDL in the atherosclerotic apolipoprotein E deficient mouse: inhibitory role for vitamin E, *Atherosclerosis.* **160**, 69-80.
[303]. Peralta-Videa, J. R., Zhao, L., Lopez-Moreno, M. L., de la Rosa, G., Hong, J. & Gardea-Torresdey, J. L. (2011) Nanomaterials and the environment: a review for the biennium 2008–2010, *Journal of hazardous materials.* **186**, 1-15.
[304]. Peralta-Videa, J. R., Zhao, L., Lopez-Moreno, M. L., de la Rosa, G., Hong, J. & Gardea-Torresdey, J. L. (2011) Nanomaterials and the environment: a review for the biennium 2008-2010, *Journal of hazardous materials.* **186**, 1-15.
[305]. Taylor, R., Coulombe, S., Otanicar, T., Phelan, P., Gunawan, A., Lv, W., Rosengarten, G., Prasher, R. & Tyagi, H. (2013) Small particles, big impacts: A review of the diverse applications of nanofluids, *Journal of Applied Physics.* **113**, -.
[306]. Brown, C. L., Bushell, G., Whitehouse, M. W., Agrawal, D., Tupe, S., Paknikar, K. & Tiekink, E. R. (2007) Nanogold-pharmaceutics, *Gold Bulletin.* **40**, 245-250.
[307]. Boisselier, E. & Astruc, D. (2009) Gold nanoparticles in nanomedicine: preparations, imaging, diagnostics, therapies and toxicity, *Chemical Society reviews.* **38**, 1759-82.
[308]. Zhang, L., Gu, F. X., Chan, J. M., Wang, A. Z., Langer, R. S. & Farokhzad, O. C. (2008) Nanoparticles in medicine: therapeutic applications and developments, *Clinical pharmacology and therapeutics.* **83**, 761-9.
[309]. Kawasaki, E. S. & Player, A. (2005) Nanotechnology, nanomedicine, and the development of new, effective therapies for cancer, *Nanomedicine.* **1**, 101-9.
[310]. Joachim, C. (2005) To be nano or not to be nano?, *Nat Mater.* **4**, 107-109.
[311]. Salata, O. V. (2004) Applications of nanoparticles in biology and medicine, *Journal of nanobiotechnology.* **2**, 3.
[312]. Northfelt, D. W., Dezube, B. J., Thommes, J. A., Miller, B. J., Fischl, M. A., Friedman-Kien, A., Kaplan, L. D., Du Mond, C., Mamelok, R. D. & Henry, D. H. (1998) Pegylated-liposomal doxorubicin versus doxorubicin, bleomycin, and vincristine in the treatment of AIDS-related Kaposi's sarcoma: results of a randomized phase III clinical trial, *Journal of clinical oncology : official journal of the American Society of Clinical Oncology.* **16**, 2445-51.
[313]. Farokhzad, O. C. & Langer, R. (2006) Nanomedicine: developing smarter therapeutic and diagnostic modalities, *Advanced drug delivery reviews.* **58**, 1456-9.
[314]. Lian, W., Litherland, S. A., Badrane, H., Tan, W., Wu, D., Baker, H. V., Gulig, P. A., Lim, D. V. & Jin, S. (2004) Ultrasensitive detection of biomolecules with fluorescent dye-doped nanoparticles, *Analytical biochemistry.* **334**, 135-44.
[315]. Hoshino, A., Hanaki, K., Suzuki, K. & Yamamoto, K. (2004) Applications of T-lymphoma labeled with fluorescent quantum dots to cell tracing markers in mouse body, *Biochemical and biophysical research communications.* **314**, 46-53.
[316]. Liu, Y., Miyoshi, H. & Nakamura, M. (2007) Nanomedicine for drug delivery and imaging: a promising avenue for cancer therapy and diagnosis using targeted functional nanoparticles, *International journal of cancer Journal international du cancer.* **120**, 2527-37.
[317]. Perrault, S. D. & Chan, W. C. (2010) In vivo assembly of nanoparticle components to improve targeted cancer imaging, *Proceedings of the National Academy of Sciences.* **107**, 11194-11199.
[318]. Kong, T., Zeng, J., Wang, X., Yang, X., Yang, J., McQuarrie, S., McEwan, A., Roa, W., Chen, J. & Xing, J. Z. (2008) Enhancement of radiation cytotoxicity in breast-cancer cells by localized attachment of gold nanoparticles, *Small (Weinheim an der Bergstrasse, Germany).* **4**, 1537-43.

[319]. Nie, S., Xing, Y., Kim, G. J. & Simons, J. W. (2007) Nanotechnology applications in cancer, *Annu Rev Biomed Eng.* **9**, 257-288.
[320]. Davis, M. E., Zuckerman, J. E., Choi, C. H. J., Seligson, D., Tolcher, A., Alabi, C. A., Yen, Y., Heidel, J. D. & Ribas, A. (2010) Evidence of RNAi in humans from systemically administered siRNA via targeted nanoparticles, *Nature.* **464**, 1067-1070.
[321]. Porcel, E., Liehn, S., Remita, H., Usami, N., Kobayashi, K., Furusawa, Y., Le Sech, C. & Lacombe, S. (2010) Platinum nanoparticles: a promising material for future cancer therapy?, *Nanotechnology.* **21**, 85103.
[322]. Hainfeld, J. F., Slatkin, D. N. & Smilowitz, H. M. (2004) The use of gold nanoparticles to enhance radiotherapy in mice, *Physics in medicine and biology.* **49**, N309-15.
[323]. Hamada, N., Imaoka, T., Masunaga, S., Ogata, T., Okayasu, R., Takahashi, A., Kato, T. A., Kobayashi, Y., Ohnishi, T., Ono, K., Shimada, Y. & Teshima, T. (2010) Recent advances in the biology of heavy-ion cancer therapy, *Journal of radiation research.* **51**, 365-83.
[324]. Niederberger, M. & Pinna, N. (2009) *Metal oxide nanoparticles in organic solvents: synthesis, formation, assembly and application*, Springer.
[325]. Carp, O., Huisman, C. L. & Reller, A. (2004) Photoinduced reactivity of titanium dioxide, *Progress in solid state chemistry.* **32**, 33-177.
[326]. Chen, X. & Mao, S. S. (2007) Titanium dioxide nanomaterials: synthesis, properties, modifications, and applications, *Chemical reviews.* **107**, 2891-2959.
[327]. Weir, A., Westerhoff, P., Fabricius, L., Hristovski, K. & von Goetz, N. (2012) Titanium dioxide nanoparticles in food and personal care products, *Environmental science & technology.* **46**, 2242-2250.
[328]. Skocaj, M., Filipic, M., Petkovic, J. & Novak, S. (2011) Titanium dioxide in our everyday life; is it safe?, *Radiology and oncology.* **45**, 227-47.
[329]. Yuan, Y., Ding, J., Xu, J., Deng, J. & Guo, J. (2010) TiO2 nanoparticles co-doped with silver and nitrogen for antibacterial application, *Journal of nanoscience and nanotechnology.* **10**, 4868-74.
[330]. Lucky, S. S., Muhammad Idris, N., Li, Z., Huang, K., Soo, K. C. & Zhang, Y. (2015) Titania coated upconversion nanoparticles for near-infrared light triggered photodynamic therapy, *ACS nano.* **9**, 191-205.
[331]. Zeisser-Labouèbe, M., Vargas, A. & Delie, F. (2007) Nanoparticles for photodynamic therapy of cancer, *Nanotechnologies for the Life Sciences*.
[332]. Lagopati, N., Kitsiou, P., Kontos, A., Venieratos, P., Kotsopoulou, E., Kontos, A., Dionysiou, D., Pispas, S., Tsilibary, E. & Falaras, P. (2010) Photo-induced treatment of breast epithelial cancer cells using nanostructured titanium dioxide solution, *Journal of Photochemistry and Photobiology A: Chemistry.* **214**, 215-223.
[333]. Dransfield, G. (2000) Inorganic sunscreens, *Radiation protection dosimetry.* **91**, 271-273.
[334]. Wiesenthal, A., Hunter, L., Wang, S., Wickliffe, J. & Wilkerson, M. (2011) Nanoparticles: small and mighty, *International journal of dermatology.* **50**, 247-54.
[335]. Papakostas, D., Rancan, F., Sterry, W., Blume-Peytavi, U. & Vogt, A. (2011) Nanoparticles in dermatology, *Archives of dermatological research.* **303**, 533-50.
[336]. Thomas, T., Thomas, K., Sadrieh, N., Savage, N., Adair, P. & Bronaugh, R. (2006) Research strategies for safety evaluation of nanomaterials, part VII: evaluating consumer exposure to nanoscale materials, *Toxicological sciences : an official journal of the Society of Toxicology.* **91**, 14-9.
[337]. Bermudez, E., Mangum, J. B., Wong, B. A., Asgharian, B., Hext, P. M., Warheit, D. B. & Everitt, J. I. (2004) Pulmonary responses of mice, rats, and hamsters to subchronic inhalation of

ultrafine titanium dioxide particles, *Toxicological sciences : an official journal of the Society of Toxicology*. **77**, 347-57.
[338]. Wang, J., Zhou, G., Chen, C., Yu, H., Wang, T., Ma, Y., Jia, G., Gao, Y., Li, B., Sun, J., Li, Y., Jiao, F., Zhao, Y. & Chai, Z. (2007) Acute toxicity and biodistribution of different sized titanium dioxide particles in mice after oral administration, *Toxicology letters.* **168**, 176-85.
[339]. Gheshlaghi, Z. N., Riazi, G. H., Ahmadian, S., Ghafari, M. & Mahinpour, R. (2008) Toxicity and interaction of titanium dioxide nanoparticles with microtubule protein, *Acta biochimica et biophysica Sinica.* **40**, 777-82.
[340]. Barnard, A. S. (2010) One-to-one comparison of sunscreen efficacy, aesthetics and potential nanotoxicity, *Nature nanotechnology.* **5**, 271-4.
[341]. Li, N., Xia, T. & Nel, A. E. (2008) The role of oxidative stress in ambient particulate matter-induced lung diseases and its implications in the toxicity of engineered nanoparticles, *Free radical biology & medicine.* **44**, 1689-99.
[342]. Buzea, C., Pacheco, I. I. & Robbie, K. (2007) Nanomaterials and nanoparticles: sources and toxicity, *Biointerphases.* **2**, MR17-MR71.
[343]. Manke, A., Wang, L. & Rojanasakul, Y. (2013) Mechanisms of Nanoparticle-Induced Oxidative Stress and Toxicity, *BioMed Research International.* **2013**, 15.
[344]. Niska, K., Pyszka, K., Tukaj, C., Wozniak, M., Radomski, M. W. & Inkielewicz-Stepniak, I. (2015) Titanium dioxide nanoparticles enhance production of superoxide anion and alter the antioxidant system in human osteoblast cells, *International journal of nanomedicine.* **10**, 1095-107.
[345]. Shi, H., Magaye, R., Castranova, V. & Zhao, J. (2013) Titanium dioxide nanoparticles: a review of current toxicological data, *Particle and fibre toxicology.* **10**, 15.
[346]. Baan, R. A. (2007) Carcinogenic hazards from inhaled carbon black, titanium dioxide, and talc not containing asbestos or asbestiform fibers: recent evaluations by an IARC Monographs Working Group, *Inhalation toxicology.* **19 Suppl 1**, 213-28.
[347]. da Rosa, E. L. (2013) Kinetic effects of TiO2 fine particles and nanoparticles aggregates on the nanomechanical properties of human neutrophils assessed by force spectroscopy, *BMC biophysics.* **6**, 11.
[348]. Huang, C. C., Aronstam, R. S., Chen, D. R. & Huang, Y. W. (2010) Oxidative stress, calcium homeostasis, and altered gene expression in human lung epithelial cells exposed to ZnO nanoparticles, *Toxicology in vitro : an international journal published in association with BIBRA.* **24**, 45-55.
[349]. Knaapen, A. M., Borm, P. J., Albrecht, C. & Schins, R. P. (2004) Inhaled particles and lung cancer. Part A: Mechanisms, *International journal of cancer Journal international du cancer.* **109**, 799-809.
[350]. Rotello, V. M. (2004) *Nanoparticles: Building Blocks for Nanotechnology*, Kluwer Academic/Plenum Publishers.
[351]. Rosenberg, B., Vancamp, L. & Krigas, T. (1965) inhibition of cell division in escherichia coli electrolysis products from platinum electrode *Nature.* **205**, 698-9.
[352]. Rosenberg, B., VanCamp, L., Trosko, J. E. & Mansour, V. H. (1969) Platinum compounds: a new class of potent antitumour agents, *Nature.* **222**, 385-6.
[353]. Yamada, M., Foote, M. & Prow, T. W. (2014) Therapeutic gold, silver, and platinum nanoparticles, *Wiley interdisciplinary reviews Nanomedicine and nanobiotechnology*.
[354]. Pelka, J., Gehrke, H., Esselen, M., Türk, M., Crone, M., Bräse, S., Muller, T., Blank, H., Send, W., Zibat, V., Brenner, P., Schneider, R., Gerthsen, D. & Marko, D. (2009) Cellular

Uptake of Platinum Nanoparticles in Human Colon Carcinoma Cells and Their Impact on Cellular Redox Systems and DNA Integrity, *Chemical research in toxicology.* **22**, 649-659.
[355]. Asharani, P. V., Xinyi, N., Hande, M. P. & Valiyaveettil, S. (2009) DNA damage and p53-mediated growth arrest in human cells treated with platinum nanoparticles, *Nanomedicine.* **5**, 51-64.
[356]. Gehrke, H., Pelka, J., Hartinger, C. G., Blank, H., Bleimund, F., Schneider, R., Gerthsen, D., Brase, S., Crone, M., Turk, M. & Marko, D. (2011) Platinum nanoparticles and their cellular uptake and DNA platination at non-cytotoxic concentrations, *Archives of toxicology.* **85**, 799-812.
[357]. Manikandan, M., Hasan, N. & Wu, H. F. (2013) Platinum nanoparticles for the photothermal treatment of Neuro 2A cancer cells, *Biomaterials.* **34**, 5833-42.
[358]. Kajita, M., Hikosaka, K., Iitsuka, M., Kanayama, A., Toshima, N. & Miyamoto, Y. (2007) Platinum nanoparticle is a useful scavenger of superoxide anion and hydrogen peroxide, *Free radical research.* **41**, 615-626.
[359]. Watanabe, A., Kajita, M., Kim, J., Kanayama, A., Takahashi, K., Mashino, T. & Miyamoto, Y. (2009) In vitro free radical scavenging activity of platinum nanoparticles, *Nanotechnology.* **20**, 455105.
[360]. Onizawa, S., Aoshiba, K., Kajita, M., Miyamoto, Y. & Nagai, A. (2009) Platinum nanoparticle antioxidants inhibit pulmonary inflammation in mice exposed to cigarette smoke, *Pulmonary pharmacology & therapeutics.* **22**, 340-9.
[361]. Martin, R., Menchon, C., Apostolova, N., Victor, V. M., Alvaro, M., Herance, J. R. & Garcia, H. (2010) Nano-jewels in biology. Gold and platinum on diamond nanoparticles as antioxidant systems against cellular oxidative stress, *ACS nano.* **4**, 6957-65.
[362]. Yamagishi, Y., Watari, A., Hayata, Y., Li, X., Kondoh, M., Tsutsumi, Y. & Yagi, K. (2013) Hepatotoxicity of sub-nanosized platinum particles in mice, *Die Pharmazie.* **68**, 178-82.
[363]. Yamagishi, Y., Watari, A., Hayata, Y., Li, X., Kondoh, M., Yoshioka, Y., Tsutsumi, Y. & Yagi, K. (2013) Acute and chronic nephrotoxicity of platinum nanoparticles in mice, *Nanoscale research letters.* **8**, 395.
[364]. Park, E. J., Kim, H., Kim, Y. & Park, K. (2010) Intratracheal instillation of platinum nanoparticles may induce inflammatory responses in mice, *Archives of pharmacal research.* **33**, 727-35.
[365]. Akasaki, T., Koga, H. & Sumimoto, H. (1999) Phosphoinositide 3-kinase-dependent and -independent activation of the small GTPase Rac2 in human neutrophils, *The Journal of biological chemistry.* **274**, 18055-9.
[366]. Light, D. R., Walsh, C., O'Callaghan, A. M., Goetzl, E. J. & Tauber, A. I. (1981) Characteristics of the cofactor requirements for the superoxide-generating NADPH oxidase of human polymorphonuclear leukocytes, *Biochemistry.* **20**, 1468-76.
[367]. Baciou, L., Erard, M., Dagher, M. C. & Bizouarn, T. (2009) The cytosolic subunit p67phox of the NADPH-oxidase complex does not bind NADPH, *FEBS letters.* **583**, 3225-9.
[368]. Ligeti, E., Doussiere, J. & Vignais, P. V. (1988) Activation of the O2(.-)-generating oxidase in plasma membrane from bovine polymorphonuclear neutrophils by arachidonic acid, a cytosolic factor of protein nature, and nonhydrolyzable analogues of GTP, *Biochemistry.* **27**, 193-200.
[369]. Greenwood, C. & Palmer, G. (1965) Evidence for the existence of two functionally distinct forms cytochrome c manomer at alkaline pH, *The Journal of biological chemistry.* **240**, 3660-3.
[370]. Micsonai, A., Wien, F., Kernya, L., Lee, Y. H., Goto, Y., Refregiers, M. & Kardos, J. (2015) Accurate secondary structure prediction and fold recognition for circular dichroism

spectroscopy, *Proceedings of the National Academy of Sciences of the United States of America.* **112**, E3095-103.
[371]. Zhou, M., Diwu, Z., Panchuk-Voloshina, N. & Haugland, R. P. (1997) A stable nonfluorescent derivative of resorufin for the fluorometric determination of trace hydrogen peroxide: applications in detecting the activity of phagocyte NADPH oxidase and other oxidases, *Analytical biochemistry.* **253**, 162-8.
[372]. Mohanty, J. G., Jaffe, J. S., Schulman, E. S. & Raible, D. G. (1997) A highly sensitive fluorescent micro-assay of H2O2 release from activated human leukocytes using a dihydroxyphenoxazine derivative, *Journal of immunological methods.* **202**, 133-41.
[373]. Christian, A. E., Haynes, M. P., Phillips, M. C. & Rothblat, G. H. (1997) Use of cyclodextrins for manipulating cellular cholesterol content, *Journal of lipid research.* **38**, 2264-72.
[374]. Rodal, S. K., Skretting, G., Garred, O., Vilhardt, F., van Deurs, B. & Sandvig, K. (1999) Extraction of cholesterol with methyl-beta-cyclodextrin perturbs formation of clathrin-coated endocytic vesicles, *Molecular biology of the cell.* **10**, 961-74.
[375]. Atger, V. M., de la Llera Moya, M., Stoudt, G. W., Rodrigueza, W. V., Phillips, M. C. & Rothblat, G. H. (1997) Cyclodextrins as catalysts for the removal of cholesterol from macrophage foam cells, *The Journal of clinical investigation.* **99**, 773-80.
[376]. Kilsdonk, E. P., Yancey, P. G., Stoudt, G. W., Bangerter, F. W., Johnson, W. J., Phillips, M. C. & Rothblat, G. H. (1995) Cellular cholesterol efflux mediated by cyclodextrins, *The Journal of biological chemistry.* **270**, 17250-6.
[377]. Berne, B. J. & Pecora, R. (2000) *Dynamic light scattering: with applications to chemistry, biology, and physics*, Courier Corporation.
[378]. Williams, D. B. & Carter, C. B. (1996) *The transmission electron microscope*, Springer.
[379]. Woods, R. J. & Pikaev, A. K. (1994) *Applied radiation chemistry: radiation processing*, John Wiley & Sons.
[380]. Silverstein, R. M., Webster, F. X., Kiemle, D. & Bryce, D. L. (2014) *Spectrometric identification of organic compounds*, John Wiley & Sons.
[381]. Spinks, J. W. T. & Woods, R. J. (1990) An introduction to radiation chemistry.
[382]. Dagher, M. C. & Pick, E. (2007) Opening the black box: lessons from cell-free systems on the phagocyte NADPH-oxidase, *Biochimie.* **89**, 1123-32.
[383]. Zhu, Y., Marchal, C. C., Casbon, A. J., Stull, N., von Lohneysen, K., Knaus, U. G., Jesaitis, A. J., McCormick, S., Nauseef, W. M. & Dinauer, M. C. (2006) Deletion mutagenesis of p22phox subunit of flavocytochrome b558: identification of regions critical for gp91phox maturation and NADPH oxidase activity, *The Journal of biological chemistry.* **281**, 30336-46.
[384]. Pilloud, M. C., Doussiere, J. & Vignais, P. V. (1989) Parameters of activation of the membrane-bound O2- generating oxidase from bovine neutrophils in a cell-free system, *Biochemical and biophysical research communications.* **159**, 783-90.
[385]. Park, H. S. & Park, J. W. (1998) Conformational changes of the leukocyte NADPH oxidase subunit p47(phox) during activation studied through its intrinsic fluorescence, *Biochimica et biophysica acta.* **1387**, 406-14.
[386]. Winterbourn, C. C. & Kettle, A. J. (2013) Redox reactions and microbial killing in the neutrophil phagosome, *Antioxidants & redox signaling.* **18**, 642-60.
[387]. Souabni, H. (2013) *Modulation de l'activité du flavocytochrome b558: Etude fonctionnelle*, Paris Sud university.

[388]. Morgan, D., Cherny, V. V., Murphy, R., Xu, W., Thomas, L. L. & DeCoursey, T. E. (2003) Temperature dependence of NADPH oxidase in human eosinophils, *The Journal of physiology.* **550**, 447-58.
[389]. Quinn, M. T. & Gauss, K. A. (2004) Structure and regulation of the neutrophil respiratory burst oxidase: comparison with nonphagocyte oxidases, *Journal of leukocyte biology.* **76**, 760-81.
[390]. Ezzine, A., Souabni, H., Bizouarn, T. & Baciou, L. (2014) Recombinant form of mammalian gp91(phox) is active in the absence of p22(phox), *The Biochemical journal.* **462**, 337-45.
[391]. Babior, B. M., Kuver, R. & Curnutte, J. T. (1988) Kinetics of activation of the respiratory burst oxidase in a fully soluble system from human neutrophils, *The Journal of biological chemistry.* **263**, 1713-8.
[392]. Dhalla, N. S., Temsah, R. M. & Netticadan, T. (2000) Role of oxidative stress in cardiovascular diseases, *Journal of hypertension.* **18**, 655-73.
[393]. Victor, V. M., Rocha, M., Sola, E., Banuls, C., Garcia-Malpartida, K. & Hernandez-Mijares, A. (2009) Oxidative stress, endothelial dysfunction and atherosclerosis, *Current pharmaceutical design.* **15**, 2988-3002.
[394]. Rodino-Janeiro, B. K., Paradela-Dobarro, B., Castineiras-Landeira, M. I., Raposeiras-Roubin, S., Gonzalez-Juanatey, J. R. & Alvarez, E. (2013) Current status of NADPH oxidase research in cardiovascular pharmacology, *Vascular health and risk management.* **9**, 401-28.
[395]. Jin, S. & Zhou, F. (2009) Lipid raft redox signaling platforms in vascular dysfunction: features and mechanisms, *Current atherosclerosis reports.* **11**, 220-6.
[396]. Simons, K. & Ehehalt, R. (2002) Cholesterol, lipid rafts, and disease, *The Journal of clinical investigation.* **110**, 597-603.
[397]. Allen, J. A., Halverson-Tamboli, R. A. & Rasenick, M. M. (2007) Lipid raft microdomains and neurotransmitter signalling, *Nature reviews Neuroscience.* **8**, 128-40.
[398]. Smart, E. J. & Anderson, R. G. (2002) Alterations in membrane cholesterol that affect structure and function of caveolae, *Methods in enzymology.* **353**, 131-9.
[399]. Bao, J. X., Xia, M., Poklis, J. L., Han, W. Q., Brimson, C. & Li, P. L. (2010) Triggering role of acid sphingomyelinase in endothelial lysosome-membrane fusion and dysfunction in coronary arteries, *American journal of physiology Heart and circulatory physiology.* **298**, H992-H1002.
[400]. Li, P. L., Zhang, Y. & Yi, F. (2007) Lipid raft redox signaling platforms in endothelial dysfunction, *Antioxidants & redox signaling.* **9**, 1457-70.
[401]. Ushio-Fukai, M. (2006) Localizing NADPH oxidase-derived ROS, *Science's STKE : signal transduction knowledge environment.* **2006**, re8.
[402]. Ushio-Fukai, M. (2009) Compartmentalization of redox signaling through NADPH oxidase-derived ROS, *Antioxidants & redox signaling.* **11**, 1289-99.
[403]. Zhang, C. & Li, P. L. (2010) Membrane raft redox signalosomes in endothelial cells, *Free radical research.* **44**, 831-42.
[404]. Gorudko, I. V., Mukhortava, A. V., Caraher, B., Ren, M., Cherenkevich, S. N., Kelly, G. M. & Timoshenko, A. V. (2011) Lectin-induced activation of plasma membrane NADPH oxidase in cholesterol-depleted human neutrophils, *Archives of biochemistry and biophysics.* **516**, 173-81.
[405]. Rao Malla, R., Raghu, H. & Rao, J. S. (2010) Regulation of NADPH oxidase (Nox2) by lipid rafts in breast carcinoma cells, *International journal of oncology.* **37**, 1483-93.
[406]. Fuhler, G. M., Blom, N. R., Coffer, P. J., Drayer, A. L. & Vellenga, E. (2007) The reduced GM-CSF priming of ROS production in granulocytes from patients with myelodysplasia is associated with an impaired lipid raft formation, *Journal of leukocyte biology.* **81**, 449-57.

[407]. Yang, B. & Rizzo, V. (2007) TNF-alpha potentiates protein-tyrosine nitration through activation of NADPH oxidase and eNOS localized in membrane rafts and caveolae of bovine aortic endothelial cells, *American journal of physiology Heart and circulatory physiology.* **292**, H954-62.
[408]. Li, H., Yao, Z., Degenhardt, B., Teper, G. & Papadopoulos, V. (2001) Cholesterol binding at the cholesterol recognition/ interaction amino acid consensus (CRAC) of the peripheral-type benzodiazepine receptor and inhibition of steroidogenesis by an HIV TAT-CRAC peptide, *Proceedings of the National Academy of Sciences of the United States of America.* **98**, 1267-72.
[409]. Wyrwoll, A. J., Lautenschläger, P., Bach, A., Hellack, B., Dybowska, A., Kuhlbusch, T. A. J., Hollert, H., Schäffer, A. & Maes, H. M. (2016) Size matters – The phototoxicity of TiO2 nanomaterials, *Environmental Pollution.* **208, Part B**, 859-867.
[410]. Jovanovic, B. (2015) Review of titanium dioxide nanoparticle phototoxicity: Developing a phototoxicity ratio to correct the endpoint values of toxicity tests, *Environmental toxicology and chemistry / SETAC.* **34**, 1070-7.
[411]. Kumar, C. S. S. R. (2010) *Nanocomposites*, John Wiley & Sons.
[412]. Kumazawa, R., Watari, F., Takashi, N., Tanimura, Y., Uo, M. & Totsuka, Y. (2002) Effects of Ti ions and particles on neutrophil function and morphology, *Biomaterials.* **23**, 3757-64.
[413]. Goncalves, D. M., Chiasson, S. & Girard, D. (2010) Activation of human neutrophils by titanium dioxide (TiO2) nanoparticles, *Toxicology in vitro : an international journal published in association with BIBRA.* **24**, 1002-8.
[414]. Marucco, A., Catalano, F., Fenoglio, I., Turci, F., Martra, G. & Fubini, B. (2015) Possible Chemical Source of Discrepancy between in Vitro and in Vivo Tests in Nanotoxicology Caused by Strong Adsorption of Buffer Components, *Chemical research in toxicology*.
[415]. Masoud, R., Bizouarn, T. & Houée-Levin, C. (2014) Cholesterol: A modulator of the phagocyte NADPH oxidase activity - A cell-free study, *Redox Biology.* **3**, 16-24.
[416]. Xia, T., Kovochich, M., Brant, J., Hotze, M., Sempf, J., Oberley, T., Sioutas, C., Yeh, J. I., Wiesner, M. R. & Nel, A. E. (2006) Comparison of the abilities of ambient and manufactured nanoparticles to induce cellular toxicity according to an oxidative stress paradigm, *Nano letters.* **6**, 1794-807.
[417]. Wilhelmi, V., Fischer, U., Weighardt, H., Schulze-Osthoff, K., Nickel, C., Stahlmecke, B., Kuhlbusch, T. A., Scherbart, A. M., Esser, C., Schins, R. P. & Albrecht, C. (2013) Zinc oxide nanoparticles induce necrosis and apoptosis in macrophages in a p47phox- and Nrf2-independent manner, *PloS one.* **8**, e65704.
[418]. Sharma, V., Singh, P., Pandey, A. K. & Dhawan, A. (2012) Induction of oxidative stress, DNA damage and apoptosis in mouse liver after sub-acute oral exposure to zinc oxide nanoparticles, *Mutation research.* **745**, 84-91.
[419]. Sharma, V., Anderson, D. & Dhawan, A. (2012) Zinc oxide nanoparticles induce oxidative DNA damage and ROS-triggered mitochondria mediated apoptosis in human liver cells (HepG2), *Apoptosis : an international journal on programmed cell death.* **17**, 852-70.
[420]. Gupta, S. M. & Tripathi, M. (2011) A review of TiO2 nanoparticles, *Chin Sci Bull.* **56**, 1639-1657.
[421]. Hedenborg, M. (1988) Titanium dioxide induced chemiluminescence of human polymorphonuclear leukocytes, *International archives of occupational and environmental health.* **61**, 1-6.

[422]. Goncalves, D. M., de Liz, R. & Girard, D. (2011) Activation of neutrophils by nanoparticles, *TheScientificWorldJournal.* **11**, 1877-85.
[423]. Jovanovic, B., Anastasova, L., Rowe, E. W., Zhang, Y., Clapp, A. R. & Palic, D. (2011) Effects of nanosized titanium dioxide on innate immune system of fathead minnow (Pimephales promelas Rafinesque, 1820), *Ecotoxicology and environmental safety.* **74**, 675-83.
[424]. Gurr, J. R., Wang, A. S., Chen, C. H. & Jan, K. Y. (2005) Ultrafine titanium dioxide particles in the absence of photoactivation can induce oxidative damage to human bronchial epithelial cells, *Toxicology.* **213**, 66-73.
[425]. Alarifi, S., Ali, D., Al-Doaiss, A. A., Ali, B. A., Ahmed, M. & Al-Khedhairy, A. A. (2013) Histologic and apoptotic changes induced by titanium dioxide nanoparticles in the livers of rats, *International journal of nanomedicine.* **8**, 3937-43.
[426]. Aderem, A. & Underhill, D. M. (1999) Mechanisms of phagocytosis in macrophages, *Annual review of immunology.* **17**, 593-623.
[427]. Babin, K., Goncalves, D. M. & Girard, D. (2015) Nanoparticles enhance the ability of human neutrophils to exert phagocytosis by a Syk-dependent mechanism, *Biochimica et biophysica acta.* **1850**, 2276-2282.
[428]. Allouni, Z. E., Gjerdet, N. R., Cimpan, M. R. & Hol, P. J. (2015) The effect of blood protein adsorption on cellular uptake of anatase TiO2 nanoparticles, *International journal of nanomedicine.* **10**, 687-95.
[429]. Simon-Vazquez, R., Lozano-Fernandez, T., Peleteiro-Olmedo, M. & Gonzalez-Fernandez, A. (2014) Conformational changes in human plasma proteins induced by metal oxide nanoparticles, *Colloids and surfaces B, Biointerfaces.* **113**, 198-206.
[430]. Wang, C. & Li, Y. (2012) Interaction and nanotoxic effect of TiO2 nanoparticle on fibrinogen by multi-spectroscopic method, *Science of The Total Environment.* **429**, 156-160.
[431]. Elder, A., Yang, H., Gwiazda, R., Teng, X., Thurston, S., He, H. & Oberdörster, G. (2007) Testing Nanomaterials of Unknown Toxicity: An Example Based on Platinum Nanoparticles of Different Shapes, *Advanced Materials.* **19**, 3124-3129.
[432]. Otsuka, H., Nagasaki, Y. & Kataoka, K. (2012) PEGylated nanoparticles for biological and pharmaceutical applications, *Advanced drug delivery reviews.* **64, Supplement**, 246-255.
[433]. Kelland, L. (2007) The resurgence of platinum-based cancer chemotherapy, *Nature reviews Cancer.* **7**, 573-84.
[434]. Bryde, S. & de Kroon, A. I. (2009) Nanocapsules of platinum anticancer drugs: development towards therapeutic use, *Future medicinal chemistry.* **1**, 1467-80.
[435]. Lok, C. N., Zou, T., Zhang, J. J., Lin, I. W. & Che, C. M. (2014) Controlled-release systems for metal-based nanomedicine: encapsulated/self-assembled nanoparticles of anticancer gold(III)/platinum(II) complexes and antimicrobial silver nanoparticles, *Advanced materials (Deerfield Beach, Fla).* **26**, 5550-7.
[436]. Mironava, T., Simon, M., Rafailovich, M. H. & Rigas, B. (2013) Platinum folate nanoparticles toxicity: cancer vs. normal cells, *Toxicology in vitro : an international journal published in association with BIBRA.* **27**, 882-9.
[437]. Vadiei, K., Siddik, Z. H., Khokhar, A. R., al-Baker, S., Sampedro, F. & Perez-Soler, R. (1992) Pharmacokinetics of liposome-entrapped cis-bis-neodecanoato-trans-R,R-1,2-diaminocyclohexane platinum(II) and cisplatin given i.v. and i.p. in the rat, *Cancer chemotherapy and pharmacology.* **30**, 365-9.
[438]. Hamasaki, T., Kashiwagi, T., Imada, T., Nakamichi, N., Aramaki, S., Toh, K., Morisawa, S., Shimakoshi, H., Hisaeda, Y. & Shirahata, S. (2008) Kinetic analysis of superoxide anion

radical-scavenging and hydroxyl radical-scavenging activities of platinum nanoparticles, *Langmuir : the ACS journal of surfaces and colloids.* **24**, 7354-64.
[439]. Zheng, W., Jiang, B., Hao, Y., Zhao, Y., Zhang, W. & Jiang, X. (2014) Screening reactive oxygen species scavenging properties of platinum nanoparticles on a microfluidic chip, *Biofabrication.* **6**, 045004.

List of publications

R. Masoud, T. Bizouarn, C. Houée Levin. Cholesterol: a modulator of the phagocyte NADPH oxidase activity. A cell-free study, Redox Biology (2014)

R. Masoud, T. Bizouarn, S. Trepout, F. Wein, L. Baciou, S. Marco C. Houée Levin. Titanium dioxide nanoparticles increase superoxide ion production by acting on NADPH oxidase. PloS One (2015)

T. Bizouarn, G. Karimi, **R. Masoud**, H. Souabni, P. Machillot, X. Serfati, F. Wien, M. Réfrégiers, C. Houée-Levin, L. Baciou. Exploring the structural changes of $p47^{phox}$ and p67phox from phagocyte NADPH oxidase induced by arachidonic acid via thiol accessibility and SRCD spectroscopy (submitted in FEBS).

Y. Izumi, K. Fujii, F.Wien, C. Houée-Lévin, S. Lacombe, D. Salado, E. Parcel, **R. Masoud**, S. Yamamoto, M. Réfrégiers, M. Hervé du Penhoat, A. Yokoya. Structural transition from β-strand and turn to α-helix in histone H2A-H2B induced by DNA damage response (submitted in Biophysical Journal).

Conferences

-Vascular inflammation, November, 2015 (Pasteur Institute, Paris) oral presentation

-International Symposium on advances in nanoparticulate carriers-Applications in diseases and infections, October, 2015 (Pasteur Institute, Paris) Poster

-18ème Congrès du GFB, September, 2015 (Mittelwihr, France) oral presentation

-15th International Conference on Oxidative Stress Reduction, Redox Homeostasis & Antioxidants, June, 2015 (Pasteur Institute, Paris) oral presentation

-2nd Mediterranean Conference of Young Researchers, October, 2014 (Marseille, France) oral
-Second Event of the Great Paris Membrane Club, June, 2014 (Institute Curie, Paris)

-GREMI symposium, May, 2014 (Institute Pasteur, Paris)

-Gordon Research Conference on Oxygen Radicals, February, 2014 (United State) Poster

-International conference on Nanosciences and healthcare, November, 2013 (Paris, France)

-8thClub Oxidase, May, 2013 (Paris, France) Poster
-Gordon Research Conference and Seminar on NOX Biology and its Translation to Human Disease and Therapy, June, 2012 (United States) Poster

Redox Biology 3 (2014) 16–24

Contents lists available at ScienceDirect

Redox Biology

journal homepage: www.elsevier.com/locate/redox

Research Paper

Cholesterol: A modulator of the phagocyte NADPH oxidase activity - A cell-free study

Rawand Masoud, Tania Bizouarn, Chantal Houée-Levin *

Laboratoire de chimie physique, UMR 8000, Université Paris Sud-CNRS, Orsay 91405, France

ARTICLE INFO

Article history:
Received 7 August 2014
Received in revised form
2 October 2014
Accepted 12 October 2014

Keywords:
NADPH oxidase
Cholesterol
Cell-free system
Arachidonic acid activation
Superoxide production

ABSTRACT

The NADPH oxidase Nox2, a multi-subunit enzyme complex comprising membrane and cytosolic proteins, catalyzes a very intense production of superoxide ions $O_2^{\bullet -}$, which are transformed into other reactive oxygen species (ROS). *In vitro*, it has to be activated by addition of amphiphiles like arachidonic acid (AA). It has been shown that the membrane part of phagocyte NADPH oxidase is present in lipid rafts rich in cholesterol. Cholesterol plays a significant role in the development of cardio-vascular diseases that are always accompanied by oxidative stress. Our aim was to investigate the influence of cholesterol on the activation process of NADPH oxidase. Our results clearly show that, in a cell-free system, cholesterol is not an efficient activator of NADPH oxidase like arachidonic acid (AA), however it triggers a basal low superoxide production at concentrations similar to what found in neutrophile. A higher concentration, if present during the assembly process of the enzyme, has an inhibitory role on the production of $O_2^{\bullet -}$. Added cholesterol acts on both cytosolic and membrane components, leading to imperfect assembly and decreasing the affinity of cytosolic subunits to the membrane ones. Added to the cytosolic proteins, it retains their conformations but still allows some conformational change induced by AA addition, indispensable to activation of NADPH oxidase.

Introduction

The damaging role of reactive oxygen species (ROS) in cardiovascular diseases (atherosclerosis, vascular inflammation, and endothelial dysfunction) leading to coronary heart disease, stroke or *angina pectoris* has been known for some decades. NADPH oxidase Nox2 is one of the major actors at the origin of oxidative stress. Actually Nox2 is one of the main isomers involved in the cardiovascular field [1]. On the other hand, high cholesterol level is linked to an elevated risk of cardiovascular disease [2], through high concentration of LDL-cholesterol in blood [3,4]. High cholesterol has also been associated with diabetes and high blood pressure [5,6]. Interestingly, NADPH oxidases have been found in lipid rafts (LR), which are dynamic, detergent-resistant plasma membrane microdomains highly enriched in cholesterol and sphingolipids [7,8]. Cytoplasmic proteins are efficiently recruited to these raft-associated flavocytochrome b_{558} upon activation to reconstitute the active complex [9]. Moreover, distribution and regulation of NADPH oxidase by LRs were reported in murine microglial cells and bovine aortic endothelial and coronary arterial endothelial cells [10–14]. These facts prompted us to study the effect of cholesterol on the functioning of NADPH oxidase. In this paper, we investigated the consequences of the presence of cholesterol on the production of reactive oxygen species.

The NADPH oxidase catalyzes the formation of superoxide anion ($O_2^{\bullet -}$) by a single-electron reduction of the molecular oxygen using NADPH as the electron donor [15–17]. $O_2^{\bullet -}$ is considered to be the starting point for the generation of a vast assortment of reactive oxidants since it is subsequently transformed into hydrogen peroxide, hypochlorous acid, hydroxyl radical and peroxynitrite [18,19]. Deregulation of NADPH-oxidase activity is linked with a large panel of pathologies in addition to cardiovascular ones, involving inflammatory processes, renal damage, central nervous system diseases, immune system disorders, induction of apoptosis after irradiation by low doses of ionizing radiations etc., [20–31].

Abbreviations: AA, arachidonic acid; PBS, phosphate buffer saline; Cyt b_{558}, cytochrome b_{558}; Cytc, cytochrome c; DTT, dithiotreitol; EDTA, ethylenediaminetetraacetic acid; FAD, flavin adenine dinucleotide; FMLP, formyl-methionyl-leucyl-phenylalanine; GTP, guanosine-5′-triphosphate; HEPES, [4-(2-hydroxyethyl)piperazine-1-yl]ethanesulfonic acid; IPTG, isopropylthiogalatoside; LB, Luria Bertoni; LDL, low density lipoprotein; LR, lipid raft; MF, membrane fractions; MβCD, methyl-β-cyclodextrin; NADPH, reduced β-nicotinamide adenine dinucleotide phosphate; PMSF, phenylmethanesulfonyl fluoride; PtdIns(3)P, phosphatidyl-inositol3-phosphate; PtdIns(3,4)P2, phosphatidylinositol(3,4)-bisphosphate; PX, phox homology domain; ROS, reactive oxygen species; SDS-PAGE, sodium dodecyl sulfate polyacrylamide gel electrophoresis

* Corresponding author.
E-mail address: Chantal.houee@u-psud.fr (C. Houée-Levin).

http://dx.doi.org/10.1016/j.redox.2014.10.001

The functionally competent oxidase complex consists of a membrane-bound flavocytochrome *b*558 (Cyt b_{558}), comprising two subunits (Nox2 also known as gp91^{phox}, and p22^{phox}) and four cytosolic components. Nox2 harbors the redox carriers (bound FAD and two hemes) and the NADPH binding site. The cytosolic components include p47^{phox}, p67^{phox}, p40^{phox}, and a small GTPase Rac1 or Rac2 [32]. Because of the high toxicity of the reactive oxygen species (ROS), the NADPH-oxidase activity is tightly regulated spatially and temporally. In resting phagocytes, the components of the complex exist as separated entities but upon cell activation by pro-inflammatory mediators, the cytosolic subunits undergo posttranslational modifications such as phosphorylation [33,34] and migrate to the membrane bound Cyt b_{558} to constitute the activated NADPH–oxidase complex [35]. Actually this process involves a complicated set of protein–protein and protein–lipid interactions to conduct to oxidase assembly [36–39].

Studies on binding between the different soluble subunits p47^{phox}, p67^{phox}, p40^{phox} performed *in vitro* suggested that these three cytosolic subunits are preassembled [40–42]. Recently, different constructions of chimeras were designed, in which individual cytosolic subunits were fused [p47^{phox}–p67^{phox}] [43] or [p67^{phox}–Rac1] [44–48] and supplemented by the missing third subunit (Rac1 and p47^{phox}, respectively). Another strategy was to construct a trimera which consisted of the following domains [p47^{phox} (aa 1–286), p67^{phox} (aa 1–212) and a full length Rac1 (aa 1–192)] in which interactions among cytosolic subunits were replaced by fusion. This trimera was found to act as potent amphiphile-dependent oxidase protein activator upon assembly to native phagocyte membrane or purified Cyt b_{558}[49]. The subsequent change from this construction was performed by adding isoprenyl group to the C-terminus of Rac1 part, mimicking *in vivo* reality, where Rac is found exclusively in the prenylated form. Further modification was the introduction of Q61L mutation in the Rac part of the trimera, making Rac constitutively in the GTP-bound form. It ensures that in the trimera an intramolecular bond was built between Rac1 and p67^{phox} which is essential for oxidase activity ability of trimera [50,51].

The development of a cell-free oxidase activation system was a great help in the understanding of the mechanism of NADPH oxidase activation. This system was designed to mimic *in vivo* oxidase activity under *in vitro* conditions. In cell-free systems, the activation process is bypassed by the introduction of an activator, an anionic amphiphile such as arachidonic or other fatty acids or surfactants [52–57]. We took advantage of this system, which permits strict quantification of the components of interest, and modifications of membrane composition. In addition, for simplicity, we have replaced the cytosolic subunits by the trimera [49,50]. A precondition for using the trimera was to ascertain that it is functionally comparable with the separated cytosolic subunits. We have verified that the rates of production of superoxide anions were similar (supplementary material) and that the dependences of the activity in function of AA concentration were also comparable with the cytosolic fractions and the trimera [58]. In addition, the presence of two states in the activation process, a sensitive one followed by a resistant one against ROS damages, observed with the separated cytosolic subunits [59] was also found with the trimera (data not shown). Consequently, we have chosen the trimera instead of the separated subunits in order to diminish the number of independent parameters to consider and to facilitate the interpretation.

Material and methods

Materials

Equine heart cytochrome c (cyt *c*), arachidonic acid (*cis*-AA), phenylmethanesulfonyl fluoride (PMSF), isopropylthiogalatoside (IPTG), cholesterol, Dulbecco PBS and methyl-β-cyclodextrin (MβCD) were from Sigma (Saint-Quentin Fallavier, France). Reduced β-nicotinamide adenine dinucleotide phosphate (NADPH) was from Acros. Ni-sepharose, superdex 75 and Ficoll-Paque Plus was from GE Healthcare, France.

Neutrophil membrane preparation

The neutrophils were prepared from human blood from healthy donors (ESF, Paris, France) as described in [60]. Briefly, 500 mL of blood was sedimented in 2% dextran solution for 40 min. PBS was added to the pellets, and then the neutrophils were separated from lymphocytes and the red cells by centrifugation for 30 min at 400*g* on Ficoll. The red cells were further eliminated after their lysis by centrifugation for 8 min, 400*g*, 4 °C. The pellet resuspended in PBS pH 7.4 containing 340 mM sucrose, 7 mM magnesium sulfate, 1 mM PMSF, 0.5 mM leupeptin was sonicated in the 30% pulse mode at power pulses (6) in an ice-cooled beaker 6 times during 10 s with interval of 1 min between the sonications (sonicator XL, Misonix Inc.). Neutrophil membranes and cytosol were separated by centrifugation for 1 h 30 min at 200,000*g* at 4 °C. The membrane fractions were resolubilized, aliquoted and stored at −80 °C for further experiments.

Expression of the trimera

The plasmid of the trimera was a generous gift from Prof. E. Pick. Trimera (p47^{phox} aa 1–286, p67^{phox} aa 1–212, and RacQ61L full length) was expressed and isolated from *Escherichia coli* BL21-DE3-plys. A stock culture of *E. coli* (glycerated, stored at −80 °C) expressing the trimera was used to inoculate a Petri dish of Luria Bertani (LB) agar, supplemented with kanamycin and chloramphenicol and incubated at 37 °C for 16 h. A colony was then cultured in 60 mL of LB medium supplemented with 50 mg/L of kanamycin and 34 mg/L of chloramphenicol, incubated at 37 °C for about 16 h. 20 mL of this culture were added to 1.5 L of Terrific Broth medium (TB) supplemented with 50 mg/L of kanamycin and 34 mg/L of chloramphenicol. The flask was incubated in shaking condition at 37 °C until it reached an absorbance of 0.9 at 600 nm, then 0.5 mM IPTG were added to induce the synthesis of protein and the culture was incubated overnight at 30 °C. The culture was pelleted and placed in the freezer at −20 °C until use.

Extraction of the trimera from bacteria

The bacterial pellet, containing the trimera obtained previously, was dissolved in a buffer containing 50 mM HEPES (pH 7.5), 200 mM NaCl and 1 mM EDTA to which was added 1 mg of DNase, 1 mM PMSF, 1 mM DTT and 1 mM benzamidine. The bacteria were sonicated during 4 times 2 min in a 50% pulse mood at power pulses (6) in an ice-cooled beaker with pauses of 2 min. The bacterial lysate was centrifuged at 160,000*g* for 1 h 30 min at 6 °C. The cleared cell-free supernatant was filtered to remove all traces of debris and bacteria.

Purification of the trimera

The trimera was expressed as fusion protein. Thus it was purified by metal chelate affinity chromatography. The above supernatant was applied to nickel affinity column after being diluted

twice with buffer (0.5 M NaCl, 30 mM Na_2HPO_4, 20 mM imidazole and 1 mM PMSF, pH 7.4). The mixture was loaded for 1 h 30 min so that the proteins of interest effectively cling to the nickel resin. Then the column was washed with the same buffer to remove unwanted bound proteins. The proteins bound to the beads were eluted from the resin with elution buffer (0.1 M NaCl, 30 mM Na_2HPO_4 and 300 mM imidazole, pH 7.4). Then size exclusion chromatography was carried out to better purify the trimera. Proteins concentration was determined using a NanoDrop2000 spectrophotometer (Thermo scientific, France) and the extinction coefficient of 1.5 mg^{-1}/mL cm. The purities of all proteins were checked by migration on 10% BisTris-NuPAGE SDS gels (Invitrogen), stained with Coomassie Brilliant Blue (Fig. S1 in Supplementary material).

Dialysis and storage of the trimera

Trimera fractions were pooled in a dialysis tube whose membrane was of 10 kDa porosity. The tube was placed in 2 L dialysis buffer (100 mM NaCl and 30 mM Na_2HPO_4, pH 7.5) at 4 °C overnight. The dialyzate was recovered and trimera was stored at −80 °C.

Quantification of intrinsic cholesterol

Intrinsic cholesterol concentration in human neutrophil membrane fractions was measured by the Amplex Red Cholesterol Assay Kit purchased from Invitrogen [61,62]. The intrinsic cholesterol concentration was estimated by three independent measurements on different blood donors.

Depletion of cholesterol from neutrophil membrane

Methyl-β-cyclodextrin (MβCD) is a well established cholesterol depleting reagent of phospholipidic membrane without affecting their permeability and it is the most commonly used reagent [63–66]. The neutrophil membranes were incubated for 1 h, at 4 °C, in presence of 10 mM MβCD. The mixture was centrifuged at 148,000*g* for 1 h 30 min at 4 °C. Neutrophil membranes were found in the pellet and the cyclodextrin–cholesterol complexes were in the supernatant. The neutrophil membranes were resolubilized in PBS.

Measurement of superoxide production in cell-free assays

Superoxide anion production rates were quantified by the initial rate of cytochrome *c* (Cyt*c*) reduction, as described before [67]. The reaction is as follows:

$$\text{Cyt } c_{ox} + O_2^{\bullet -} \rightarrow O_2 + \text{Cyt } c_{red}$$

Unless indicated, the components of the cell-free system were added as follows: (2–5 nM Cyt b_{558}) membrane fractions, (100–200 nM) trimera and (40 μM) arachidonic acid in 500 μL Phosphate Buffer Saline supplemented with 10 mM $MgSO_4$ for 4 min of incubation at 25 °C in order to allow the Nox complex assembly. The production was initiated by addition of (250 μM) NADPH and the rate of $O_2^{\bullet -}$ was quantified by the reduction of cytochrome *c* (50 μM). The rate was measured at 550 nm in a Thermo evolution500 Spectrophotometer. The amount of superoxide was calculated using a molar extinction coefficient ($\Delta\varepsilon$ of the reduced *minus* oxidized form of Cyt*c*) of 21 mM^{-1} cm^{-1}. 20 mM stock solution of cholesterol was prepared in ethanol. Further dilutions have been done in ethanol to get a concentration range of cholesterol (0.1–16 mM), which was mixed with AA 65 mM. 3 μL of each mixture was introduced in the cell free system to finally have cholesterol 0.25–40 μM in a mixture with 40 μM AA in the final reaction volume. This allowed keeping the volume constant.

2.10. Determination of enzymatic parameters and curve plotting

The enzymatic parameters EC_{50} and V_{max} were calculated by non-linear least square fitting of the curves of superoxide rate of production *vs.* protein concentration using the following expression.

$$v = \frac{v_{max}[P]}{EC_{50} + [P]} \quad (1)$$

where [*P*] is the concentration of the considered protein (trimera). Plotting and calculation were performed using Graph Pad Prism Version 6.

Intrinsic fluorescence assays

Steady-state fluorescence spectra were performed on a Photon Technology International scanning fluorimeter at 25 °C. Various concentrations of AA and/or cholesterol were added as indicated to a final volume of 3 mL of buffer (phosphate buffer saline supplemented with 10 mM $MgSO_4$) containing trimera (60 nM) in a quartz cuvette. The tryptophan fluorescence spectra of trimera were obtained by exciting the samples at 290 nm (2 nm bandwidth) and recorded between 300 and 400 nm (5 nm bandwidth). The excitation wavelength was chosen at 290 nm to optimize the signal to noise ratio and to reduce the contribution of tyrosine residues to the signal [68].

Results

Intrinsic cholesterol concentration and effect of cholesterol depletion by methyl-β-cyclodextrin on superoxide production rate

We first measured the intrinsic cholesterol concentration in human neutrophil membrane fractions. We found 3 ± 1 μM cholesterol in the final reaction volume of cell free system assay (2 nM Cyt b_{558}, 40 μg/mL membrane proteins) in three independent measurements. Then to investigate the role of cholesterol that is naturally present in the neutrophil membrane on NADPH oxidase, 10 μM MβCD was used to disrupt lipid rafts by removing cholesterol from membranes [66,69,70]. The rate was measured as described in Material and methods. We found that cholesterol depletion decreased superoxide production rate relative to the non-treated membrane neutrophil to (44 ± 7)%.

In the following studies, the level of cholesterol was increased to a range corresponding to hypercholesterolemia (up to *ca.* 33% of the normal concentration) and above, to enlighten the effects of this addition.

Cholesterol as an activating molecule?

Having established the most propitious conditions for activation (see Materials and methods), we aimed at determining whether cholesterol could have an activator effect on NADPH oxidase. The results expressed as percentages of NADPH oxidase activity as a function of cholesterol are displayed in Fig. 1. Addition of cholesterol in the range 0.2–1 μM (*ca.* 7–33% increase compared to the intrinsic value) provoked slight but significant activation of NADPH oxidase complex, but not at an equivalent level to AA. The rate of production of $O_2^{\bullet -}$ stayed at around 15% of the rate value obtained with AA for concentrations above 1 μM. Comparable results were obtained using the separated subunits where a

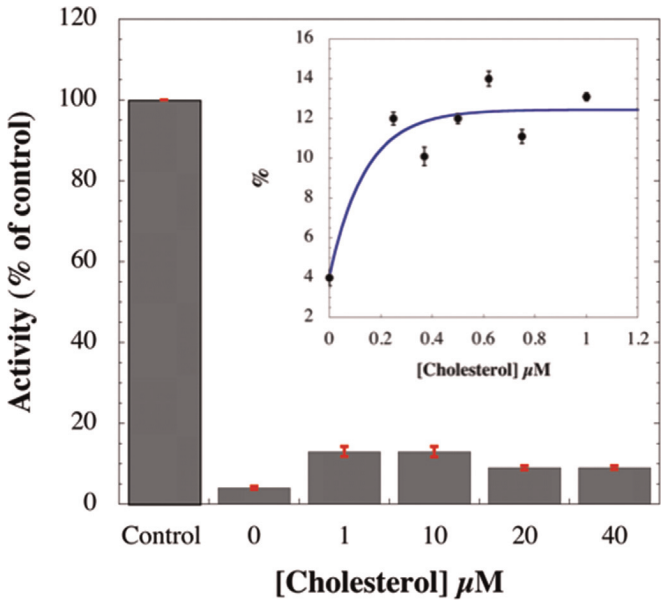

Fig. 1. Dependence of NADPH oxidase activity as a function of cholesterol concentration in the absence of arachidonic acid. Membrane fractions (2 nM Cyt b_{558}) with trimera 200 nM were incubated 4 min in presence of different concentrations of cholesterol. Control experiment representing 100% (68 mol $O_2^{\bullet -}$/s/mol Cyt b_{558}) of the activity was realized in presence of 40 μM AA and in absence of cholesterol. The rates of superoxide production were measured as described in Materials and methods. The data are the average of 3 independent measurements ± SEM.

maximum activity of (20 ± 2)% of AA-dependent activity was reached (data not shown).

Superoxide production in the presence of AA plus added cholesterol

NADPH oxidase activity was inhibited by the addition of cholesterol

Since cholesterol alone does not activate NADPH oxidase, we have tested the cholesterol effect on activation by AA.The AA induced NADPH-oxidase activity was followed upon increasing concentrations of cholesterol (Fig. 2). To avoid an increase of solvent volume, a mixture of cholesterol added with AA for each cholesterol concentration was prepared. The rate of production with AA alone was considered as 100%. Surprisingly, when membrane fractions and trimera were incubated together with 0.25 μM cholesterol and 40 μM AA, the activity dropped to about 86 ± 5%. The AA-induced NADPH oxidase activity was thus reduced by addition of less than 10% of the intrinsic cholesterol amount. The decrease of the activity could be fitted by a two inhibitory sites equation (Fig. 2) and the parameters of the fit are given in Table 1.

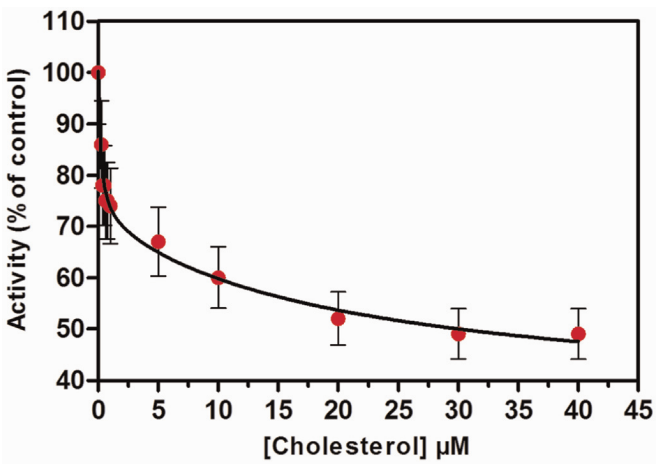

Fig. 2. NADPH-oxidase activity inhibition by cholesterol. Neutrophil membrane fractions and trimera were incubated together in the presence of a mixture of 40 μM AA plus cholesterol. The oxidase activity was expressed as the percent of activity measured in the absence of cholesterol (79 mol $O_2^{\bullet -}$/s/mol Cyt b_{558}) as described in Materials and methods. The values are an average of 3 independent measurements ± SEM. Table 1 shows the kinetic parameters of the fit.

Table 1

*Parameters of the fits of Fig. 2. $Y=Y_{min}+\frac{Y_1}{(1+[chol]/K_{i1})}+\frac{Y_2}{(1+[chol]/K_{i2})}$

	Value	Error
Y_{min} (%)	35	9.6
Y_1 (%)	30	4.6
K_{i1} (μM)	0.19	0.09
Y_2 (%)	35	7.3
K_{i2} (μM)	21.2	16.7

Effect of cholesterol on AA activation profile

To probe the effect of cholesterol on the NADPH activation profile by AA, we performed titrations of the activity *vs.* AA concentration in the absence and in the presence of two concentrations of cholesterol (0.5 and 20 μM). In this experiment cholesterol was added at the same time as Arachidonic acid (Fig. 3).

In the presence of cholesterol, the $O_2^{\bullet -}$ production was lower on the full range of concentrations of AA, which confirms the inhibitory effect of cholesterol in a concentration-dependent manner. However the maximum activity was achieved with the same AA concentration and the bell-shape curve was kept.

Modification of kinetic parameters in the presence of added cholesterol

The absence of effect of cholesterol on the AA activation profile described above raised the question of the mechanism by which addition of cholesterol decreases the activity of the complex. In that purpose, the rate of superoxide production for increasing concentrations of trimera with and without cholesterol was determined. This dependence could always be fitted using a Michaelis–Menten-like equation (see materials and methods) and from each curve one could determine EC_{50} and V_{max} values. There was a marked loss in the oxidase activity in the presence of cholesterol for the whole range of concentrations of trimera, with important variations for both the EC_{50} and V_{max} values (Fig. 4, Table 2). In the

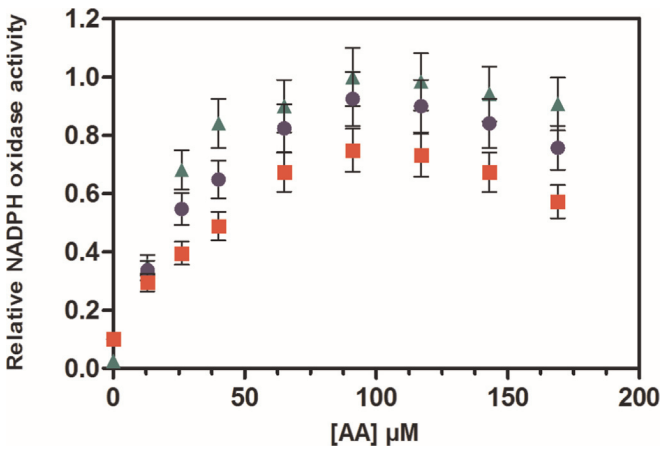

Fig. 3. Effect of cholesterol on the AA-dependent activation profile. Neutrophil membrane fractions and trimera were incubated together in the presence of a mixture of varying amounts of AA plus cholesterol. The cholesterol concentration was as follow, ▲: no cholesterol; ●: 0.5 μM cholesterol; ■: 20 μM cholesterol. Oxidase activities were expressed relative to the maximum activity (119 ± 12 mol $O_2^{\bullet -}$/s/mol Cyt b_{558}). The rate of $O_2^{\bullet -}$ production was achieved as described in Materials and methods.

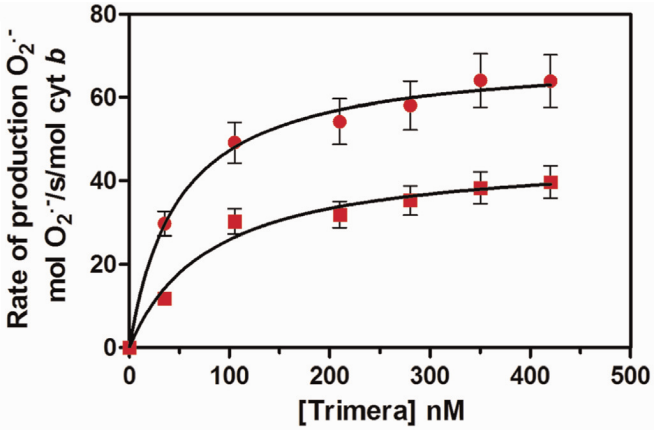

Fig. 4. Effect of cholesterol on the trimera dependence NADPH oxidase activity. The assays mixtures consisted of trimera at varying concentrations (from 0 to 420 nM) and membrane fractions of human neutrophils (3 nM Cyt b_{558}) to which were added • 40 μM AA or ■ a mixture of 40 μM AA and 10 μM cholesterol. The superoxide formation was measured as indicated in Materials and methods. Each curve was fitted by Michaelis–Menten like equation leading to the determination of the EC_{50} and V_{max} values related to the trimera. The values of these kinetic parameters in the presence of AA alone or AA plus cholesterol are in Table 2. The values are an average of three independent measurements ± SEM.

Table 2
Kinetic parameters of NADPH oxidase activation by trimera.

Assay enriched with	*Vmax* (*mol $O_2^{\bullet-}$/s/mol cytb*)	EC_{50} (nM trimera)
AA 40 μM	70.3 ± 2	48.6 ± 3
AA 40 μM, cholesterol 10 μM	46.6 ± 6	79.8 ± 19

presence of cholesterol, the complex exhibited 1.5 times lower V_{max} value and the EC_{50} was 1.6 times higher than its values measured in absence of cholesterol, which might reflect a decrease of affinity of trimera for the Cyt b_{558}.

Effect of cholesterol addition during assembly phase

To examine whether cholesterol had an effect on the oxidase assembly process, 10 μM of cholesterol were added at different times during the 4-min phase of assembly (Fig. 5). Depending on the time at which cholesterol was added, various levels of

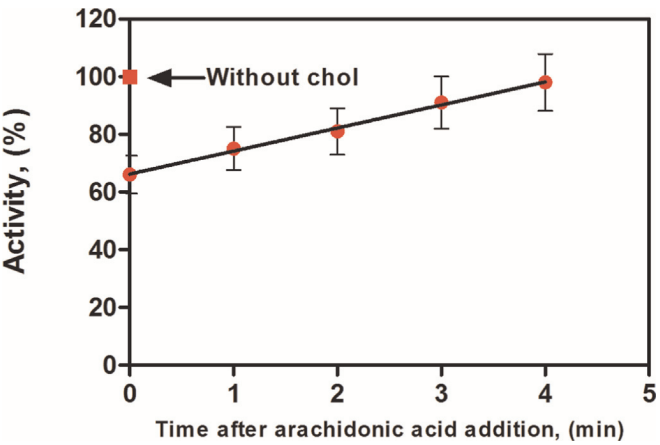

Fig. 5. Effect of the addition time of cholesterol on NADPH-oxidase activity. Membrane fractions (MF), trimera, and 40 μM AA were incubated 4 min in reaction buffer. 10 μM cholesterol were added at various times after the addition of AA. Conditions are as described under Materials and methods. Results are expressed as percentages of the control activity (without cholesterol addition). The values represent the means ± SEM of three independent experiments.

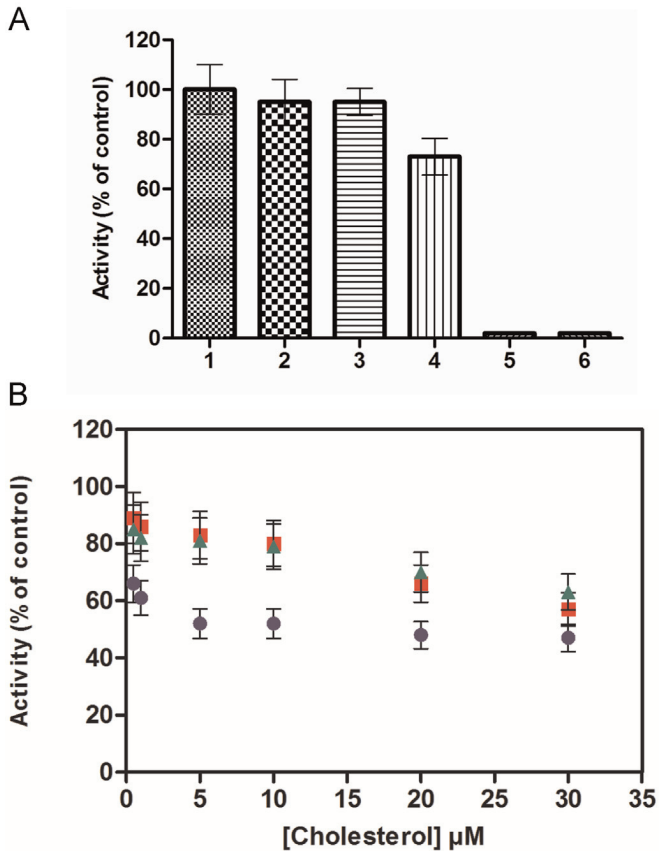

Fig. 6. Effect of cholesterol on AA activation of membrane fraction and trimera. (A) AA activation of membrane fraction and trimera (1) In the control experiment, membrane fraction and the trimera were incubated together during 4 min in the presence of 40 μM AA. The rate obtained corresponds to the 100% value (75 mol $O_2^{\bullet-}$/s/mol Cyt b_{558}). (2–4) Membrane fractions (MF) and trimera were separately preincubated during 10 s and mixed together for 4 min as follow: (2) both were preincubated with 40 μM AA, (3) only MF was preincubated with 40 μM AA, (4) only the trimera were preinicubated with 40 μM AA. (5) The rate was measured in absence of trimera. (6) The rate was measured in absence of MF. (B) Membrane fractions (MF) and trimera were separately preincubated during 10 s and mixed together for 4 min as follow: ■ only MF was preincubated with 40 μM AA plus cholesterol as indicated, ▲ only the trimera was preincubated with 40 μM AA plus cholesterol as indicated and • both were preincubated with 40 μM AA plus cholesterol. Activities in Fig. 6B were expressed as the percent of activities measured of Fig. 6A corresponding to each state to assess the cholesterol effect only.

inhibition were noticed. $O_2^{\bullet-}$ production was drastically lowered to ~66% of the control when cholesterol was added immediately after all the NADPH-oxidase components. The inhibition was less and less important (up to 100% activity) for times longer than 1 min. If cholesterol addition took place 4 min after the mixing, the oxidase activity remained comparable to that of the control. Both results (Figs. 4 and 5) suggest that cholesterol interferes in the interaction between trimera and Cyt b_{558}.

Structural effects of added cholesterol

Effect of cholesterol on soluble and membrane proteins

To evaluate the sensitivity of each component, the membrane part and the trimera, to cholesterol, superoxide anion production rate was measured after pre-incubation of membrane components or trimera or both, either with AA alone (Fig. 6A) or with a mixture of cholesterol and AA (Fig. 6B). After 10 s of separate pre-incubations of the membrane and of the trimera, both solutions were mixed and left for a second incubation for 4 min. We chose to pre-incubate for 10 s because a preincubation for longer time (30 s) led

to a drastic decrease of the activity. This was also observed in the case of separated subunits [71].

First, when both membrane fractions and trimera were pre-incubated separately with AA, the activity was maintained to about 95% of the observed one in standard conditions. The same level of activity (95%) was measured when AA was incorporated only to the membrane fractions. On the other hand, when AA was added only to the trimera, the activity dropped to 73% (Fig. 6A).

The experiment with AA (Fig. 6A) served as control for the ones with cholesterol. In all cases, addition of cholesterol+AA either to the membrane or to the trimera or to both separately led to a decreased rate of superoxide production (Fig. 6B). Incorporating cholesterol+AA only to the membrane fractions or only to the trimera gave comparable effect, indicating that cholesterol could act on both partners. When cholesterol was added to both counterparts, the activity drop was more important, the addition of 5 μM or more of cholesterol to both fractions led to a decrease of the activity down to ~50%. The inhibition always increased by increasing cholesterol concentration, in agreement with the results presented Fig. 2.

Effect of AA and cholesterol on the tryptophan intrinsic fluorescence of the trimera

To probe the effect of AA and cholesterol on the trimera conformational state, we followed the variation of intrinsic tryptophan fluorescence spectra upon addition of AA and/or cholesterol (Fig. 7). Trimera contains a total of 13 tryptophan residues. It was previously shown that addition of AA to the cytosolic subunits p67phox and p47phox induced changes reflected by measurable decrease of the intrinsic tryptophan fluorescence level [68,72].

By increasing AA concentration up to 140 μM, the fluorescence yield of the trimera underwent a concentration dependent decrease (Fig. 7A). A small blue shift up to 5 nm was observed, consistent with a slightly more hydrophobic tryptophan environment.

Surprisingly, the addition of cholesterol had no effect on the fluorescence yield of the trimera but a similar blue shift up to 5 nm was detected by increasing cholesterol concentration to 50 μM (Fig. 7B), indicating that addition of cholesterol does not induce conformational changes in the trimera, as AA does. When cholesterol was added to the trimera treated with 40 μM AA, the initial quenching of 25% due to the presence of AA still was visible, but there was no further lowering due to cholesterol (Fig. 7C). In addition to that the same blue shift up to 5 nm was observed after the addition of both AA and cholesterol.

4. Discussion

In this work we have explored the effect of added cholesterol on the activity of the phagocyte NADPH oxidase. This study is related to events that could happen to Nox2 following hypercholesterolemia. It is also related to the hypothesis of modulation of NADPH oxidase activity by lipid rafts rich in cholesterol. In fact, some studies have reported the distribution and regulation of Nox proteins and oxidase subunits in LRs, (most of the studies were performed in non-human cells [11–14] except those in human neutrophils) [9,73]. Given that, NADPH oxidase activation demands many partners to work together, LRs can provide a useful platform for Nox2 and its subunits to aggregate and then function as an active enzyme complex that produces $O_2^{\bullet-}$ [13,14,74–78]. In particular, it has been demonstrated that NADPH oxidase was assembled and activated in LR of neutrophils, producing $O_2^{\bullet-}$, causing respiratory bursts and killing bacteria [9]. The integrity of LRs would play a crucial role in the regulation of NADPH oxidase activity and cholesterol would be an essential component in LRs for NADPH oxidase in agreement with previous reports [11,79].

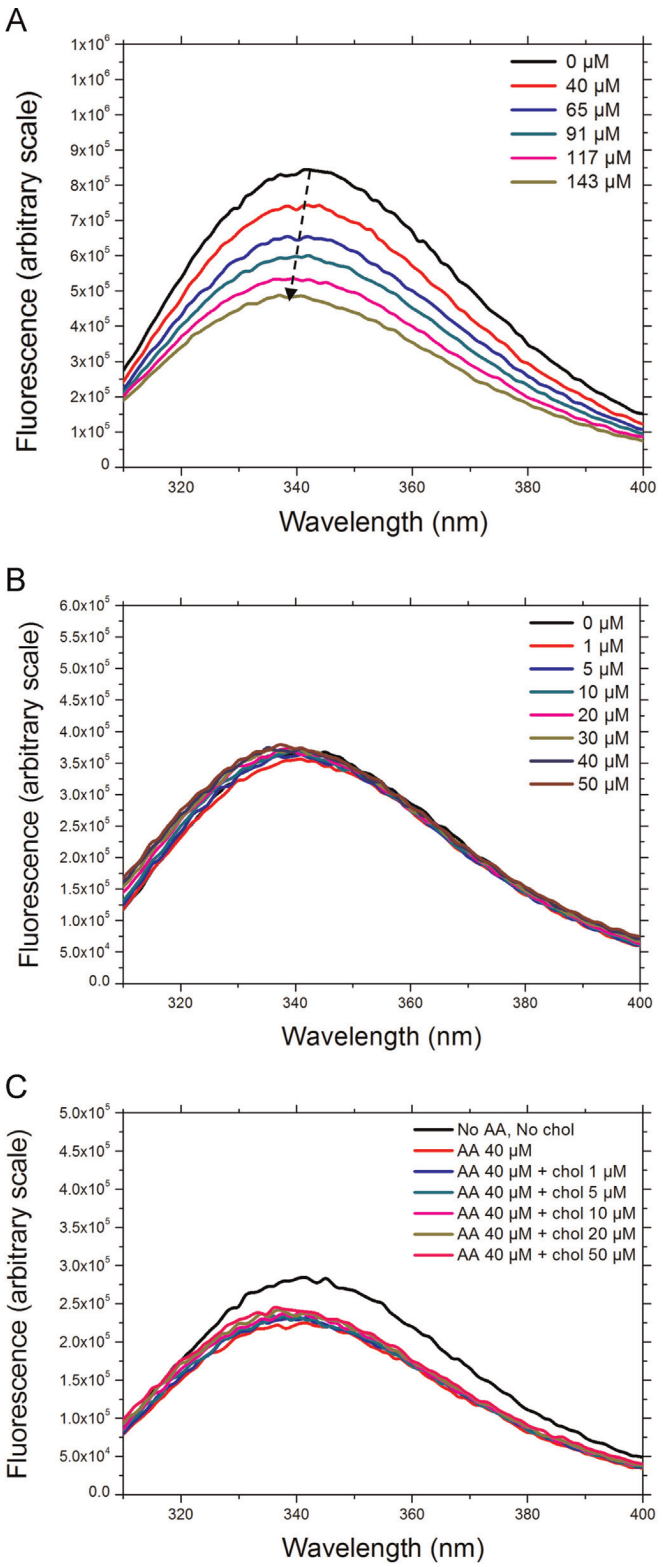

Fig. 7. Intrinsic fluorescence of trimera treated with either AA or cholesterol or both. The emission spectra were measured using an excitation wavelength of 290 nm as described in Materials and methods. Results are representative of at least three independent experiments. A: trimera 60 nM, AA as stated in the figure legend. B: trimera 60 nM, cholesterol as stated in the figure legend. C: trimera 60 nM, AA 40 μM, cholesterol as stated in the figure legend.

Actually, the role of specific protein–lipid interactions in oxidase assembly has been studied in the last decades [32,36,38]. It has been shown that the interaction of the PX domains of $p40^{phox}$ and

p47^{phox} with phospholipids constitutes an essential mechanism to orchestrate the assembly of the cytoplasmic components with the phagosomal membrane. The PX domain of p40^{phox} interacts selectively with phosphatidyl-inositol3-phosphate, (PtdIns(3)P) [80,81], while the PX domain of p47^{phox} preferentially recognizes (PtdIns(3,4)P2) [80,82].

On the required cholesterol concentration in neutrophils

The regulatory role of LR was rationalized by the fact that cholesterol exerts a stabilizing role in LRs by filling the void space between sphingolipids and forming hydrogen bonds with them. Thus, cholesterol depletion by MβCD would lead to the breakdown of LRs as it suppresses the glue effect of cholesterol on sphingolipids [83,84]. In addition to that, removal of raft cholesterol leads to dissociation of most proteins from the rafts, rendering them nonfunctional [85]. Shao et al. showed that incubation of the cells with MβCD resulted in a loss of association of gp91^{phox} with the LR fractions [9] while Vilhardt et al. reported that cholesterol depletion by MβCD reduced significantly $O_2^{\bullet -}$ production in both intact cells and a cell-free reconstituted system and MβCD effect was joined with a parallel reduction of the translocation of cytosolic components to the membrane [11]. Later, Fuhler et al. further demonstrated that treatment of neutrophils with the MβCD, abrogated fMLP-induced ROS production and activation of protein kinases ERK1/2 and B/Akt in both unprimed and primed neutrophils, further assisting the opinion that LR-associated NADPH oxidase produces ROS and contributes importantly to the onset of phagocytic respiratory bursts [86]. Our results about removal of cholesterol by MβCD are in agreement with the preceding findings since the oxidase activity was decreased to $(44 \pm 7)\%$.

On the effect of cholesterol

Our results indicated slight but significant activation of NADPH oxidase complex in cell free system by addition of cholesterol alone at physiological concentrations (*ca.* 10–30% above the normal level), without AA. Conversely, addition of cholesterol in this range has an inhibitory effect on AA activation of NADPH oxidase activity. Similar amplitude was also observed at 37 °C (data not shown). The effect of cholesterol did not interfere with that of AA (same profile), indicating different binding sites for both compounds. Several facts indicate the presence of two independent inhibitory binding sites. Effectively, in Fig. 2, the curve could be fitted only with a two-site inhibition equation. In addition, cholesterol effect has been observed when it was preincubated either with the membrane or with the trimera alone. When cholesterol (0.2–10 μM) was added to one component (membrane or trimera) (Fig. 7B) a small inhibition was observed (~20%), but when both components were preincubated with the same concentration, a higher inhibition was measured (~50%). It strengthens the idea that cholesterol affects not only the membrane fraction but also the cytosolic ones.

The kinetic parameters in the presence of cholesterol revealed that V_{max} for trimera is lower while EC_{50} is higher, which points out a less stable and imperfect assembly of the complex. Furthermore, cholesterol acts before assembly (Fig. 5), which might reflect that, one of the cholesterol binding sites is in the interaction region between membrane and cytosolic components, in the region hindered after assembly. Indeed, once the complex is formed, cholesterol cannot have access to it and makes no inhibitory effect. This effect has to be related to the observation that the depletion of cholesterol by MβCD also reduced the translocation of cytosolic proteins [10]. The cholesterol concentration found in membrane neutrophil seems to be optimal for NADPH oxidase activity.

4.3. On the conformation of the cytosolic partner

We have shown recently that AA modified the environment of tryptophan residues in the separated cytosolic subunits: both p47^{phox} and p67^{phox} underwent fluorescence decrease, which would be related to structural modifications necessary for their interaction with Cyt b_{558}[58,68]. A similar tryptophan fluorescence decrease was observed for the trimera upon addition of AA. No comparable effect of cholesterol on the trimera was observed, indicating that cholesterol cannot adapt the protein to the membrane subunit.

In conclusion, while the presence of cholesterol at physiological concentration (*e.g.* in lipid rafts) is important for the NADPH oxidase function, an increase of cholesterol amount might have several consequences: (i) a slight but significant activity in the absence of the usual pro-inflammatory signals such as AA with the possibility of a permanent mild inflammatory state and (ii) an inhibition of the activity of NADPH oxidase in the presence of pro-inflammatory signals. In both cases there would be a modification of the response to the signaling regulation.

Acknowledgments

We are grateful to Prof. E. Pick for the plasmids, to Dr. L. Baciou for helpful discussions and to Dr. F. Lederer for the preparation of neutrophiles. We acknowledge the financial support of the COSTCM1201 Action (Biomimetic models) and of ANR2010-blan-1536-01. We are indebted to EDF for financial support (contract RB 2013-15).

Appendix A. Supplementary material

Supplementary data associated with this article can be found in the online version at http://dx.doi.org/10.1016/j.redox.2014.07.004.

References

[1] B.K. Rodiño-Janeiro, B. Paradela-Dobarro, M.I. Castiñeiras-Landeira, S. Raposeiras-Roubín, J.R. González-Juanatey, E. Alvarez, Current status of NADPH oxidase research in cardiovascular pharmacology, Vascular Health and Risk Management 9 (2013) 401–428. http://dx.doi.org/10.2147/VHRM.S33053 23983473.

[2] C.E. James, S.S.C. Underwood, General and Systematic Pathology, Churchill Livingstone, London, 2009.

[3] M.S. Brown, J.L. Goldstein, How LDL receptors influence cholesterol and atherosclerosis, Scientific American 251 (5) (1984) 58–66. http://dx.doi.org/10.1038/scientificamerican1184-58 6390676.

[4] D. Bhatnagar, H. Soran, P.N. Durrington, Hypercholesterolaemia and its management, BMJ (Clinical Research Ed.) 337 (2008) a993. http://dx.doi.org/10.1136/bmj.a993 18719012.

[5] F.V. CrallJr., W.C. Roberts, The extramural and intramural coronary arteries in juvenile diabetes mellitus: Analysis of nine necropsy patients aged 19–38 years with onset of diabetes before age 15 years, American Journal of Medicine 64 (2) (1978) 221–230. http://dx.doi.org/10.1016/0002-9343(78)90049-9 629271.

[6] J.V. Selby, G.D. Friedman, C.P. QuesenberryJr., Precursors of essential hypertension: pulmonary function, heart rate, uric acid, serum cholesterol, and other serum chemistries, American Journal of Epidemiology 131 (6) (1990) 1017–1027 2343854.

[7] S. Jin, F. Zhou, Lipid raft redox signaling platforms in vascular dysfunction: features and mechanisms, Current Atherosclerosis Reports 11 (3) (2009) 220–226. http://dx.doi.org/10.1007/s11883-009-0034-6 19361354.

[8] K. Simons, R. Ehehalt, Cholesterol, lipid rafts, and disease, Journal of Clinical Investigation 110 (5) (2002) 597–603. http://dx.doi.org/10.1172/JCI16390 12208858.

[9] D. Shao, A.W. Segal, L.V. Dekker, Lipid rafts determine efficiency of NADPH oxidase activation in neutrophils, FEBS Letters 550 (1–3) (2003) 101–106. http://dx.doi.org/10.1016/S0014-5793(03)00845-7 12935894.

[10] W. Han, H. Li, V.A. Villar, A.M. Pascua, M.I. Dajani, X. Wang, A. Natarajan, M. T. Quinn, R.A. Felder, P.A. Jose, P. Yu, Lipid rafts keep NADPH oxidase in the

inactive state in human renal proximal tubule cells, Hypertension 51 (2) (2008) 481–487. http://dx.doi.org/10.1161/HYPERTENSIONAHA.107.103275 18195159.
[11] F. Vilhardt, B. van Deurs, The phagocyte NADPH oxidase depends on cholesterol-enriched membrane microdomains for assembly, EMBO Journal 23 (4) (2004) 739–748. http://dx.doi.org/10.1038/sj.emboj.7600066 14765128.
[12] B. Yang, T.N. Oo, V. Rizzo, Lipid rafts mediate H_2O_2 prosurvival effects in cultured endothelial cells, FASEB Journal: Official Publication of the Federation of American Societies for Experimental Biology 20 (9) (2006) 1501–1503. http://dx.doi.org/10.1096/fj.05-5359fje 16754746.
[13] A.Y. Zhang, F. Yi, G. Zhang, E. Gulbins, P.L. Li, Lipid raft clustering and redox signaling platform formation in coronary arterial endothelial cells, Hypertension 47 (1) (2006) 74–80. http://dx.doi.org/10.1161/10.1161/01.HYP.0000196727.53300.62 16344372.
[14] L. Zuo, M. Ushio-Fukai, L.L. Hilenski, R.W. Alexander, Microtubules regulate angiotensin II type 1 receptor and Rac1 localization in caveolae/lipid rafts: role in redox signaling, Arteriosclerosis, Thrombosis, and Vascular Biology 24 (7) (2004) 1223–1228. http://dx.doi.org/10.1161/01.ATV.0000132400.25045.2a 15142861.
[15] W.M. Nauseef, How human neutrophils kill and degrade microbes: an integrated view, Immunological Reviews 219 (2007) 88–102. http://dx.doi.org/10.1111/j.1600-065X.2007.00550.x 17850484.
[16] A.W. Segal, How neutrophils kill microbes, Annual Review of Immunology 23 (2005) 197–223. http://dx.doi.org/10.1146/annurev.immunol.23.021704.115653 15771570.
[17] B.M. Babior, Oxidants from phagocytes: agents of defense and destruction, Blood 64 (5) (1984) 959–966 6386073.
[18] K. Bedard, K.H. Krause, The NOX family of ROS-generating NADPH oxidases: physiology and pathophysiology, Physiological Reviews 87 (1) (2007) 245–313. http://dx.doi.org/10.1152/physrev.00044.2005 17237347.
[19] B.M. Babior, NADPH oxidase, Current Opinion in Immunology 16 (1) (2004) 42–47. http://dx.doi.org/10.1016/j.coi.2003.12.001 14734109.
[20] K.K. Griendling, D. Sorescu, M. Ushio-Fukai, NAD(P)H oxidase: role in cardiovascular biology and disease, Circulation Research 86 (5) (2000) 494–501. http://dx.doi.org/10.1161/01.RES.86.5.494 10720409.
[21] T. Kamata, Roles of Nox1 and other Nox isoforms in cancer development, Cancer Science 100 (8) (2009) 1382–1388. http://dx.doi.org/10.1111/j.1349-7006.2009.01207.x 19493276.
[22] J.D. Lambeth, T. Kawahara, B. Diebold, Regulation of Nox and Duox enzymatic activity and expression, Free Radical Biology and Medicine 43 (3) (2007) 319–331. http://dx.doi.org/10.1016/j.freeradbiomed.2007.03.028 17602947.
[23] B. Lassègue, K.K. Griendling, NADPH oxidases: functions and pathologies in the vasculature, Arteriosclerosis, Thrombosis, and Vascular Biology 30 (4) (2010) 653–661. http://dx.doi.org/10.1161/ATVBAHA.108.181610 19910640.
[24] R.A. Seger, Chronic granulomatous disease: recent advances in pathophysiology and treatment, Netherlands Journal of Medicine 68 (11) (2010) 334–340 21116026.
[25] S. Sorce, K.H. Krause, NOX enzymes in the central nervous system: from signaling to disease, Antioxidants and Redox Signaling 11 (10) (2009) 2481–2504. http://dx.doi.org/10.1089/ARS.2009.2578 19309263.
[26] H. Li, S. Horke, U. Förstermann, Oxidative stress in vascular disease and its pharmacological prevention, Trends in Pharmacological Sciences 34 (6) (2013) 313–319. http://dx.doi.org/10.1016/j.tips.2013.03.007 23608227.
[27] Z.V. Varga, K. Kupai, G. Szűcs, R. Gáspár, J. Pálóczi, N. Faragó, A. Zvara, L. G. Puskás, Z. Rázga, L. Tiszlavicz, P. Bencsik, A. Görbe, C. Csonka, P. Ferdinandy, T. Csont, MicroRNA-25-dependent up-regulation of NADPH oxidase 4 (NOX4) mediates hypercholesterolemia-induced oxidative/nitrative stress and subsequent dysfunction in the heart, Journal of Molecular and Cellular Cardiology 62 (2013) 111–121. http://dx.doi.org/10.1016/j.yjmcc.2013.05.009 23722270.
[28] A. Neumann, G. Brogden, N. Jerjomiceva, S. Brodesser, H.Y. Naim, M. von Köckritz-Blickwede, Lipid alterations in human blood-derived neutrophils lead to formation of neutrophil extracellular traps, European Journal of Cell Biology 93 (2014) 347–354. http://dx.doi.org/10.1016/j.ejcb.2014.07.005 25172775.
[29] G.R. Drummond, C.G. Sobey, Endothelial NADPH oxidases: which NOX to target in vascular disease? Trends in Endocrinology and Metabolism: TEM 25 (9) (2014) 452–463. http://dx.doi.org/10.1016/j.tem.2014.06.012 25066192.
[30] R. Carnevale, L. Loffredo, V. Sanguigni, A. Plebani, P. Rossi, C. Pignata, B. Martire, A. Finocchi, M.C. Pietrogrande, C. Azzari, A.R. Soresina, S. Martino, E. Cirillo, F. Martino, P. Pignatelli, F. Violi, Different degrees of NADPH oxidase 2 regulation and in vivo platelet activation: lesson from chronic granulomatous disease, Journal of the American Heart Association 3 (3) (2014) e000920. http://dx.doi.org/10.1161/JAHA.114.000920 24973227.
[31] L. Račková, Cholesterol load of microglia: contribution of membrane architecture changes to neurotoxic power? Archives of Biochemistry and Biophysics 537 (1) (2013) 91–103. http://dx.doi.org/10.1016/j.abb.2013.06.015 23831332.
[32] W.M. Nauseef, Assembly of the phagocyte NADPH oxidase, Histochemistry and Cell Biology 122 (4) (2004) 277–291. http://dx.doi.org/10.1007/s00418-004-0679-8 15293055.
[33] J. El-Benna, P.M. Dang, M.A. Gougerot-Pocidalo, J.C. Marie, F. Braut-Boucher, p47phox, the phagocyte NADPH oxidase/NOX2 organizer: structure, phosphorylation and implication in diseases, Experimental and Molecular Medicine 41 (4) (2009) 217–225. http://dx.doi.org/10.3858/emm.2009.41.4.058 19372727.
[34] F.R. Sheppard, M.R. Kelher, E.E. Moore, N.J. McLaughlin, A. Banerjee, C. C. Silliman, Structural organization of the neutrophil NADPH oxidase: phosphorylation and translocation during priming and activation, Journal of Leukocyte Biology 78 (5) (2005) 1025–1042. http://dx.doi.org/10.1189/jlb.0804442 16204621.
[35] H. Raad, M.H. Paclet, T. Boussetta, Y. Kroviarski, F. Morel, M.T. Quinn, M. A. Gougerot-Pocidalo, P.M. Dang, J. El-Benna, Regulation of the phagocyte NADPH oxidase activity: phosphorylation of gp91phox/NOX2 by protein kinase C enhances its diaphorase activity and binding to Rac2, p67phox, and p47phox, FASEB Journal: Official Publication of the Federation of American Societies for Experimental Biology 23 (4) (2009) 1011–1022. http://dx.doi.org/10.1096/fj.08-114553 19028840.
[36] Y. Groemping, K. Rittinger, Activation and assembly of the NADPH oxidase: a structural perspective, Biochemical Journal 386 (3) (2005) 401–416. http://dx.doi.org/10.1042/BJ20041835 15588255.
[37] M.T. Quinn, K.A. Gauss, Structure and regulation of the neutrophil respiratory burst oxidase: comparison with nonphagocyte oxidases, Journal of Leukocyte Biology 76 (4) (2004) 760–781. http://dx.doi.org/10.1189/jlb.0404216 15240752.
[38] H. Sumimoto, Structure, regulation and evolution of Nox-family NADPH oxidases that produce reactive oxygen species, FEBS Journal 275 (13) (2008) 3249–3277. http://dx.doi.org/10.1111/j.1742-4658.2008.06488.x 18513324.
[39] S. Grizot, N. Grandvaux, F. Fieschi, J. Fauré, C. Massenet, J.P. Andrieu, A. Fuchs, P.V. Vignais, P.A. Timmins, M.C. Dagher, E. Pebay-Peyroula, Small angle neutron scattering and gel filtration analyses of neutrophil NADPH oxidase cytosolic factors highlight the role of the C-terminal end of p47phox in the association with p40phox, Biochemistry 40 (10) (2001) 3127–3133. http://dx.doi.org/10.1021/bi0028439 11258927.
[40] F.B. Wientjes, G. Panayotou, E. Reeves, A.W. Segal, Interactions between cytosolic components of the NADPH oxidase: p40phox interacts with both p67phox and p47phox, Biochemical Journal 317 (3) (1996) 919–924 8760383.
[41] A. Fuchs, M.C. Dagher, J. Fauré, P.V. Vignais, Topological organization of the cytosolic activating complex of the superoxide-generating NADPH-oxidase. Pinpointing the sites of interaction between p47phoz, p67phox and p40phox using the two-hybrid system, Biochimica et Biophysica Acta 1312 (1) (1996) 39–47. http://dx.doi.org/10.1016/0167-4889(96)00020-1 8679714.
[42] K. Lapouge, S.J. Smith, Y. Groemping, K. Rittinger, Architecture of the p40-p47-p67phox complex in the resting state of the NADPH oxidase. A central role for p67phox, Journal of Biological Chemistry 277 (12) (2002) 10121–10128. http://dx.doi.org/10.1074/jbc.M112065200 11796733.
[43] K. Ebisu, T. Nagasawa, K. Watanabe, K. Kakinuma, K. Miyano, M. Tamura, Fused p47phox and p67phox truncations efficiently reconstitute NADPH oxidase with higher activity and stability than the individual components, Journal of Biological Chemistry 276 (27) (2001) 24498–24505. http://dx.doi.org/10.1074/jbc.M101122200 11333262.
[44] N. Alloul, Y. Gorzalczany, M. Itan, N. Sigal, E. Pick, Activation of the superoxide-generating NADPH oxidase by chimeric proteins consisting of segments of the cytosolic component p67(phox) and the small GTPase Rac1, Biochemistry 40 (48) (2001) 14557–14566. http://dx.doi.org/10.1021/bi0117347 11724569.
[45] K. Miyano, S. Ogasawara, C.H. Han, H. Fukuda, M. Tamura, A fusion protein between rac and p67phox (1–210) reconstitutes NADPH oxidase with higher activity and stability than the individual components, Biochemistry 40 (46) (2001) 14089–14097. http://dx.doi.org/10.1021/bi010882u 11705402.
[46] A. Mizrahi, Y. Berdichevsky, Y. Ugolev, S. Molshanski-Mor, Y. Nakash, I. Dahan, N. Alloul, Y. Gorzalczany, R. Sarfstein, M. Hirshberg, E. Pick, Assembly of the phagocyte NADPH oxidase complex: chimeric constructs derived from the cytosolic components as tools for exploring structure-function relationships, Journal of Leukocyte Biology 79 (5) (2006) 881–895. http://dx.doi.org/10.1189/jlb.1005553 16641134.
[47] R. Sarfstein, Y. Gorzalczany, A. Mizrahi, Y. Berdichevsky, S. Molshanski-Mor, C. Weinbaum, M. Hirshberg, M.C. Dagher, E. Pick, Dual role of Rac in the assembly of NADPH oxidase, tethering to the membrane and activation of p67phox: a study based on mutagenesis of p67phox-Rac1 chimeras, Journal of Biological Chemistry 279 (16) (2004) 16007–16016. http://dx.doi.org/10.1074/jbc.M312394200 14761978.
[48] Y. Gorzalczany, N. Alloul, N. Sigal, C. Weinbaum, E. Pick, A prenylated p67phox-Rac1 chimera elicits NADPH-dependent superoxide production by phagocyte membranes in the absence of an activator and of p47phox: conversion of a pagan NADPH oxidase to monotheism, Journal of Biological Chemistry 277 (21) (2002) 18605–18610. http://dx.doi.org/10.1074/jbc.M202114200 11896062.
[49] Y. Berdichevsky, A. Mizrahi, Y. Ugolev, S. Molshanski-Mor, E. Pick, Tripartite chimeras comprising functional domains derived from the cytosolic NADPH oxidase components p47phox, p67phox, and Rac1 elicit activator-independent superoxide production by phagocyte membranes: an essential role for anionic membrane phospholipids, Journal of Biological Chemistry 282 (30) (2007) 22122–22139. http://dx.doi.org/10.1074/jbc.M701497200 17548354.
[50] A. Mizrahi, Y. Berdichevsky, P.J. Casey, E. Pick, A prenylated p47phox-p67phox-Rac1 chimera is a quintessential NADPH oxidase activator: membrane association and functional capacity, Journal of Biological Chemistry 285 (33) (2010) 25485–25499. http://dx.doi.org/10.1074/jbc.M110.113779 20529851.
[51] K. Miyano, H. Fukuda, K. Ebisu, M. Tamura, Remarkable stabilization of neutrophil NADPH oxidase using RacQ61L and a p67phox-p47phox fusion protein, Biochemistry 42 (1) (2003) 184–190. http://dx.doi.org/10.1021/bi0269052 12515553.
[52] Y. Bromberg, E. Pick, Unsaturated fatty acids stimulate NADPH-dependent superoxide production by cell-free system derived from macrophages, Cellular Immunology 88 (1) (1984) 213–221. http://dx.doi.org/10.1016/0008-8749(84)90066-2 6090027.

[53] Y. Bromberg, E. Pick, Activation of NADPH-dependent superoxide production in a cell-free system by sodium dodecyl sulfate, Journal of Biological Chemistry 260 (25) (1985) 13539–13545 2997168.
[54] J.T. Curnutte, Activation of human neutrophil nicotinamide adenine dinucleotide phosphate, reduced (triphosphopyridine nucleotide, reduced) oxidase by arachidonic acid in a cell-free system, Journal of Clinical Investigation 75 (5) (1985) 1740–1743. http://dx.doi.org/10.1172/JCI111885 2987311.
[55] R.A. Heyneman, R.E. Vercauteren, Activation of a NADPH oxidase from horse polymorphonuclear leukocytes in a cell-free system, Journal of Leukocyte Biology 36 (6) (1984) 751–759 6594417.
[56] L.C. McPhail, P.S. Shirley, C.C. Clayton, R. Snyderman, Activation of the respiratory burst enzyme from human neutrophils in a cell-free system. Evidence for a soluble cofactor, Journal of Clinical Investigation 75 (5) (1985) 1735–1739. http://dx.doi.org/10.1172/JCI111884 2987310.
[57] D. Qualliotine-Mann, D.E. Agwu, M.D. Ellenburg, C.E. McCall, L.C. McPhail, Phosphatidic acid and diacylglycerol synergize in a cell-free system for activation of NADPH oxidase from human neutrophils, Journal of Biological Chemistry 268 (32) (1993) 23843–23849 8226922.
[58] H. Souabni, V. Thoma, T. Bizouarn, C. Chatgilialoglu, A. Siafaka-Kapadai, L. Baciou, C. Ferreri, C. Houée-Levin, M.A. Ostuni, Arachidonic acid isomers inhibit NADPH-oxidase activity by direct interaction with enzyme components, Biochimica et Biophysica Acta 1818 (2012) 2314–2324. http://dx.doi.org/10.1016/j.bbamem.2012.04.018 22580228.
[59] M.A. Ostuni, M. Gelinotte, T. Bizouarn, L. Baciou, C. Houée-Levin, Targeting NADPH-oxidase by reactive oxygen species reveals an initial sensitive step in the assembly process, Free Radical Biology and Medicine 49 (5) (2010) 900–907. http://dx.doi.org/10.1016/j.freeradbiomed.2010.06.021 20600833.
[60] T. Akasaki, H. Koga, H. Sumimoto, Phosphoinositide 3-kinase-dependent and -independent activation of the small GTPase Rac2 in human neutrophils, Journal of Biological Chemistry 274 (25) (1999) 18055–18059. http://dx.doi.org/10.1074/jbc.274.25.18055 10364257.
[61] J.G. Mohanty, J.S. Jaffe, E.S. Schulman, D.G. Raible, A highly sensitive fluorescent micro-assay of H_2O_2 release from activated human leukocytes using a dihydroxyphenoxazine derivative, Journal of Immunological Methods 202 (2) (1997) 133–141. http://dx.doi.org/10.1016/S0022-1759(96)00244-X 9107302.
[62] M. Zhou, Z. Diwu, N. Panchuk-Voloshina, R.P. Haugland, A stable nonfluorescent derivative of resorufin for the fluorometric determination of trace hydrogen peroxide: applications in detecting the activity of phagocyte NADPH oxidase and other oxidases, Analytical Biochemistry 253 (2) (1997) 162–168. http://dx.doi.org/10.1006/abio.1997.2391 9367498.
[63] V.M. Atger, M. de la Llera Moya, G.W. Stoudt, W.V. Rodrigueza, M.C. Phillips, G. H. Rothblat, Cyclodextrins as catalysts for the removal of cholesterol from macrophage foam cells, Journal of Clinical Investigation 99 (4) (1997) 773–780. http://dx.doi.org/10.1172/JCI119223 9045882.
[64] E.P. Kilsdonk, P.G. Yancey, G.W. Stoudt, F.W. Bangerter, W.J. Johnson, M. C. Phillips, G.H. Rothblat, Cellular cholesterol efflux mediated by cyclodextrins, Journal of Biological Chemistry 270 (29) (1995) 17250–17256. http://dx.doi.org/10.1074/jbc.270.29.17250 7615524.
[65] A.E. Christian, M.P. Haynes, M.C. Phillips, G.H. Rothblat, Use of cyclodextrins for manipulating cellular cholesterol content, Journal of Lipid Research 38 (11) (1997) 2264–2272 9392424.
[66] S.K. Rodal, G. Skretting, O. Garred, F. Vilhardt, B. van Deurs, K. Sandvig, Extraction of cholesterol with methyl-beta-cyclodextrin perturbs formation of clathrin-coated endocytic vesicles, Molecular Biology of the Cell 10 (4) (1999) 961–974. http://dx.doi.org/10.1091/mbc.10.4.961 10198050.
[67] E. Pick, Y. Bromberg, S. Shpungin, R. Gadba, Activation of the superoxide forming NADPH oxidase in a cell-free system by sodium dodecyl sulfate. Characterization of the membrane-associated component, Journal of Biological Chemistry 262 (34) (1987) 16476–16483 2824496.
[68] S.D. Swain, S.L. Helgerson, A.R. Davis, L.K. Nelson, M.T. Quinn, Analysis of activation-induced conformational changes in p47phox using tryptophan fluorescence spectroscopy, Journal of Biological Chemistry 272 (47) (1997) 29502–29510. http://dx.doi.org/10.1074/jbc.272.47.29502 9368011.
[69] J.A. Allen, R.A. Halverson-Tamboli, M.M. Rasenick, Lipid raft microdomains and neurotransmitter signalling, Nature Reviews. Neuroscience 8 (2) (2007) 128–140. http://dx.doi.org/10.1038/nrn2059 17195035.
[70] E.J. Smart, R.G. Anderson, Alterations in membrane cholesterol that affect structure and function of caveolae, Methods in Enzymology 353 (2002) 131–139. http://dx.doi.org/10.1016/S0076-6879(02)53043-3 12078489.
[71] G. Karimi, C. Houée Levin, M.C. Dagher, L. Baciou, T. Bizouarn, Assembly of phagocyte NADPH oxidase: a concerted binding process? Biochimica et Biophysica Acta 1840 (11) (2014) 3277–3283. http://dx.doi.org/10.1016/j.bbagen.2014.07.022 25108064.
[72] H.S. Park, J.W. Park, Conformational changes of the leukocyte NADPH oxidase subunit p47(phox) during activation studied through its intrinsic fluorescence, Biochimica et Biophysica Acta 1387 (1–2) (1998) 406–414. http://dx.doi.org/10.1016/S0167-4838(98)00152-6 9748657.
[73] C. Guichard, E. Pedruzzi, C. Dewas, M. Fay, C. Pouzet, M. Bens, A. Vandewalle, E. Ogier-Denis, M.A. Gougerot-Pocidalo, C. Elbim, Interleukin-8-induced priming of neutrophil oxidative burst requires sequential recruitment of NADPH oxidase components into lipid rafts, Journal of Biological Chemistry 280 (44) (2005) 37021–37032. http://dx.doi.org/10.1074/jbc.M506594200 16115878.
[74] J.X. Bao, M. Xia, J.L. Poklis, W.Q. Han, C. Brimson, P.L. Li, Triggering role of acid sphingomyelinase in endothelial lysosome-membrane fusion and dysfunction in coronary arteries, American Journal of Physiology. Heart and Circulatory Physiology 298 (3) (2010) H992–H1002. http://dx.doi.org/10.1152/ajpheart.00958.2009 20061541.
[75] P.L. Li, Y. Zhang, F. Yi, Lipid raft redox signaling platforms in endothelial dysfunction, Antioxidants and Redox Signaling 9 (9) (2007) 1457–1470. http://dx.doi.org/10.1089/ars.2007.1667 17661535.
[76] M. Ushio-Fukai, Localizing NADPH oxidase-derived ROS, Science's STKE: Signal Transduction Knowledge Environment 2006 (349) (2006) re8. http://dx.doi.org/10.1126/stke.3492006re8 16926363.
[77] M. Ushio-Fukai, Compartmentalization of redox signaling through NADPH oxidase-derived ROS, Antioxidants and Redox Signaling 11 (6) (2009) 1289–1299. http://dx.doi.org/10.1089/ARS.2008.2333 18999986.
[78] C. Zhang, P.L. Li, Membrane raft redox signalosomes in endothelial cells, Free Radical Research 44 (8) (2010) 831–842. http://dx.doi.org/10.3109/10715762.2010.485994 20528560.
[79] R. Rao Malla, H. Raghu, J.S. Rao, Regulation of NADPH oxidase (Nox2) by lipid rafts in breast carcinoma cells, International Journal of Oncology 37 (6) (2010) 1483–1493 21042717.
[80] F. Kanai, H. Liu, S.J. Field, H. Akbary, T. Matsuo, G.E. Brown, L.C. Cantley, M. B. Yaffe, The PX domains of p47phox and p40phox bind to lipid products of PI (3)K, Nature Cell Biology 3 (7) (2001) 675–678. http://dx.doi.org/10.1038/35083070 11433300.
[81] J. Bravo, D. Karathanassis, C.M. Pacold, M.E. Pacold, C.D. Ellson, K.E. Anderson, P.J. Butler, I. Lavenir, O. Perisic, P.T. Hawkins, L. Stephens, R.L. Williams, The crystal structure of the PX domain from p40(phox) bound to phosphatidylinositol 3-phosphate, Molecular Cell 8 (4) (2001) 829–839. http://dx.doi.org/10.1016/S1097-2765(01)00372-0 11684018.
[82] T. Ago, R. Takeya, H. Hiroaki, F. Kuribayashi, T. Ito, D. Kohda, H. Sumimoto, The PX domain as a novel phosphoinositide-binding module, Biochemical and Biophysical Research Communications 287 (3) (2001) 733–738. http://dx.doi.org/10.1006/bbrc.2001.5629 11563857.
[83] C.R. Bollinger, V. Teichgräber, E. Gulbins, Ceramide-enriched membrane domains, Biochimica et Biophysica Acta 1746 (3) (2005) 284–294. http://dx.doi.org/10.1016/j.bbamcr.2005.09.001 16226325.
[84] E. Gulbins, P.L. Li, Physiological and pathophysiological aspects of ceramide, American Journal of Physiology. Regulatory, Integrative and Comparative Physiology 290 (1) (2006) R11–R26. http://dx.doi.org/10.1152/ajpregu.00416.2005 16352856.
[85] S. Jin, F. Zhou, F. Katirai, P.L. Li, Lipid raft redox signaling: molecular mechanisms in health and disease, Antioxidants and Redox Signaling 15 (4) (2011) 1043–1083. http://dx.doi.org/10.1089/ars.2010.3619 21294649.
[86] G.M. Fuhler, N.R. Blom, P.J. Coffer, A.L. Drayer, E. Vellenga, The reduced GM-CSF priming of ROS production in granulocytes from patients with myelodysplasia is associated with an impaired lipid raft formation, Journal of Leukocyte Biology 81 (2) (2007) 449–457. http://dx.doi.org/10.1189/jlb.0506311 17079651.

PLOS | ONE

RESEARCH ARTICLE

Titanium Dioxide Nanoparticles Increase Superoxide Anion Production by Acting on NADPH Oxidase

Rawand Masoud[1,2☯], Tania Bizouarn[1,2☯], Sylvain Trepout[3,4,5‡], Frank Wien[6‡], Laura Baciou[1,2☯], Sergio Marco[3,4,5‡], Chantal Houée Levin[1,2☯]*

1 Laboratoire de Chimie Physique, UMR 8000, Université Paris Sud Orsay France, **2** CNRS, UMR 8000, Orsay, France, **3** Institut Curie, Centre de Recherche, Centre Universitaire, Orsay, France, **4** INSERM U1196, Centre Universitaire, Orsay, France, **5** CNRS UMR9187, Centre Universitaire, Orsay, France, **6** Synchrotron SOLEIL, L'Orme des Merisiers, Gif-sur-Yvette, France

☯ These authors contributed equally to this work.
‡ These authors also contributed equally to this work.
* Chantal.houee@u-psud.fr

OPEN ACCESS

Citation: Masoud R, Bizouarn T, Trepout S, Wien F, Baciou L, Marco S, et al. (2015) Titanium Dioxide Nanoparticles Increase Superoxide Anion Production by Acting on NADPH Oxidase. PLoS ONE 10(12): e0144829. doi:10.1371/journal.pone.0144829

Editor: Elena A. Rozhkova, Argonne National Laboratory, UNITED STATES

Received: July 22, 2015

Accepted: November 23, 2015

Published: December 29, 2015

Data Availability Statement: All relevant data are within the paper and its Supporting Information files.

Funding: The financial support of ANR 2010-blan-1536-01 is acknowledged. The funders had no role in study design, data collection and analysis, decision to publish, or preparation of the manuscript.

Competing Interests: The authors have declared that no competing interests exist.

Abstract

Titanium dioxide (TiO_2) anatase nanoparticles (NPs) are metal oxide NPs commercialized for several uses of everyday life. However their toxicity has been poorly investigated. Cellular internalization of NPs has been shown to activate macrophages and neutrophils that contribute to superoxide anion production by the NADPH oxidase complex. Transmission electron micrososcopy images showed that the membrane fractions were close to the NPs while fluorescence indicated an interaction between NPs and cytosolic proteins. Using a cell-free system, we have investigated the influence of TiO_2 NPs on the behavior of the NADPH oxidase. In the absence of the classical activator molecules of the enzyme (arachidonic acid) but in the presence of TiO_2 NPs, no production of superoxide ions could be detected indicating that TiO_2 NPs were unable to activate by themselves the complex. However once the NADPH oxidase was activated (i.e., by arachidonic acid), the rate of superoxide anion production went up to 140% of its value without NPs, this effect being dependent on their concentration. In the presence of TiO_2 nanoparticles, the NADPH oxidase produces more superoxide ions, hence induces higher oxidative stress. This hyper-activation and the subsequent increase in ROS production by TiO_2 NPs could participate to the oxidative stress development.

Introduction

Titanium dioxide (TiO_2) nanoparticles (NPs) are metal oxides NPs manufactured in large quantities and commercialized for several uses because of their high stability, anticorrosive and photocatalytic properties [1]. For example, they are present in household products, plastics industry, electronics, pharmaceutical additives and food colorants [2,3]. In nanomedicine, TiO_2 NPs are under investigation as useful tools in advanced imaging and nanotherapeutics [4]. TiO_2 NPs are being explored in cancer diagnosis. They bring many benefits in cancer

therapy by absorbing near infrared light [5], and thus being considered as potential photosensitizers for photodynamic therapy [6]. Very promising is the finding that photo-activated nanostructured TiO_2 exhibited selective cytotoxicity against breast epithelial cancer cells [7]. Furthermore, the physical properties of TiO_2 NPs make them very interesting products for a use in various skin care and cosmetic products such as sunscreens [8]. TiO_2 NPs are under investigation as novel treatments for acne vulgaris, atopic dermatitis, hyperpigmented skin lesions, and other non-dermatologic diseases [2,3].

Despite their omnipresence in everyday life, modest research effort has been made in studying their potential adverse effects on living bodies and environment. TiO_2 NPs can be absorbed into the human body by inhalation, ingestion, and dermal penetration, then they can be distributed to vital organs, including lymph, brain, lung, liver, and kidney [9–11]. TiO_2 NPs can enter not only in cells, but also mitochondria and nuclei [12]. Most work to date has shown that TiO_2 NPs toxicity is strongly related to reactive oxygen species (ROS) generation and consequent oxidative stress [12–16].

TiO_2 NP-mediated ROS responses have been reported to orchestrate a series of pathological events leading to genotoxicity, immunotoxicity, neurotoxicity and carcinogenicity [17,18]. Neutrophils have been shown to be quickly recruited to titanium dioxide areas [19]. Moreover, cellular internalization of TiO_2 and ZnO NPs has been shown to activate immune cells including macrophages and neutrophils that contribute to ROS production [20–24]. TiO_2 NPs increased respiratory burst when fish neutrophils were incubated with these NPs [25]. Moreover, they lead to the activation of human ones [23,24]. Recently the same group showed that these nanoparticles enhance the ability of human neutrophils to exert phagocytosis by acting on Syk-dependent signaling pathway [26]. ROS production involves the activation of NADPH oxidase enzymes [22,27], a key player of oxidative stress in immune system cells but also in many other cell types (thyroid, kidney, neurons, and skin) [28–32].

NADPH-oxidase is the only enzyme whose function is to generate superoxide free radicals, which are transformed subsequently into other ROS [33–36]. It is a multi-subunit enzyme complex composed of membrane-bound flavocytochrome *b558* (cyt *b558*), comprising two subunits (Nox2 also known as $gp91^{phox}$, and $p22^{phox}$), present in the membranes phagocytes, and four cytosolic components. Nox2 harbors all the redox carriers (bound FAD, two hemes and the NADPH binding site) that transfer electrons from one side of the membrane cell to the other. The cytosolic components include $p47^{phox}$, $p67^{phox}$, $p40^{phox}$, and a small GTPase Rac1 or Rac2 [37].

In resting phagocytes, the components of the complex exist as separated entities but upon cell activation by pro-inflammatory mediators, the cytosolic subunits undergo posttranslational modifications such as phosphorylation and migrate to the membrane bound cyt *b558* to constitute the activated NADPH-oxidase complex, the only form able to produced superoxide ions [38].

The aim of our study was to investigate the enzymatic behavior of NADPH oxidase in the presence of TiO_2 NPs and to check if NADPH oxidase could be a pathway involved in ROS generation by TiO_2 NPs as it has been suggested [27]. We have developed a cell-free system [39–41] that allows controlling the environment, testing and identifying the potential effects of different molecules in various steps of oxidase activation [42,43]. In such cell-free systems, activation is obtained by mixing all proteins with an activator, arachidonic acid (AA). In this study, we have used a construction called trimera, which consisted of the following domains Nter-p47*phox* (amino acids 1-286) linked to the N-ter p67*phox* (amino acids 1-212), and the full length Rac1 Q61L [44]. In a previous paper, we have verified that the rates of production of superoxide anions were similar when the classic cytosolic proteins are replaced by trimera protein to activate the cyt *b558* and also that the dependences of the activity in function of the

enzyme activator AA concentration were also found comparable with the cytosolic fractions and the trimera [45]. Thus, the trimera was chosen in order to avoid complications due to some assembly steps and to activate the cyt *b558* in a reproducible manner. We have constantly validated our main conclusions with the separated subunits. We studied not only the effect of TiO_2 NPs on the function of NADPH oxidase but we also examined their effects on proteins conformations by different methods (fluorescence, synchrotron radiation circular dichroism (SRCD), transmission electron microscope (TEM), dynamic light scattering (DLS)). The use of these combined methods has provided a broad view of how TiO_2 NPs influence NADPH oxidase functioning and hypotheses about the origin of oxidative stress TiO_2 NPs dependent.

Material and Methods

Materials

Equine heart cytochrome c (cyt *c*), superoxide dismutase from bovine erythrocyte, arachidonic acid (AA), phenylmethanesulfonyl fluoride (PMSF) and Dulbecco phosphate buffer saline (PBS) and standard PBS were from Sigma (Saint Quentin Fallavier, France). Reduced nicotinamide adenine dinucleotide phosphate (NADPH) was from Acros. Ni-sepharose, superdex 75 and Ficoll-Paque Plus were from GE Healthcare, France. Anatase TiO_2 NPs were a generous gift of Dr Hynd Remita. They were suspended in deionized water (1 mg/mL) and sonicated in an ultra-sound bath for 10 min before use. The experiments were performed in phosphate buffer saline (PBS buffer). It is known that TiO_2 NPs are affected by the buffer and especially by phosphate [46]. We chose this buffer to be as close as possible to living medium.

Neutrophil membrane preparation

The neutrophils were prepared from human blood from healthy donors (ESF Paris, France) as described in [47]. Briefly, 500 mL of blood was sedimented in 2% dextran solution for 40 min and centrifuged 400 x g 8 min. Dulbecco PBS was added to the pellets, and then the neutrophils were separated from lymphocytes and the red cells by centrifugation for 30 min at 400 x g on Ficoll solution. The red cells were further eliminated after their lysis by centrifugation for 8 min, 400 g, 4°C. The pellet resuspended in PBS pH 7.4 containing 340 mM sucrose, 7 mM magnesium sulphate, 1 mM PMSF, 0.5 mM leupeptin was sonicated in the 30% pulse mode at power pulses (6) in an ice-cooled beaker 6 times during 10 s with resting time of 1 min between the sonications (sonicator XL, Misonix inc.). Neutrophil membranes and cytosol were separated by centrifugation for 1h30 at 200 000 g at 4°C. The membrane fractions were resuspended, aliquoted and stored at -80°C for further experiments.

Trimera preparation

The plasmid coding for the trimera was kindly provided by Prof. E. Pick (University of Tel Aviv, Israel). It codes for the Nter-p47*phox* (amino acids 1-286) linked to the N-ter p67*phox* (amino acids 1-212), and the full length Rac1 Q61L [44]. The trimera was expressed and isolated from *E.coli BL21-(DE)3-plysS*. Purification of trimera was performed mainly as previously described [45]. Briefly, after a first step through a nickel affinity chromatography, the protein was further purified by size exclusion chromatography; the protein was then dialyzed overnight against a phosphate buffer (100 mM NaCl and 30 mM Na_2HPO_4, pH 7.5) and stored at −80°C. The protein concentration was estimated using a NanoDrop2000 spectrophotometer (Thermo scientific, France) and the extinction coefficient of 124,000 mol^{-1} L cm^{-1} at 280 nm (Expasy, Protparam). The purity of all proteins were checked by migration on 10% BisTris-NuPAGE

SDS gels (Invitrogen), stained with Coomassie Brilliant Blue and quantified by the ImageJ software.

Dynamic light scattering measurements

Dynamic light scattering (DLS) experiments were performed to estimate the NPs size. DLS measurements were performed at room temperature on a Malvern NanoZS equipped with a 633 nm laser. Data were collected with a scattering angle of 173°. A range between 2 and 60 μg/mL of TiO_2 NPs suspensions prepared in PBS or water was tested.

Transmission electron microscopy measurement

The morphology and size of NPs were also determined by transmission electron microscopy (TEM). The solutions contained 0.5 mg/mL TiO_2 NPs +/-50 μg/mL trimera and +/-1 mg/mL membrane proteins containing 25μg/mL cyt *b558*. 4 μL of the suspension was deposited onto glow-discharged carbon-coated copper grids and after 1 minute of interaction, the excess of solution was removed with a filter paper (Whatman). As a result, the sample is dried onto the support. Zero-loss (20 eV window) images of TiO_2 NPs were acquired on field emission gun transmission electron microscope operating at 200 kV (JEOL 2200FS, JEOL LTD®).

Intrinsic fluorescence Assays

Steady-state fluorescence spectra were performed on Fluorolog3- Horiba spectrofluorimeter at 25°C. Various concentrations of TiO_2 NP suspensions (10- 100 μg/mL) were added as indicated to a final volume of 3 mL of buffer (PBS supplemented with 10 mM $MgSO_4$,) containing trimera (5 μg/mL, 60 nM) in a quartz cuvette. The tryptophan fluorescence spectra of trimera were obtained by exciting the samples at 290 nm (2 nm bandwidth) and recorded between 300 to 550 nm (5 nm bandwidth). The excitation wavelength was chosen at 290 nm to optimize the signal to noise ratio and to reduce the contribution of tyrosine residues to the signal [48]. 3 mL of buffer was used as baseline.

Circular dichroism spectroscopy

Synchrotron radiation circular dichroism (SRCD) spectra were measured on the DISCO beam Line at the synchrotron radiation SOLEIL, Gif/Yvette, France. The calibration was made using a solution of camphorsulphonic acid (CSA). Spectra were measured over the wavelength range from 170 to 260 nm. Three scans were measured and averaged for the samples and the baseline. The averaged baseline was subtracted from the samples and the curves obtained smoothed. SRCD spectra were recorded at 25°C. The solutions contained 1.5 mg/mL (18 μM) trimera +/-60 μg/mL TiO_2 NPs, +/- 300 μM AA prepared in 100 mM sodium fluoride; 10 mM sodium phosphate pH 7.0. Spectra are expressed in delta epsilon units, calculated using mean residue weights of 82,681 Da for the trimera. They were fitted using the free software BestSel [49]. Control spectra were recorded with TiO_2 NPs.

Measurement of superoxide ion production rates

Superoxide anion production rates were indirectly quantified by the initial rate of cytochrome *c* (cyt *c*) reduction, as previously described [50]. The reaction is the following:

$$Cyt\ c\ Fe^{3+} + O_2^{\bullet -} \rightarrow Cyt\ c\ Fe^{2+} + O_2^{\bullet}$$

Unless indicated, the components of the cell-free system were added as follows: membrane fractions (MF; 2-5 nM cyt b_{558}), trimera (100-200 nM) and arachidonic acid (40 μM) in 500 μl

PBS supplemented with 10 mM $MgSO_4$ and incubated for 4 minutes at 25°C in order to allow the NADPH oxidase complex to assemble. The production was initiated by addition of NADPH (250 μM) and the rate of $O_2^{-\bullet}$ was quantified by the reduction of cyt *c* (50 μM). The rate was measured at 550 nm in a Thermo evolution 500 spectrophotometer, using a molar extinction coefficient (Δε of the reduced *minus* oxidized form of cyt *c*) of 21 mM^{-1} cm^{-1}. Control of the production of the $O_2^{\bullet-}$ species was performed by addition of 50 μg/mL superoxide dismutase (SOD).

Results

3.1 TiO2 NPs size characterization

The hydrodynamic size of TiO_2 NPs in water and PBS was estimated by DLS. The average size of the NPs aggregates in water was about 350 ± 50 nm for the concentration range of 2-80 μg/mL of TiO_2. This NP aggregate population was predominant (100%) for TiO_2 NPs concentration lower than 20 μg/mL but another population of larger agglomerates whose sizes were estimated to about ~2000 nm (5%) appeared when TiO_2 NPs concentration was higher than 20 μg/mL. We noticed also that the size of the NP aggregates in a physiological medium, such as PBS, is similar (460 ± 50 nm) to that in water. By TEM we can also observe particle aggregation (Fig 1A). The aggregates are constituted by particles of about 30± 5 nm (Fig 1B). These results are in accordance with those in the literature where it was shown that TiO_2 NPs tend to associate to form relatively strongly bonded aggregates or soft agglomerates [17]. TEM images also showed that TiO_2 NPs are in contact with the membrane fractions (Fig 1C). Moreover, aggregation of TiO_2 NPs is similar when they were together with the proteins, (Fig 1C). Similarly, DLS measurements showed that the size of TiO_2 NPs aggregates did not change when MF (0.5μg/mL cyt *b558*) and trimera 18 μg/mL were added to 20 μg/mL TiO_2 NPs. The concentrations were similar to what we have in the cell free system assays for the measurements of NADPH oxidase activities.

3.2 Tryptophan fluorescence of trimera in the presence of TiO2 NPs

The conformation changes of the trimera were evaluated by measuring the intrinsic fluorescence spectra of tryptophan residues, before and after addition of TiO_2 NPs. Trimera contains a total of thirteen tryptophan residues (seven, four and two in the p47*phox*, p67*phox* and Rac portions, respectively). The amplitude of the emission spectrum decreased linearly by the addition of TiO_2 NPs without any change of the wavelength at the maximum (340 nm) (Fig 2, S1 Fig).The decrease of fluorescence intensity might indicate a quenching due to proximity of TiO_2 NPs and some tryptophan residues without change in the surrounding of these residues. The intensity of the shoulder at around 440 nm increased concomitantly with the decrease of the intensity of the 340 nm band and is due to emission from TiO_2 NPs (inset of Fig 2). A similar quenching happens with Trp amino acid in solution with a bathochromic effect on the maximum. This indicates some affinity between Trp and TiO_2 NPs (S2 Fig)

The eventual changes of the secondary structure due to the NPs were investigated by SRCD spectroscopy. We have recorded the SRCD spectra of 1.5 mg/mL (18μM) trimera in the absence and in the presence of 60 μg/mL TiO_2 NPs and 300 μM AA (Fig 3). In S1 Table are gathered the percentages of α-helices and β-sheets obtained by fitting the spectra with the Bestsel software [49]. Analysis of the SRCD spectra of the trimera indicates that this chimeric protein is mostly in random coil (ca. 40%) and that the content of helices is very low (3-4%) (S1 Table). Although it was supposed that the addition of an amphiphile like AA would induce larger changes in the structure of the cytosolic proteins, [48,51] we observe only slight modifications of trimera secondary structure upon addition of AA. Similarly, only slight changes in

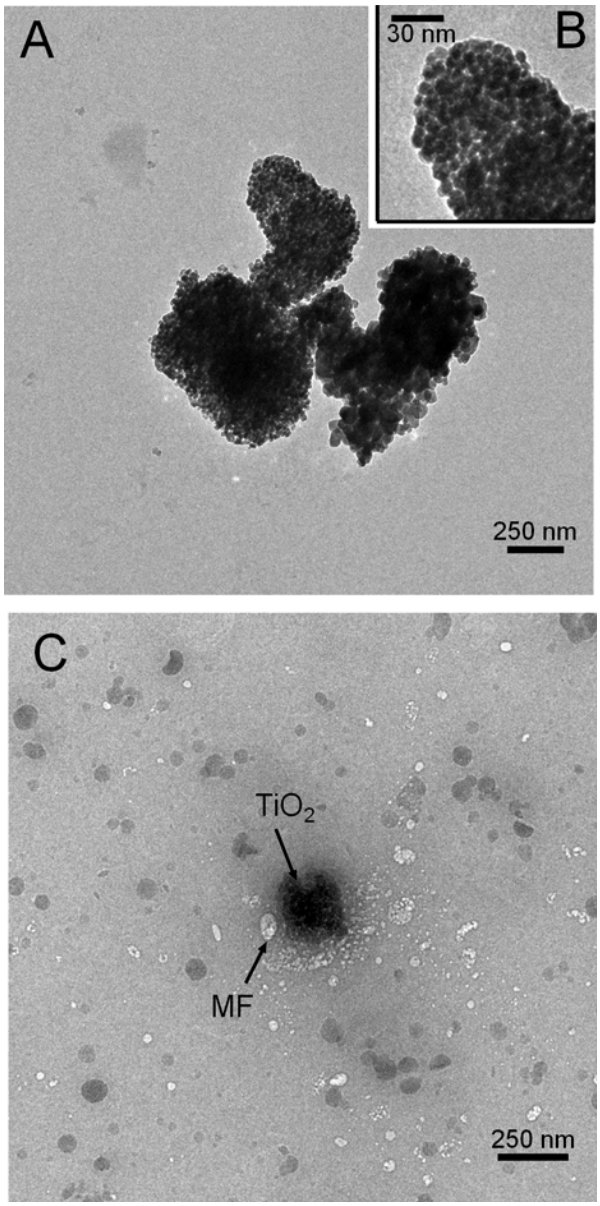

Fig 1. TEM images of (A) 0.5 mg/mL TiO_2 NPs alone; (B): enlarged view of the cluster; (C) 0.5 mg/mL TiO_2 NPs with membrane fraction (MF) (25μg/mL cyt *b558*) and 50 μg/mL aggregated trimera;. (The black bar gives the scale: 250 nm for Fig 1A and 1C and 30 nm for Fig 1B). The samples are dried (see materials and methods).

doi:10.1371/journal.pone.0144829.g001

the structure are observed with NPs. There is a loss of α-helixes and an increase of the disorder (S1 Table).

Altogether these results show that the interaction between NPs and trimera, indicated by fluorescence quenching, have no big consequence on the secondary structure of trimera.

3.3 Effects on the functionality

3.3.1 Effects of TiO2 NPs on the NADPH oxidase activity. First, we have checked that TiO_2 NPs alone did not reduce cyt *c* (data not shown), which means that in these conditions,

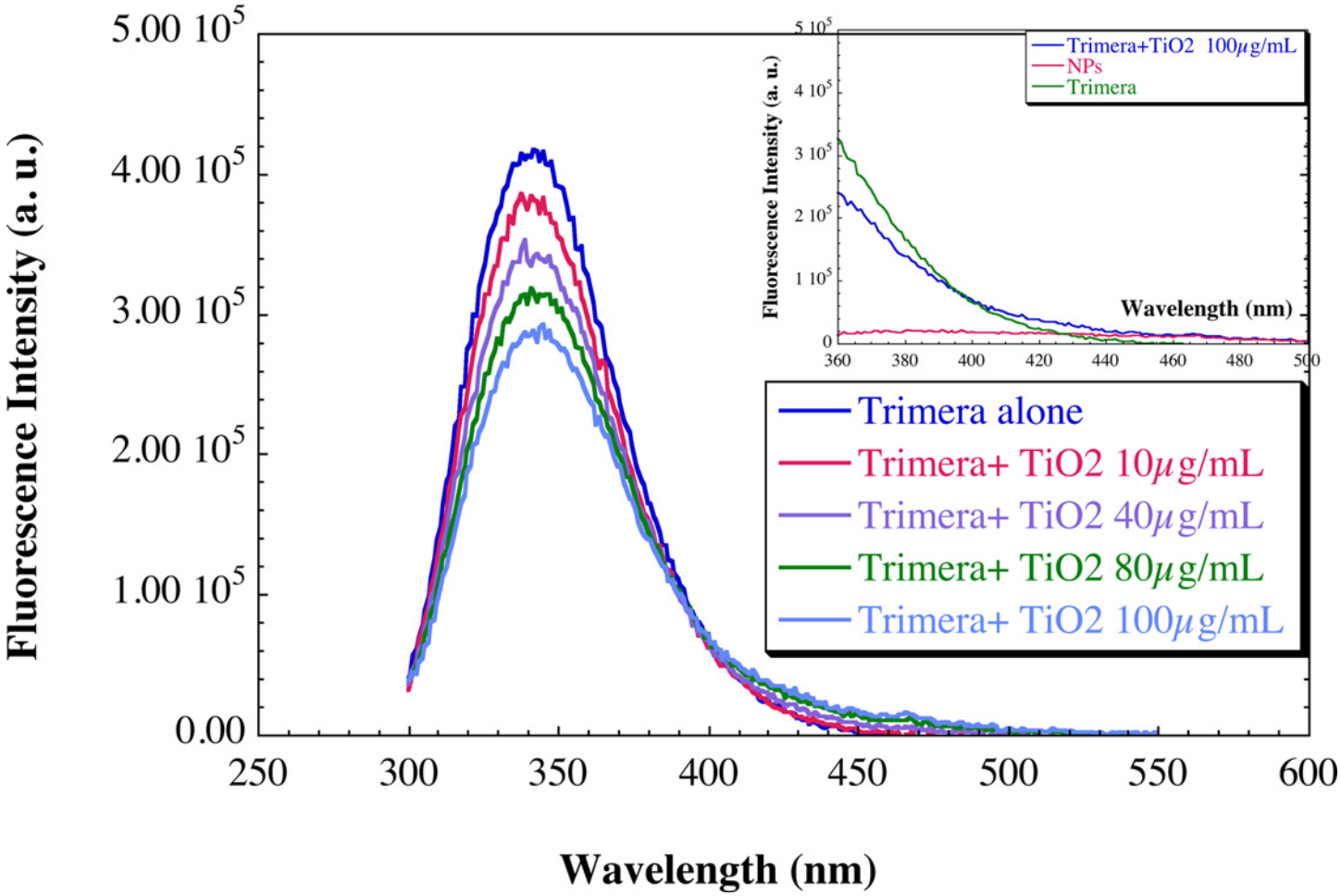

Fig 2. Fluorescence emission spectra of the trimera-TiO_2 NPs suspensions. The solution contains 5 μg/mL (60 nM) trimera and TiO_2 NPs at the concentrations of 0, 10, 40, 80 and 100 μg/mL in a final volume of 3 mL of buffer (PBS supplemented with 10 mM $MgSO_4$). The emission spectra were measured using an excitation wavelength of 290 nm as described in the Materials and Methods section. Results are representative of at least three independent experiments. In inset: enlargement of the fluorescence spectrum in the region 360-500 nm for three solutions. Fluorescence spectra of 5 μg/mL trimera alone (green), 100 μg/ mL TiO_2 NPs alone (red) 5 μg/mL trimera in the presence of 100 μg/ mL TiO_2 NPs (blue).

doi:10.1371/journal.pone.0144829.g002

NPs by themselves do not produce superoxide ions. In order to investigate the effect of NPs on the NADPH oxidase, the rate of superoxide anion production was measured upon addition of TiO_2 NPs in the cell free assay conditions previously optimized with trimera [45] (Fig 4). The initial slope of the kinetic curve is equal to the rate of superoxide anion formation. This rate was faster in the presence of TiO_2 NP. The identification of $O_2^{\cdot\bullet}$ was performed by addition of 50 μg/mL SOD.

The activity of the complex was investigated in parallel with either the trimera or the mix of cytosolic proteins $p47^{phox}$, $p67^{phox}$ and Rac. All components were incubated together with TiO_2 NPs (2-60) μg/mL and 40 μM AA. The rate of superoxide anion production in the absence of NPs was considered as 100% of NADPH oxidase activity. No major difference was noticed between the trimera and the cytosolic proteins (Fig 5). In both cases we clearly observed an increase in the NADPH oxidase activity in the presence of NPs. The curves of Fig 5 exhibit a bell shape profile with a maximum (140% of the reference) at around 20 μg/mL of TiO_2 NPs. For higher concentrations of TiO_2 NPs (> 20 μg/mL), the rate returned close to the activation level of the control. This result indicates that TiO_2 NPs potentiate the NADPH

oxidase activity. The activity remains constant for concentrations higher than 40 μg/mL probably due to some aggregations of NPs at higher concentrations.

Thus, we further questioned whether TiO_2 NPs alone (20 or 40 μg/mL) could activate the NADPH oxidase complex and thus replace AA as activator (Fig 6). Almost no NADPH oxidase activity (5 ± 2%) was detected with NPs instead of AA (control). Comparable results were obtained using the separated subunits where a maximum activity of 4 ± 2% of AA- dependent activity was reached (data not shown).

Since TiO_2 NPs cannot be considered as activating molecules, the significant increase in the rate of $O_2^{\bullet-}$ production with NPs might be due to an indirect effect on the optimized oxidase condition by disturbing the optimal AA concentration. We therefore investigated the effect of TiO_2 NPs on the AA activation profile. To probe this effect, we performed titrations of the oxidase activity vs. AA concentration in the absence and in the presence of 20 μg/mL TiO_2 NPs added after arachidonic acid (Fig 7). The rate of production with 40 μM AA alone (the concentration used as reference in this paper), was considered as 100%. In agreement with the above -mentioned results, in the presence of TiO_2 NPs, the $O_2^{\bullet-}$ production rate was higher on the full range of AA concentrations. Both curves exhibited bell-shapes as usual but the optimal concentration of AA was lower (ca. 62 μM) in the presence than in the absence (ca. 90 μM) of NPs. Similar results were obtained when NPs were added before AA (data not shown).

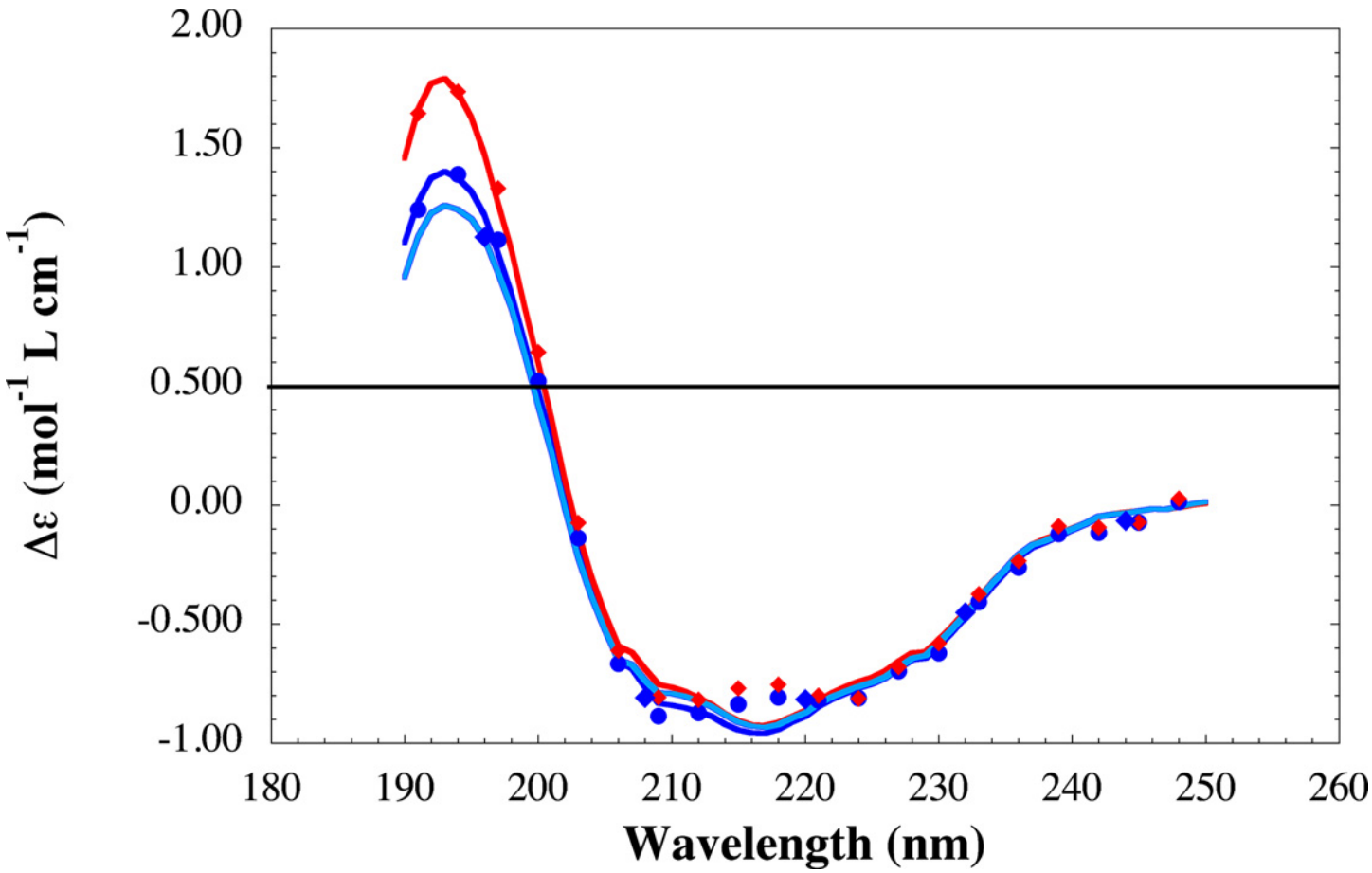

Fig 3. SRCD spectra of trimera alone and in the presence of either TiO2 NPs or AA. SRCD spectra of the trimera (18 μM) alone (Blue) and in the presence of TiO_2 nanoparticles (60 μg/mL) (sky blue) and AA (300μM) (red). The solvent was NaF 100mM /NaPi 10 mM pH 7, 25°C. The points are experimental, the curves are the fits using BeStSel [49].

doi:10.1371/journal.pone.0144829.g003

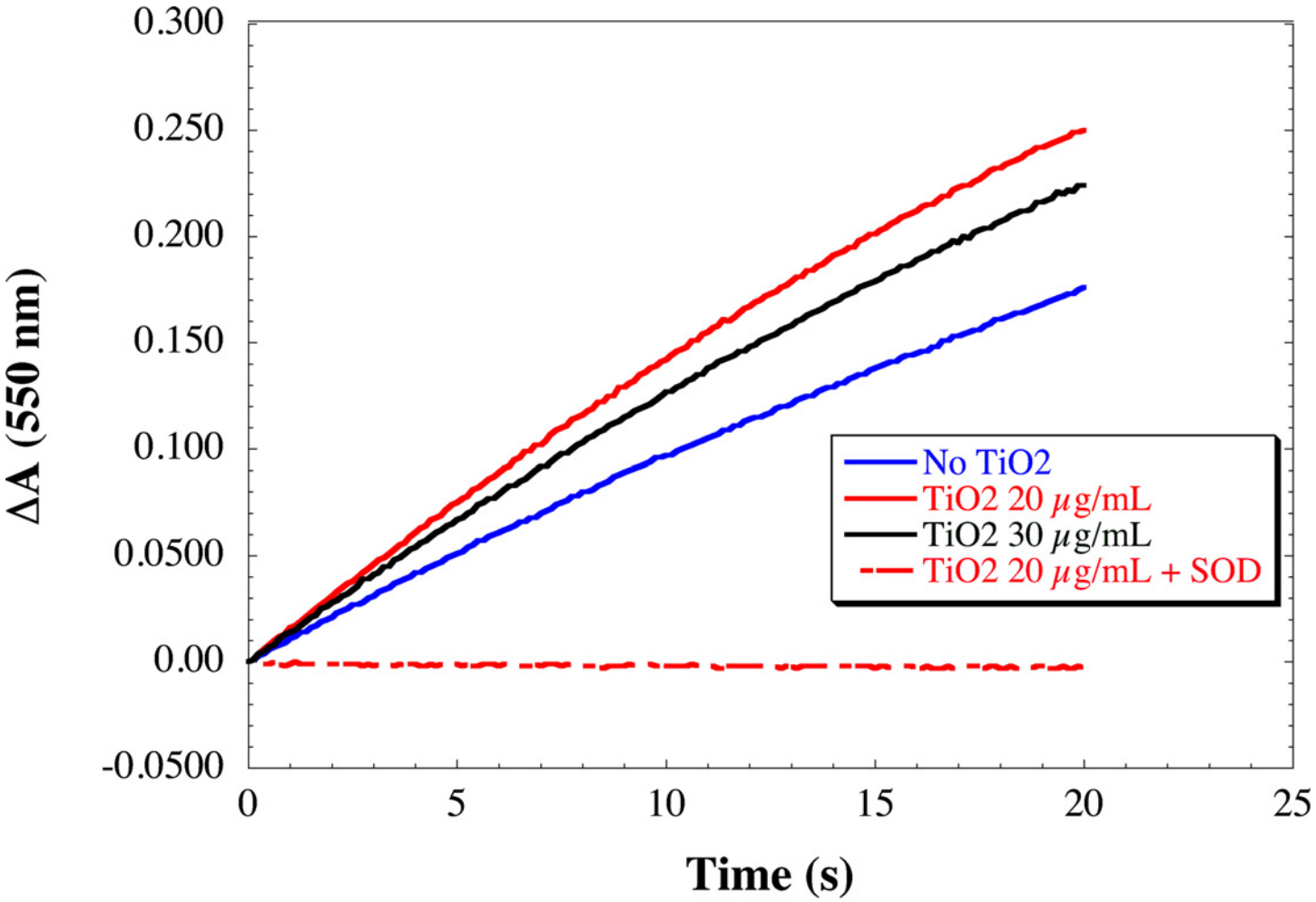

Fig 4. Kinetics of superoxide anion production in presence of TiO_2 NPs. Neutrophil membrane fractions (5 nM cyt *b558*) and trimera 200 nM were incubated together in the presence of 40 μM AA and (0, 20, 30 μg/mL) TiO_2 NPs. The production was initiated by addition of NADPH (250 μM) and the rate of $O_2^{\bullet}$ was quantified by the reduction of cyt *c* (50 μM). Control was performed by the addition of 50 μg/mL SOD. (on the fig: 20μg/mL TiO_2 in the presence of SOD). The initial rates of production of superoxide are the following: 92.0±0.3, 134.0±0.5, 119.2±0.4 mol $O_2^{\bullet}$/s/Mol Cyt b_{558} for TiO2 NPs 0, 20, 30 μg/m respectively.

doi:10.1371/journal.pone.0144829.g004

3.3.2 Effect of TiO2 NPs addition at different sequences of cell free system assay. To examine whether TiO_2 NPs have effects on specific steps of the assembly, several concentration of TiO_2 NPs (10, 20, 40 μg/mL) were added at different times: (i) to the membrane fractions alone before mixing to the cytosolic subunits; (ii) to mixed membrane fractions and trimera; (iii) to the membrane fractions plus trimera plus AA (Fig 8). Regardless the stages at which TiO_2 NPs were added, the rates of production of superoxide were the same within uncertainty. The highest $O_2^{\bullet-}$ production was still observed when 20 μg/mL TiO_2 NPs were incorporated in the system whatever the sequence of addition of NPs.

Discussion and Conclusion

Oxide nanoparticles are widely used and their toxicity levels seem to be quite different albeit always related to induction of oxidative stress [27]. Some work has been done on the toxicity of ZnO NPs. A ROS formation enhancement was observed in ZnO-treated liver cells [22,52,53] and on macrophages from wt mice, whereas this formation was impaired in the treated

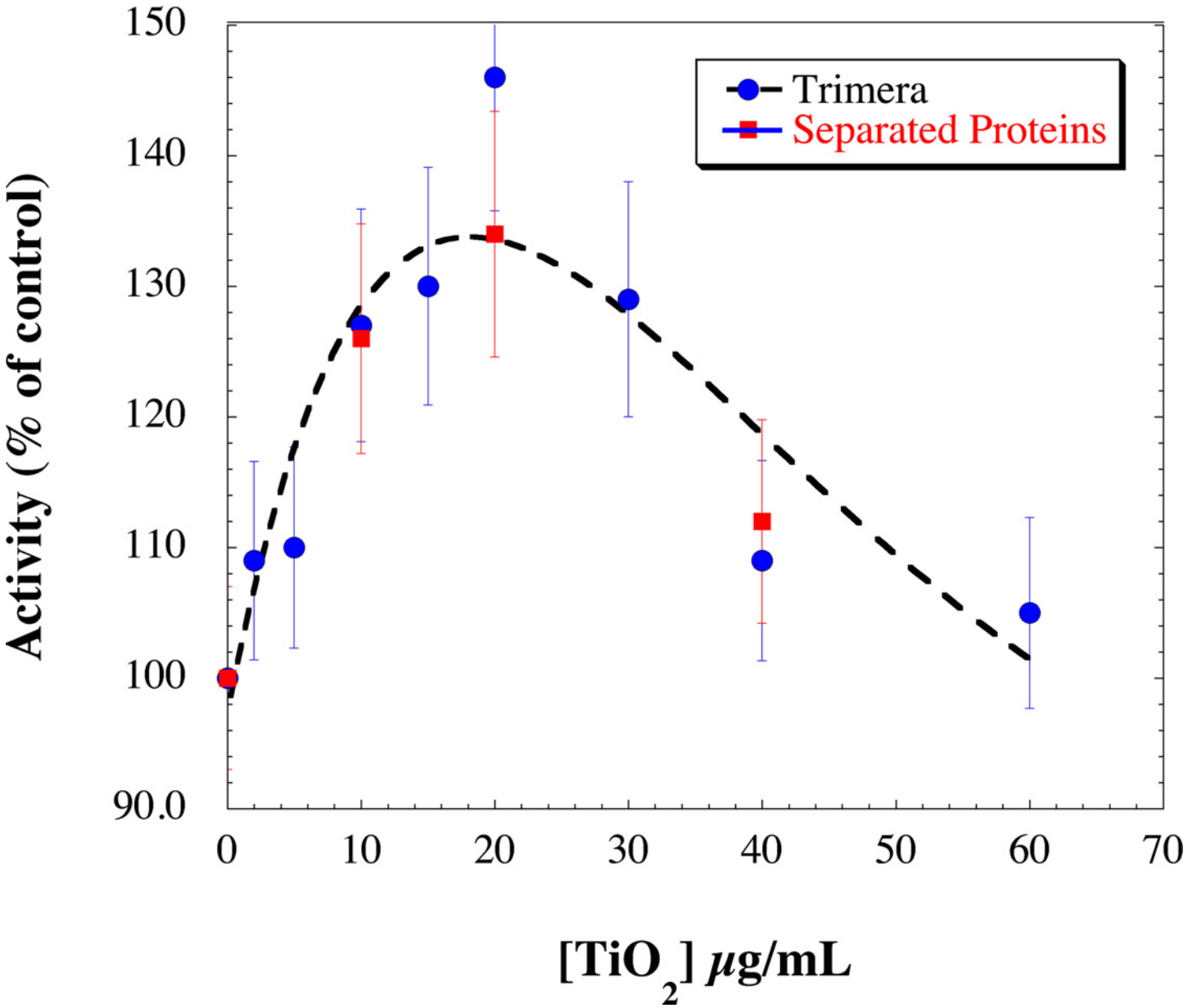

Fig 5. Dependence of NADPH oxidase activity as a function of TiO_2 NPs concentration. Neutrophil membrane fractions (5 nM cyt *b558*) and trimera 200 nM (blue dots) or the cytosolic subunits ($p67^{phox}$ 200 nM, $p47^{phox}$ 260 nM and Rac 580 nM) (red squares) were incubated together in the presence of 40 μM AA and TiO_2 NPs. Oxidase activities were expressed as the percent of activity measured in the absence of TiO_2 NPs (90 mol $O_2^{\cdot-}$/s/mol cyt *b558*), and determined as 100%. Points are an average of 3 independent measurements. The dotted curve is a visual fit for both systems.

doi:10.1371/journal.pone.0144829.g005

macrophages from the $p47^{phox-/-}$ animals. To our knowledge, this is the only work involving NADPH oxidase. [22]. The use of TiO_2 NPs has become widespread including in situations where they can be absorbed by living bodies. The photocatalytic activity of TiO_2 is well known [54], however UVA and visible light do not penetrate inside the body. Thus there is no light exposure and no activation of TiO_2 NPs by photo-catalysis.

The toxic effects of TiO_2 NPs seem to be mainly due to indirect production of ROS and therefore to induction of oxidative stress. One of the first studies about interaction between NPs and neutrophils was done in 1988; Hedenborg demonstrated that TiO_2 induced the

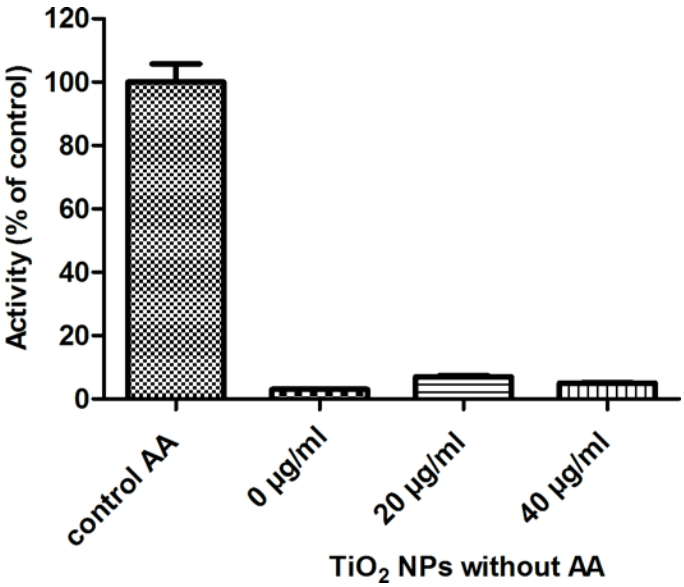

Fig 6. Dependence of NADPH oxidase activity as a function of TiO_2 NPs concentrations in the absence of arachidonic acid. Membrane fractions (4 nM cyt *b558*) with trimera 200 nM were incubated 4 min in the presence of 0, 20 or 40 µg/mL TiO_2 NPs. Control experiment representing 100% (83 mol $O_2^{\bullet-}$/s/mol cyt *b558*) of the activity was realized in presence of 40 µM AA and in absence of TiO_2 NPs. The rates of superoxide production were measured as described in Materials and Methods. Data are the average of 3 independent measurements.

doi:10.1371/journal.pone.0144829.g006

production of ROS by human neutrophils [55]. It has also been shown that TiO_2 NPs can induce oxidative damage to human bronchial epithelial cells in the absence of photoactivation [54,56]. They are known to enhance superoxide production in osteoblasts [16]. TiO_2 NPs were shown to interact with proteins and enzymes in hepatic tissues, interfering with antioxidant defense mechanisms and leading to generation of ROS [57]. Since NADPH oxidase is a major actor of oxidative stress by producing superoxide ions, it was evident that investigating the effect of TiO_2 NPs on this enzyme constitutes a relevant issue.

The aim of this paper was to obtain comprehensive information on the interaction of TiO_2 NPs with the NADPH oxidase. To facilitate such studies, we used a model system that allows performing deeper studies. The different tests performed either with the trimera or with the three separated subunits showed similar results.

It is known that the cytosolic proteins must undergo conformational changes to lead to active enzyme. TiO_2 NPs have no significant effect on the secondary structure, as shown by the CD spectra (Fig 3). However the fluorescence of the Tryptophan residues is affected by the presence of NPs. Both results are similar to those obtained with fibrinogen [58]. The quenching of fluorescence of the endogenous tryptophans of the trimera indicates that the NPs are probably close to one or several Trp residues and implies that a complex may be formed between the NPs and the cytosolic protein. *In vivo*, it was shown that proteins adsorb on TiO_2 NPs. In some cases, these NPs induced conformational changes in proteins and affected their functions [12,59,60].

The CD spectra of the trimera in the presence of TiO_2 NPs and in the presence of AA (Fig 1 and S1 Table [61]) do not exhibit much difference. The Nps have no significant effect on the secondary structure of the trimera as suggested by the CD spectra. Yet, we do not observe any ROS production from NADPH complex in the absence of AA suggesting that TiO_2 NPs are unable by themselves to activate the enzyme. TEM images showed that membrane fractions

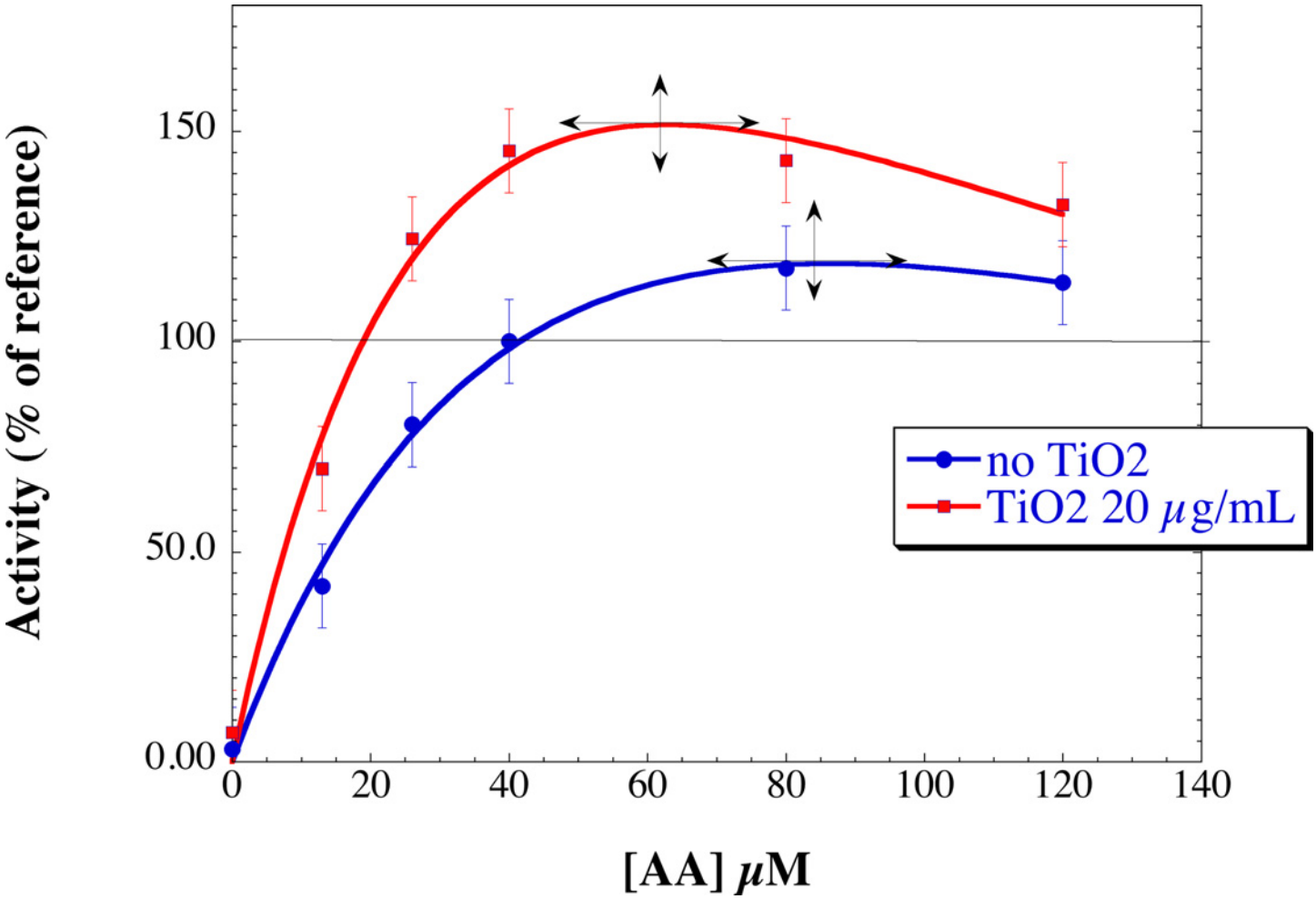

Fig 7. Effect of TiO_2 NPs on the AA-dependent activation profile. Neutrophil membrane fractions and trimera were incubated together in the presence of different concentration of AA. The TiO_2 NPs concentration was as follow, blue dots: no TiO_2 NPs; red squares: 20 μg/mL TiO_2 NPs. Oxidase activities were expressed as the percent of activity measured in the presence of 40 μM AA (85 mol $O_2^{\bullet-}$/s/mol cyt *b558*) set as 100%. The curves are visual fits of the experimental points and the maxima have been indicated by crosses. The rate of $O_2^{\bullet-}$ production was measured as described in Materials and Methods.

doi:10.1371/journal.pone.0144829.g007

are close to TiO_2 NPs and suggest also an interaction between TiO_2 NPs and the membranous proteins. Obviously this interaction with the MF does not replace that of the trimera and of AA for activation, and does not prevent AA from having access to the MF, however it might be responsible for the hyperactivation.

Surprisingly, the presence of NPs increases the rate of superoxide anion production (up to 140% of its value without NPs), this effect being dependent on the NPs concentration. They do not interact at a specific step of activation, indicating that their targets are indifferently the membrane fraction as well as the cytosolic proteins and that they can work on the system even when the entire complex is assembled and active. Since the presence of TiO_2 NPs modifies the AA-dependent activation profile of the enzyme shown in Fig 7, we can postulate that more efficient structure of the NADPH oxidase complex is attained in the presence of NPs. We can exclude a consequence of AA availability due to NPs since the higher NADPH oxidase activity is observed at lower concentration of AA in the presence of NPs than in their absence. This phenomenon cannot be attributed only to an interaction with the sole membrane fraction since the sequence of addition of the NP has no effect on it. An effect on the cytosolic fractions

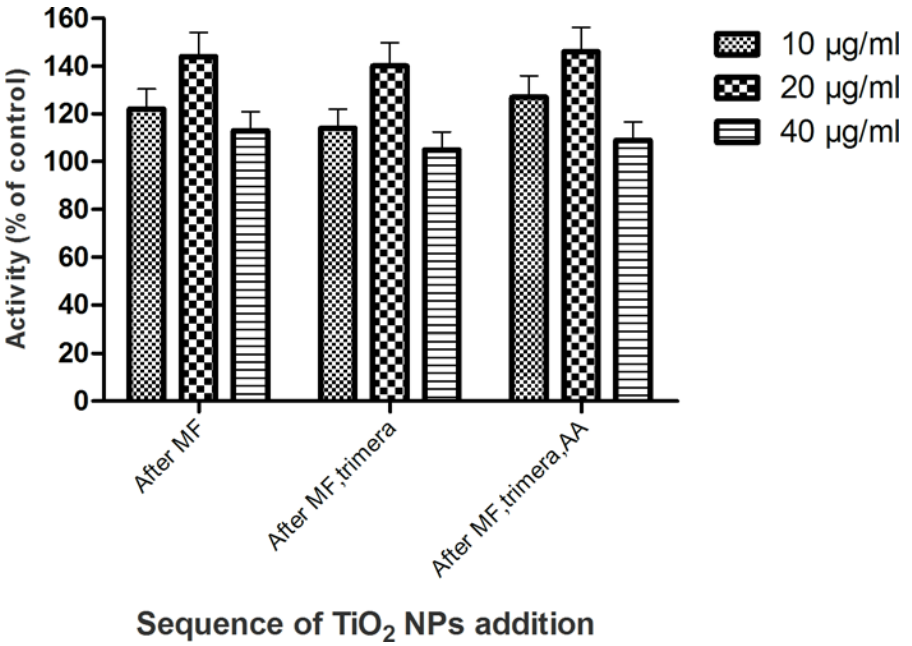

Fig 8. Effect of TiO_2 NPs as a function of its sequence of addition in the cell free system. Neutrophil membrane fractions (4 nM cyt *b558*) and 200 nM trimera were incubated together in the presence of 40 μM AA and TiO_2 NPs (10, 20, 40 μg/mL). TiO_2 NPs was added to the solution either after the membrane fractions or after the membrane fractions and trimera or after the membrane fractions, trimera and AA. Oxidase activity was expressed as the percent of activity measured in the absence of TiO_2 NPs (84 mol $O_2^{\cdot-}$/s/mol cyt *b558*) set as 100%. Results are presented as the mean±SD of 3 independent experiments.

doi:10.1371/journal.pone.0144829.g008

is also likely. Taken together, these facts indicate that the secondary structure of the cytosolic proteins may be conserved and at the same time modifications must have happened to lead to hyperactivation.

Our TEM images showed that NPs remain in the aggregation state even when they are in contact with the proteins. It was demonstrated that particles bigger than 100 nm, can enter phagocytes [62]. Additionally, it was reported that NPs enhance the ability of human neutrophils to exert phagocytosis by a Syk-dependent mechanism [26]. Thus, the TiO_2 NPs we used can enter cells by phagocytosis and may lead consequently to activation of NADPH oxidase. TiO_2 NPs aggregates are known to interact with neutrophils. Recent work by SEM [19] showed increased stiffness of the membrane and cell morphology alteration. Our present results indicate that this stiffness would not impede the NADPH oxidase functioning. In conclusion, NADPH oxidase hyper-activation and the subsequent increase in ROS production in the presence of TiO_2 NPs could be one of the pathways involved in ROS generation by TiO2 NPs, thus participate to their toxicity, which is strongly related to oxidative stress development.

Supporting Information

S1 Fig. Variation of the fluorescence intensity as a function of TiO2 concentration. 340 nm (blue), 440 nm (red). The mixture contained 5 μg/ml (60 nM) trimera and TiO_2 concentrations of 0, 10, 40, 80 and 100 μg/ml in a final volume of 3 mL of buffer (PBS supplemented with 10 mM $MgSO_4$,). The emission spectra were measured using an excitation wavelength of 290 nm as described in the Materials and Methods section. Results are representative of at least three independent experiments.
(TIF)

S2 Fig. Fluorescence emission spectra of the tryptophan residues-TiO_2 NPs suspensions. The solution contains 8μM L-tryptophan and TiO_2 NPs at the concentrations of 0, 10, 20, 40, 60, 80 and 100 μg/mL in a final volume of 3 mL of buffer (PBS supplemented with 10 mM $MgSO_4$). The emission spectra were measured using an excitation wavelength of 290 nm as described in the Materials and Methods section.
(TIF)

S1 Table. Analysis of the SRCD spectra of the trimera alone or with cis-AA or with TiO2 NPs. For definition of helixes, sheets and turns, see for instance [60].
(DOCX)

Acknowledgments

We are grateful to Dr H. Remita for a generous gift of nanoparticles, to Prof. E. Pick for the trimera plasmids and to Dr F. Lederer for the preparation of neutrophils. The financial support of ANR 2010-blan-1536-01 is acknowledged. We thank the COST Action CM1201 (Biomimetic Radical Chemistry) for very fruitful discussions.

Author Contributions

Conceived and designed the experiments: CHL TB. Performed the experiments: RM ST TB FW. Analyzed the data: CHL TB LB SM. Contributed reagents/materials/analysis tools: RM TB ST. Wrote the paper: RM CHL LB.

References

1. Niederberger M, Pinna N (2009) Metal oxide nanoparticles in organic solvents: synthesis, formation, assembly and application: Springer.
2. Wiesenthal A, Hunter L, Wang S, Wickliffe J, Wilkerson M (2011) Nanoparticles: small and mighty. Int J Dermatol 50: 247–254. doi: 10.1111/j.1365-4632.2010.04815.x PMID: 21342155
3. Papakostas D, Rancan F, Sterry W, Blume-Peytavi U, Vogt A (2011) Nanoparticles in dermatology. Arch Dermatol Res 303: 533–550. doi: 10.1007/s00403-011-1163-7 PMID: 21837474
4. Yuan Y, Ding J, Xu J, Deng J, Guo J (2010) TiO2 nanoparticles co-doped with silver and nitrogen for antibacterial application. J Nanosci Nanotechnol 10: 4868–4874. PMID: 21125821
5. Lucky SS, Muhammad Idris N, Li Z, Huang K, Soo KC, et al. (2015) Titania coated upconversion nanoparticles for near-infrared light triggered photodynamic therapy. ACS Nano 9: 191–205. doi: 10.1021/nn503450t PMID: 25564723
6. Zeisser-Labouèbe M, Vargas A, Delie F (2007) Nanoparticles for photodynamic therapy of cancer. Nanotechnologies for the Life Sciences.
7. Lagopati N, Kitsiou P, Kontos A, Venieratos P, Kotsopoulou E, et al. (2010) Photo-induced treatment of breast epithelial cancer cells using nanostructured titanium dioxide solution. Journal of Photochemistry and Photobiology A: Chemistry 214: 215–223.
8. Dransfield G (2000) Inorganic sunscreens. Radiation protection dosimetry 91: 271–273.
9. Thomas T, Thomas K, Sadrieh N, Savage N, Adair P, et al. (2006) Research strategies for safety evaluation of nanomaterials, part VII: evaluating consumer exposure to nanoscale materials. Toxicol Sci 91: 14–19. PMID: 16476686
10. Bermudez E, Mangum JB, Wong BA, Asgharian B, Hext PM, et al. (2004) Pulmonary responses of mice, rats, and hamsters to subchronic inhalation of ultrafine titanium dioxide particles. Toxicol Sci 77: 347–357. PMID: 14600271
11. Wang J, Zhou G, Chen C, Yu H, Wang T, et al. (2007) Acute toxicity and biodistribution of different sized titanium dioxide particles in mice after oral administration. Toxicol Lett 168: 176–185. PMID: 17197136
12. Gheshlaghi ZN, Riazi GH, Ahmadian S, Ghafari M, Mahinpour R (2008) Toxicity and interaction of titanium dioxide nanoparticles with microtubule protein. Acta Biochim Biophys Sin (Shanghai) 40: 777–782.

13. Barnard AS (2010) One-to-one comparison of sunscreen efficacy, aesthetics and potential nanotoxicity. Nat Nanotechnol 5: 271–274. doi: 10.1038/nnano.2010.25 PMID: 20208548
14. Buzea C, Pacheco II, Robbie K (2007) Nanomaterials and nanoparticles: sources and toxicity. Biointerphases 2: MR17–MR71. PMID: 20419892
15. Manke A, Wang L, Rojanasakul Y (2013) Mechanisms of Nanoparticle-Induced Oxidative Stress and Toxicity. BioMed Research International 2013: 15.
16. Niska K, Pyszka K, Tukaj C, Wozniak M, Radomski MW, et al. (2015) Titanium dioxide nanoparticles enhance production of superoxide anion and alter the antioxidant system in human osteoblast cells. Int J Nanomedicine 10: 1095–1107. doi: 10.2147/IJN.S73557 PMID: 25709434
17. Skocaj M, Filipic M, Petkovic J, Novak S (2011) Titanium dioxide in our everyday life; is it safe? Radiol Oncol 45: 227–247. doi: 10.2478/v10019-011-0037-0 PMID: 22933961
18. Shi H, Magaye R, Castranova V, Zhao J (2013) Titanium dioxide nanoparticles: a review of current toxicological data. Part Fibre Toxicol 10: 15. doi: 10.1186/1743-8977-10-15 PMID: 23587290
19. da Rosa EL (2013) Kinetic effects of TiO2 fine particles and nanoparticles aggregates on the nanomechanical properties of human neutrophils assessed by force spectroscopy. BMC Biophys 6: 11. doi: 10.1186/2046-1682-6-11 PMID: 23957965
20. Huang CC, Aronstam RS, Chen DR, Huang YW (2010) Oxidative stress, calcium homeostasis, and altered gene expression in human lung epithelial cells exposed to ZnO nanoparticles. Toxicol In Vitro 24: 45–55. doi: 10.1016/j.tiv.2009.09.007 PMID: 19755143
21. Knaapen AM, Borm PJ, Albrecht C, Schins RP (2004) Inhaled particles and lung cancer. Part A: Mechanisms. Int J Cancer 109: 799–809. PMID: 15027112
22. Wilhelmi V, Fischer U, Weighardt H, Schulze-Osthoff K, Nickel C, et al. (2013) Zinc oxide nanoparticles induce necrosis and apoptosis in macrophages in a p47phox- and Nrf2-independent manner. PLoS One 8: e65704. doi: 10.1371/journal.pone.0065704 PMID: 23755271
23. Goncalves DM, de Liz R, Girard D (2011) Activation of neutrophils by nanoparticles. ScientificWorldJournal 11: 1877–1885. doi: 10.1100/2011/768350 PMID: 22125444
24. Goncalves DM, Chiasson S, Girard D (2010) Activation of human neutrophils by titanium dioxide (TiO2) nanoparticles. Toxicol In Vitro 24: 1002–1008. doi: 10.1016/j.tiv.2009.12.007 PMID: 20005940
25. Jovanovic B, Anastasova L., Rowe E. W., Zhang Y., Clapp A. R. & Palic D. (2011) Effects of nanosized titanium dioxide on innate immune system of fathead minnow (Pimephales promelas Rafinesque, 1820). Ecotoxicology and environmental safety 74: 675–683 doi: 10.1016/j.ecoenv.2010.10.017 PMID: 21035856
26. Babin K, Goncalves DM, Girard D (2015) Nanoparticles enhance the ability of human neutrophils to exert phagocytosis by a Syk-dependent mechanism. Biochim Biophys Acta 1850: 2276–2282. doi: 10.1016/j.bbagen.2015.08.006 PMID: 26277637
27. Xia T, Kovochich M, Brant J, Hotze M, Sempf J, et al. (2006) Comparison of the abilities of ambient and manufactured nanoparticles to induce cellular toxicity according to an oxidative stress paradigm. Nano Lett 6: 1794–1807. PMID: 16895376
28. Nauseef WM (2007) How human neutrophils kill and degrade microbes: an integrated view. Immunological Reviews 219: 88–102. PMID: 17850484
29. Segal AW (2005) How neutrophils kill microbes. Annu Rev Immunol 23: 197–223. PMID: 15771570
30. Babior BM (1984) Oxidants from phagocytes: agents of defense and destruction. Blood 64: 959–966. PMID: 6386073
31. Sumimoto H (2008) Structure, regulation and evolution of Nox-family NADPH oxidases that produce reactive oxygen species. FEBS Journal 275: 3249–3277. doi: 10.1111/j.1742-4658.2008.06488.x PMID: 18513324
32. Valencia A, Kochevar IE (2007) Nox1-based NADPH oxidase is the major source of UVA-induced reactive oxygen species in human keratinocytes. Journal of Investigative Dermatology 128: 214–222. PMID: 17611574
33. El-Benna J, Dang PM, Gougerot-Pocidalo MA, Marie JC, Braut-Boucher F (2009) p47phox, the phagocyte NADPH oxidase/NOX2 organizer: structure, phosphorylation and implication in diseases. Exp Mol Med 41: 217–225. doi: 10.3858/emm.2009.41.4.058 PMID: 19372727
34. Sheppard FR, Kelher MR, Moore EE, McLaughlin NJ, Banerjee A, et al. (2005) Structural organization of the neutrophil NADPH oxidase: phosphorylation and translocation during priming and activation. J Leukoc Biol 78: 1025–1042. PMID: 16204621
35. Bedard K, Krause KH (2007) The NOX family of ROS-generating NADPH oxidases: physiology and pathophysiology. Physiol Rev 87: 245–313. PMID: 17237347
36. Babior BM (2004) NADPH oxidase. Current Opinion in Immunology 16: 42–47. PMID: 14734109

37. Nauseef W (2004) Assembly of the phagocyte NADPH oxidase. Histochemistry and Cell Biology 122: 277–291. PMID: 15293055

38. Raad H, Paclet MH, Boussetta T, Kroviarski Y, Morel F, et al. (2009) Regulation of the phagocyte NADPH oxidase activity: phosphorylation of gp91phox/NOX2 by protein kinase C enhances its diaphorase activity and binding to Rac2, p67phox, and p47phox. FASEB J 23: 1011–1022. doi: 10.1096/fj.08-114553 PMID: 19028840

39. Baciou L, Erard M, Dagher MC, Bizouarn T (2009) The cytosolic subunit p67phox of the NADPH-oxidase complex does not bind NADPH. FEBS Lett 583: 3225–3229. doi: 10.1016/j.febslet.2009.09.011 PMID: 19751728

40. Ostuni MA, Gelinotte M, Bizouarn T, Baciou L, Houee-Levin C (2010) Targeting NADPH-oxidase by reactive oxygen species reveals an initial sensitive step in the assembly process. Free Radic Biol Med 49: 900–907. doi: 10.1016/j.freeradbiomed.2010.06.021 PMID: 20600833

41. Karimi G, Houee Levin C, Dagher MC, Baciou L, Bizouarn T (2014) Assembly of phagocyte NADPH oxidase: A concerted binding process? Biochim Biophys Acta 1840: 3277–3283. doi: 10.1016/j.bbagen.2014.07.022 PMID: 25108064

42. Souabni H, Machillot P, Baciou L Contribution of lipid environment to NADPH oxidase activity: Influence of sterol. Biochimie.

43. Souabni H, Thoma V, Bizouarn T, Chatgilialoglu C, Siafaka-Kapadai A, et al. (2012) trans Arachidonic acid isomers inhibit NADPH-oxidase activity by direct interaction with enzyme components. Biochim Biophys Acta 1818: 2314–2324. doi: 10.1016/j.bbamem.2012.04.018 PMID: 22580228

44. Berdichevsky Y, Mizrahi A, Ugolev Y, Molshanski-Mor S, Pick E (2007) Tripartite chimeras comprising functional domains derived from the cytosolic NADPH oxidase components p47phox, p67phox, and Rac1 elicit activator-independent superoxide production by phagocyte membranes: an essential role for anionic membrane phospholipids. J Biol Chem 282: 22122–22139. PMID: 17548354

45. Masoud R, Bizouarn T., Houée-Levin C. (2014) Cholesterol: A modulator of the phagocyte NADPH oxidase activity - A cell-free study. Redox Biology 3: 16–24. doi: 10.1016/j.redox.2014.10.001 PMID: 25462061

46. Marucco A, Catalano F, Fenoglio I, Turci F, Martra G, et al. (2015) Possible Chemical Source of Discrepancy between in Vitro and in Vivo Tests in Nanotoxicology Caused by Strong Adsorption of Buffer Components. Chem Res Toxicol.

47. Akasaki T, Koga H, Sumimoto H (1999) Phosphoinositide 3-kinase-dependent and -independent activation of the small GTPase Rac2 in human neutrophils. J Biol Chem 274: 18055–18059. PMID: 10364257

48. Swain SD, Helgerson SL, Davis AR, Nelson LK, Quinn MT (1997) Analysis of activation-induced conformational changes in p47phox using tryptophan fluorescence spectroscopy. J Biol Chem 272: 29502–29510. PMID: 9368011

49. Micsonai A, Wien F, Kernya L, Lee YH, Goto Y, et al. (2015) Accurate secondary structure prediction and fold recognition for circular dichroism spectroscopy. Proc Natl Acad Sci U S A 112: E3095–3103. doi: 10.1073/pnas.1500851112 PMID: 26038575

50. Pick E, Bromberg Y, Shpungin S, Gadba R (1987) Activation of the superoxide forming NADPH oxidase in a cell-free system by sodium dodecyl sulfate. Characterization of the membrane-associated component. J Biol Chem 262: 16476–16483. PMID: 2824496

51. Shiose A, Sumimoto H (2000) Arachidonic acid and phosphorylation synergistically induce a conformational change of p47phox to activate the phagocyte NADPH oxidase. J Biol Chem 275: 13793–13801. PMID: 10788501

52. Sharma V, Singh P, Pandey AK, Dhawan A (2012) Induction of oxidative stress, DNA damage and apoptosis in mouse liver after sub-acute oral exposure to zinc oxide nanoparticles. Mutat Res 745: 84–91. doi: 10.1016/j.mrgentox.2011.12.009 PMID: 22198329

53. Sharma V, Anderson D, Dhawan A (2012) Zinc oxide nanoparticles induce oxidative DNA damage and ROS-triggered mitochondria mediated apoptosis in human liver cells (HepG2). Apoptosis 17: 852–870. doi: 10.1007/s10495-012-0705-6 PMID: 22395444

54. Jovanovic B (2015) Review of titanium dioxide nanoparticle phototoxicity: Developing a phototoxicity ratio to correct the endpoint values of toxicity tests. Environ Toxicol Chem 34: 1070–1077. doi: 10.1002/etc.2891 PMID: 25640001

55. Hedenborg M (1988) Titanium dioxide induced chemiluminescence of human polymorphonuclear leukocytes. Int Arch Occup Environ Health 61: 1–6. PMID: 3198275

56. Gurr JR, Wang AS, Chen CH, Jan KY (2005) Ultrafine titanium dioxide particles in the absence of photoactivation can induce oxidative damage to human bronchial epithelial cells. Toxicology 213: 66–73. PMID: 15970370

57. Alarifi S, Ali D, Al-Doaiss AA, Ali BA, Ahmed M, et al. (2013) Histologic and apoptotic changes induced by titanium dioxide nanoparticles in the livers of rats. Int J Nanomedicine 8: 3937–3943. doi: 10.2147/IJN.S47174 PMID: 24143098

58. Wang C, Li Y (2012) Interaction and nanotoxic effect of TiO2 nanoparticle on fibrinogen by multi-spectroscopic method. Science of The Total Environment 429: 156–160. doi: 10.1016/j.scitotenv.2012.03.048 PMID: 22607744

59. Allouni ZE, Gjerdet NR, Cimpan MR, Hol PJ (2015) The effect of blood protein adsorption on cellular uptake of anatase TiO2 nanoparticles. Int J Nanomedicine 10: 687–695. doi: 10.2147/IJN.S72726 PMID: 25632230

60. Simon-Vazquez R, Lozano-Fernandez T, Peleteiro-Olmedo M, Gonzalez-Fernandez A (2014) Conformational changes in human plasma proteins induced by metal oxide nanoparticles. Colloids Surf B Biointerfaces 113: 198–206. doi: 10.1016/j.colsurfb.2013.08.047 PMID: 24095988

61. Voet D, Voet J. (2011) Biochemistry 4th edition. New York: Wiley.

62. Aderem A, Underhill DM (1999) Mechanisms of phagocytosis in macrophages. Annu Rev Immunol 17: 593–623. PMID: 10358769

Résumé

La NADPH oxydase de phagocyte est un complexe enzymatique impliqué dans la défense immunitaire contre les pathogènes. Elle est constituée du flavocytochrome b_{558} membranaire (Cyt b_{558}), composé de deux sous-unités (gp91^{phox} et p22^{phox}) et de quatre sous-unités cytosoliques, p47^{phox}, p67^{phox}, p40^{phox}, et Rac. Sa fonction est de produire les anions superoxyde ($O_2^{\bullet -}$) qui sont transformés en d'autres espèces réactives de l'oxygène (ROS) qui vont détruire les agents pathogènes mais aussi dans certains situations pathologiques attaquer les lipides, les protéines et l'ADN environnants. Après activation du phagocyte, les sous-unités cytosoliques subissent des modifications post-traductionnelles et transloquent vers la membrane pour former avec le Cyt b_{558} le complexe NADPH oxydase activé (Figure 1). Le rôle délétère des ROS dans les maladies inflammatoires est connu depuis longtemps. Le but de ma thèse a été d'étudier l'influence de molécules exogènes qui induisent une augmentation du stress oxydatif, sur l'activité de la NADPH oxydase.

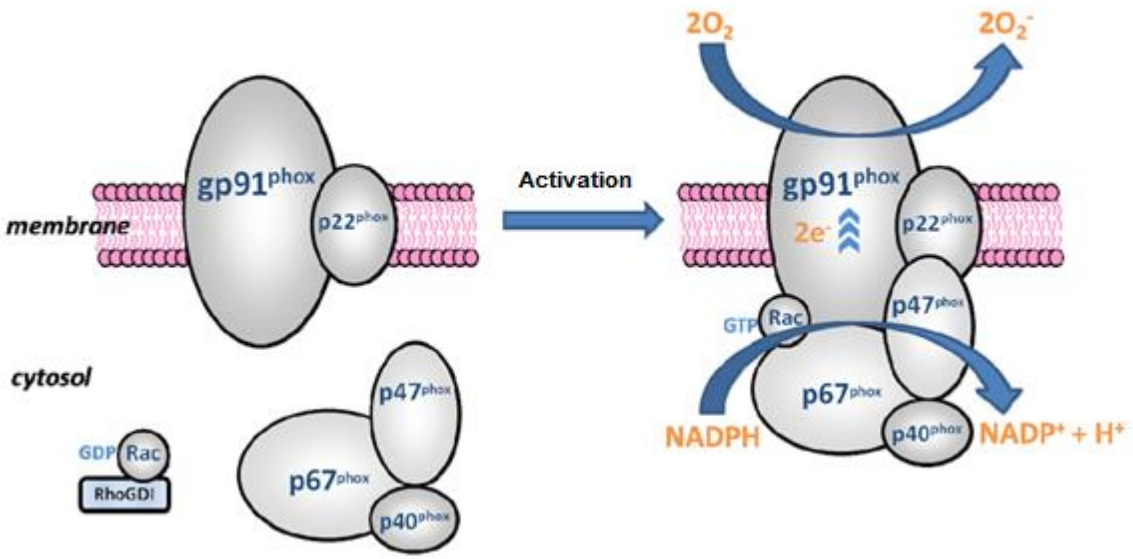

Figure1: Activation de la NADPH oxydase de phagocyte

(D'après *McCaan et al, 2013*)

Dans ce travail, nous avons étudié le fonctionnement de la NADPH oxydase dans un système *in vitro* dans lequel l'enzyme était activée par la présence d'acide arachidonique (AA). J'ai étudié

l'influence de deux types de molécules: une classe de lipides et des nanoparticules (NPs). Pour simplifier le système, nous avons remplacé l'ensemble des sous-unités cytosoliques par une protéine unique appelé trimère qui correspond à une fusion des trois protéines cytosoliques $p47^{phox}$, $p67^{phox}$ et Rac. Nous avons montré que le trimère est fonctionnellement comparable aux sous-unités cytosoliques séparées. La vitesse de production de $O_2^{\bullet-}$, sa dépendances en fonction de la concentration en AA et et sa sensibilité aux radicaux libres sont comparables lorsque le trimère ou les sous-unités séparées sont utilisés.

J'ai étudié les conséquences de la présence du cholestérol et de ses formes oxydées sur la production de $O_2^{\bullet-}$ par la NADPH oxydase. Nos résultats montrent clairement que le cholestérol et les oxystérols ne sont pas des activateurs efficaces de la NADPH oxydase. L'addition d'une quantité physiologique de cholestérol déclenche une faible production d'anions superoxyde. L'addition de cholestérol à des concentrations du même ordre de grandeur pendant le processus d'assemblage (en présence de AA), a un rôle inhibiteur sur la production d' $O_2^{\bullet-}$. Le cholestérol ajouté agit sur les composantes cytosoliques et membranaires, conduisant à un assemblage imparfait. En conclusion, le cholestérol déjà présent dans la membrane des neutrophiles est optimal pour le fonctionnement de la NADPH oxydase.

Il était intéressant de vérifier l'influence des nanoparticules de dioxyde de titane (TiO_2) et de platine (Pt) sur le comportement de la NADPH oxydase sachant que l'internalisation cellulaire de ces NPs a pour effet d'activer les neutrophiles et les macrophages et contribue à une sur-production de ROS. En l'absence d'activateur mais en présence de NPs de TiO_2 ou Pt, aucune production de $O_2^{\bullet-}$ n'était détectée indiquant que les NPs de TiO_2 et Pt sont incapables d'activer le complexe par eux-mêmes aussi bien dans le système acellulaire que dans les neutrophiles. Cependant, une fois la NADPH oxydase activée (par AA), les NPs de TiO_2 entrainent une augmentation de la production des $O_2^{\bullet-}$ jusqu'à 40% en comparaison aux conditions où elles sont absentes. Cet effet est dépendent de leur concentration. Par contre, les NPs de Pt n'ont aucun effet sur l'activité de la NADPH oxydase aussi bien *in vitro* que dans les neutrophiles. En conclusion, l'hyperactivation de la NADPH oxydase et l'augmentation subséquente de la production des ROS induites par les NPs de TiO_2 pourraient participer au développement du stress oxydatif ce qui ne serait pas le cas de Pt NPs étant donnée leur absence d'effet.